UNIVERSITÀ DEGLI STUDI DI CAMERINO

School of Advanced Studies

Doctorate course in

"Architecture Design and Planning"

Curriculum "Sustainable Urban Planning"

XXXIII Cycle

**RISK ASSESSMENT METHODS
AND APPLICATIONS TO CULTURAL HERITAGE**

Ph.D. Candidate   Supervisors

Claudia Canuti   Prof. Andrea Dall'Asta

                                                       Prof. Graziano Leoni

                                                       Co-supervisor

                                                       Dr. Michele Morici

May 2021

Table of Contents

List of Figures

List of Tables

Ai nonni.

Acknowledgements

Chapter 1.
Introduction

Seismic risk assessment is one of the engineering's most complex challenges. From this perspective, understanding earthquakes and the risks they pose, is a matter that has stretched scientists and engineers for centuries.

The seismic events in the last years represent one of the most devastating natural disasters. The destructive feature of the last earthquakes is highlighted by seismic events over the years in Italy such as Irpinia 1980, Marche-Umbria 1997, Molise 2002, L'Aquila 2009, Emilia 2012, Central Italy 2016 and worldwide such as Tohoku Earthquake 2011, Off west coast of northern Sumatera, Indonesia, 2012, Nepal 2015 and many others. The seismic events influence across scales from economic to social and psychological aspects, from individual to regional communities in a short and long-term development.

Reasons of their destructive feature certainly include the increase in world population, but also the development of cities located in high seismic hazard with high vulnerabilities structures, such as cultural heritage assets or buildings with project deficiencies or the ones located in prone areas.

It became increasingly important as urban populations and communities, to estimate the potential impact of future earthquakes using the previous knowledge in the engineering, science, social sciences and economics so that effective decisions could be made to reduce the disastrous effects of the seismic events. It is evident the importance of this topic from all the point of view, and scientists and engineers have the tools to deal with it, in order to mitigate the risk.

In this light, the importance of having a strategy and a comprehensive understanding that minimize and reduce the risk of losses became crucial. The risk evaluation must include a proper assessment of the hazard, as well as the assessment of the vulnerability of the structures and infrastructures and the exposure of the site considered. The seismic hazard is the probability that an earthquake will occur in a given area, within a given time period, and with ground motion intensity exceeding a given threshold. The seismic vulnerability generally refers to the probability of a damage given the occurrence of a hazard and, the presence of people, livelihoods, environmental functions and infrastructure are indicated as exposure, a sort of "scale factor" of the vulnerability problem. Of course, these specific evaluations cannot be based only on a qualitative approach and on the observation of the building behaviour from the past.

The analysis of the hazard, based on the probabilistic seismic hazard analysis (PSHA), is an analytical methodology that estimates the likelihood that will be exceeded at a given location in a given time period by a seismic event (Baker, 2013). The results of such analysis are expressed as estimated probabilities per unit time or estimated frequencies (such as expected number of events per year). Buldninz et al. in 1997 published

a guidance and recommendations for PSHA, taking into account the importance of the uncertainties in the analysis. This confirms the complexity of the hazard evaluation, that for this reason is not deeply analysed and not being the main topic of this work.

On the contrary, the level of accuracy of the seismic vulnerability evaluation is one of the main topics of this Thesis and it depends on the size of the study performed. In particular, the estimation of buildings vulnerability is performed mainly relying on complex models, which have to consider large amounts of in-situ data and they are generally capable of covering only a limited geographical area. On the other hand, the evaluation of seismic vulnerability at territorial level allows using both empirical and analytical methods, which could cover larger regions. Moreover, the vulnerability assessment can be achieved by classes' vulnerability, and the size of these classes is a direct consequence of the final variability of the response.

Prediction of potential economic losses and, more generally, consequences due to hazardous events, is a key point for prevention planning and emergency organization. To this aim, it is necessary to define reliable models for event predictions, both empirical or analytical, building response and consequences evaluation. Indeed historically, the impact of an earthquake on the economy of a country may be remarkable. Evaluations and management on architectural resources from an economic point of view should be deeply analysed and considered.

The Performance Based Earthquake Engineering framework (PBEE) presented by the Pacific Earthquake Engineering Research (PEER) Center (Deierlein et al., 2003) is a robust methodology that allows to evaluate the structural performance in a rigorous probabilistic manner without relying on expert opinion, considering the uncertainty in the seismic hazard, structural response, potential damage and economic losses.

The PBEE involves four different stages: hazard analysis, structural analysis, damage analysis and loss analysis (Cornell and Krawinkler 2000, Deierlein et al., 2003) in order to quantify the decision variables. Cornell and Krawinkler presented a scheme that can be considered an effective foundation for the development of performance-based guidelines. In particular, they suggested a generic structure for coordinating, combining, and evaluating the implicit considerations in performance-based seismic assessment. The main challenge is to provide a direction toward which the various PEER research efforts should converge, identifying two different options. The first one is to develop a general methodology for estimating the annual expected costs associated with the seismic risk (initial, maintenance, insurance, etc., plus annualized earthquake losses). This building loss estimation option is very attractive because it permits an evaluation of retrofit or design alternatives, but should be "compatible" with seismic retrofit projects and new designs. The second option is the development of a methodology that focuses on specific performance levels, from continuous operation to collapse prevention and the annual probability of exceeding these levels. Finally, the authors stated that the final challenge for PEER researchers is not the estimation of losses or performance prediction, but it is based on the effective contribution in the reduction of losses and the improvement of safety.

Deierlein et al., described the performance assessment process through four generalized variables that characterize information in a logical manner. The process identified by Deierlein et al. starts with the definition of a parameter describing the ground motion intensity at the site of the structure, the Intensity Measure (e.g., peak ground acceleration, spectral acceleration, etc.), whose probabilistic features are described by means of seismic hazard curve expressing the mean annual rate of exceedance for different intensity values. Next, Engineering Demand Parameters, such as interstory drift, floor accelerations or other engineering response quantities, are calculated (e.g., via simulation approaches and through numerical analyses of structural systems) to characterize the response of the system conditional to the earthquake occurrence. The Engineering Demand Parameters can be then easily linked to Damage Measures, which describe the physical damage to the structure and its components. Moreover, damage states are delineated by their consequences on Decision Variables, consisting of economic losses, downtimes, and casualty rates. To summarize, Deierlein et al. stated that the key aspect of the methodology is a representation and tracking of uncertainties in predicting performance metrics that are relevant to decision making for seismic risk mitigation.

In 2003 also Porter summarized the development of a performance-based earthquake engineering methodology by the Pacific Earthquake Engineering Research Center (Porter, 2003).

A complete methodology of loss estimation is presented in various works such as Risk-UE (Milutinovic and Trendafiloski, 2003) and Hazus (FEMA, 2003). The Risk-UE project developed vulnerability models describing the relation between potential building damage and their specific seismic hazard, followed by their fragility models and damage probability matrices based on analytical studies and expert judgment. Then a standardized damage survey and building inventory form is proposed. This is useful for rapid collection of relevant data, building damage and post-earthquake building usability classification. Hazus project described the methods for performing earthquake loss estimation. A simple illustration of the scheme used in Hazus is proposed in Figure 1-1.
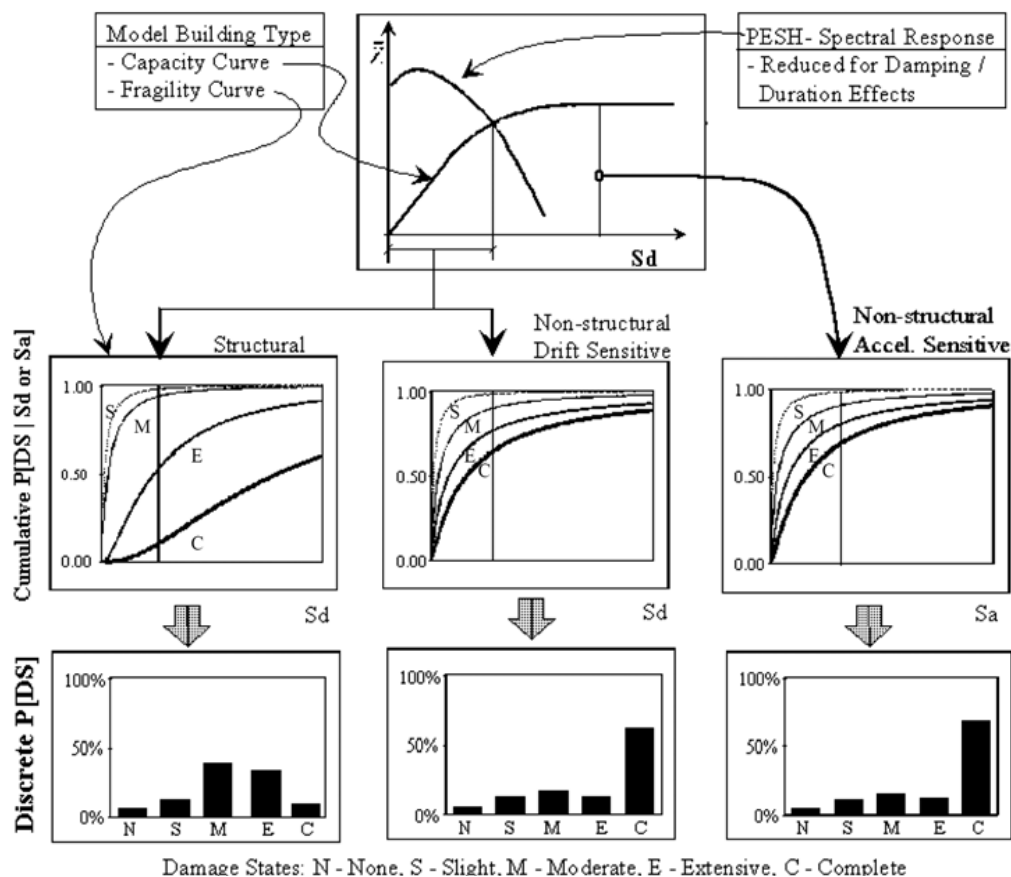
Figure 1-1: Illustration of the estimation of damage from ground shaking in HAZUS (FEMA, 2003)

The primary purpose of that project is the development of guidelines and procedures for making earthquake loss estimates at a regional scale. A secondary purpose of the project is to provide a basis for assessing nationwide risk of earthquake losses. In that project, the authors pointed out the importance of studying this method considering the uncertainties that are inherent in any loss estimation methodology. The uncertainties may derive from incomplete scientific knowledge concerning earthquakes and their effects upon buildings and facilities. They can be also the result of the approximations and simplifications that are necessary for comprehensive analyses, especially at territorial level.

In this light, understanding and quantifying uncertainty is essential to develop a reliable probabilistic model for structural seismic risk assessment (Ellingwood and Kinali 2009).

In order to rigorously assess the seismic risk of a structure, all the uncertainties related to the ground motions affecting a given site, the structural response, the associated damage and the cost to repair a damaged structure should be accounted for.

A number of uncertainties are present in the earthquake action, in the choice of the materials and geometrical structural properties, in the modelling and analysis of the structure and in the numerical prediction of structural seismic performance.

In particular, the work of Ellingwood and Kinali pointed out the fact that all sources of uncertainty should be included in risk assessment, basing this choice on the preferences of the stakeholders and decision-makers. In detail, they illustrated how such uncertainties are propagated through seismic risk assessment of steel frame building structures, typical of regions of low-to-moderate seismicity in the Central and Eastern United States.

For structural risk assessment, the uncertainties analysis is part of the evaluation. In particular, in this Thesis the uncertainties analysis will be focalized on the vulnerability assessment, where the response variability of classes' vulnerability depends on the size of the class itself.

This Thesis aims to provide a contribution to the understanding of the uncertainty propagation in the seismic risk assessment. This topic has been investigated using two different approaches; in the former approach vulnerability is described by empirical models, and in the latter one vulnerability is described by analytical models. The first approach has been used to evaluate the seismic risk of historical churches and an original empirical model is proposed, starting from the damage survey carried out after the 2016 Central Italy seismic sequence. The main aspect of originality is provided by the statistical analysis of the dataset, and by the probabilistic model developed for the damage and consequences prediction. A major specificity is that the dataset used to develop the probabilistic models, includes also undamaged and collapsed churches instead of damaged constructions only. The model presented can be of applicable in the risk assessment at territorial level and may be a useful tool to select the most promising mitigation actions, and to support the related decision making process. The strategy used to define the historical church model can be of interest in the development of damage and consequences predictive models of other type of constructions (e.g. masonry buildings, reinforced concrete buildings, etc.).

The second approach, based on an analytical description of construction vulnerability, has been investigated in the last part of the Thesis. In particular, existing analytical models have been used and the analysis focuses on the uncertainties propagation by studying the sensitivity of the risk metric to the variance of the response models. This approach has been applied to a set of reinforced concrete structures highly damaged after a seismic sequence, classified based on the height of the buildings and that may be considered part of the Italian cultural heritage, due to a construction technique that it is now obsolete and abandoned (Morabito and Podestà, 2015). In this case, all the steps of the seismic risk framework have been investigated. Finally, a comparison between predictions coming from analytical models and the real damage observed after the Central Italy seismic events is presented, in order to understand the level of reliability of analytical methods.

Chapter 2 contains an introduction to the main problem of the vulnerability analysis and a review of the state of the art related to the practical methods for the probabilistic evaluation of the seismic vulnerability, focusing on the empirical and analytical approaches, the main methods used in the applications of the Thesis.

Chapter 3 presents the main sources of uncertainties that could affect the variability of the response of the churches in one case, and reinforced concrete buildings in the other case, strictly linked to the vulnerability classes' size. The sources of uncertainties include seismic input, model parameter uncertainties related to the observed data in the case of the empirical method or geometrical and mechanical structural properties if the analytical method is used. Epistemic uncertainties are also considered, related to the limited data and knowledge in the adopted model. In this chapter, a review of the state of the art of this topic, in particular of the statistical models, is presented.

Chapter 4 and 5 will treat the two case studies using the different methods. In particular, Chapter 4 begins with an analysis of observational damage from post earthquake investigations carried out on churches of the Marche Region hit by the 2016 Central Italy seismic sequence. Then, these data are collected and processed to give a better view of the vulnerability of this type of structures. An improvement in a probabilistic way of this study has made, firstly related to the seismic damage and then to the consequences. The damage is expressed by a continuous index and a complete database of damaged, undamaged and collapsed churches is considered. This empirical model is applied to illustrate the potential application of this risk analysis in decision-making process. Then, a probabilistic response consequence model is presented, by considering also a deep analysis on the soil features. This probabilistic response consequence model may be of interest in the development of effective strategies to mitigate and prevent the risk and can be a tool of supporting the reduction of direct economic losses.

Chapter 5 presents the analytical method using a sample formed by reinforced concrete buildings classified on the basis of their height. In this case, the seismic response of the structures is described by means of fragility curves proposed in literature according with the typologies of building of the area considered. A loss analysis is also carried out in terms of expected annual losses. Moreover, a comparison with the observed damage experienced by the buildings after the 2016 Central Italy seismic sequence is provided. The propagation of the uncertainties in the framework of the risk has been considered as well, and in particular, the variability in the fragility curves parameters. The sensitivity analysis has been conducted evaluating the First-Order sensitivity index and the Total sensitivity index and considering different hazard references curves.

Finally, in Chapter 6, some conclusions are drawn and future developments are discussed.

Chapter's references

Baker, J.W., 2013. Introduction to Probabilistic Seismic Hazard Analysis White Paper Version 2.0.1, 79.

Budnitz, R.J., Apostolakis, G., Boore, D.M., 1997. Recommendations for probabilistic seismic hazard analysis: Guidance on uncertainty and use of experts (No. NUREG/CR--6372-Vol.1, UCRL-ID--122160, 479072). https://doi.org/10.2172/479072

Cornell, C.A., Krawinkler, H., 2000. Progress and Challenges in Seismic Performance Assessment PEER Center News, 3(2).

Deierlein, G., Krawinkler, H., Cornell, C., 2003. A framework for performance-based earthquake engineering. Presented at the 2003, Pacific Conference on Earthquake Engineering, Christchurch, New Zealand.

Ellingwood, B.R., Kinali, K., 2009. Quantifying and communicating uncertainty in seismic risk assessment. Structural Safety 31, 179–187. https://doi.org/10.1016/j.strusafe.2008.06.001

FEMA, 2003. Hazus–MH MR5 Technical Manual. Department of Homeland Security Federal Emergency Management Agency Mitigation Division Washington, D.C.

Hastings, W.K., 1970. Monte Carlo Sampling Methods Using Markov Chains and Their Applications. Biometrika 57, 97–109. https://doi.org/10.2307/2334940

Krawinkler, H., 1999. Challenges and progress in performance-based earthquake engineering. Presented at the International Seminar on Seismic Engineering for Tomorrow, Tokyo, Japan, p. 10.

Milutinovic, Z.V., Trendafiloski, G.S., 2003. RISK-UE-An advanced approach to earthquake risk scenarios with applications to different European towns, WP4 Vulnerability of current buildings.

Morabito, G., Podestà S., 2015, Edifici storici in conglomerato cementizio armato, D. Flaccovio, Palermo, ISBN 9788857904306©

Porter, K.A., 2003. An Overview of PEER's Performance-Based Earthquake Engineering Methodology, in: Applications of Statistics and Probability in Civil Engineering.

Chapter 2.
Seismic Vulnerability Evaluation

To introduce the methods useful for the seismic vulnerability evaluation, some premises and some definitions need to be assessed.

Seismic risk is the probability of harm if someone or something is exposed to a hazard, or in other words, it is the likelihood that humans will incur loss or damage to their environment if they are exposed to a seismic hazard during a specific time.

The evaluation of the seismic risk is strictly connected with the assessment of the seismic loss, defined as (i) direct economic losses associated with repairing damage within a structure; (ii) direct losses associated with injuries and casualties; and (iii) indirect losses associated with the loss of income due to business disruption. Generally, these three forms of losses (damage, deaths and downtime) are known as the '3D's'(Bradley et al. 2008) and the analysis of the seismic loss is important for the decision making process.

However, the distinction between all the terms included in the seismic risk evaluation, is often not precise and the components definition of the process are interchangeable (Wang, 2009).

Therefore, it can be said that seismic risk is an interaction between seismic hazard and vulnerability (humans or their built environment). In general, seismic risk can be expressed qualitatively as:

Seismic Risk=Seismic Hazard × Vulnerability

The seismic hazard is the probability that an earthquake will occur in a given area, within a given time period, and with ground motion intensity exceeding a given threshold.

The seismic vulnerability generally refers to the probability of a damage given the occurrence of a hazard. Generally, the presence of people, livelihoods, species or ecosystems, environmental functions, services, and resources, infrastructure is indicated as exposure that is a sort of "scale factor" of the vulnerability problem.

The most known results of a vulnerability analysis are the fragility functions, mathematical function that express the probability that some undesirable events occur (generally that a structure exceed a threshold or limit state or damage state) as a function of some intensity measure (measure of acceleration, measure of displacement or other measure of seismic excitation). In other word, as reported in Porter's guide (Porter, 2018), the fragility functions represent the probability that an uncertain quantity will be less or equal to a given value, as a function of that value (cumulative distribution function). The most common form of a seismic fragility function is the lognormal cumulative distribution function (CDF)

$$F_d\left(x\right)=P\left[D\geq d\,|X=x\right]=\phi\left(\frac{\ln(x/\theta_d)}{\beta_d}\right)\qquad\qquad d\in\left\{1,2,...,N_D\right\}\qquad\qquad(2.1)$$

where

D = uncertain damage state of a particular component

d= particular value of D that goes from 0 to the number of possible damage states N_D

X= uncertain excitation for example peak ground acceleration, and x is a particular value

ϕ = standard normal cumulative distribution function

F_d= fragility function for damage state d evaluated at x

θ= median capacity of the structure to resist to a damage state d

β= standard deviation of the natural logarithm of the capacity of the building to resist at damage state d (logarithmic standard deviation).

The capacity of the fragility curves to correctly predict the damage probability distribution, depends on the level of details of the collected data generating numerical models that could best simulate the building behaviours. This shows the importance of defining damage levels for seismic hazard by taking into account the variability in building types through probabilistic distributions of the damage levels. Indeed, methods for deriving fragility curves can model the damage on a discrete damage scale. The scale is used in reconnaissance efforts to produce post-earthquake damage statistics (observational approached/empirical method), whereas in mechanical procedures the scale is related to limit state mechanical properties of the buildings, such as displacement capacity or inter-storey drift capacity (analytical method).

In particular, the fragility functions are a probabilistic tool, since uncertainties are present in the hazard, in the demand and in the capacity; therefore epistemic uncertainties due to a lack of knowledge, and aleatory uncertainties due to the intrinsic randomness, are both considered in the process (Figure 2-1).
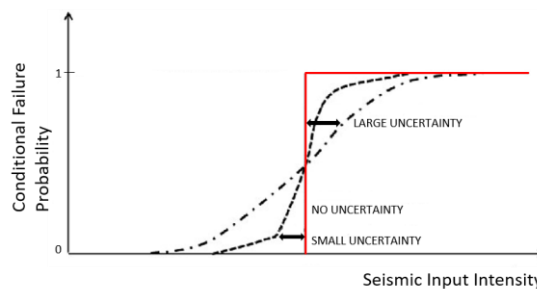
Figure 2-1: Fragility function with the effect of uncertainties

Every structure or group of buildings, classified according some features in order to estimate the seismic risk at territorial level, has its own fragility function. The fragility functions can be used for seismic risk assessment, for example Pinto et al. in 2005 provided quantitative predictions of future economic losses as well as safety levels, accounting for the many uncertainties involved in the earthquake assessment problem.

Moreover, these functions can be used for retrofitting techniques, such as risk mitigation efforts but also for disaster response planning.

Based on the literature review, there are four approaches to develop fragility functions:

- Judgmental or expert based opinions
- Empirical method
- Analytical method
- Hybrid method

The first method is the one based only on the knowledge of group of experts in the field of earthquake engineering. They provide the probability distribution of the expected damage resulting from the occurrence of an earthquake of a given intensity. It is a simple method and it is generally based on the use of questionnaires, the experience of the consulted experts and on the number of experts. However, the strong disadvantages of this approach are the underestimation of uncertainties and the lack of credibility because the fragility functions are built based only on the individual experience of the scientists and engineers and therefore, the information cannot be tested or cross-validated.

The empirical approach is based on the development of fragility function based on previous earthquake events. Data are derived entirely from the observation of the actual performance of an asset in the past earthquakes. Indeed, it is assumed that the damage derived from past earthquakes for certain class of structures, will be the same for future earthquakes. The main advantage of this approach is the credibility of the data: they represent a realistic picture of the location analysed, that can be useful to analyse the risk at territorial level, grouping the structures into classes' vulnerability. On the other hand, the main drawbacks of the empirical method are the incompleteness of the observational data for some case studies and the fact that many buildings types have not yet experienced strong motion.

The analytical vulnerability method uses stochastic or numerical simulations of the seismic response of any type of structure and it is useful when observed data or expert judgments are not fully available or when there are buildings that not have experienced strong motion. However, it is a time consuming method in terms of estimating the behaviour of a building or class of buildings. Moreover, it is an approach that introduces a significant variability. The problem can be separated in blocks, as proposed in the PEER framework (Porter, 2003; Günay and. Mosalam, 2013) starting from the hazard analysis, knowing already the definition of the location and site conditions. Once the seismic input model is well identified, an evaluation of the structural

analysis is provided that will be then the input of the fragility function useful to estimate the damage analysis. Finally, a loss analysis is made in order to estimate the cost to repair damage and cost in terms of deaths and/or downtime. In most of the cases, the analytical methods use the same steps identified above, as Porter in 2003 illustrated in Figure 2-2.

Facility info	Hazard analysis	Struct'l analysis	Damage analysis	Loss analysis	Decision-making
	$g[IM/O,D]$	$p[EDP/IM]$	$p[DM/EDP]$	$p[DV/DM]$	
O, D	$g[IM]$	$p[EDP]$	$p[DM]$	$p[DV]$	*Select O, D*
O: Location *D*: Design	*IM*: intensity measure	*EDP*: engineering demand param.	*DM*: damage measure	*DV*: decision variable	
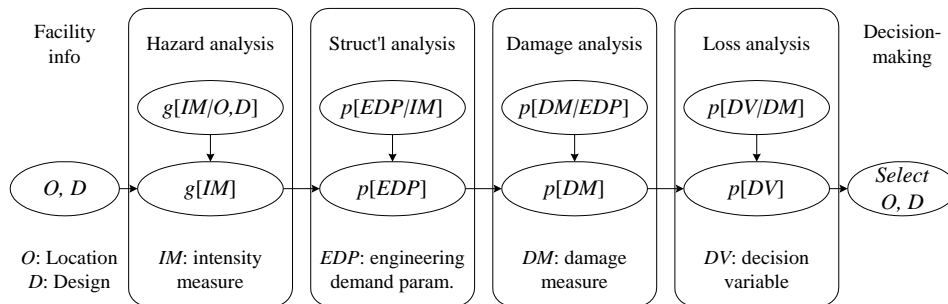
Figure 2-2: Analytical method to estimate seismic vulnerability (Porter, 2003)

Finally, the hybrid vulnerability method is based on the combination of the experimental and analytical method (Kappos et al., 1995; Kappos et al 1998). In 1998, Kappos presented a seismic risk scenario based on the so-called "hybrid" approach of vulnerability assessment. This work combined the empirical approach with the advanced analysis based procedure of Reinforced Concrete (RC) buildings in Thessaloniki, Greece. In particular, the vulnerability analysis is carried out by constructing the part of each damage probability matrixes for which the statistical data from past earthquakes are available, and the remaining part of the damage matrix from the results obtained by the inelastic time history analysis of models that simulate the behaviour of the building class. In 2006, the same author (Kappos et al. 2006) improved the work by using a more rigorous approach to derive the fragility curves, and the hybrid approach involve non-linear static analysis rather than dynamic analysis. However, the main drawback of this approach is the requirement of multiple data because of the combination of experimental and analytical method.

Calvi et al. provided a deep analysis of the main methodologies that have been proposed over the past 50 years. In that study, it was analysed the most important contributions in the field of vulnerability evaluation on the empirical, analytical and hybrid side, highlighting the advantages and disadvantages of these approaches (Calvi et al., 2006). Also in the study of Giovinazzi, a proposal for the vulnerability assessment of built-up area and their implementation for damage scenario estimation is illustrated, considering observed damage and mechanical methods being worldwide recognized approaches for scenario seismic vulnerability assessment. In that work, also the drawbacks have been analysed. In particular, a unique procedure for observational methods is not yet recognized due to the difference in the way of which data have been collected and processed.

On the other hand, the mechanical methods provide reliable results for built-up area characterized by consolidated seismic design codes, but their application for traditional non-designed masonry constructions is not always obvious. Moreover, due to their conceptual differences, these methods are not well comparable and in terms of seismic risk analysis, the results they provide are not always similar. In this work, the authors wanted to overcome the limitations of the vulnerability methods, making the most of the positive characteristics of these approaches (Giovinazzi, 2005).

On the basis of what discussed above, in this Thesis, the focus will be on the empirical and analytical method, which will be applied at two different case studies.

2.1 Empirical Vulnerability Functions

The evaluation of the vulnerability through the empirical approach derives from observation of damage distribution in buildings after past seismic events. This approach is the most realistic and the majority of the details are taken into account such as soil-structure interaction, topography, site, path and source characteristic. However, this realistic condition means the requirements of large quantities of observational data after the earthquake that cover a wide range of ground motion intensities.

Indeed, all the observational data derives from surveys and investigations carried out for a large databank of buildings of similar features and in similar area conditions. This is an important characteristic for uniform seismic demand to be assumed over the population and to collect data after seismic events useful to develop empirical fragility functions.

This considerable number of data bring a great measure of uncertainties due to lack of local ground motion recording or due to intrinsic uncertainties. The sources of this kind of uncertainties are many, such as errors in the building form compilation during the investigations, incorrect classification of the observed damage due to rapid execution of survey, and errors due to the poor experience of the technicians to identify the damage or that badly define the damage scales. Others uncertainties could come from differences in geometric/material properties and seismic design of structures of a given class, or to structural irregularities of a given class. On the intensity measure side, the uncertainties can derived from a variation of the estimated level of intensity measure or from a lack of observed ground motion intensity levels. These uncertainties are considered in the main well known probabilistic tool and in the fragility functions specific for each typology of building.

Even if fragility function shape changes for different structural types, the same general procedure is followed for the derivation of the curves in all the structural cases. Rossetto et al. (Rossetto et al., 2014) proposed a framework for vulnerability assessment as guidance for the construction of vulnerability relationship form post-earthquake survey data. The choices to be made at each stage are firstly the parameters of the ground

motion, then the building typologies class determination. The selection of the damage scale and the definition of the limit states with their thresholds represent the following steps. Finally, in the last step, the main alternatives are the choice of the methodology for damage data combination, the selection of the shape function and the regression procedure.

For what concern the damage scale, in the early 1960s the first proposal was the Mercalli-Cancani-Sieberg Scale (MCS), followed by the Modified Mercalli Intensity scale (MMI) and then by the Medvedev-Sponheuer-Karnik scale (Medvev and Sponheuer, 1969) with slight noticeably changes into the MSK-64, proposed by Medvedev in 1976 and 1978 (MSK-64).

Then, another update was developed and the whole process of establishing first the European Macroseismic Scale in 1992 (EMS-92) and finally the EMS-98 in 1998 went on for almost ten years, and so the final version of the EMS represented a subsequent final stage of upgrading activities in the intensity scale.

The EMS-98 (Grünthal et al.1998) proposed a new macroseismic intensity scale for different building types, classifying the damage into five levels from "Grade 1" (negligible damage associable to damage level 1) to "Grade 5" (collapse associable to damage level 5) for different types of buildings and using the definition of quantities (such as "few", "most", "many"). Moreover, in this study a differentiation of structures into vulnerability classes is provided. In this document, the term macroseismic intensity means the classification of the severity of ground shaking, based on the observed effects of a specific area. In Figure 2-3 on the left is illustrated the vulnerability table of the EMS-98 that shows for each type of structure (masonry, RC buildings steel and wood) the associate vulnerable class, considering for each of them the most likely vulnerable class but also the probable and less probable range of class. On the right, it is displayed the damage classification of a specific type of building (masonry), where each grade level is described by using specific damage description in which the construction building type (masonry, RC..) can be fallen into that specific damage level.
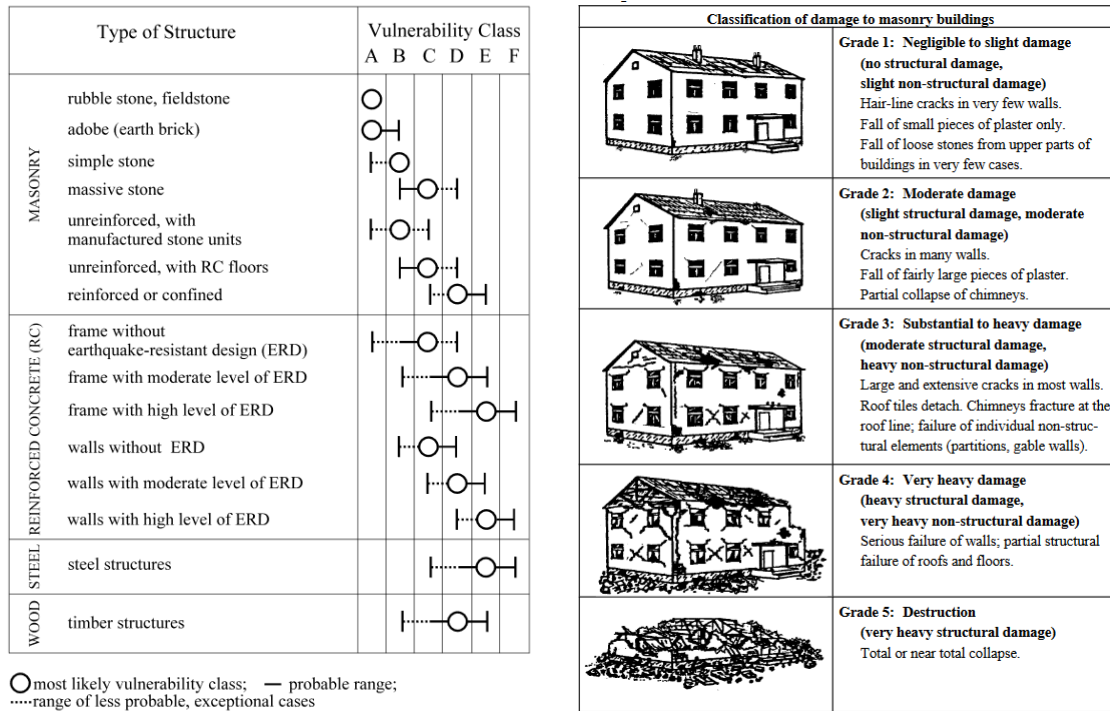
Figure 2-3. European Macroseismic Scale-1998 (Grunthal et al., 1998); Left: Vulnerability Table; Right: Damage Scale for masonry buildings.

The choice of the damage scale is fundamental for the definition of the fragility function and different classifications are made during the past years. The fragility function set is described according to different limit states that define the threshold between different damage conditions; generally a correlation between damage level and limit state is provided. For example, if the performance of a building is described by two limit states, there will be three damage states, as illustrated in Figure 2-4.
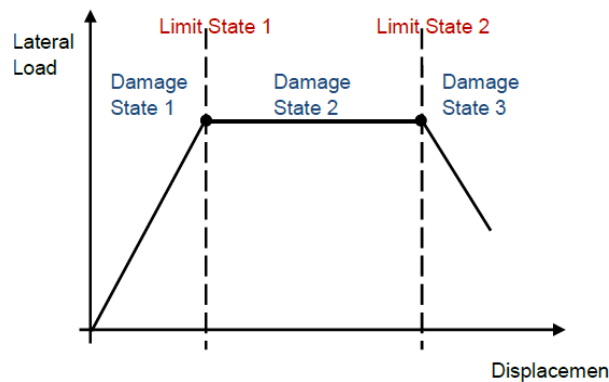
Figure 2-4. Correlation between damage levels and limit states (Pitilakis et al., 2014)

Other studies (Rossetto et al., 2014) stated that the damage scale should consist of at least three limit states and each of them is required to be defined in terms of structural and non-structural damage expected in different building classes.

However, the number of damage levels and consequently the number of limit states, depends on the damage scale used. An example of comparison is proposed by Rossetto and Elnashai (Rossetto and Elnashai, 2003) that represents a reinterpretation of heterogeneous observational data in terms of a new damage scale called Homogenised Reinforced Concrete (HRC). In Table 2-1 the main damage scales references are reported.

Table 2-1. Correlation of damage scales for ductile RC moment resisting frame (Rossetto and Elnashai , 2003)

Damage Index HRC	HRC	HAZUS 1999 (FEMA, 2003)	FEMA 273 (FEMA 273, 1997)	EMS-98 (Grünthal et al.1998)	MSK (Medvev and Sponheuer, 1969)
0	None	No damage			
10	Slight	Slight damage	Immediate Occupancy	Grade 1	D1
20	Light				
30				Grade 2	D2
40			Damage Control		
50	Moderate	Moderate damage		Grade 3	D3
60			Life Safe		
70					
80	Extensive	Extensive damage	Limited Safety	Grade 4	D4
90					
100	Partial Collapse		Collapse Prevention		
	Collapse	Collapse			

The empirical methods can be grouped in the three main categories:

- Damage Probability matrix (DPM)

  This method is based on site observation and expresses the conditional probability that a damage level is attained given a seismic intensity in a discrete form. Their main use is the probabilistic prediction of damage levels on buildings. Indeed, this method is based on damage data of past earthquakes and it considers the correlation between the seismic intensity, between the material, and between construction methods of different seismic regions.

  Therefore, each matrix is applied to a particular type of structure and particular design strategy, giving the probability of damage levels as a result from earthquakes of various intensities.

However, the main limitations of this approach are the discrete definition of the damage and its limited applicability due to the strong dependence to the seismic area and geographical and architectural context. Therefore, the matrixes are not valid for different areas and buildings due to the absence of direct damage data.

The main hypothesis on this method is the same structural features and same seismic response of the structures. It follows that these groups of buildings have the same damage probability, as Whitman presented after the S. Fernando earthquake in California (Whitman, 1973). This condition implies that the DPMs have to be retested for a new case study. Moreover, another issue could be the heterogeneity of the building district, formed by different building typologies. A large epistemic uncertainty will be collected in this case due the inability of taking into account the variety of geometric features of the heterogeneous buildings.

This method was widely used in the past for different applications. An example is the study of Braga in 1982 after the Irpinia Earthquake (Braga et al., 1982) that proposed a statistical study on damage building using the MSK-76 scale. Also after Friuli earthquake, a conceptual frame for a large scale evaluation of the seismic vulnerability of building by using the DPM was proposed. A methodology for forecasting the vulnerability of residential buildings in three seismic zones of Veneto-Friuli region is shown, classifying them into vulnerability classes according to the macroseismic scale of EMS98 (Bernardini et al., 2008). Dolce et al. proposed a damage scenarios relevant to the building stock of the town of Potenza, in south Italy where the vulnerability evaluation is made by using the DPM's of four classes of vulnerability ranging from high (class A) to low (class D) class according to the EMS-98 (Dolce et al., 2003).

Nowadays, this approach is widely used especially in regions with extensive seismicity records; for example it is presented a prediction of potential seismic damage to low and mid-rise RC buildings in Turkey using the DPM approach (Askan and Yucemen, 2010).

- Vulnerability Index (VI)

This method assesses the seismic vulnerability of historic buildings by calculating a vulnerability index, using specific parameters that affect the seismic response of the building and making a weighted sum.

One of the first proposal of this method was made by Benedetti and Petrini, where they proposed an evaluation of the seismic vulnerability of isolated buildings (Benedetti and Petrini, 1984). The results obtained from this study allowed making a classification of the cultural heritage of a specific area according to a vulnerability scale. In particular, the procedure consists of giving to eleven geometrical and mechanical parameters specific of the buildings, one of the vulnerability class proposed by the EMS-98 (class A to D). Then, to each class corresponds a score, while to each parameter corresponds a weight that represents the influence of the parameter on the global vulnerability of the structure.

Finally, the vulnerability index is calculated as the sum of the scores, identified by the attribution to classes, multiplied by the respective weights.

Some example using the VI method have been developed over the years. For the city of Lisbon (Oliveira et al., 2005), a comparison of two methods for estimating the vulnerability of building stock is proposed; the first used a damage database of worldwide statistics of earthquakes occurred essentially in the 90', while the second assesses the vulnerability of a variety of construction types representing the different situations present in Lisbon. Another example is the study for historic centre of Faro where an analysis of the reason of damages, injuries and losses is presented based on statistical data. Then a comparison of different vulnerability methods base on the EMS-98 is illustrated (Oliveira et al., 2004).

Considering the VI method and comparing it with the DPM method, the main improvement is the definition of a continuous vulnerability function respect to a discrete function provided by the DPM.

- Continuous vulnerability curves

This approach defines continuous functions to express the vulnerability of a building or classes of buildings. It describes the probability of exceedance of a specific damage state given a seismic intensity. The reported damage of buildings is the observed damage over the past seismic events.

All the vulnerability functions have a value of dispersion for all damage states given a building class, in order to consider the uncertainties. Moreover, it is assumed that all the damage levels are correlated and one level can be derived from the others.

However, the main drawback of this approach is the possibility of having a lack of data: if for a case of study the damage data are partial, the applicability of this approach is limited. Indeed, this approach is considered robust only if a considerable database is furnished and if it is made by extensive data, useful to calibrate the curves and to correlate observed damage with the expected one.

In the first studies of the literature, most of the vulnerability curves were expressed in terms of discrete intensity level of seismic intensity scales, such as the MMI scale and later EMS. Then, the work of Spence et al. (Spence et al., 1992) showed a new scale named the Parameterless Scale of Intensity (PSI). The authors have been derived vulnerability functions by using this seismic intensity for different building types and then correlated them with the parameters of acceleration (Figure 2-5).
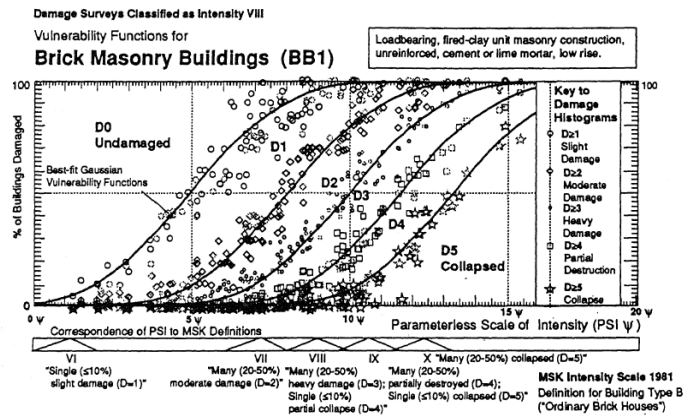
Figure 2-5. Vulnerability functions for damage levels (D1 to D5) for unreinforced brick masonry buildings (Spence et al., 1992) and comparison with other seismic intensities

Other studies based on the PSI intensity measure were made also in Italy after Irpinia earthquake (Orsini, 1999), where the Italian Government promoted a deep damage survey. These data have been elaborated and a damage prediction model has been developed and compared with the DPM.

In literature, many studies have been made using vulnerability empirical functions on different type of buildings such as churches, monumental buildings, aggregate buildings, RC structures and masonry structures. In particular, the protection of cultural heritage above all is a topic of high importance in Italy, given the large number of historical constructions characterized by the high architectural and cultural value.

The state of the art of empirical approach for churches is deeply analysed during years due to the importance and complexity of these structures. The problem of seismic vulnerability assumes particular significance when the historical and architectonic heritage is concerned. The main reasons are the structural elements and geometric proportions of these buildings; the need of building conservation and their artistic value.

However, these structures highlight common features after different seismic events in almost 20 years.

Indeed, Doglioni in 1994 (Doglioni et al., 1994) showed these recurrent features, called macroelements, in the seismic response of churches after Friuli earthquake in 1976. This approach allows an effective qualitative interpretation for churches and demonstrate that the structural behaviour is almost autonomous for each macroelement (façade, bell tower, side chapels, apse..).

Lagomarsino and Podestà proposed a deep investigation on churches vulnerability empirical function after Umbria Marche 1997 earthquake (Lagomarsino and Podestà in 2004a). In the first part of the work, they described a new methodology to assess the seismic damage focusing on macroelements, to identify damage modes and collapse mechanisms and to get then a damage score from these data. Later, the authors proposed the new methodology for the vulnerability analysis based on the DPM approach. Moreover, they provided a definition of the vulnerability curves as a function of the macroseismic intensity by considering the VI of each church.

The DPM method consists of the subdivision of buildings belonging to a certain typology into classes of comparable vulnerability on the basis of structural and architectonic characteristics. In this work, it was useful

19

to estimate the global level of damage in the churches, by considering the damage score, with the goal to define a mean expected damage for classes of churches after specific seismic events. The damage score, continuous index from 0 to 1, was transformed in a discrete one, using the six levels of damage of the EMS-98 scale. The statistical analysis of the global damage (expressed by the global damage index), performed by computing the DPM for churches, follows the binomial distribution proposed by Braga et al. (Braga et al, 1982). The following binomial expression represents the probability mass function of the binomial distribution p_k with damage levels defined by k=0,..,5:

$$p_k = \frac{5!}{k!(5-k)!}\left(\frac{\mu_D}{5}\right)^k\left(1-\frac{\mu_D}{5}\right)^{1-k} \tag{2.2}$$

and it is described by the mean damage for each intensity measure by the expression:

$$\mu_D = 2.5\cdot\left[1+\tanh\left(\frac{I+3.4375\cdot i_v-8.9125}{3}\right)\right] \tag{2.3}$$

where *tanh* is the iperbolic tangent and i_v is the vulnerability score directly obtained from the survey form(Lagomarsino and Podestà, 2004b). The work compared the obtained vulnerability curve with massive stone vulnerability curves, confirming the highest vulnerability of churches respect other building. Finally, it proposed the fragility curves for churches for all damage grades.

From this study, the same approach has been used also after the same seismic event of Umbria-Marche 1997 (Lagomarsino, 2006).

After Molise earthquake of 2002, Lagomarsino and Podestà in 2004 (Lagomarsino and Podestà, 2004c) presented the results of an extensive survey of churches' damage useful for understanding the complex seismic response of churches and for building the DPM referred to 586 monumental buildings, including 296 churches. In 2009, another seismic event struck the Abruzzo Region and many teams surveyed historical monuments, collecting damage data and proving the high vulnerability of cultural heritage, with particular reference to churches. The approach developed after the Umbria Marche earthquake, started to be widely used from L'Aquila earthquake, understanding its importance in the seismic prevention and identifying the most vulnerable structures. In the Lagomarsino's work of 2012 (Lagomarsino, 2012), an assessment of the damage on more than 700 churches was carried out, recognizing the collapse mechanisms in different architectonic elements of the churches. It is highlighted the importance of the prior knowledge of the construction types and transformations sequence conducted by the church. These data are then compared with vulnerability curves from literature using damage observed data after Italian earthquake of the last 50 years. Da Porto et al., (Da Porto et al., 2012) presented a statistical study on the information collected after L'Aquila earthquake, evaluating the damage and the seismic effects on several churches. In particular, the work showed that the

damage index and the safety of the structures are not directly related to distance from the epicentre. Moreover, the relative percentage of activation of the churches mechanisms are evaluated and investigations on the seismic vulnerability of structural and non-structural elements of churches are analysed in order to define hierarchy of interventions. Another campaign has been carried out after the same seismic events in 2009 in the study of De Matteis (De Matteis et al., 2014). A detailed investigation on three nave churches is presented, defining the local and global level of damage and the DPM. Then, a predictive model obtained according to the methodology given by the Italian Guidelines for Cultural heritage is proposed, in order to build the fragility functions using the macroseismic scale as intensity measure.

A deep analysis and assessment of the seismic vulnerability of three nave churches after L'Aquila earthquake is also proposed. Typological, structural and architectural features have been classified, and the main failure mechanisms with the damage related to the local mechanisms have been detected (De Matteis et al., 2016). In other studies, the aim was to calibrate a procedure for assessing a vulnerability index of the same types of churches (three nave) and define suitable fragility curves (De Matteis et al., 2019a; De Matteis et al., 2019b, De Matteis et al., 2019c).

The Emilia earthquake in 2012 hit the Emilia-Romagna Region and surroundings, and several cultural heritage structures collapsed or were severely damaged. Some works were focused on the collection of data of observed damage and diagnostics experimental campaigns on construction materials were conducted, together with structural dynamic characterizations and numerical analyses (Indirli et al., 2012). In other works, the observed damage has been analysed by means of the local collapse mechanism approach, highlighting that the damage is often concentrated at the top section of the façade, in the clerestory walls, in the vaults and in the bell towers (Sorrentino et al., 2014). In addition, the building safety assessments were carried out and the most vulnerable structural and non-structural elements of the Emilia and Veneto churches have been determined (Taffarel et al., 2016).

Numerous studies have been made after the Central Italy seismic sequence in 2016, due to the strong sequence that caused several damages to the structures, and in particular to the cultural heritage.

The majority of the works started with a data collection process to carry out a damage evaluation. This collection of data is accomplished by compiling in situ the II level survey during the post-earthquake survey activities. The detection of the most common failure mechanisms for the main macroelements is implemented, classifying such mechanisms according with their severity and estimating the damage index. This classification allowed to compute the DPM for different values of macroseismic intensities (Casapulla et al., 2017; Salzano et al., 2019).

In some works, the effectiveness of past retrofitting interventions and the damage progression due to cumulated effect of shaking was monitored (Penna et al., 2019). In other studies, a simplified method that evaluates separately hazard and vulnerability is proposed, giving a quick screening of intervention priorities and a possible comparison with seismic risk evaluation performed in different geographical area (Fabbrocino et al., 2019).

Other works (Hofer et al., 2018, Carbonari et al., 2019; De Matteis and Zizi, 2019) provided the empirical fragility functions calibrated on the basis of the global damage index and using as seismic intensity the Peak Ground Acceleration (PGA). At the same time, in the work of Cescatti (Cescatti et al., 2020) a deep typological description of the inspected churches, an evaluation of the input action and an analysis of the various literature correlations between PGA and macroseismic intensities are performed. The results were very useful in the risk analysis at regional level and provided applicable insights for the seismic vulnerability assessment obtained by using an empirical approach.

The empirical approach is well used also for other buildings of the cultural heritage such as historical masonry buildings, monumental buildings, and aggregates.

Moreover, the seismic vulnerability that characterizes the architectural heritage requires the applicability of method at urban level. A particular study at territorial level was made for the buildings belonging to the Italian rationalism architectural movement. In particular, RC buildings belonging to the architectural heritage have been analysed starting from a vulnerability model based on the EMS-98, providing new scores assigned to the parameters identified (Podestà and Romano, 2014).

Deep studies for the seismic vulnerability assessment of historic centre are presented, providing analysis of the structural damage at urban level with homogenous building characteristics after L'Aquila earthquake. The preliminary evaluation of these studies were about the structural VI approach modified by physical indicators that could affect the seismic response of the buildings. Moreover, the method collected data that could oriented the decision making process for seismic risk mitigation policies (Brando et al., 2017). Useful information on the most effective anti-seismic strategies to be implemented at urban scale with the support of GIS representations are presented (Rapone et al., 2018). Fragility curves and sensitivity analysis have been developed, in order to highlight the discrepancies due to the uncertainties in the methodology (Rapone et al., 2015). Nevertheless, also other types of structures such as traditional masonry construction, RC and stone buildings structures were studied in literature in the field of empirical vulnerability approach at territorial level. An example is the proposal of the macroseismic approach for the vulnerability assessment of urban area, considering a distinction between rating and typological method. In particular, the use of fuzzy set theory (Dubois et al., 1980) helped to solve the issue of the vagueness of the qualitative definition of the EMS-98 vulnerability scale (Figure 2-6).
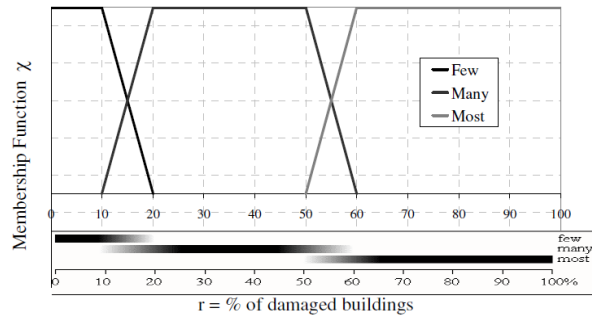
Figure 2-6: Percentage ranges and membership functions χ of the quantitative terms Few Many Most (Lagomarsino and Giovinazzi 2004)

The membership function X, visible from Figure 2-6, defines the belonging of a parameter to a specific set from 1 to 0 where 1 means plausible value and 0 a value not belong to set. Then the DPM are evaluated considering the vulnerability scale proposed by the EMS-98 scale, and finally the vulnerability classes are drawn for different type of buildings (Giovinazzi and Lagomarsino, 2004; Bernardini et al., 2007). A deep study on the buildings types of several municipalities has been conducted, investigating the seismic behaviour of ordinary masonry buildings and the performance of modern buildings after studies on the historical seismicity of the area and on the construction standards (Sorrentino et al., 2019).

Another form used to collect data of ordinary buildings and to evaluate the seismic risk, is the AEDES form. Many works have been used this form to provide empirical vulnerability functions. In particular, some works were more focused on the descriptions of the procedures of the form, in order to get the empirical damage and vulnerability distribution, highlighting the role of several vulnerability factors and analysed the usability outcomes (Dolce and Goretti, 2015). Other works developed a Web-Gis platform named Da.D.O. (Observed Damage Database) in order to store and share data from past-earthquakes surveys, inserting data from AEDES form (Dolce et al., 2019).

The data collected in the AEDES form have been used also to develop fragility functions for ordinary masonry (Rosti et al., 2019a) and RC buildings (Del Gaudio et al., 2019) and classifying the fragility curves for classes of vulnerability. Moreover, the results of these works have been used to carry out the National Italian risk platform, in order to evaluate seismic risk at territorial level for specific consequences such as collapses, or number of evacuated people (Rosti et al., 2019b).

The impact of the field of risk assessment is well known all over the world and in particular, the use of empirical vulnerability approach. Indeed, the Italian form has been widely used also worldwide due to the large amount of literature on the topic. An example is the vulnerability assessment for unreinforced masonry churches located in New Zealand, hit by the Canterbury earthquake sequence 2010–2011, based on the Italian macroelements approach. In some studies, the macroelements were considered in a separate way or as the seismic damage mode they might developed (Lagomarsino et al., 2019). In other works, the authors compared the seismic performance of these churches with the structural classification used in Italy (Leite et al., 2013).

Another study developed a contribution to the seismic vulnerability mitigation at territorial scale, using regression models and correlating mean damage level with macroseismic intensity for all observed mechanisms (Marotta et al., 2016). With the same approach of correlation, the vulnerability of churches is assessed after the Colima Mexico earthquake by qualitative method (Preciado and Orduña, 2014). The most significant types of damage and the activated mechanisms sustained by unreinforced stone masonry structures hit by the Azores Island earthquake were studied (Guerriero et al., 2000).

Also other types of existing buildings have been analysed using the empirical approach presented by the Italian methodology. In particular, an extensive survey on the historic centre of Cusco, Perù has been provided, implementing an empirical model from Italian studies. Also the fragility curves have been developed to reduce the potential seismic vulnerability by applying proper retrofitting intervention at territorial scale (Brando et al., 2019). The same approach was used in the assessment of the seismic vulnerability of existing buildings in Europe. In particular, the central region of Portugal was chosen as case study in which the index based seismic vulnerability assessment method has been used (Blyth et al., 2020). After the Murcia earthquake in 2011, an overview of the damage with the analysis of the performance of the construction both historical and recent, was addressed (Romão et al., 2013).

2.2 Analytical Vulnerability Functions

To define the seismic performance of class of buildings typologies, the analytical vulnerability function is an alternative to the empirical approach. The analytical vulnerability function is a method slightly more detailed than the empirical one, that allows a calibration to various features of building classes and sensitivity studies could be taken, with the aim of define retrofitting, risk mitigation policies and urban planning. Moreover, it has the advantage of framing the seismic vulnerability problem in structural engineering terms, directly connected to the structural behaviour of constructions.

Some studies have been published as guidelines useful for performing earthquake loss estimation that represent comprehensive technical collection of methods and data (FEMA 2001; FEMA 2003). In these technical manuals, that want to associate to each building typologies a capacity curve, the overall approach and the framework of the methodology with its components is well described, as presented in Figure 2-7. The methodology includes standard approaches for:

- Inventory data collection

- Using database maps of soil type, ground motion

- Classifying occupancy of buildings

- Classifying building structure type

- Describing damage states

- Developing building damage functions

- Grouping, ranking and analysing lifelines

- Using technical terminology

- Providing output.
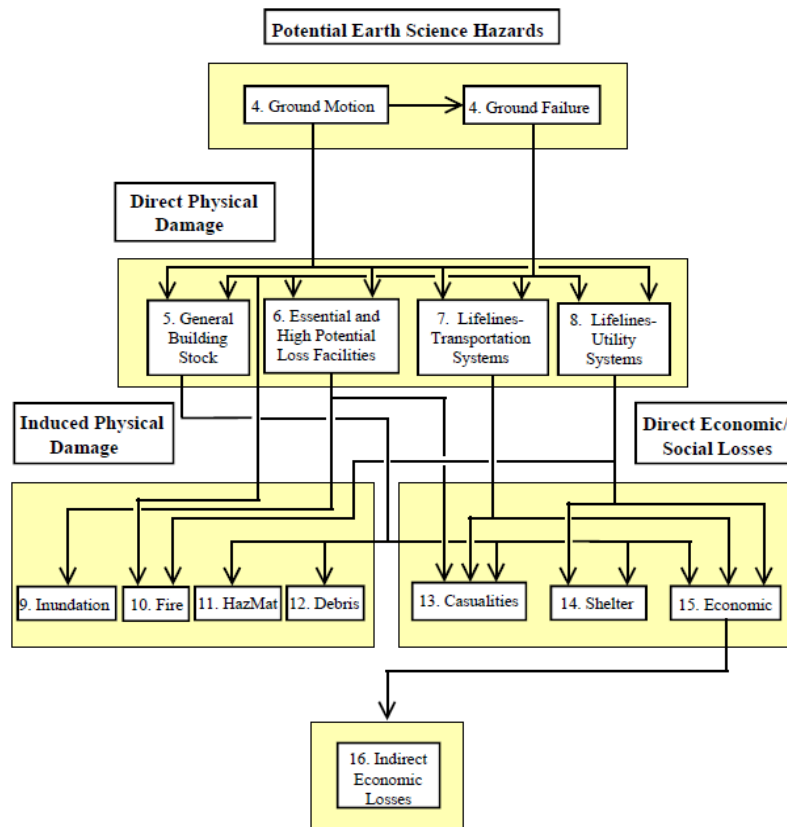
Figure 2-7: Flowchart of the earthquake loss estimation methodology (FEMA 2003)

Another project that involves the earthquake scenario assessment at city scale within the European context is the RISK-UE Project (RISK-UE, 2001), where two levels of approaches have been proposed. The first concerned the macroseismic methods, while the second concerns the mechanical method that it is based on capacity and fragility models. In that project, the damage assessment became a crucial step and for an individual building or building group allows to estimate the expected seismic losses based on detailed evaluation of the vulnerability features of the building/building group at a given level of seismic intensity (Figure 2-8).

Risk-UE Building Typology Matrix			
Number	Label	Description	Name
1	M11L		Low-Rise
2	M11M		Mid-Rise
3	M12L	Simple Stone	Low-Rise
4	M12M		Mid-Rise
5	M12H		High-Rise
6	M13L	Massive Stone	Low-Rise
7	M13M		Mid-Rise
8	M13H		High-Rise

Damage States
N = None; **Mi** = Minor; **Mo** = Moderate; **S** = Severe; **C** = Collapse
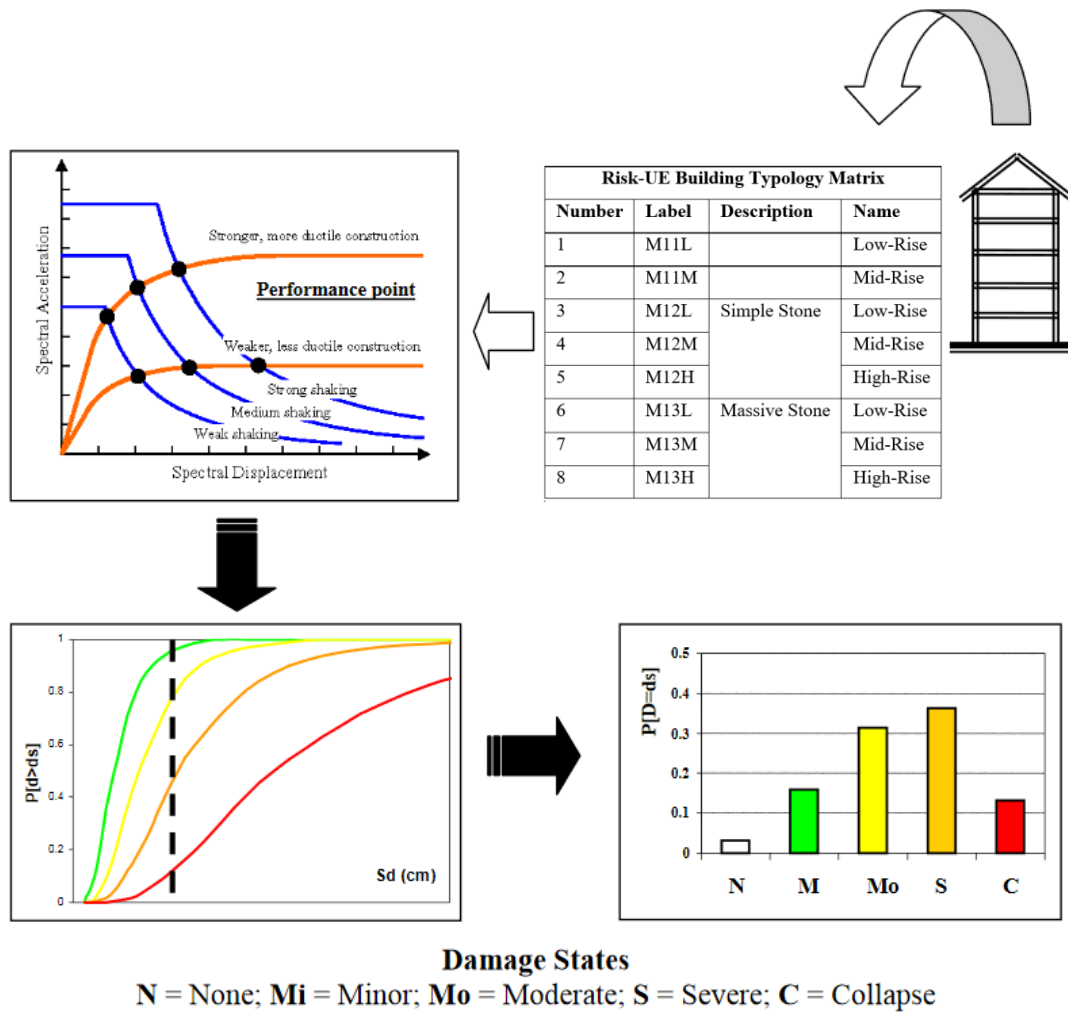
Figure 2-8: Damage Estimation Process (RISK-UE, 2001)

Applications of the Risk-UE project framework are proposed in literature. In particular, in the work of Lagomarsino and Giovinazzi (Lagomarsino and Giovinazzi, 2006) two vulnerability models have been proposed with different hazard but with the same building typologies classification representative of the European built up environment: a macroseismic model, a mechanical based model and subsequently cross-validation is proposed. Another example is the case of Barcelona, Spain, a city located in a low to moderate seismic hazard region, where the capacity spectrum based method developed in the framework of the European project Risk-UE has been applied to evaluate the seismic risk for that city. Starting from a deep description of the hazard and a collection of data for the buildings of the city, the capacity spectrum based method is applied, in order to develop fragility curves and DPMs for six building classes and for four city areas. The results of this study, allowed providing scenarios of expected losses (Irizarry et al., 2011).

Other studies at territorial scale used the analytical approach in comparison with the empirical method, especially when a large number of data of urban area are present and when it is required a validation between results of the two approaches. In particular, some studies (Lagomarsino et al., 2004; Lagomarsino 2006)

26

displayed methods with different level of detail, depending on the information available. It started with a general estimation of the vulnerability of monumental heritage after quick survey; then the capacity curves furnished a more useful data in case of damage prevention plan. Finally, simulations on macroelements of monumental buildings or directly on the entire building are developed in order to get results comparable with other monuments and to develop a damage scenario. Another example is the study that showed the limits of the comparison between the empirical vulnerability with the mechanics-based vulnerability curves, highlighting the difficulties found, and showing that a valid comparison is not possible mainly due to a number of drawbacks in the database of the observed buildings (Colombi et al., 2008).

Buildings in historical city are particularly vulnerable to seismic events, so it is important to assess the seismic vulnerability considering the geometric, structural features and deficiencies, which have an impact on seismic failures modes. In the development of analytical fragility functions for masonry structures, two approaches are identified, that correlate different elements:

- Damage levels to the vulnerability index for example the mechanical methods VULNUS (Bernardini et al., 1990) and FaMIVE (D'Ayala and Speranza, 2003).
  Both mechanical methods are based on grouping of masonry buildings in different vulnerability classes, and their use produce damage scenarios through fragility curves.

- Spectral demand curves to acceleration/displacement capacity curves (capacity spectrum based method), such as HAZUS-MH (FEMA 2001; FEMA 2003), nonlinear time history analysis (Jalayer and Cornell, 2009), N2 method (Fajfar, 2000), where the seismic performance of buildings is estimated by comparing seismic demand and seismic capacity directly in the acceleration-displacement response spectra. The Hazus framework, already discussed previously in this chapter, is classified as capacity spectrum based method and provide fragility curves assuming lognormal distribution of available data. The Non Linear Time History analysis are considered a very accurate method for predicting building response to ground motion, but at territorial level these analysis are a time consuming methodology.

The peculiarities of these procedures are the link between the damage levels and fragility curves with the demand parameters, which are generally expressed in terms of drift or displacement. The fragility curves are referred to engineering demand parameters, derived from the capacity curves, and also to the ground motion intensity parameters for a given building or group buildings type.

Other studies on the masonry buildings or old buildings using the approaches described above, are provided. To characterize classes of building to assess the risk, capacity curves are defined for masonry buildings of the European and Mediterranean regions, and constant-ductility inelastic spectra are adopted for the demand spectrum (Cattari et al., 2004). Also for the Italian historic centres, procedures aimed at the evaluation of

seismic vulnerability of masonry historic buildings are provided. In particular, an example is the case study of the historic centre of Marche region where the approach is based on a failure analysis of structures, identifying the probable collapse mechanisms and calculating their load factors (D'Ayala and Speranza 2002). Another case is the unreinforced masonry buildings of the city of Benevento, where a new procedure for the seismic risk assessment at territorial scale is developed. This procedure is based on four features: (i) the structural capacity and response that are identified in terms of mechanics concepts; (ii) the demand, represented by a displacement response spectrum; (iii) the inclusion of sources of uncertainty, and the (iv) consideration of failure mechanisms in particular the in-plane and out-of-plane mechanisms (Restrepo-Vélez and Magenes, 2004).

Another application concerns the case of the Casbah of Algiers, a world heritage site formed by buildings from the Ottoman to the French period. A total number of around 150 houses have been selected and the seismic vulnerability assessment was evaluated through the FaMIVE approach, which allows computing collapse load factor, deriving capacity curves and determining fragility functions. Therefore, there are evaluated the effects of strengthening interventions at territorial level in order to improve the seismic performance of the whole sample (Novelli et al., 2015). The case of building stock of the neighborhood in Lisbon assessed the seismic vulnerability and the risk analysis for three frequent buildings typologies in Portugal. Equivalent frame method was used to model reference buildings for each typology and pushover analysis was performed to derive the vulnerability features of the reference buildings but also to more general buildings (Lamego et al., 2017).

A work that has a conceptual nature merit is the one of Calvi, which wants to apply a unique approach to evaluate the response and the vulnerability of buildings for different levels of knowledge and refinement in analysis and modelling. The work is based on the evaluation of displacement capacity of different kind of buildings (masonry and RC), and when very poor data are provided, only an expected damage scenario is yielded but not the collapse modes. By increasing the level of refinement and knowledge, more detailed structural models can be developed by applied the same principles and obtained more reliable results (Calvi 1999). Another proposal of a probabilistic framework using a probabilistic displacement-based vulnerability assessment procedure is illustrated, bringing the method closer to practical application. Indeed, this procedure used mechanically derived formula in terms of material and geometrical properties to describe the displacement capacity of classes of buildings considering three different limit states. The original concept of the approach is displayed in Figure 2-9, proposed first by Pinho et al. and then developed by Glaister and Pinho (Pinho et al., 2002; Glaister and Pinho 2003). In the proposal the range of periods are obtained and transformed into a range of heights using the relationship between limit state period and height, then superimposed into the CDF of building stock to find the buildings failing in the given limit state.
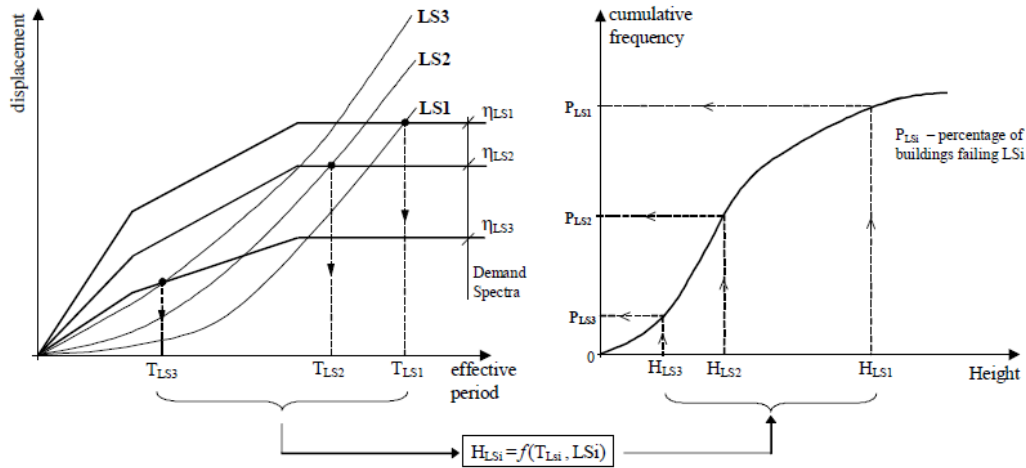
Figure 2-9: Deformation-based seismic vulnerability procedure (Glaister and Pinho, 2003)

In summary, in this study for the first time have been derived non-structural displacement capacity formulae, at different limit states, considering the influence of infill panels on the displacement capacity of RC structures, the shear deformation capacity of non-flexure controlled members, and the inclusion of the displacement capacity formulae for dual-system structures and for RC wall. Another consideration of this work is the inclusion of the uncertainty in the fully probabilistic framework. The main evidence is that the presented procedure is suitable for loss estimation studies due to its theoretical accuracy and computational efficiency (Crowley et al., 2004).

Another example based on the same displacement-based approach to estimate the losses, is applied to a test case of buildings along the northern side of the Sea of Marmara in Turkey. In this work, the main focus is on the treatment of the uncertainties. In particular, systematic variations of the parameters related to the demand and to the capacity are used in order to identify the impact of the losses. As a result, the capacity parameters related to the vulnerabilities such as the geometrical properties, have a higher impact on the resulting losses respect to the demand for a single earthquake scenario (Crowley et al., 2005).

Studies at large scale for RC buildings are also made by using analytical approaches. An example is the work based on representative building types widely present in the Italian building stock of the last 50 years. The seismic response, of some frame structures, typical of existing RC buildings designed only to vertical loads is calculated using non linear dynamic analyses with artificial and natural accelerograms. Three main typologies of RC buildings have been examined: bare frames, regularly infilled frames and pilotis frames, showing a high vulnerability for the pilotis buildings (Masi, 2003). Another procedure is proposed for the derivation of analytical displacement-based vulnerability curves for the seismic assessment of RC buildings stock, in particular applied to low-rise, infilled RC frames with inadequate seismic provisions. Pushover analysis is adapted within a capacity spectrum framework assessment. The building model group is generated from a

single design experiment techniques used to optimize the population size and considering material parameter uncertainty (Rossetto and Elnashai, 2005).

The rational mechanical based approach proposed by Cosenza et al. wanted to highlight the dispersion of the results with the knowledge level of the building environment (Cosenza et al., 2005). The examined case study was the town district in Campania region formed by RC frame structures built in the 1960, classified in terms of number of stories and construction year. The capacity curves are derived in terms of ultimate strength and deformation capacities.

A systematic approach is proposed to develop damage-motion relationships based on nonlinear dynamic analysis of the structure rather than on heuristics or on empirical data. The probability of having a damaged structure is estimated by a Monte Carlo-simulation approach, in order to obtain fragility curves and damage probability matrices for RC frames. The non linear properties of the structure have been considered in these fragility curves and DPM. Therefore, they represented a set of fragility curves that can be used for estimating damage states for a large range of RC frames, and the estimated damage can be used for a cost-benefits analysis in terms of retrofitting and potential losses (Singhal and Kiremidjian, 1996). Another example that used the Monte Carlo simulation technique concerned the RC buildings stock on a high seismic area in Southern Italy. In this work, it is considered the presence of infills, taking into account their influence on the structural response but also evaluating the damage to such non-structural elements. Using the Monte Carlo simulation technique, material characteristics, capacity models and uncertainties in the seismic demand are taken into account. Finally, fragility curves are obtained and the key parameters that influenced the seismic fragility was illustrated. A comparison with empirical-based fragility curves from literature was also shown (Del Gaudio et al., 2015).

A last work useful for this Thesis are the guidelines named SYNER-G (Pitilakis et al., 2014a; Pitilakis et al., 2014b). In this project an innovative methodological framework for the assessment of physical and socio-economic seismic vulnerability to assess the seismic risk at the urban/regional level was proposed. The built environment was modelled according to a refined taxonomy and grouped into categories such as buildings, transportation and utility networks, and critical facilities, where each category have several types of components and systems. The proposed framework took into account all aspects of the chain, from hazard to the vulnerability assessment of components and systems, and also the socio-economic impacts of a seismic event, accounting for uncertainties and modelling interactions between the components of the system. The objective of this guide is to propose the most appropriate fragility function for the building typologies in Europe. To do that, a collection of the fragility function from literature was made, reviewed and validated. Several approaches have been used to establish the fragility curves, grouped under empirical, judgmental, analytical and hybrid criteria.

In this study also an harmonization was tackled, due to different parameters for intensity measure, different number of limit states and different building typologies. Indeed, in the reviewed papers collected from

literature to develop the fragility functions, different types of intensity measure have been used to describe the level of ground shaking but also different number of limit states have been adopted. Thus, in order to compare the fragility functions selected by the state of the art, an essential step is the harmonization. Three different steps have been followed in this process:

1. Harmonization of the intensity measure types: all the intensity measure types have been converted into PGA due to the facility with which it can be used in seismic risk assessment,

2. Harmonization of limit states: a different number of limit states were found in accordance with the damage scale used in the literature reviewed. The choice in that study was to use two limit states, considering it as the simplest way of harmonizing the limit states for a large number of fragility functions, since the majority of fragility functions already have these two thresholds (yielding and collapse).

3. Harmonization of the building typology: a taxonomy has been assigned to all of the collected fragility functions. However, a reduced number of attributes has been used for the purposes of comparing fragility functions, due to the different taxonomical descriptions adopted when deriving fragility functions in Europe

After these important steps, the most appropriate fragility functions are proposed for buildings, lifelines, transportation infrastructures and critical facilities. Figure 2-10 presents an example to illustrate the building typologies for which fragility functions of RC can be compared. The guidelines developed also a software tool for the storage, harmonization and estimation of the uncertainty of fragility functions.
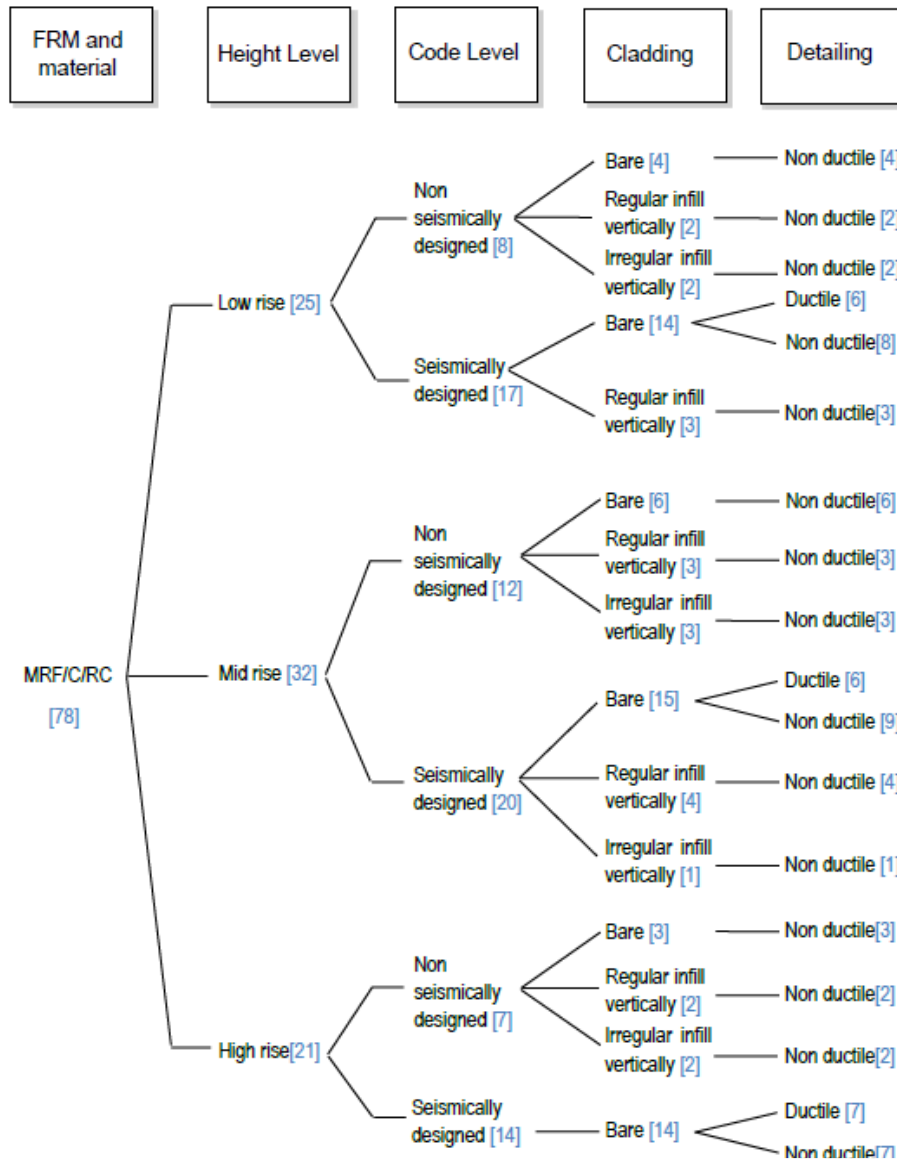
Figure 2-10: Example of a flow chart of a building type, with the indication of different attributes in column, and the number of available fragility functions in blue brackets (Pitilakis et al., 2014b)

Chapter's references

Askan, A., Yucemen, M., 2010. Probabilistic methods for the estimation of potential seismic damage: Application to reinforced concrete buildings in Turkey. Structural Safety 32, 262–271. https://doi.org/10.1016/j.strusafe.2010.04.001

Benedetti, D., Petrini, V., 1984. Sulla Vulnerabilità Di Edifici in Muratura: Proposta Di Un Metodo Di Valutazione 149, 66–74.

Bernardini, A., Giovinazzi, S., Lagomarsino, S., Parodi, S., 2007. The vulnerability assessment of current buildings by a macroseismic approach derived from the EMS-98 scale.

Bernardini, A., Gori, R., Modena, C., 1990. An application of coupled analytical models and experiential knowledge for seismic vulnerability analyses of masonry buildings. 3, 161–180.

Bernardini, A., Salmaso, L., Solari, A., 2008. Statistical evaluation of vulnerability and expected seismic damage of residential buildings in the Veneto-Friuli area (NE Italy) Bollettino di Geofisica Teorica ed Applicata, Vol. 49, 427–446.

Blyth, A., Napoli, B., Parisse, F., Namourah, Z., Anglade, E., Giatreli, A.-M., Rodrigues, H., Ferreira, T., 2020. Assessment and mitigation of seismic risk at the urban scale: an application to the historic city center of Leiria, Portugal. Bulletin of Earthquake Engineering. https://doi.org/10.1007/s10518-020-00795-2

Bradley, B.A., Dhakal, R.P., Cubrinovski, M., MacRae, G.A., Lee, D.S., 2008. Seismic loss estimation for efficient decision making. BNZSEE 42, 96–110. https://doi.org/10.5459/bnzsee.42.2.96-110

Braga, F., Dolce, M., Liberatore, D., 1982. A statistical study on damaged buildings and an ensuing review of the MSK-76 scale. Presented at the Proceedings of the 7th European Conference on Earthquake Engineering, Athens, pp. 431–450.

Brando, G., Cocco, G., Mazzanti, C., Peruch, M., Spacone, E., Alfaro, C., Sovero, K., Tarque, N., 2019. Structural Survey and Empirical Seismic Vulnerability Assessment of Dwellings in the Historical Centre of Cusco, Peru. International Journal of Architectural Heritage 0, 1–29. https://doi.org/10.1080/15583058.2019.1685022

Brando, G., De Matteis, G., Spacone, E., 2017. Predictive model for the seismic vulnerability assessment of small historic centres: Application to the inner Abruzzi Region in Italy. Engineering Structures 153, 81–96. https://doi.org/10.1016/j.engstruct.2017.10.013

Calvi, G., Pinho, R., Magenes, G., Bommer, J., Restrepo-Vélez, L., Crowley, H., 2006. Development of seismic vulnerability assessment methodologies over the past 30 years. ISET Journal of Earthquake Technology 43.

Calvi, G.M., 1999. A Displacement-Based Approach for Vulnerability Evaluation of Classes of Buildings. Journal of Earthquake Engineering 3, 411–438. https://doi.org/10.1080/13632469909350353

Carbonari, S., Dall'Asta, A., Dezi, Gara, F., Leoni, G., Morici, M., Prota, Zona, A., 2019. First analysis of data concerning damage occurred to churches of the Marche region following the 2016 central Italy earthquakes. Bollettino di Geofisica Teorica ed Applicata 60, 183–196. https://doi.org/10.4430/bgta0271

Casapulla, C., Salzano, P., Sandoli, A., Argiento, L., Ceroni, F., Calderoni, B., Prota, A., 2017. Statistical Analysis of the Structural Damage to Churches affected by the 2016-17 Central Italy Earthquake Sequence - Analisi Statistica del Danno Strutturale Rilevato nelle Chiese Colpite dai Terremoti Centro Italia 2016-17.

Cattari, S., Curti, E., Giovinazzi, S., Lagomarsino, S., Parodi, S., Penna, A., 2004. Un modello meccanico per l'analisi di vulnerabilità del costruito in muratura a scala urbana. Presented at the XI Congresso Nazionale "L'ingegneria Sismica in Italia," Genova.

Cescatti, E., Salzano, P., Casapulla, C., Ceroni, F., da porto, F., Prota, A., 2020. Damages to masonry churches after 2016–2017 Central Italy seismic sequence and definition of fragility curves. Bulletin of Earthquake Engineering 18. https://doi.org/10.1007/s10518-019-00729-7

Colombi, M., Borzi, B., Crowley, H., Onida, M., Meroni, F., Pinho, R., 2008. Deriving vulnerability curves using Italian earthquake damage data. Bulletin of Earthquake Engineering 6. https://doi.org/10.1007/s10518-008-9073-6

Cosenza, E., Manfredi, G., Polese, M., Verderame, G.M., 2005. A multilevel approach to the capacity assessment of existing rc buildings. J. Earth. Eng. 09, 1–22. https://doi.org/10.1142/S1363246905001931

Crowley, H., Bommer, J.J., Pinho, R., Bird, J., 2005. The impact of epistemic uncertainty on an earthquake loss model. Earthquake Engineering & Structural Dynamics 34, 1653–1685. https://doi.org/10.1002/eqe.498

Crowley, H., Pinho, R., Bommer, J.J., 2004. A Probabilistic Displacement-based Vulnerability Assessment Procedure for Earthquake Loss Estimation. Bull Earthquake Eng 2, 173–219. https://doi.org/10.1007/s10518-004-2290-8

Da Porto, F., Silva, B., Costa, C., Modena, C., 2012. Macro-Scale Analysis of Damage to Churches after Earthquake in Abruzzo (Italy) on April 6, 2009. Journal of Earthquake Engineering 16, 739–758. https://doi.org/10.1080/13632469.2012.685207

D'Ayala, D., Speranza, E., 2003. Definition of Failure modes and Seismic Vulnerability of Historic Masonry Buildings. Earthquake Spectra 19, 479–509.

D'Ayala, D., Speranza, E., 2002. An Integrated Procedure for the Assessment of Seismic Vulnerability of Historic Buildings, in: Proceedings of the 12th European Conference on Earthquake Engineering.

De Matteis, G., Brando, G., Corlito, V., September 1, 2019a. Predictive model for seismic vulnerability assessment of churches based on the 2009 L'Aquila earthquake. Bulletin of Earthquake Engineering 17, 1–28. https://doi.org/10.1007/s10518-019-00656-7

De Matteis, G., Brando, G., Corlito, V., January 1, 2019b. Simplified Assessment of the Seismic Vulnerability of Churches After the 2009 L'Aquila Earthquake: An Interdisciplinary Approach. pp. 1280–1289. https://doi.org/10.1007/978-3-319-99441-3_137

De Matteis, G., Brando, G., Corlito, V., Criber, E., Guadagnuolo, M., January 1, 2019c. Seismic vulnerability assessment of churches at regional scale after the 2009 L'Aquila earthquake. International Journal of Masonry Research and Innovation 4, 174. https://doi.org/10.1504/IJMRI.2019.096824

De Matteis, G., Criber, E., Brando, G., 2016. Damage Probability Matrices for Three-Nave Masonry Churches in Abruzzi After the 2009 L'Aquila Earthquake. International Journal of Architectural Heritage 10, 120–145. https://doi.org/10.1080/15583058.2015.1113340

De Matteis, G., Criber, E., Brando, G., 2014. Damage evaluation on churches belonging to the sulmona-valva diocese after the 2009 L'Aquila earthquake.,. Presented at the Proceeding of the 2nd International Conference on Protection of Historical Constructions (PROHITECH 2014), Antalya, Turkey.

De Matteis, G., Zizi, M., 2019. Seismic Damage Prediction of Masonry Churches by a PGA-based Approach. International Journal of Architectural Heritage 13, 1165–1179. https://doi.org/10.1080/15583058.2019.1597215

Del Gaudio, C., Ricci, P., Verderame, G., Manfredi, G., 2015. Development and urban-scale application of a simplified method for seismic fragility assessment of RC buildings. Engineering Structures 91. https://doi.org/10.1016/j.engstruct.2015.01.031

Del Gaudio, C., Rosti, A., Rota, M., Ricci, P., Penna, A., Verderame, G., 2019. Derivazione di curve di fragilità empiriche per edifici residenziali italiani in c.a., in: ANIDIS 2019 - XVIII Convegno.

Doglioni, F., Moretti, A., Petrini, V., Angeletti, P., 1994. Le chiese e il terremoto. Dalla vulnerabilità constatata nel terremoto del Friuli al miglioramento antisismico nel restauro. Verso una politica di prevenzione., Lint Editoriale Associati. ed, 9788886179362.

Dolce, M., Goretti, A., 2015. Building damage assessment after the 2009 Abruzzi earthquake. Bull Earthquake Eng 13, 2241–2264. https://doi.org/10.1007/s10518-015-9723-4

Dolce, M., Masi, A., Marino, M., Vona, M., 2003. Earthquake Damage Scenarios of the Building Stock of Potenza (Southern Italy) Including Site Effects Bulletin of Earthquake Engineering, 115–140.

Dolce, M., Speranza, E., Giordano, F., Borzi, B., Bocchi, F., Conte, C., Di Meo, A., Faravelli, M., Pascale, V., 2019. Observed damage database of past Italian earthquakes: the Da.D.O. WebGIS. BGTA. https://doi.org/10.4430/bgta0254

Dubois, D., Prade, H., 1980. Fuzzy sets and systems: Theory and applications. New York.

European Commission, 2001. RISK-UE, An advanced approach to earthquake risk scenarios with applications to different european towns.

Fabbrocino, F., Vaiano, G., Formisano, A., D'Amato, M., 2019. Large-Scale Seismic Vulnerability and Risk of Masonry Churches in Seismic-Prone Areas: Two Territorial Case Studies. Front. Built Environ. 5. https://doi.org/10.3389/fbuil.2019.00102

Fajfar, P., 2000. A Nonlinear Analysis Method for Performance-Based Seismic Design. Earthquake Spectra 16, 573–592. https://doi.org/10.1193/1.1586128

FEMA, 2001. FEMA-HAZUS99 Estimated Annualized Earthquake Loss for the United States. FEMA P-366, Washington, DC, U.S.A.

FEMA, 1997. NEHRP Guidelines for seismic rehabilitation of buildings. FEMA 273, Federal Emergency Management Agency, Washington D.C.

FEMA "HAZUS-MH Technical Manual," 2003. Federal Emergency Management Agency,Washington, DC, U.S.A.

Giovinazzi, S., 2005. The vulnerability assessment and the damage scenario in seismic risk analysis. PhD thesis, Department of Civil Engineering of the Technical University Carolo-Wilhelmina at Braunschweig and the Faculty of Engineering Department of Civil Engineering of the University of Florence.

Giovinazzi, S., Lagomarsino, S., 2004. A Macroseismic Method for the Vulnerability Assessment of Buildings. Presented at the 13th World Conference on Earthquake Engineering, Vancouver, B.C., Canada, pp. 16, Paper No. 896.

Glaister, S., Pinho, R., 2003. Development of a simplified deformation-based method for seismic vulnerability assessment. Journal of Earthquake Engineering - J EARTHQU ENG 7, 107–140. https://doi.org/10.1080/13632460309350475

Grünthal, G., 1998. European macroseismic scale 1998 (EMS-98). Cahiers du Centre Européen de Géodynamique et de Séismologie.

Guerreiro, L., Azevedo, J., Proença, J., Bento, R., Lopes, M., 2000. Damage in ancient churches during the 9th of July 1998 Azores earthquake. Presented at the 12WCEE, p. 8.

Günay, S., Mosalam, K.M., 2013. PEER Performance-Based Earthquake Engineering Methodology, Revisited. Journal of Earthquake Engineering 17, 829–858. https://doi.org/10.1080/13632469.2013.787377

Hofer, L., Zampieri, P., Zanini, M., Faleschini, F., Pellegrino, C., 2018. Seismic damage survey and empirical fragility curves for churches after the August 24, 2016 Central Italy earthquake. Soil Dynamics and Earthquake Engineering 111. https://doi.org/10.1016/j.soildyn.2018.02.013

Indirli, M., Marghella, G., Marzo, A., 2012. Damage and collapse mechanisms in churches during the Pianura Padana Emiliana earthquake Energia Ambiente Innovazione, 26.

Irizarry Padilla, J., Lantada, N., Beneit, L., Barbat, A., Goula, X., Susagna, T., Roca, A., 2011. Ground-shaking scenarios and urban risk evaluation of Barcelona using the Risk-UE capacity spectrum based method. Bulletin of Earthquake Engineering 9, 441–466. https://doi.org/10.1007/s10518-010-9222-6

Jalayer, F., Cornell, C., 2009. Alternative non-linear demand estimation methods for probability-based seismic assessments. Earthquake Engineering & Structural Dynamics 38, 951–972. https://doi.org/10.1002/eqe.876

Kappos, A., Pitilakis, K., Stylianidis, K., Morfidis, K., Asimakopoulos, D., 1995. Cost – Benefit Analysis for the Seismic Rehabilitation of Buildings in Thessaloniki, Based on A Hybrid Method of Vulnerability Assessment.

Kappos, A.J., Panagopoulos, G., Panagiotopoulos, C., Penelis, G., 2006. A hybrid method for the vulnerability assessment of R/C and URM buildings. Bull Earthquake Eng 4, 391–413. https://doi.org/10.1007/s10518-006-9023-0

Kappos, A.J., Stylianidis, K.C., Pitilakis, K., 1998. Development of Seismic Risk Scenarios Based on a Hybrid Method of Vulnerability Assessment Natural Hazards 17, 177–192.

Lagomarsino, S., 2012. Damage assessment of churches after L'Aquila earthquake (2009). Bull Earthquake Eng 10, 73–92. https://doi.org/10.1007/s10518-011-9307-x

Lagomarsino, S., 2006. On the vulnerability assessment of monumental buildings. Bull Earthquake Eng 4, 445–463. https://doi.org/10.1007/s10518-006-9025-y

Lagomarsino, S., Cattari, S., Ottonelli, D., Giovinazzi, S., 2019. Earthquake damage assessment of masonry churches: proposal for rapid and detailed forms and derivation of empirical vulnerability curves. Bulletin of Earthquake Engineering 17. https://doi.org/10.1007/s10518-018-00542-8

Lagomarsino, S., Giovinazzi, S., 2006. Macroseismic and mechanical models for the vulnerability and damage assessment of current buildings. Bull Earthquake Eng 4, 415–443. https://doi.org/10.1007/s10518-006-9024-z

Lagomarsino, S., Podestà, S., July 1, 2004c. Damage and Vulnerability Assessment of Churches after the 2002 Molise, Italy, Earthquake. Earthquake Spectra - EARTHQ SPECTRA 20. https://doi.org/10.1193/1.1767161

Lagomarsino, S., Podestà, S., May 1, 2004a. Seismic Vulnerability of Ancient Churches: I. Damage Assessment and Emergency Planning. Earthquake Spectra 20, 377–394. https://doi.org/10.1193/1.1737735

Lagomarsino, S., Podestà, S., May 1, 2004b. Seismic Vulnerability of Ancient Churches: II. Statistical Analysis of Surveyed Data and Methods for Risk Analysis. Earthquake Spectra 20, 395–412. https://doi.org/10.1193/1.1737736

Lagomarsino, S., Podesta, S., Resemini, S., 2004. Observational and Mechanical Models for the Vulnerability Assessment of Monumental Buildings. Presented at the 13th World Conference on Earthquake Engineering, Vancouver, B.C., Canada, pp. 15, Paper No. 942.

Lamego, P., Lourenco, P., Sousa, M., Marques, R., 2017. Seismic vulnerability and risk analysis of the old building stock at urban scale: application to a neighbourhood in Lisbon. Bulletin of Earthquake Engineering 15, 2901–2937. https://doi.org/10.1007/s10518-016-0072-8

Leite, J., Lourenco, P.B., Ingham, J.M., 2013. Statistical Assessment of Damage to Churches Affected by the 2010–2011 Canterbury (New Zealand) Earthquake Sequence. Journal of Earthquake Engineering 17, 73–97. https://doi.org/10.1080/13632469.2012.713562

Marotta, A., Sorrentino, L., Liberatore, D., Ingham, J., 2016. Vulnerability Assessment of Unreinforced Masonry Churches Following the 2010–2011 Canterbury Earthquake Sequence. Journal of Earthquake Engineering 21. https://doi.org/10.1080/13632469.2016.1206761

Masi, A., 2003. Seismic Vulnerability Assessment of Gravity Load Designed R/C Frames. Bulletin of Earthquake Engineering 1, 371–395. https://doi.org/10.1023/B:BEEE.0000021426.31223.60

Medvev, S., Sponheuer, W., 1969. MSK Scale of seismic intensity. In:, ,. Presented at the Proceedings of the 4th World Conference on Earthquake Engineering: Chilean Association of Seismology and EarthquakeEngineering, Santiago, p. A2.

Novelli, V.I., D'Ayala, D., Makhloufi, N., Benouar, D., Zekagh, A., 2015. A procedure for the identification of the seismic vulnerability at territorial scale. Application to the Casbah of Algiers. Bull Earthquake Eng 13, 177–202. https://doi.org/10.1007/s10518-014-9666-1

Oliveira, C.S., Ferreira, M.A., de Sá, F.M., 2004. Seismic Vulnerability and Impact Analysis: Elements for Mitigation Policies 29.

Oliveira, C.S., Sá, F.M.D., Ferreira, M.A., 2005. Application of Two Different Vulnerability Methodologies to Assess Seismic Scenarios in Lisbon. Presented at the 250th anniversary of the 1755 Lisbon earthquake, p. 6.

Orsini, G., 1999. A model for buildings' vulnerability assessment using the parameterless scale of seismic intensity (PSI) Earthquake Spectra, 463–483.

Penna, A., Calderini, C., Sorrentino, L., Carocci, F., Cescatti, E., Sisti, R., Borri, A., Modena, C., Prota, A., 2019. Damage to churches in the 2016 central Italy earthquakes Bulletin of Earthquake Engineering. https://doi.org/10.1007/s10518-019-00594-4.

Pinho, R., Bommer, J.J., Glaister, S., 2002. A simplified approach to displacement-based earthquake loss estimation analysis, in: No. 738. Presented at the Proceedings of the 12th European Conference on Earthquake Engineering, London, England.

Pinto, P.E., Giannini, R., Franchin, P., Fardis, M., 2005. Seismic Reliability Analysis of Structures. Journal of Earthquake Engineering 9, 943–943. https://doi.org/10.1080/13632460509350573

Pitilakis, K., Crowley, H., Kaynia, A. (Eds.), 2014a. SYNER-G: Typology Definition and Fragility Functions for Physical Elements at Seismic Risk: Buildings, Lifelines, Transportation Networks and Critical Facilities, Geotechnical, Geological and Earthquake Engineering. Springer Netherlands. https://doi.org/10.1007/978-94-007-7872-6

Pitilakis, K., Franchin, P., Khazai, B., Wenzel, H. (Eds.), 2014b. SYNER-G: Systemic Seismic Vulnerability and Risk Assessment of Complex Urban, Utility, Lifeline Systems and Critical Facilities: Methodology and Applications, Geotechnical, Geological and Earthquake Engineering. Springer Netherlands. https://doi.org/10.1007/978-94-017-8835-9

Podestà, S., Romano, C., 2014. A Macroseismic Method for Vulnerability Assessment of Rationalist Architectural Heritage. Procedia Economics and Finance, 4th International Conference on Building Resilience, Incorporating the 3rd Annual Conference of the ANDROID Disaster Resilience Network, 8th – 11th September 2014, Salford Quays, United Kingdom 18, 173–180. https://doi.org/10.1016/S2212-5671(14)00928-9

Porter, K., 2021. A Beginner's Guide to Fragility, Vulnerability, and Risk, in: Beer, M., Kougioumtzoglou, I.A., Patelli, E., Au, I.S.-K. (Eds.), Encyclopedia of Earthquake Engineering. Springer Berlin Heidelberg, Berlin, Heidelberg, pp. 1–29. https://doi.org/10.1007/978-3-642-36197-5_256-1

Porter, K.A., 2003. An Overview of PEER's Performance-Based Earthquake Engineering Methodology, in: Applications of Statistics and Probability in Civil Engineering.

Preciado, A., Orduña, A., 2014. A correlation between damage and intensity on old masonry churches in Colima, Mexico by the 2003 M7.5 earthquake. Case Studies in Structural Engineering 2, 1–8. https://doi.org/10.1016/j.csse.2014.05.001

Rapone, D., Brando, G., Spacone, E., De Matteis, G., 2015. Valutazione della Vulnerabilità Sismica del centro storico di Scanno. Presented at the Atti del XVI Convegno ANIDIS.

Rapone, D., Brando, G., Spacone, E., Matteis, G.D., 2018. Seismic vulnerability assessment of historic centers: description of a predictive method and application to the case study of scanno (Abruzzi, Italy). International Journal of Architectural Heritage 12, 1171–1195. https://doi.org/10.1080/15583058.2018.1503373

Restrepo-Velez, L.F., Magenes, G., 2004. Simplified Procedure for the Seismic Risk Assessment of Unreinforced Masonry Buildings. Presented at the 13th World Conference on Earthquake Engineering, Vancouver, B.C., Canada, pp. 15, Paper No. 2561.

Romão, X., Costa, A.A., Paupério, E., Rodrigues, H., Vicente, R., Varum, H., Costa, A., 2013. Field observations and interpretation of the structural performance of constructions after the 11 May 2011 Lorca earthquake. Engineering Failure Analysis 34, 670–692. https://doi.org/10.1016/j.engfailanal.2013.01.040

Rossetto, T., Elnashai, A., 2005. A new analytical procedure for the derivation of displacement-based vulnerability curves for population of RC structures. Engineering Structures 27, 397–409. https://doi.org/10.1016/j.engstruct.2004.11.002

Rossetto, T., Elnashai, A., 2003. Derivation of vulnerability functions for European-type RC structures based on observational data. Engineering Structures 25, 1241–1263. https://doi.org/10.1016/S0141-0296(03)00060-9

Rossetto, T., Ioannou, I., Grant, D.N., Maqsood, T., 2014. Guidelines for the empirical vulnerability assessment. (GEM Technical Report). GEM Foundation, Pavia, Italy.

Rosti, A., Del Gaudio, C., Di Ludovico, M., Magenes, G., Penna, A., Polese, M., Prota, A., Ricci, P., Rota, M., Verderame, G., 2019b. Uso di curve di fragilità empiriche per la valutazione del rischio sismico a scala nazionale, in: ANIDIS 2019 - XVIII Convegno.

Rosti, A., Rota, M., Magenes, G., Penna, A., September, 2019a. Derivazione di curve di fragilità empiriche per edifici residenziali in muratura, in: ANIDIS 2019 - XVIII Convegno.

Salzano, P., Cescatti, E., Casapulla, C., Ceroni, F., Prota, A., 2019. 2016-17 Central Italy: macroscale assessment of masonry churches vulnerability. https://doi.org/10.7712/120119.6974.19936

Singhal, A., Kiremidjian, A., 1996. Method for Probabilistic Evaluation of Seismic Structural Damage. https://doi.org/10.1061/(ASCE)0733-9445(1996)122:12(1459)

Sorrentino, L., Cattari, S., da porto, F., Magenes, G., Penna, A., 2019. Seismic behaviour of ordinary masonry buildings during the 2016 central Italy earthquakes. Bulletin of Earthquake Engineering 17. https://doi.org/10.1007/s10518-018-0370-4

Sorrentino, L., Liberatore, L., Decanini, L.D., Liberatore, D., 2014. The performance of churches in the 2012 Emilia earthquakes. Bull Earthquake Eng 12, 2299–2331. https://doi.org/10.1007/s10518-013-9519-3

Spence, R., Coburn, A.W., Pomonis, A., 1992. Correlation of Ground Motion with Building Damage: The Definition of a New Damage-Based Seismic Intensity Scale. Presented at the Proceedings of the Tenth World Conference on Earthquake Engineering, Madrid, Spain, pp. 551–556.

Taffarel, S., Giaretton, M., Da Porto, F., Modena, C., 2016. Damage and vulnerability assessment of URM buildings after the 2012 Northern Italy earthquakes. pp. 2455–2462. https://doi.org/10.1201/b21889-321

Wang, Z., 2009. Seismic Hazard vs. Seismic Risk. Seismological Research Letters 80, 673–674. https://doi.org/10.1785/gssrl.80.5.673

Whitman, R.V., 1973. Damage probability matrices for prototype buildings (No. R73-57, Structures Publication No. 380). Seismic Design Decision Analysis.

Chapter 3.

Sources of uncertainties in seismic risk assessment

3.1 Classification of the uncertainties

In statistics the term uncertainty means a risk that has not been measured, in particular it reflects the difference of an observable quantity from its real values.

The uncertainties have a crucial role in the analysis and modelling of disasters in general, both natural and human, having a meaningful impact on the risk-based decisions.

The effects of the uncertainties in the decision-making process is not still well understood even by mathematicians and risk analysts. In literature, still few studies have been developed to investigate the impact of the uncertainties in the decision-making process.

An example is the study of Bier and Lin (Bier and Lin, 2013) that had the objective of illustrating the potential effects and dependence in making decisions about risk of the involved uncertainties. They presented the ways of uncertainties impact communication and suggested future developments in this direction. However, these suggestions are preliminary because a little research has been done on efficient methods of communicating the risk analysis results to decision makers that consider the dependence on uncertainties at the same time.

The challenges for risk analysts and managers have been presented by Thompson (Thompson, 2002). This topic is analysed in different fields, studying the variability of risk of dying from crashing airplane and the activation of motor vehicle airbags. The objective is to show how a better characterization and investigation of uncertainty in the risk assessment bring to a better risk communication.

In the field of nuclear safety, the risk informed decision-making process (Figure 3-1) is developed. It is studied the way in which the risk can be used in making decisions. In this case, the operating experience and the consideration of the uncertainties are integrated in the process, helping the risk decision in a coherent and balanced manner (INSAG-25, 2011).
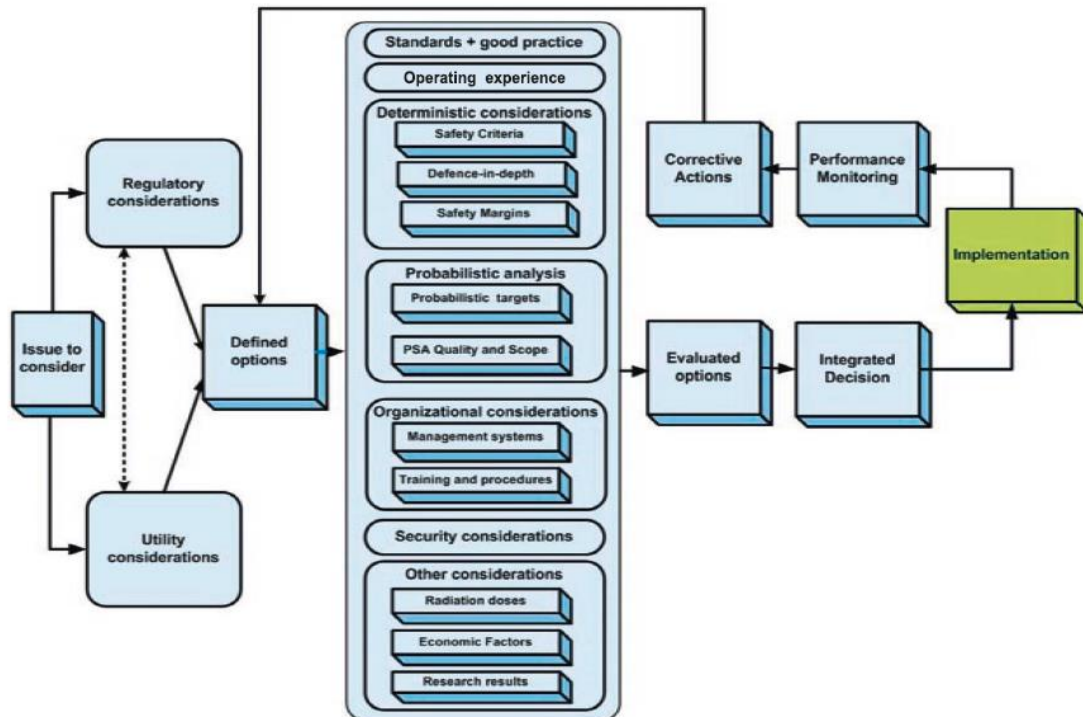
Figure 3-1. Key elements of the integrated risk informed decision-making process (INSAG-25, 2011).

Therefore, it is evident that nowadays most studies that want to quantify environmental impact, do not always consider the impact of variability; in particular they do not take into account uncertainties of input data on their results. Standardised methodology on the propagation of the uncertainties and on the impact of them, are not widely investigated.

A proposal of conceptual framework for the systematic treatment of uncertainties, in order to support the management of uncertainties in decision process has been performed (Walker et al., 2003). The reasons of the uncertainties consideration in this process of decision support are investigated, starting from a better communication between the policy analysts, policy makers and stakeholders. Indeed, coherent definitions of the terms for the uncertainties in the decision framework help the communication between experts from different fields, such as scientists and policy managers, the understanding of the process and also the facilitation of policy choices and the resources allocation. The study performed a harmonization of the terminology and a tool proposal in order to characterize the uncertainties in the model-based decision support. To reach the target, it is important to identify the location of the various sources of uncertainties within the whole model. The generic location of the uncertainties are: (i) the contexts that identify the boundaries of the system to be modelled; (ii) the model uncertainties such as the variables and their relationships that are chosen to describe the system located within the boundaries and the computer implementation of the model; (iii) the inputs to the model; (iv) the parameters uncertainties associated with data used to calibrate the model and, finally, (v) the model outcome uncertainties. Figure 3-2 shows the location of the uncertainties, in particular it is shown the context that defines the system boundaries (Figure 3-2a) and its uncertainties that display the

ambiguity on the definition of the confines (Figure 3-2b). Then in Figure 3-2 c-d, the model structure with its uncertainties is illustrated.

(a)   (b)

(c)   (d)
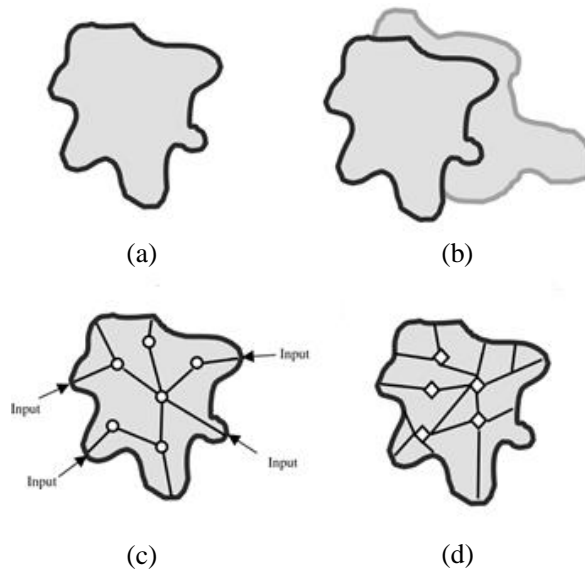
Figure 3-2. The location of uncertainties: (a) and (b) represent the context uncertainties; (c) and (d) represent the model structure uncertainties, showing also the input uncertainty (Walker et al., 2003)

In the Life Cycle Assessment field, the importance of uncertainties consideration and how it can help in supporting and improving the mitigation strategies have been explored (Groen, 2016). Some studies show that only a single value per each data point in the environmental model overlooked the range of possible realisations (Björklund, 2002), while in other cases, if the results of different models must be compared and the magnitude of uncertainty is larger, it is difficult to provide precise information (De Koning et al., 2010).

Earthquake engineering and decision-making problems are solved within the bounds of a model universe. This model universe contains physical and probabilistic features that are used to represent the real world in order to find a solution at the problem at hand, plenty of uncertainties. The analysis and definition of the uncertainties became crucial in these models, which should be defined within the confines of the model itself.

Therefore, the definition of reliable models for structural seismic risk assessment is one of the main objectives to achieve in earthquake engineering; moreover, understanding and quantifying uncertainties are crucial parts that allow to characterize validated models. The main advantages of a process that takes into account the dependence of the uncertainties are the evaluation of the effectiveness of the risk mitigation strategies and a good plan of the resources for managing the risk (Ellingwood and Kinali, 2009).

In this field, it is common to distinguish between intrinsic and reducible uncertainties (Porter, 2021). The first class is the case of the aleatory uncertainties that are supposed to be irreducible. Due to their existence in nature, they are considered to be inherent in the involved process. Even though it is possible to strive for the reduction of natural variability in space or time, the observed variation cannot be reduced. The term aleatory is used for addressing uncertainties that reflect physical randomness. Their outcome probability is intrinsic in

the process in question and the probability can be determined with numerous trials but will not change. From earthquake engineering field, an example of aleatory uncertainty is the structural response derived from randomness in the ground motion, generally called record-to-record variability. The seismic response variability due to record-to-record uncertainties, indeed, depends on different factors such as the intensity measure type, the set of earthquakes ground motion and the limit states.

The epistemic uncertainties represent, instead, the reducible ones. They can be carried by gaining more and/or better data and by improving the knowledge of the models, using more refined structural models or by adding experimental tests on specific components. This type of uncertainties does not exist in nature, neither it is inherent in the process under consideration. Different kind of uncertainties are:

- Parameters statistical distribution estimation uncertainty: parameters such as the material stiffness or parameters that defined the fragility curves are addressed based on available data. This is the case of low data availability, strictly connected with a small number of observations. This allows considering uncertainty in the probability distribution as random variables and it is considered to be statistical uncertainty. Another source of error is the fitting of probability distribution to the available data.

- Model uncertainty: the choice of mathematical model can generate uncertainties. Sometimes, the models are incomplete due to the dependence from variables that may be not considered in the model, such as the velocity rupture propagation of a fault that generally creates numerous troubles in the measurement. Moreover, the uncertainty can be caused by the inaccuracy of the model form, or by the relationship between dependent and independent variables. This can happen when the model uses a linear form but the relation is nonlinear.

-Discretization uncertainty: when an analytical approach is used, uncertainties in the discretization process could happen. For example, the structural members can be modelled as discrete elements in finite element analysis and issues in the definition of the mesh may be run into.

The study of Der Kiureghian detected three dominant types of uncertainties in the structural engineering field that could be associated to the two classes identified above (Der Kiureghian, 1996).

The author defined the inherent randomness, that express the intrinsic variability in materials and in environmental effects; the statistical uncertainty, that want to estimate the parameters of probability distributions derived from observational sample of limited size; finally, the model uncertainty, that express the limit of the mathematical models used to describe more complex processes. The first case is referred to

irreducible uncertainties, while the statistical and model uncertainties can be reduced using more data and/or by refining the models. It still matter other sources of uncertainties such as the human or measurement errors that deserve attention and should be considered in the analysis.

To sum up, in risk analysis the sources of uncertainties and their characterization and classification into aleatory and epistemic, became a significant issue to take into account. The work of Der Kiureghian and Ditlevsen (Der Kiureghian and Ditlevsen, 2009) provided a deep study on the sources of uncertainties in engineering risk modelling by using different application contexts. The categorization of the uncertainties within a model is useful for making clear which of them could be reduced near term. This distinction, according with their work, is determined by the modelling choice and depends on the context and application. They showed that for a proper formulation of the risk assessment, a careful attention should be carried out to the type of uncertainty, demonstrating it with results of underestimation or of overestimation probability if this aspect is not well analysed.

To this end, the uncertainty analysis can be used to propagate epistemic and aleatory uncertainties. In the study of Groen (Groen, 2016) for example, the term uncertainty is referred to the analysis of the magnitude and consequences of both epistemic and aleatory variability of the input parameters. In particular, this kind of analysis quantifies the uncertainty of the output based on the uncertainty of the input parameters. To do so, the knowledge of the distribution function such as normal distribution, lognormal distribution, as well as its dispersion is required. In addition to the uncertainty analysis, the sensitivity analysis is another way to study the effect of the input uncertainty on the output. The main approaches used for sensitivity analysis are the local sensitivity analysis and the global sensitivity analysis (Saltelli et al., 2008). The local sensitivity analysis manages what happens to the output when input parameters are changed, and the parameters that have the largest effect on the model output are referred to as the most influential parameters. These types of methods are generally useful when poor data are available and they are limited to point values (Figure 3-3).
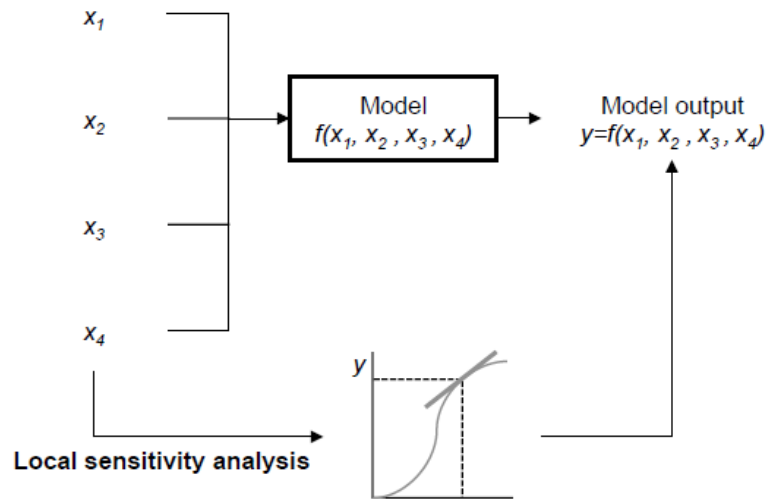
Figure 3-3. Local sensitivity analysis illustration (Groen, 2016)

The global sensitivity analysis is based on how much the uncertainty around each input parameter contributes to the output variance. This analysis considers the actual variation over all input parameters simultaneously (Figure 3-4). The parameters that mostly change the model output are referred to as the most important parameters. Generally, the global sensitivity analysis requires full knowledge of the input uncertainties, such as its distribution functions and its covariance, if the input parameters are correlated. The study of Goen helped to explore how uncertainty and sensitivity analysis reduce the efforts for data collection, support the development of mitigation strategies and improve overall reliability of decision-making in environmental impact assessments models.
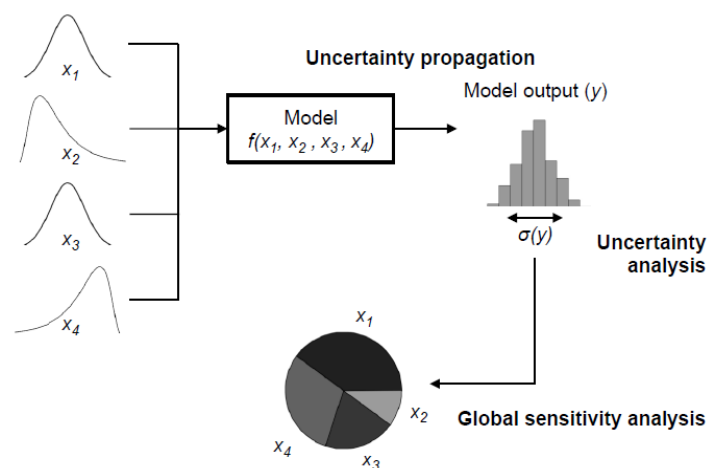
Figure 3-4. Global sensitivity analysis illustration: given the distribution functions of the input parameters, the variance decomposition represented in the pie chart, explains the output variance represented by the histogram (Groen, 2016).

3.2 Seismic Input Uncertainty

Seismic input uncertainty is considered one of the most influencing sources of uncertainty in the probabilistic risk assessment of structures. The study of Ioannou et al. (Ioannou et al, 2015) confirmed that the ground motion variability has a dramatic impact in the uncertainties of the seismic risk assessment. In particular, they showed how the ground motion uncertainty affects the empirical fragility curve by undertaking a series of experiments. They illustrated that one of the potential reasons for the dispersion in the evaluation of the final risk, is the neglect of the spatial variability and the epistemic uncertainty in ground-motion prediction. They summarized that this variability leads to flatter the fragility curves and the lack of dense ground motion recording network allows a higher uncertainty in the empirical curves.

Among all sources of uncertainty, such as the material properties and the design assumptions, the earthquake-induced ground motion has a significant impact on the observed variability in the structural response (Padgett and Desroches, 2007). In particular, Padgett and Desroches demonstrated that the propagation of the variable model parameters tends to be overshadowed by the uncertainty in the ground motion and base geometry of the structural class.

The features of a seismic event, such as the amplitude, frequency content, and duration may show a high variability earthquake to earthquake.

Ground motion appears to be random in space and time, due to the complexity of the path that induced waves that travel from the fault source through bedrock reaching the foundation level of a structure. In fact, during seismic events, the seismic waves interact with the foundations of the structures that once again interact with the superstructures. Soil-foundation-structure interaction is the term used to describe this phenomenon.

To this end, all these aspects are useful to understand the complexity of a reliable model and generally, simplifications are applied.

A good balance between the realistic modelling of the seismic action, a detailed analysis of the response and an efficient mathematical model for probability computation, allow having a valid risk analysis.

In literature, there are descriptions of models available for identifying ground motion and its uncertainties.

The study of Atkinson (Atkinson, 2011) showed that an examination of ground-motion variability from an empirical perspective could be useful to represent its epistemic and aleatory components in a better way. In this work, the epistemic uncertainty was considered in the median ground motion prediction curve reflecting the inter-event variability at the ground motion level and that can be reduced if the source, path, and site characteristics are known. On the other hand, the aleatory variability is made by the intra-event variability for a given event in a given distance range.

The study of Pinto (Pinto, 2001) focused on the used models for representing the action, which are classified into four categories: random processes, simulated accelerograms, recorded accelerograms and synthetic accelerograms. It is stated that a proper selection of recorded accelerograms or synthetic accelerograms,

satisfies the requirement of realism better than random processes and samples. The reason of the use of accelerograms is the necessity of simulations, considering the sample-to-sample variability.

According to this last concept, the work of Jalayer et al. (Jalayer et al., 2004) studied different approaches to describe the uncertainties in the ground motion. A complete probability distribution based on a stochastic ground motion model used the subset simulation technique.

The complexity of the selection of ground motion is analysed in literature. Signals recorded at specific site constitute a random process that is hard if not impossible to reproduce. Numerous efforts have been made on processing the records to became them representative of future seismic input. Moreover, there have been expended effort to minimize the dispersion in the structural response due to the usage of different seismic records.

Given the above uncertainties, it is still a responsibility of the designer to find an appropriate way for selecting a set of earthquake records. This task can be accomplished with a deep understanding of the selection process concepts and of the earthquake records scaling. In fact, the current code framework for ground motion record selection is simplified, if compared to the potential impact of the selection process on the dynamic analyses. This gives the impression that structural analyses results are robust as much as the finite element model analysis is refined.

In particular, some studies presented the review of the state of the art on current methods developed for selecting and scaling appropriate set of records that can be used for dynamic analysis of structural systems in performance-based design. Moreover, the record selection techniques have not yet been included in contemporary seismic code provisions (Katsanos et al., 2010). Because of that, the current seismic code framework is presented to be a simplified version of the full picture, considering being adequate for conventional structures but may not be true for more complex situations, where deep analysis and more refined models need to be assessed.

Another study addressed the question of selection and scaling of accelerograms for predicting the nonlinear dynamic response of a structure at a specific site (Iervolino and Cornell, 2005). The selection of real records based on strong motion parameters allow to address the problem of excessive number of accelerograms required for reliable analyses. In fact, the study of Iervolino and Cornell, found that there are no evidences to suggest that it is necessary to take in great consideration the magnitude and distance in the selection of records process.

The parameters that quantify the effect of record on a structure are known as Intensity Measure (IM), and examples of most used IM are the PGA or the spectral acceleration at the fundamental period of vibration of the structure $S_a(T_1)$.

The uncertainties present in the seismic input assessment, in the structural response, in the resulting damage, and in the cost estimation need to be assessed in terms of probabilities. A formal approach, generally used for

solving this problem, has been developed by the Pacific Earthquake Engineering Research Center (PEER), characterized by stages performed in formal probabilistic terms. These stages consist in quantifying the seismic ground motion hazard, structural response, damage to the building, and potential consequences. The process is modular, allowing the phases to be identified and executed independently, and then linked back together (Figure 3-5). In the PEER methodology the intermediate variables are termed IM, Engineering Demand Parameter (EDP) and Damage Measure (DM). The final consequences, termed Decision Variable (DV), could also be considered a pinch point (Baker, 2005).
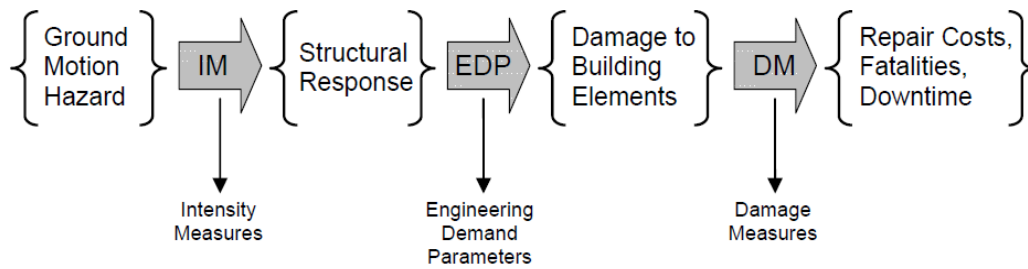
Figure 3-5. Schematic illustration of the Performance-Based Earthquake Engineering model and the pinch points IM, EDP and DM. (Baker, 2005).

Focusing on the seismic input, the IM variable links the ground motion hazard with the structural response. The ground motion hazard is computed using the Probabilistic Seismic Hazard Analysis (PSHA), and generally the final output is the mean annual frequency of exceeding various levels of IM. The probabilistic seismic hazard assessment evaluates the probability that a selected scalar measure of seismic intensity IM at a specific site exceeds a given value in a given time interval, generally fixed at one year.

The result of the seismic analysis for the site under consideration is the so-called hazard curve that furnishes the annual frequency of which the seismic excitation is estimated to exceed various levels of IM.

For the evaluation of the seismic hazard a procedure is proposed in literature. In particular, some studies (Cornell 1968, Cornell et al., 2002, Jalayer and Cornell, 2003) provided curves that gives the relation between ground motion parameters and return period at specific site. The procedure for the evaluation of the hazard curve proposed by Cornell (Cornell, 1968) required the knowledge of different seismogenetic sources, the recurrence law that provide the description of the activities of each seismogenetic source, and the attenuation relationship that provide the relation between the seismological parameters at the site of interest.

The work of Jalayer and Cornell (Jalayer and Cornell, 2003) had the performance objective in terms of mean annual frequency of exceeding the desired performance level. The expression is derived by considering the uncertainty in the estimation of seismic hazard, of structural response (as a function of the ground motion intensity level), and of structural capacity for the desired performance level. Therefore, the objective is the mean annual frequency of exceeding a specified limit state H_{LS}. This expression is the product of the mean

53

rate of occurrence of event with a seismic intensity larger than a threshold ν and the probability that the demand D exceeds the capacity C

$$H_{LS} = \nu \cdot P[D > C] \tag{3.1}$$

In their work, in order to determine H_{LS}, they used two different strategies. In the first, they decomposed the problem into tractable pieces and then re-assemble them, using the total probability theorem:

$$H_{LS} = \nu \cdot P[D > C] = \nu \cdot \sum_{im} P[D > C \mid IM = im] \cdot P[IM = im] \tag{3.2}$$

So, the first piece $P[IM = im]$ that represents the likelihood that the spectral acceleration will equal a specific level, can get from the PSHA of the site. The second piece that is the conditional limit state probability for a given level of ground motion intensity, means understand the response /demand variability from record-to-record of the same intensity. This strategy is called IM-based solution approach.

An alternative solution strategy they proposed, consists in decomposing the derivation in two different steps. The first is to decompose the limit state probability with respect to the displacement-based demand using the total probability theorem.

$$H_{LS} = \nu \cdot P[D > C] = \nu \cdot \sum_{d} P[D > C \mid D = d] \cdot P[D = d] \tag{3.3}$$

Then the second step, concerns in the decomposition of the term $P[D = d]$ with respect to the chosen intensity measure:

$$H_{LS} = \nu \cdot P[D > C] = \nu \cdot \sum_{d} \sum_{im} P[D > C \mid D = d] \cdot P[D = d \mid IM = im] \cdot P[IM = im] \tag{3.4}$$

This strategy is called displacement-based solution strategy and it is the one used by the PEER framework as a basis of probabilistic design and assessment, valid for discrete interface variables.

In their work, Jalayer and Cornell presented also the parallel expression on continuous interface variables and they assumed that randomness is the only source of uncertainty in the demand and capacity variables.

Generally, the Gutenberg-Richter recurrence law is used to model the activity of the seismic sources (Gutenberg and Richter, 1956, Gutenberg and Richter, 1944), which provides an estimation of the mean number of seismic events of magnitude greater or equal than a fixed one during a period of interest. The expression is the following:

$$N(m) = 10^{a-bm} \tag{3.5}$$

where m is the fixed magnitude, while a and b are the parameters of the law source-dependent. In particular, the first defines the number of seismic events with a magnitude greater or equal than 0 and the second parameter defines the frequency of occurrence between events of different size, generally equal to 1.

Several studies have been proposed improving the Gutenber-Richeter law. The study of De Santis et al. (De Santis et al., 2011) recalled theoretical expressions for the probability of occurrence of an earthquake with a specific magnitude in terms of the constants a and b. The study gave a physical interpretation of the constants by introducing the definition of the Shannon entropy of earthquakes. These concepts have been applied to two different case studies referred to L'Aquila earthquake of 2009 and to the Umbria-Marche earthquake of 1997, confirming the importance of the physical meaning of a and b values and their relation with the entropy. In Figure 3-6 the application of the study of De Santis et al., to Abruzzi earthquake is showed. A linear fit over the number of events in each magnitude bin is highlighted, and the choice for the value of minimum magnitude is made by inspecting the magnitude frequency and cumulative distributions.
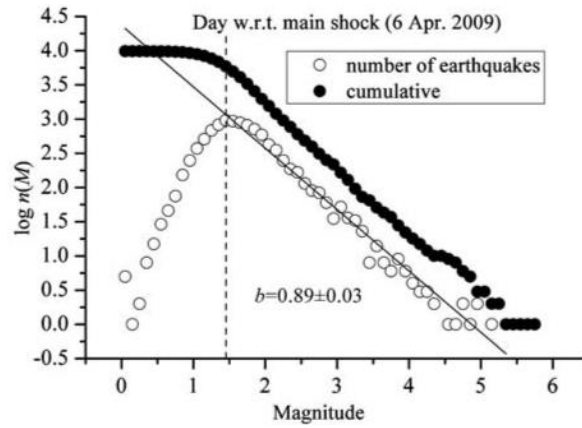
Figure 3-6. Application to L'Aquila earthquake: the white circles represent the number of events in each magnitude bin, while the black ones represent the cumulative frequency magnitude distribution of events for all seismic event. The vertical dashed line represents an estimate of the minimum magnitude for the catalogue completeness (De Santis et al., 2011).

The work of Tinti and Mulargia (Tinti and Mulargia, 1985) showed that the greater is the uncertainty of observed magnitudes, the greater is the bias. The authors have been calculated the probability density for the observed magnitude given normal estimation errors with a common standard deviation.

Generally, in most of the applications is used a truncated Gutenberg-Richter law, considering an upper and lower bound defined by the values that the magnitude can assume. In particular, the lower bound m_l is defined such that the earthquakes with magnitude lower than that value are insignificant, while the upper bound m_u is defined such that the probability of having earthquakes higher than that value is zero. It is possible to define the mean number of events of magnitude $M > m$ by using:

$$N(m) = \alpha \left(\frac{e^{-\beta m} - e^{-\beta mu}}{e^{-\beta ml} - e^{-\beta mu}} \right)$$

(3.6)

where the quantity in brackets represents the probability of having a magnitude of the earthquake larger than m and α coefficient is the mean number of seismic events of any magnitude bounded between m_l and m_u.

It is important to note that the attenuation relationship correlates the seismic intensity with the magnitude M and the source-site distance R as follow:

$$\log IM = b + g_M(m) + g_R(r) + \varepsilon$$

(3.7)

where ε is zero mean Gaussian variable of given standard deviation.

The derivation of the hazard for a site can be done by considering a single source, or in presence of several sources, their contribution to the hazard can be simply added by assuming the independence of the seismic activity of the various sources.

The first step in the evaluation of the hazard curve consists in finding the conditional probability function of IM by applying the total probability theorem. The result of this procedure multiplied by the mean annual rate of event gave the mean annual rate of exceedance $v(im)$:

$$v(im) = \Pr(IM > im) = k_0 \cdot i^{-k}$$

$$(3.8)$$

where the coefficients k_0, k are two constants that depend on the specific form of the attenuation law and on the geometric characteristics of the seismic source.

Generally, the seismic events are considered to be rare, such that the assumption of independence and absence of overlap can be accepted. In these cases, also the Poisson distribution may be applied to describe these events. In these phenomena, the events are rare enough to be counted, and to have measurable delays between them.

The work of Dall'Asta et al. (Dall'Asta et al., 2021) moved on in respect to the Poisson law, presenting some preliminary results on the time dependent seismic hazard. Indeed in the codes, the reliability assessment of structures and relevant design rules are based on the Poisson recursive model, for which the frequency of the occurrence of seismic events does not change in time. In this work, the authors proposed a comparison between the outcomes deriving from a Poisson recursive model, providing a constant hazard rate, with results coming from a time dependent recursive model.

As said, the result of the PSHA is the mean annual rate of exceeding a seismic intensity value IM.

In particular according with the PEER framework, the link between seismic hazard and seismic demand analysis can be written as:

$$\lambda_{DM}\left(dm\right) = \int_{IM} G_{EDP|IM}\left(edp \mid im\right) \cdot \left|d\lambda_{IM}\left(im\right)\right|$$

$$(3.9)$$

where $\lambda_{IM}(im)$ is the result of probabilistic seismic hazard analysis, while $G_{EDP|IM}(edp \mid im)$ is the result of probabilistic seismic demand analysis. It is directly recognised that the order of uncertainties in the $\lambda_{DM}(dm)$

is dictated mainly by the uncertainties in the hazard $\lambda_{IM}(im)$ and not by the uncertainties in the structural response $G_{EDP|IM}(edp|im)$.

However, the selection of appropriate IM is related to its sufficiency and efficiency, which are specific features related to the accuracy of the performance assessment process. From the perspective of a structural engineer, an efficient IM is defined as a result of limited variability of the structural demand measure given seismic intensity. In this way, the efficiency could reduce the number of nonlinear dynamic analysis and ground motion records. On the other hand, a sufficient IM makes the DM independent from magnitude and distance, providing an accurate estimation of the probability of exceeding each value of DM given the value of the ground-motion intensity measure independently from magnitude and distance.

Luco and Cornell (Luco and Cornell, 2007) provided a search for a scalar IM that is both "efficient" and "sufficient" for different period buildings subjected to ordinary or near-source earthquake ground motions. They stated that the efficiency and sufficiency of an IM can further depend to the structure characteristics and to the type of ground motions considered. Moreover, they summarized that the spectral acceleration considered as intensity measure, is not always efficient and sufficient especially for tall, long-period buildings or for near-source ground motions. Clearly, the computability of the ground motion for a specific site in terms of the selected IM, is an important consideration in the selection of an appropriate intensity measure.

A more accurate response prediction using IM-based approach concerned the consideration of the epsilon parameter ε associated with the ground motion. According with the study of Baker and Cornell (Baker and Cornell, 2005), ε is the number of standard deviations by which an observed logarithmic spectral acceleration differs from the mean logarithmic spectral acceleration of a ground motion prediction equation. They investigated that ε has a significant ability to predict the structural response. Indeed, ε is an indicator of spectral shape of the response spectrum and the shape does not change with scaling. Moreover, a record with positive epsilon value, so with a larger than expected spectral acceleration at the specified period, showed a peck in the response spectrum at specific period. On the other hand, a record that is lower than the expected has a valley only in a narrow range of periods, meaning that a record with negative epsilon values showed a valley in the response spectrum at specific period (Figure 3-7). Neglecting the effect of epsilon when computing the drift hazard, leads to conservative estimations of the response of the structures.
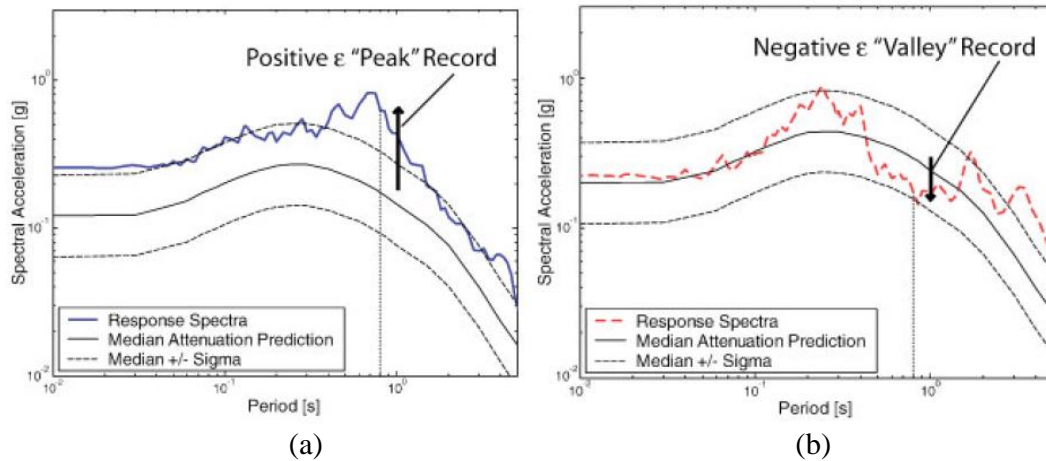
Figure 3-7. An illustration of the (a) peak and (b) valley effect (Baker and Cornell, 2005)

Another aspect of uncertainty in the seismic input is the local soil condition. The main sources of uncertainties for site response analysis are the input motion characterization and the shear-waves velocity, measured at multiple locations using in situ seismic test methods. Moreover, nonlinear property characterization of the soil can be evaluated through laboratory testing or via empirical correlation between soil types, stress conditions, or through the selection of the method of analysis such as equivalent linear or nonlinear analysis (Figure 3-8). In the work of Rathje et al. (Rathje et al., 2010) the influence of soil characterization uncertainty is assessed using Monte Carlo simulations and considering variations in the shear-waves velocity profile and nonlinear soil properties. Including the variability in soil properties results in an increase of the standard deviation of the amplification factors but this has a lower effect on the standard deviation of the surface motions.
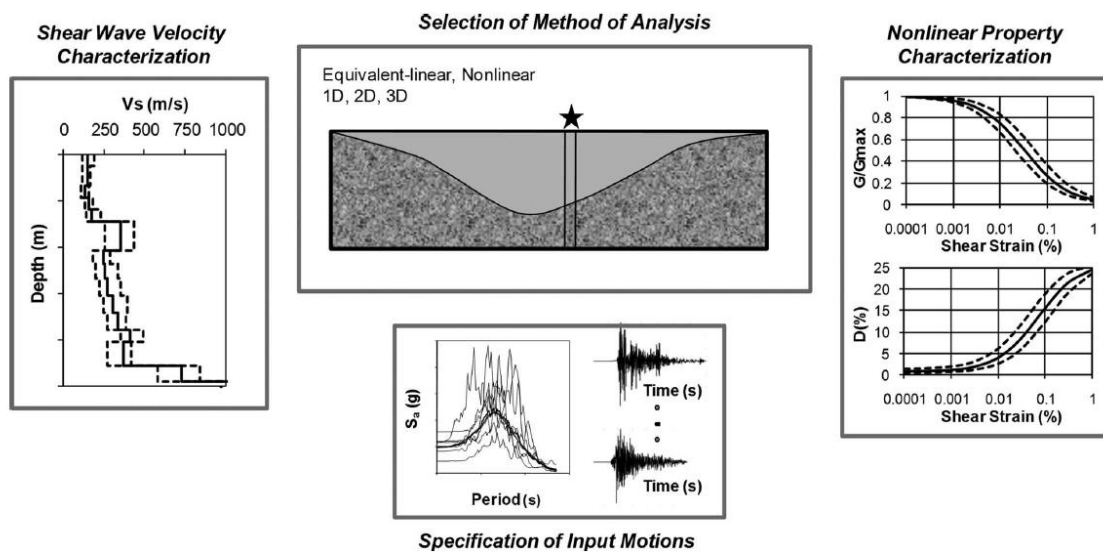
Figure 3-8. Illustration of the sources of uncertainty in seismic site response analysis (Rathje et al., 2010)

3.3 Model Uncertainties

The treatment of the uncertainties associated with modeling is another important variable to take into account because it influences the final evaluation of the risk.

To assess the seismic risk in a probabilistic way, vulnerability functions and/or fragility functions have to be derived. Regardless the derivation methodology of these functions, the characterization of the uncertainties can be made according with three categories:

- Record-to-record variability: it is related with the fact that different damage levels can be obtained by the same IM from different records (as discussed in the previous section).

- Building-to-building variability: there is a variability inside the same vulnerability class due to differences in the material and geometrical properties or structure features.

- Damage criterion: during the process of estimation of the expected damage using the EDP, large variability should be taken into account, for example the same EDP may lead to different expected damage or damage levels.

Despite the importance and recognition of these types of uncertainties, the majority of the works related to determine the seismic risk, used deterministic vulnerability functions. However, the deterministic approach underestimates the variability in the earthquake losses. This is due to higher computational costs in the process of uncertainty analyses, related to a lack of tools capable of propagating variability in vulnerability.

By the way, in the literature exist studies that have been modeled the uncertainties of the building class vulnerability in a probabilistic way. Silva et al. (Silva et al., 2014) proposed a logic tree structure in order to better characterize the epistemic uncertainty. A new vulnerability model based on analytical approach for RC building stock has been proposed. The model considers the seismic zonation and the uncertainties in the distribution of loss ratio. These curves have been generated through Monte Carlo simulations and analysed using nonlinear dynamic analysis. These RC building classes have been generated using the probabilistic distribution by considering geometric and material properties. Then the structures were allocated in the coherent damage state according to specific damage criteria in order to get the vulnerability function. The uncertainties were considered with the bootstrap sampling technique.

The study of Salgado et al. (Salgado et al., 2016) used different sets of vulnerability functions. The study wants to evaluate the direct effects of seismic events (deaths and injured estimation depending on the building class) and the consequences in terms of the possibility of occupying the buildings after the disaster (occupants in terms of homeless or unemployed people). This study performed the whole process by using a probabilistic

framework in which the uncertainties, related to physical damage and loss assessment, are considered. Indeed, the vulnerability functions are a probabilistic representation of the loss associated to different hazard seismic intensities.

In the literature referred to the probabilistic seismic risk, methods to model the uncertainties using vulnerability functions have been proposed (Silva, 2019). The author performed these analyses considering three portfolios of RC buildings in Lisbon, Portugal. Different approaches to model the variability in the vulnerability function were considered. In particular, different ways to represent the loss ratio were defined: only the mean behaviour, a non-parametric distribution and a beta distribution, or just a beta distribution. In particular, the difference between the second and third approach wanted to show that the record-to-record variability and building-to-building variability could be modeled separately. Moreover, in this study the inclusion of building-to-building variability has been taken into account by generating almost one hundred stochastically single degree of freedom system to represent each building class. Capacity curves were randomly built using the median capacity curve per each class and by considering the variability at the yielding and ultimate capacity points.

The study of Bazzurro and Luco (Bazzurro and Luco, 2007) performed a rigorous treatment of uncertainties, showing the importance of their consideration in the loss and risk evaluation process. Depending on the level of refinement of the analysis, different sources of uncertainties are present. For example, they showed that the response record-to-record variability of a structure is subjected to different earthquakes but with the same value of the seismic intensity parameter. They analysed the vulnerability function for buildings portfolio that are classified on the same construction class according with the construction type, number of stories. In Figure 3-9 an example of this kind of variability of the structural response measure is illustrated. In the Figure each gray curve is produced by the same ground motion, each time recording the maximum value of the drift. The focus of this work has been the effect of the uncertainties and the correlation of them with the annual loss of exceedance probability curves.
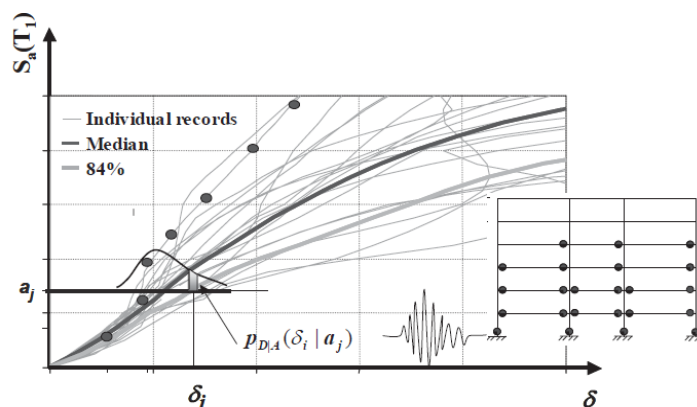
Figure 3-9. Example of variability of the structural response measure (Bazzurro and Luco, 2007)

Another example is the study on steel concrete composite bridges proposed by Tubaldi et al. (Tubaldi et al., 2012) where the influence of the model parameters was studied. In that work, a rigorous tool to evaluate the

effects of the uncertainties derived from the model such as geometric and material properties, mass, dissipative properties and gravity loads was provided. The methodology proposed and the results obtained, even though they are limited to steel concrete composite bridges, can be applied to different structural typologies.

Another study made on a different field, proved the importance of the model uncertainties, that represent an issue rarely addressed in practical applications of the risk evaluation (Linkov et al., 2003). Linkov et al. studied the model implementation problem and showed that the selection parameters process can be derived from a subjective interpretation of the problem. The authors classified an additional dimension of uncertainty with the scenario uncertainty, related to the lack of specification on the scenario. They showed that the greatest uncertainty derived from the scenario and its interpretation and approximation from the modelers. The parameter uncertainty evaluated though Monte Carlo analysis, may have contributed over one order of magnitude with respect to all the other model uncertainties.

The work of Der Kiureghian and Ditlevsen (Der Kiureghian and Ditlevsen, 2009) studied the importance of the sources of uncertainties in engineering risk modelling, considering the distinction between aleatory and epistemic uncertainty. Moreover, the model error may be derived from the potential inaccuracy of the model or from the effect of the missing variables. The parameter uncertainties can be considered epistemic in nature. Indeed, the uncertainty in their estimation decreases with the increase of number and quality of the observational data. Related to this, the concept of transparency in decision making became crucial. In fact, it requires that the stakeholders are aware that the parameters uncertainties can be reduced with an increase of computational costs.

3.4 Loss Estimation Uncertainties

The final objective of the risk assessment is the evaluation of the consequences/losses. Therefore, the whole framework of the risk evaluation gathers the uncertainties from all the steps already discussed.

In modern studies of risk assessment model, some sources of uncertainties are often neglected, leading a bias on estimation of the losses or an underestimation of the uncertainties.

Numerous studies focus on the impact of the uncertainties, quantifying and exploring them at each step of the risk loss model.

A simplified approach has been provided by Dolšek (Dolšek, 2012) in which both aleatory and epistemic uncertainties have been considered for the assessment of the seismic risk of reinforced concrete frame buildings. Risk has been expressed in terms of mean annual frequency of exceeding a given limit state. The epistemic uncertainties have been incorporated with a set of structural models using the Latin hypercube technique, while the aleatory uncertainties are represented by the ground motion records. The main result of this study is that the incorporation of epistemic and aleatory uncertainties increases the dispersion with the increase of the limit state. Moreover, neglecting the epistemic uncertainties means an underestimation of the

mean annual frequency of exceedance. Therefore, this cannot be simply ignored from the seismic risk evaluation.

Kalakonas et al. (Kalakonas et al., 2020) provided a deep analysis on the impact of uncertainties considering the case studies of Guatemala and Guatemala City. The selection of uncertainties is strictly related to the refinement of the model and the availability of other information. A sensitivity analysis was used to quantify the impact of the uncertainties, starting from a base model selecting the default options for each component and then altering it by using other options. The main considered uncertainties are referred to the seismic hazard and in particular the seismic zonation, the maximum considered magnitude and the selection of the GMPE. Moreover, also the spatial resolution and the distribution of construction materials have been considered as useful parameters to evaluate the uncertainties referred to the exposure. Finally, concerning the vulnerability aspect, the uncertainties considered were focused on the loss ratio distribution, modelled using its mean value, the beta distribution and the lognormal distribution. The correlation in the vulnerability for lognormal distribution of the vulnerability functions has been also investigated (Figure 3-10).
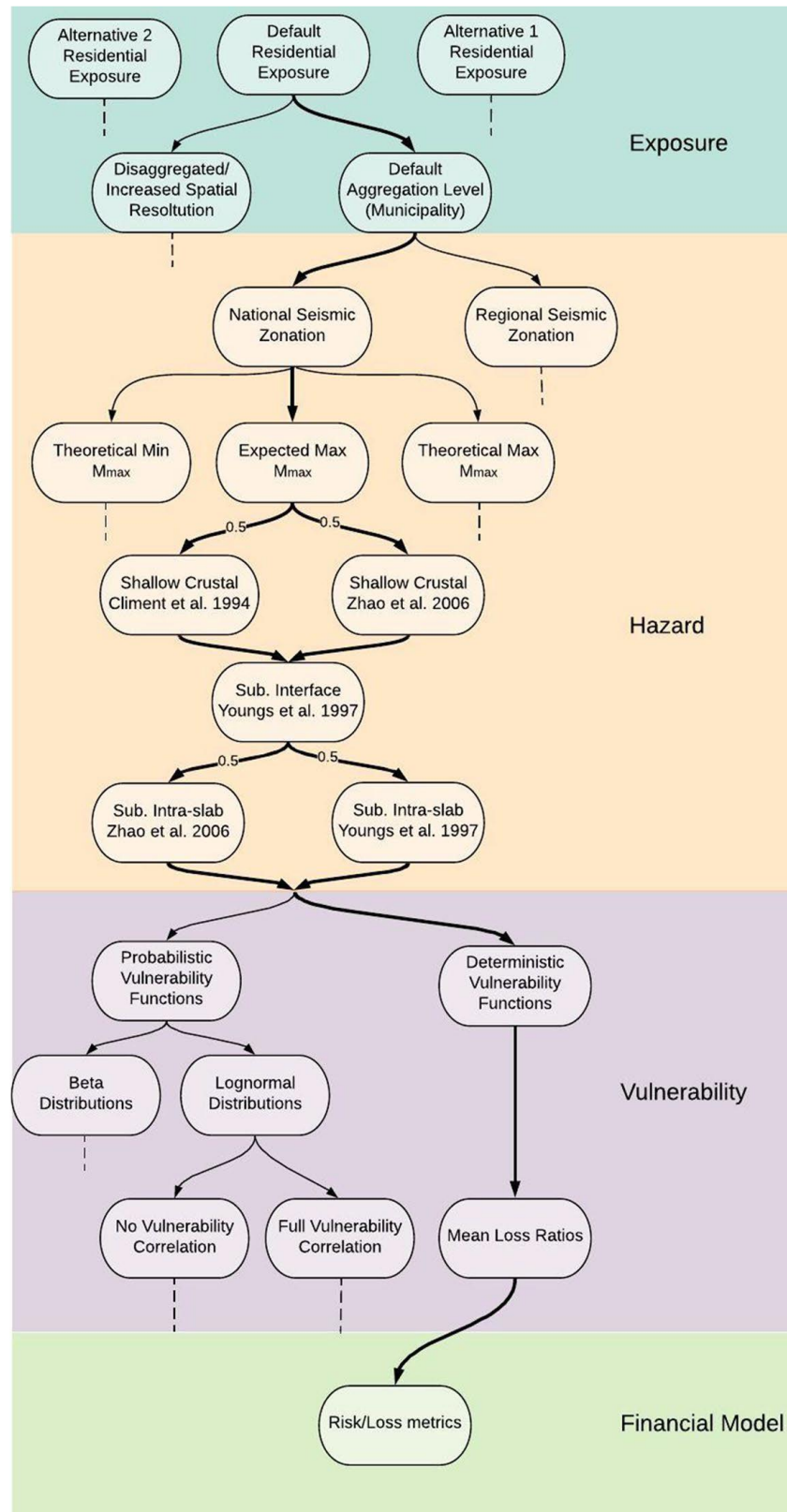
Figure 3-10. Representation of the considered uncertainties and the base model with more remarked arrows (Kalakonas et al., 2020)

The study indicated that the hazard uncertainties are the most significant, while the exposure uncertainties showed minor differences in the loss estimation. The vulnerability component, that incorporated the building-

to-building variability and record-to-record variability, illustrated a predominance in the correlation between buildings of the same class.

The correlation relations between buildings were studied in another work proposed by Silva (Silva, 2019), that would explore the statistical framework to simulate the variability in the whole process, by studying the loss exceedance curves and the average annualized losses for different building portfolios.

In particular, the study investigated three different case studies: (i) a deterministic (no uncertainty), (ii) a record-to-record and building-to building uncertainty modelled jointly and (iii) a record-to-record and building-to-building uncertainty modelled separately. The risk outcomes showed that the cases with variability without correlation are identical to the deterministic case, where no uncertainty is considered. Therefore, if the possible correlation in record-to-record variability is not simulated, all the befits in modelling the variability in loss ratio are null. Moreover, the absence of large datasets for different seismic events represents an obstacle to this process. Indeed, the expansion of damage databases, the availability of ground motion records and information about the loss, help to have a better understanding of the uncertainties and correlation in vulnerability and risk process.

The evaluation of loss uncertainty can be seen also as a logic tree approach (Silva et al., 2014). The logic tree approach helps to better characterize the epistemic uncertainties derived from the calculations. Indeed, the evaluation of seismic risk involves the combination of different components and in particular the probabilistic seismic hazard model, the vulnerability functions that describe the distribution of losses for a set of intensity measure levels, and the exposure model defining the distribution of elements that are exposed to the hazard.

Within the logic tree approach, different options have been considered to better evaluate the uncertainties present in the framework, such as the seismic sources zonation, various damage criteria and the use of different spatial resolutions for the exposure model. This method has been applied to Portugal in order to provide a recent development of the aspects that influence the hazard and the risk of that area, identifying the most vulnerable areas to seismic events with their expected losses probability.

In order to deeply evaluate a seismic risk model when an earthquake hit a city, an extensive risk management strategy that considers the direct impact, physical damage and also all the indirect impacts such as the socio-economics aspects, need to be assess. The proof of the importance of this approach is also given by the holistic approach proposed by Salgado et al. (Salgado et al., 2016). This study took into consideration all the aspects of the framework useful for decision-making processes and for quantifying the resilience of the case studies considered. This work consisted of performing a process where uncertainties related to physical damage and loss assessment are considered using probabilistic methodologies. Focusing on the whole process, in this study the Urban Seismic Risk *USR* was calculated, starting from a physical risk index R_F, which represents the level of risk for structural elements, and by considering an aggravating coefficient F in which there are included socioeconomic fragilities and lack of resilience of the context. The urban seismic risk is calculated with the expression known as Moncho's equation (Carreño et al.,2012):

$$USR_i = R_F(1+F) \qquad\qquad (3.10)$$

where the subscript i represents all the set of factors as well as their associated weights useful to calculate the physical index. Figure 3-11a and Figure 3-11b showed the R_F and the F results respectively for the considered country, while Figure 3-11c showed the urban seismic risk USR representing the combination of the two previous factors.

(a)   (b)   (c)
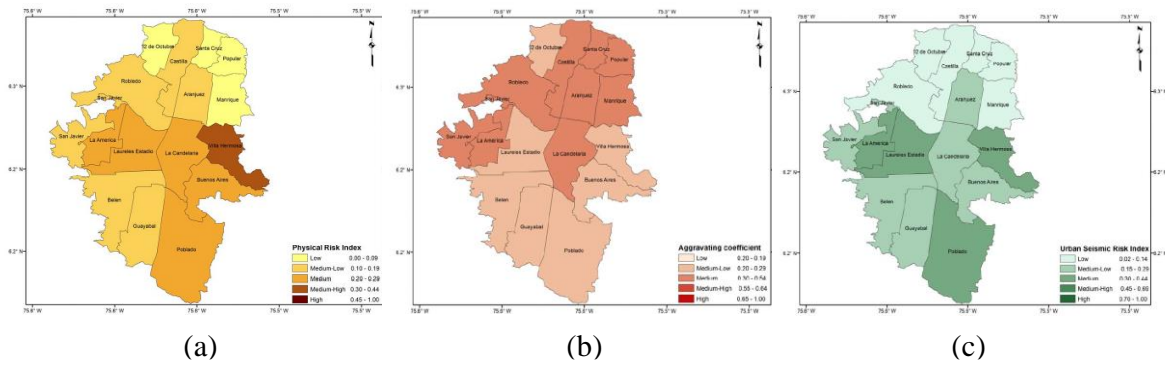
Figure 3-11. Results for the country of Medellin (Colombia): (a) R_F results; (b) F results and (c) USR results (Salgado et al., 2016)

With their work, the authors wanted to show how multidisciplinary studies on disaster risk reduction can be helpful and how they can be of relevance for decision-making processes in the disaster risk management.

The importance of a full understanding of the limitations, needs and prioritization of the risk assessment estimation is of a primary importance for the decision makers. The study of Foulser-Piggott et al. (Foulser-Piggott et al., 2020) presented a model framework that helps to avoid the underestimation or overestimation of the risk, by means of the treatment of uncertainties in inputs variables, their propagation through the model, and their effect visible on the results. In particular, four sources of uncertainties have been considered in the study: the spectral acceleration; the site condition; the conversion of spectral acceleration to Modified Mercalli Intensity MMI (these related to the seismic hazard calculation, considered independent and not correlated) and the vulnerability relationship. The assumption of uncorrelation/correlation deserves attention because it has implications on the calculation of the overall uncertainty. Indeed, if the uncertainties are assumed to be independent but they are correlated, a double counting of uncertainties and an overestimation of uncertainty is collected. On the other hand, when uncertainties are actually independent but they are assumed not to be independent, the uncertainty could be underestimated. Therefore, global sensitivity analysis has been conducted to define the importance of each of the uncertain variables. The results showed that the uncertainty

on the MMI conversion and on the mean collapse ratios have the largest effect on the calculation of the annual collapse probability for the case studies.

A deep study on the treatment of uncertainties has been made also for seismic risk analysis of transportation system (Stergiou and Kiremidjian, 2008). In that study, the authors wanted to evaluate the consequences and losses of seismic events to transportation network and then develop a probabilistic framework where the consequences are quantified.

In this framework, two different kind of uncertainties are included: those related to the replacement cost and those related to the damage factor. In the evaluation of the probability density function of the structural loss, the uncertainties related to the replacement cost are going to increase the risk, while the others do not have the same impact.

The main innovation of this work is that the framework took into account the operational losses from damage, instead of considering only the estimation of the structural loss. The uncertainties in the operational loss estimation regard the demand. Other sources of uncertainty are related with the socioeconomic factors, such as the value of the time or the passenger-car occupancy. Moreover, the study provided an accurate investigation of methods for the estimation of structural losses, seeking for more advance methodologies that took into account the uncertainties ignored so far.

For what concern the damage factor, the authors have been considered a probabilistic distribution, a truncated normal distribution, and have been assumed that the mean value were the value of the central damage factor with a variation of 30% (Figure 3-12).
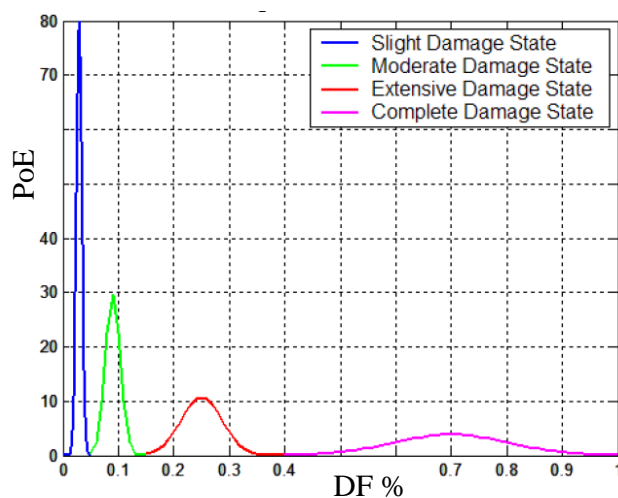
Figure 3-12. Probability density functions for damage factors for the damage states considered (Stergiou and Kiremidjian, 2008)

For what concerns the replacement cost of the structure, it is generally estimated by experts considering future predictions for labour cost, cost of materials, and the resources needed nowadays. The mean value of the replacement cost of a bridge is the product of its deck area and its comparative cost, and the standard deviation is assumed to be 50% of the mean value.

In addition to the analyses on the impact of uncertainties, also the communication and perception of the risk and of their uncertainty, became important (Bostrom et al., 2008). The decision-making process employs a competent communication of the risk and uncertainty. For risk communicators to achieve the risk communication goals, the influence of the perception and cognition is a key point in the visualizations of risk and uncertainty. Indeed, the study of Bostrom et al. proposed findings from past research and a review of the criteria to evaluate the accuracy, the accessibility, the perceived risk, the subjective measures of quality and usefulness and the effect of the risk visualization. Moreover, the work focused on the relationship between risk assessment, risk perception, risk communication and risk visualization, with the help of the GIS software to visualize natural disaster. A framework to evaluate the risk visualization is proposed. It is based on simple statistical graphics that represent a risk communication aids, and on visualization attributes that include the use of colours, interactivity, animation, virtual reality and 2D/3D dimensionality. To classify the uncertainty, they used two approaches: the first based on how the uncertainty is represented, and the second on how the uncertainty is defined into the visualization process.

Chapter's References

Atkinson, G., 2011. An empirical perspective on uncertainty in earthquake ground motion prediction. Canadian Journal of Civil Engineering 38, 1002–1015. https://doi.org/10.1139/L10-120

Baker, J., 2005. Vector-valued ground motion intensity measures for probabilistic seismic demand analysis (co-published as Blume Center Technical Report #150 and PEER Technical Report 2006/08). PhD thesis, Stanford University, Stanford, California.

Baker, J.W., Allin Cornell, C., 2005. A vector-valued ground motion intensity measure consisting of spectral acceleration and epsilon. Earthquake Engng Struct. Dyn. 34, 1193–1217. https://doi.org/10.1002/eqe.474

Bazzurro, P., Luco, N., 2007. Effects of different sources of uncertainty and correlation on earthquake-generated losses. Australian Journal of Civil Engineering 4, 1–14. https://doi.org/10.1080/14488353.2007.11463924

Bier, V.M., Lin, S.-W., 2013. On the Treatment of Uncertainty and Variability in Making Decisions About Risk. Risk Analysis 33, 1899–1907. https://doi.org/10.1111/risa.12071

Björklund, A., 2002. Survey of approaches to improve reliability in LCA. The International Journal of Life Cycle Assessment 7, 64–72. https://doi.org/10.1007/BF02978849

Bostrom, A., Anselin, L., Farris, J., 2008. Visualizing seismic risk and uncertainty: a review of related research. Ann N Y Acad Sci 1128, 29–40. https://doi.org/10.1196/annals.1399.005

Carreño Tibaduiza, M., Cardona, O., Barbat, A., 2012. New methodology for urban seismic risk assessment from a holistic perspective. Bulletin of Earthquake Engineering 10, 547–565. https://doi.org/10.1007/s10518-011-9302-2

Cornell, C.A., 1968. Engineering seismic risk analysis. Bulletin of the Seismological Society of America 58, 1583–1606.

Cornell, C.A., Jalayer, F., Hamburger, R.O., Foutch, D.A., 2002. Probabilistic Basis for 2000 SAC Federal Emergency Management Agency Steel Moment Frame Guidelines. Journal of Structural Engineering 128, 526–533. https://doi.org/10.1061/(ASCE)0733-9445(2002)128:4(526)

Dall'Asta, A., Dabiri, H., Tondi, E. Morici, M., 2021. Influence of time-dependent seismic hazard on structural design. Bulletin of Earthquake Engineering 19, 2505–2529. https://doi.org/10.1007/s10518-021-01075-3

De Koning, A., Schowanek, D., Dewaele, J., Weisbrod, A., Guinée, J., 2010. Uncertainties in a carbon footprint model for detergents; quantifying the confidence in a comparative result. Int J Life Cycle Assess 15, 79. https://doi.org/10.1007/s11367-009-0123-3

De Santis, A., Cianchini, G., Favali, P., Beranzoli, L., Boschi, E., 2011. The Gutenberg–Richter Law and Entropy of Earthquakes: Two Case Studies in Central Italy. Bulletin of the Seismological Society of America 101, 1386–1395. https://doi.org/10.1785/0120090390

Der Kiureghian, A., 1996. Structural reliability methods for seismic safety assessment: a review. Engineering Structures 18, 412–424. https://doi.org/10.1016/0141-0296(95)00005-4

Der Kiureghian, A., Ditlevsen, O., 2009. Aleatory or epistemic? Does it matter? Structural Safety, Risk Acceptance and Risk Communication 31, 105–112. https://doi.org/10.1016/j.strusafe.2008.06.020

Dolšek, M., 2012. Simplified method for seismic risk assessment of buildings with consideration of aleatory and epistemic uncertainty. Structure and Infrastructure Engineering 8, 939–953. https://doi.org/10.1080/15732479.2011.574813

Ellingwood, B.R., Kinali, K., 2009. Quantifying and communicating uncertainty in seismic risk assessment. Structural Safety, Risk Acceptance and Risk Communication 31, 179–187. https://doi.org/10.1016/j.strusafe.2008.06.001

Foulser-Piggott, R., Bowman, G., Hughes, M., 2020. A Framework for Understanding Uncertainty in Seismic Risk Assessment. Risk Anal 40, 169–182. https://doi.org/10.1111/risa.12919

Groen, E.A., 2016. An uncertain climate: the value of uncertainty and sensitivity analysis in environmental impact assessment of food. https://doi.org/10.18174/375497

Gutenberg, B., Richter, C.F., 1956. Earthquake magnitude, intensity, energy, and acceleration(Second paper). Bulletin of the Seismological Society of America 46, 105–145.

Gutenberg, B., Richter, C.F., 1944. Frequency of earthquakes in California. Bulletin of the Seismological Society of America 34, 185–188.

Iervolino, I., Cornell, C.A., 2005. Record Selection for Nonlinear Seismic Analysis of Structures. Earthquake Spectra 21, 685–713. https://doi.org/10.1193/1.1990199

International Nuclear Safety Group-INSAG-25, 2011. A Framework for an Integrated Risk Informed Decision Making Process. Vienna International Atomic Energy Agency, Vienna.

Ioannou, I., Douglas, J., Rossetto, T., 2015. Assessing the impact of ground-motion variability and uncertainty on empirical fragility curves. Soil Dynamics and Earthquake Engineering 69, 83–92. https://doi.org/10.1016/j.soildyn.2014.10.024

Jalayer, F., Beck, J.L., Porter, K.A., Hall, J.F., 2004. Effects of ground motion uncertainty on predicting the response of an existing RC frame structure. Presented at the 13th World Conference on Earthquake Engineering, Vancouver, B.C., Canada, p. 14.

Jalayer, F., Cornell, C.A., 2003. A Technical Framework for Probability-Based Demand and Capacity Factor Design (DCFD) Seismic Formats (No. PEER Report 2003/08). Pacific Earthquake Engineering Center College of Engineering University of California Berkeley.

Kalakonas, P., Silva, V., Mouyiannou, A., Rao, A., 2020. Exploring the impact of epistemic uncertainty on a regional probabilistic seismic risk assessment model. Natural Hazards: Journal of the International Society for the Prevention and Mitigation of Natural Hazards 104, 997–1020.

Katsanos, E., Sextos, A.G., Manolis, G.D., 2010. Selection of earthquake ground motion records: A state-of-the-art review from a structural engineering perspective. SOIL DYN EARTHQ ENG 30, 157–169. https://doi.org/10.1016/j.soildyn.2009.10.005

Linkov, I., Burmistrov, D., 2003. Model Uncertainty and Choices Made by Modelers: Lessons Learned from the International Atomic Energy Agency Model Intercomparisons. Risk Analysis 23, 1297–1308. https://doi.org/10.1111/j.0272-4332.2003.00402.x

Luco, N., Cornell, C.A., 2007. Structure-Specific Scalar Intensity Measures for Near-Source and Ordinary Earthquake Ground Motions. Earthquake Spectra 23, 357–392. https://doi.org/10.1193/1.2723158

Padgett, J.E., DesRoches, R., 2007. Sensitivity of Seismic Response and Fragility to Parameter Uncertainty. Journal of Structural Engineering 133, 1710–1718. https://doi.org/10.1061/(ASCE)0733-9445(2007)133:12(1710)

Pinto, P.E., 2001. Reliability methods in earthquake engineering. Progress in Structural Engineering and Materials 3, 76–85. https://doi.org/10.1002/pse.64

Porter, K., 2021. A Beginner's Guide to Fragility, Vulnerability, and Risk, in: Beer, M., Kougioumtzoglou, I.A., Patelli, E., Au, I.S.-K. (Eds.), Encyclopedia of Earthquake Engineering. Springer Berlin Heidelberg, Berlin, Heidelberg, pp. 1–29. https://doi.org/10.1007/978-3-642-36197-5_256-1

Rathje, E., Kottke, A., Trent, W., 2010. Influence of Input Motion and Site Property Variabilities on Seismic Site Response Analysis. Journal of Geotechnical and Geoenvironmental Engineering - J GEOTECH GEOENVIRON ENG 136. https://doi.org/10.1061/(ASCE)GT.1943-5606.0000255

Salgado-Gálvez, M.A., Zuloaga Romero, D., Velásquez, C.A., Carreño, M.L., Cardona, O.-D., Barbat, A.H., 2016. Urban seismic risk index for Medellín, Colombia, based on probabilistic loss and casualties estimations. Nat Hazards 80, 1995–2021. https://doi.org/10.1007/s11069-015-2056-4

Saltelli, A., Ratto, M., Andres, T., Campolongo, F., Cariboni, J., Gatelli, D., Saisana, M., Tarantola, S., 2008. Global Sensitivity Analysis. The Primer. John Wiley & Sons, Ltd, Chichester, UK. https://doi.org/10.1002/9780470725184

Silva, V., 2019. Uncertainty and Correlation in Seismic Vulnerability Functions of Building Classes. Earthquake Spectra 35, 1515–1539. https://doi.org/10.1193/013018EQS031M

Silva, V., Crowley, H., Varum, H., Pinho, R., 2014. Seismic risk assessment for mainland Portugal. Bull Earthquake Eng 13, 429–457. https://doi.org/10.1007/s10518-014-9630-0

Stergiou, E., Kiremidjian, A., 2008. Treatment of uncertainties in seismic risk analysis of transportation systems / (No. PEER Report 2008/02). Pacific Earthquake Engineering Research Center College of Engineering University of California.

Thompson, K.M., 2002. Variability and Uncertainty Meet Risk Management and Risk Communication. Risk Analysis 22, 647–654. https://doi.org/10.1111/0272-4332.00044

Tinti, S., Mulargia, F., 1985. Effects of magnitude uncertainties on estimating the parameters in the Gutenberg-Richter frequency-magnitude law. Bulletin of the Seismological Society of America 75, 1681–1697.

Tubaldi, E., Barbato, M., Dall'Asta, A., 2012. Influence of Model Parameter Uncertainty on Seismic Transverse Response and Vulnerability of Steel–Concrete Composite Bridges with Dual Load Path. Journal of Structural Engineering 138, 363–374. https://doi.org/10.1061/(ASCE)ST.1943-541X.0000456

Walker, W.E., Harremoës, P., Rotmans, J., Sluijs, J.P. van der, Asselt, M.B.A. van, Janssen, P., Krauss, M.P.K. von, 2003. Defining Uncertainty: A Conceptual Basis for Uncertainty Management in Model-Based Decision Support. Integrated Assessment 4, 5–17. https://doi.org/10.1076/iaij.4.1.5.16466.

Chapter 4.

Application of the empirical method

4.1 Introduction

Historical constructions such as churches, towers, palaces, fortresses and other defensive structures acquire cultural significance over time and constitute a significant part of the cultural heritage (International Charter of Venice, ICOMOS 1964). The awareness of the cultural heritage value contributed to the development of measures for risk prevention planning as well as risk reduction all over the world (Despotaki et al. 2019; Vicente et al. 2018). Attention to the world heritage is increasing due to its exposure to major natural risks, such as earthquakes, landslides, slope movements and groundwater activities. For example, a collection of valuable data on historic monuments worldwide, have been evaluated by the Commission 16 (Engineering Geology and Protection of Ancient Monuments and Archaeological Sites) of the International Association of Engineering Geology (IAEG, 2003), with special focus on geotechnical and geological conditions. An overview of studies on geological hazard for cultural and natural heritage can be found in Pavlova et al. (2015). Among historical masonry constructions, churches have a special role in the Italian architectural heritage as they are widespread (from urban to rural and mountainous areas), have generally significant importance for local communities, and very often present high artistic value.

Italy is known for its considerable number of historical churches constituting a very important part of the cultural heritage for the country. Unfortunately, the Italian territory is a highly seismically active area and the effects of earthquakes on the cultural heritage can be destructive, as demonstrated by the events in the last

years, such as Irpinia earthquake (1980), Umbria Marche earthquake (1997), Molise earthquake (2002), L'Aquila earthquake (2009), Emilia Romagna earthquake (2012), Central Italy seismic sequence (2016).

From a structural point of view, the seismic response of churches is complex, characterized by a mix of local and global damage mechanisms, and their seismic vulnerability is higher than that of ordinary masonry buildings (Sorrentino et al. 2019). Their poor seismic performance, demonstrated by recurrent seismic damage, is due to specific architectural configurations, characterized by large halls, slender walls, absence of internal diaphragms, and presence of vaults and arches.

This chapter presents different applications of the empirical method for the assessment of the vulnerability and risk functions of historical churches. The method, presented in Chapter 2, represents the basics for the following implementations and applications. The objective is to understand the seismic behavior of historical churches, firstly directed at analysing the observed damage and vulnerability, and comparing them to those available in literature. After this prime phase, the chapter aims to develop empirical predictive model for the seismic damage and for the economic losses in a probabilistic way, in order to fill the gap of knowledge on the seismic risk and repairing cost of the cultural heritage.

General observations and the main features of the seismic sequence that seriously damaged many historical buildings are presented and detailed. The importance of the historical churches and their architectural background related to the Marche Region is then documented and highlighted.

After this general introduction, in the first part of this Chapter the observational damage of the Marche Region churches from post seismic sequence of Central Italy 2016 is analysed. Indeed, such seismic activity seriously damaged many historical buildings and particularly churches, due to their intrinsic inability to develop an efficient box-like resisting mechanism. Collected data were then processed to give insight into the occurred damage and to evaluate the vulnerability of the religious buildings in the Region. Subsequently, the most recurring damage mechanisms are identified, and a global damage index of each church is computed. The distribution of the damage over the Region is commented, as a function of the macro-seismic intensity. Finally, the overall damage of the sample is compared to that estimated through empirical models available in literature. In addition, the churches were grouped into homogeneous typologies characterized by similar structural response, to derive empirical fragility curves. In fact, a fragility model is proposed for the considered dataset by evaluating relevant parameters using the Maximum Likelihood Estimation (MLE). From the defined fragility curves, the global damage index function is derived and compared with the curve obtained by fitting data registered on field with a Sum Square Estimation (SSE) technique, as well as with the results from past research related to previous seismic events.

In the last section of the chapter, an empirical response model is defined starting from observed damage of churches and recorded ground motions. In particular, the damage is expressed by a continuous index and the seismic action is described by a scalar intensity measure. Only churches falling into the area hit by the Central Italy 2016 seismic sequence are chosen to calibrate the parameters of the proposed predictive model. The

considered sample covers a wide range of damage and intensity levels, and it includes all the churches of the specific area and in particular the damaged, undamaged and collapsed ones. The parameters of the model have been evaluated using the MLE, considering a double step in the optimization procedure that combines a discrete with a continuous approach. Alternative proposals for the shape functions used in the numerical approximation and the results are discussed. In addition, potentiality of risk assessment in the decision-making process is shown by applying the predictive model to evaluate the damage scenario after a simulated seismic event. Finally, a repairing cost model is proposed based on a probabilistic consequence model that relates the repairing costs of historical churches with the seismic damage defined on the basis of the empirical damage model previously presented. Two different distribution functions have been proposed to infer dataset from surveys; the model parameters have been determined by using the maximum likelihood method with three different couple of polynomial expressions for the better data fit. The predictive repairing cost model and the procedure developed to evaluate relevant parameters are based on a dataset formed by historical churches that have reported a repairing cost value or an economic contribution furnished by the Italian Government after the 2016 Central Italy seismic sequence. A final demonstrative application is presented in order to illustrate the potential use of the model in the prediction of repairing cost scenarios.

4.2 Post Earthquake damage and vulnerability assessment of churches in Marche region using discrete and continuous approaches

The Italian architectural heritage is constituted by a large number of historical masonry constructions characterized by structural and typological vulnerabilities usually responsible for poor seismic performances. The latest 2016 Central Italy sequence was no exception; architectural heritage suffered serious damage and extensive collapse in the areas closer to the epicentres as well as substantial loss of artistic contents even in the case of low or moderate damage of the structural components (Rossi et al. 2019; Sextos et al. 2018; Stewart et al. 2018). These intrinsic characteristics, combined with the high cultural value of historical constructions and the medium-high seismicity of the many areas of the Italian territory, often lead to a significant seismic risk.

In fact, among historical masonry constructions in Central Italy, churches have a special role in the national architectural heritage as they are widespread (both in urban, rural, and mountainous areas), they have generally significant importance for local communities, and very often present high artistic value. Following the 2016 Central Italy seismic sequence, many churches suffered serious damage and extensive collapse, including substantial losses of the artistic contents, even in the case of low and moderate damage of the structure. Damage following the main seismic events revealed that the seismic response of churches is often complex, characterized by a mix of local and global mechanisms. Generally, local mechanisms prevail over global ones due to the typical architecture of churches, constituted by a number of parts, known as macro-elements (Doglioni et al., 1994), e.g. façade, side walls, transept, apse, nave, and side aisles, characterized by independent seismic behaviours. Such independency of the seismic response of macro-elements is typically a consequence of the considerable slenderness of walls, the absence of intermediate floors, the poor interlock of

walls, the presence of arches and vaults with not opposed thrust, and the presence of deformable wooden roofing.

This typical behaviour was confirmed by a number of subsequent analytical studies on the vulnerability assessment of single churches (Mele et al. 2003; Casarin and Modena 2008; Betti and Vignoli 2008, 2011; De Matteis and Mazzolani 2010; Baraccani et al. 2015; Fortunato et al. 2017; Berto et al. 2017), as well as by studies on sets of churches located in specific areas (D'Amato et al. 2018; Fabbrocino et al. 2019; Fuentes et al. 2019). Moreover, the analysis of the observed damage after the Umbria-Marche 1997 earthquake, (Lagomarsino and Podestà 2004a,b; Giovinazzi and Lagomarsino 2004) Molise 2002 earthquake, (Lagomarsino and Podestà, 2004c) L'Aquila 2009 earthquake, (Lagomarsino 2012; da Porto et al. 2012; De Matteis et al. 2019), Emilia 2012 earthquake (Indirli et al. 2012; Sorrentino et al. 2014) and Central Italy 2016 (Carbonari et al. 2019; Salzano et al. 2019; Penna et al. 2019; Cescatti et al. 2019; Di Ludovico et al. 2019; De Matteis and Zizi. 2019) as well as earthquakes in the Azores (Guerreiro et al. 2000), New Zealand (Goded et al. 2014; Leite et al. 2013; Marotta et al. 2017) and Mexico (Peña and Chávez 2015), confirmed their high vulnerability, and demonstrated that damage mechanisms have recurrent features, despite the peculiarities and uniqueness of each construction.

Based on these observations, Lagomarsino and Podestà (Lagomarsino 1998; Lagomarsino and Podestà 2004a, 2004b) proposed a survey form for post-earthquake damage assessment of churches, based on 18 indicators representative of collapse mechanisms associated to common macro-elements. Subsequent improvements of the survey form and of the seismic damage assessment methodology, led to the current procedure and survey form (DPCM, 2006; Modello A-DC PCM-DPC MiBAC, 2006), which is based on the classification of damage relevant to 28 mechanisms. Damage of mechanisms is graded according to a 0 to 5 numerical scale (Grünthal 1998) and the results are combined to obtain a global damage index. Furthermore, the form is completed with information on the church safe usability, suggestions about required provisional interventions to avoid collapses (e.g. due to aftershocks), brief descriptions of any artworks and valuable objects as well as their possible damage.

4.2.1 General features of the seismic sequence

The seismic sequence that struck central Italy began on August 24th, 2016 with the mainshock of magnitude Mw 6.0, whose hypocentre was located at the borders of the Lazio, Abruzzo, Marche, and Umbria regions, about 2.5 km north-east of the village of Accumoli at depth of 8 km. This first event produced 299 casualties and huge damage to both private and public buildings, including cultural heritage. Near the epicentre, Peak Ground Accelerations (PGAs) of about 0.45 g were recorded, with a maximum peak of 0.86 g in Amatrice. Another mainshock of Mw 5.9 occurred on October 26th and afterwards, on October 30th, the largest shock of the sequence, characterised by Mw 6.5, took place, with the epicentre located between the village of Norcia, Preci, and Castelsantangelo sul Nera (Umbria Region) with a 9.4 km deep hypocentre. During the latter mainshock, the maximum PGA recorded nearby the epicentre was about 0.48g with a peak of 0.76g recorded

in Arquata del Tronto, probably due to the local site amplification (Laurenzano et al. 2018). Overall, in the area interested by the seismic sequence, about 6500 aftershocks with Mw ranging between 2.3 and 5.5 occurred between August 2016 and January 2017.

The shake maps of the mainshocks in terms of PGA are shown in Figure 4-1a, b, c, together with the epicentre locations. Maps, which were obtained by post-processing data provided by the Italian National Institute of Geophysics and Volcanology (INGV) through the QGIS software (QGIS Development Team 2015), were computed assuming that the ground motion intensity at each location is lognormally distributed, combining the instrumental measurements of accelerations with information about local geology, earthquake location and magnitude (INGV Shake maps data). It should be noted that the measures of the PGAs evaluated by INGV do not consider specific amplifications due to the site effects (e.g. basin and peak effect).
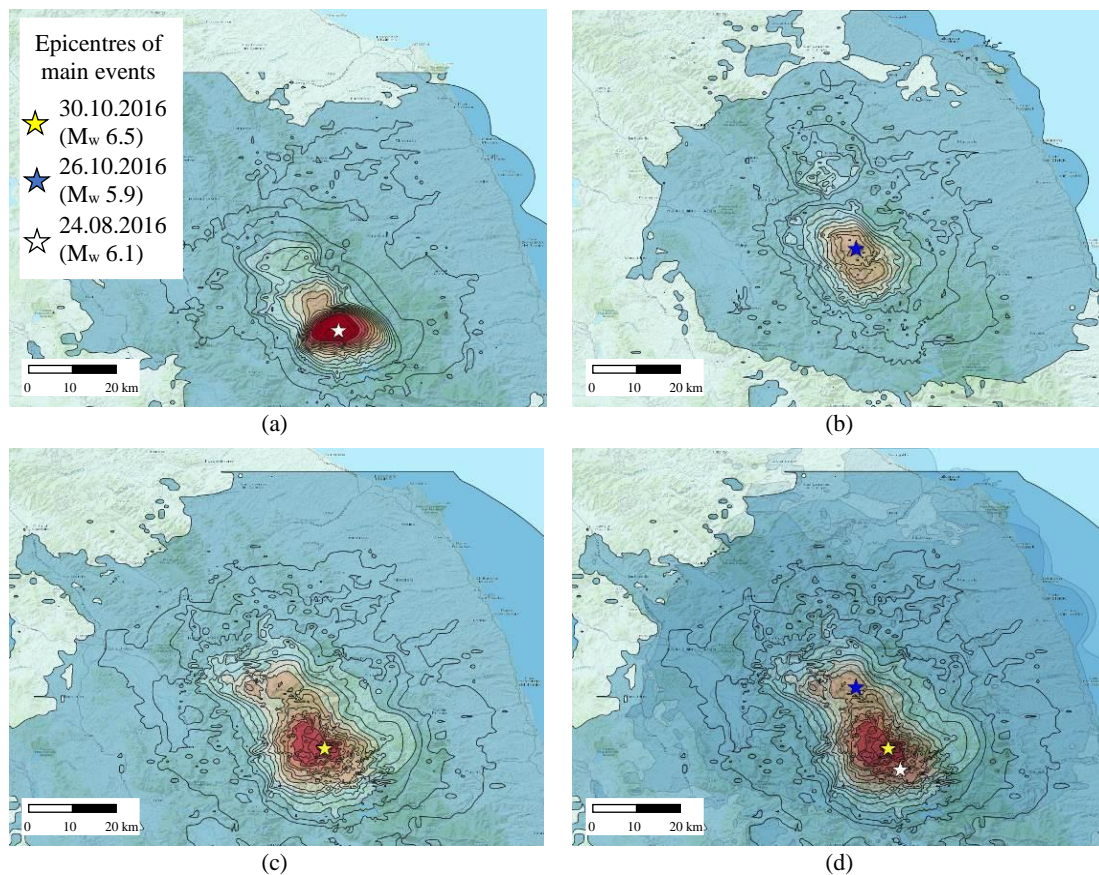
Figure 4-1. Maximum PGA registered after the mainshocks: (a) earthquake of August 24th; (b) earthquake of October 26th; (c) earthquake of October 30th; (d) envelope of the 2016 seismic sequence.

4.2.2 Database definition and statistical analysis

4.2.2.1 Architectural background of the historical churches

The Marche Region has always been a meeting point of cultures, styles, people and local traditions, which had to face the new architectural trends (Gizzi, 2017). For this reason, it is not easy to identify a common origin for the ecclesiastical architecture. Religious buildings are characterized by a variability of their architectural form, construction techniques, and adopted materials. Therefore, cataloguing churches into recurring typologies is often a not straightforward task. Different approaches could be followed, e.g., based on the construction period, architectural style, construction materials and techniques, or site geomorphological conditions.

Regarding the classification based on the construction period, attention should be made to the appropriate consideration of transformations, enlargements, and reconstructions that modified the original architectural organisms, especially after the severe earthquakes that struck the Region in the past. Indeed, the cultural heritage of the Marche Region underwent seismic damage and collapses as a consequence of poor material quality, design defects, and the non-uniform construction process.

The classification based on the architectural styles is even more complex due to the possible mixture of different architectural influences. Nevertheless, it is possible to consider the alternative of ordering churches on the basis of their architectural style, referring to the prevalent period of construction.

Accordingly, the following categories are identified:

(i)   Medieval type (construction period up to the XIV century),

(ii)   Renaissance type (construction period between the XV and XVI centuries),

(iii)   Baroque type (construction period between the XVII and XVIII centuries),

(iv)   Neoclassic type (construction period after the XIX century).

A considerable number of churches were built in the XV, XVI and XVII centuries; many of these are characterized by a typical Renaissance Latin cross plan. In the XVIII century, baroque changes of the interiors were made, in addition to the construction of new churches with a central plan, mainly elliptical, covered by complex vaults and impressive decorations, typical of the Baroque style. Medieval churches are numerically prevalent (from the XI century to the end of the XIII century) and constitute one of the greatest artistic heritage of the Region. Among them, Romanesque churches present a regular plant and are characterized by complex narrative cycles demonstrating influences from different styles (Ravenna, Dalmatia and Byzantium styles are mixed with French and Germanic themes, as well as with Umbria, Abruzzo and Tuscan styles). In the XIII century, a clear influence of the southern architecture (especially that of the Puglia Region) of the Svevo period is evident (Wagner-Rieger, 1957), enriching the simple Romanesque style with new figurative elements. Along the valleys of the Potenza, Chienti and Tenna rivers, or in remote places of the Apennines, important centres

of spirituality grow up. The monastic orders constructed abbeys and convents, in which churches are devoted to the hospitality of the local communities (Cherubini, 2000). When construction materials and techniques are examined based on the results of the inspections reported in the survey forms, difficulties related to the geographical area arise. In fact, materials and techniques could significantly vary in different towns or villages, regardless the fact that churches belong to the same period or typology. The church location, namely the geomorphological conditions of the construction site, i.e., plain, slope, backfill, valley, crest, indeed influenced the configurations of the churches. Thus, the church location could work as a possible characterization of the church for cataloguing.

4.2.2.2 Damage data processing

The peculiarities of the 2016 Central Italy seismic sequence, characterized by a significant number of important events, must be carefully considered in the damage analysis based on post-earthquake surveys, considering their actual temporal evolution. Inspections on churches began soon after the first event on 24th August and stopped after the earthquakes on 26th and 30th October, for safety reasons. Later, surveys restarted in November 2016. Thus, the damage analysis required each church being associated to the corresponding maximum value of PGA experienced during the seismic sequence up to the time of inspection. Consequently, for churches inspected until October 26th, the shake map relevant to the event of August 24th was considered (Figure 4-1a), while for churches inspected starting from November the shake map obtained from the envelope of accelerations of the three main events was assumed (Figure 4-1d).

In particular, following the seismic crisis started on August 24th, teams of specialized technicians were activated to inspect churches of the territory and to assess the occurred damage, in order to evaluate building usability, potential risks for public safety, need of immediate provisional interventions. Such teams were coordinated by the Department of Civil Protection (DPC) and the Ministry of Cultural Heritage (MiBACT), through structures operating within the Command and Control Direction (Dicomac) and the regional offices. Each team was composed by MiBACT's officials as well as structural engineers of the Seismic Engineering Laboratory Network (ReLUIS). In addition, staff of the Italian Fire Corp was included when necessary to assure safe access to the inspected buildings. During the inspection, the A-DC survey form (Modello A-DC PCM-DPC MiBACT, 2006) was compiled. The form is composed of several sections: the first one collects general information of the church (e.g. name, construction period, geographical position, the value of artworks in the building, etc.), data relevant to planar and volumetric layout and dimensions, and the overall state of preservation. In the second section, macro-elements that may be potentially activated, and the relevant visible damage (with the specification of the seismic or non-seismic origin), are addressed, together with access restrictions and requirement of urgent and/or provisional actions to assure public safety and heritage preservation. In the last part of the survey form, a description of artworks contained in the church, the damage suffered, and the urgent provisional interventions for their preservations are required.

Overall, teams composed by structural engineers of the University of Camerino and Università Politecnica delle Marche inspected 541 churches, which constitute the sample adopted for the damage analysis and the vulnerability assessment presented in the following sections. Figure 4-2 shows the distribution of the inspected churches within the Region and provides indication of their relevant position with respect to the epicentres of the mainshocks. It is worth noting a reduced concentration of churches in the areas close to the epicentres being such points located in mountainous areas with limited urban and village settlements.

It is remarked that the EMS-98 macro-seismic intensity (IMCS) was considered and computed from the PGA according to correlation

$$I_{MCS} = 6.54 + 1.96 \cdot Log\left(PGA\right) \tag{4.1}$$

proposed by Faccioli and Cauzzi (2006), selected among others proposed in the literature (Capera, et al. 2007) in view of the PGA ranges of applicability (18–600 cm/s2) and its calibration, based on Italian earthquakes. In this sense, the adopted approach can be considered a PGA based methodology; the PGA-derived seismic intensity can be very effective, even though not very commonly used, for determining vulnerability curves for exiting churches (De Matteis and Zizi 2019). Table 4-1 shows the correlation between the macro-seismic intensities and the PGA intervals. Considering that the use of the macro-seismic intensity for the derivation of observational fragility functions is widely adopted in the literature (Lagomarsino and Podestà, 2004b, 2004c; Da Porto et al. 2012; De Matteis et al. 2016; Lagomarsino 2012), according to the macro-seismic approach (Despotaki et al. 2018), the choice of IMCS as IM allowed comparison of the results obtained in this study with similar ones available in the technical literature, as later discussed.
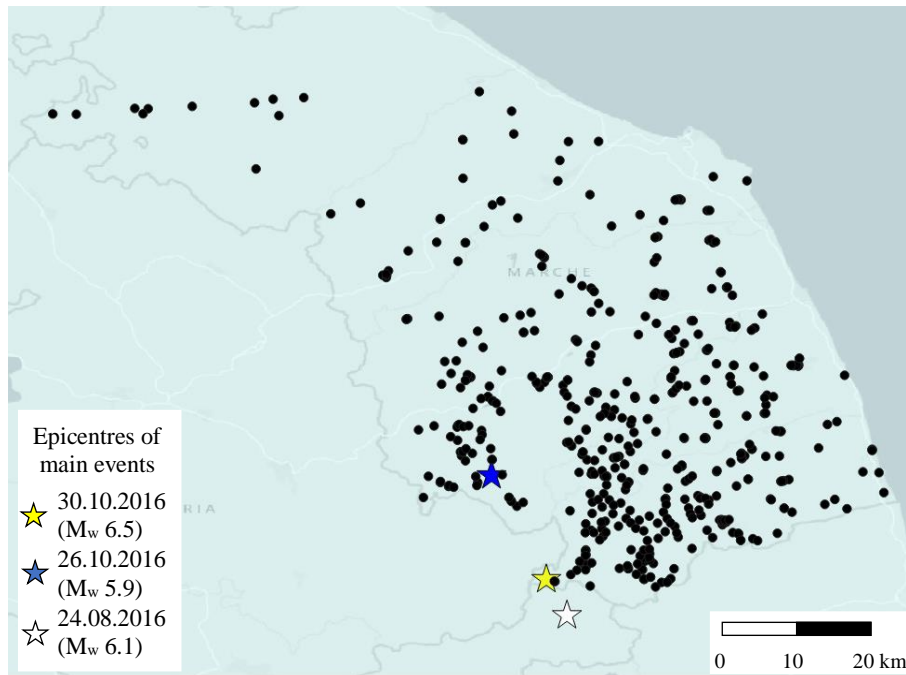
Figure 4-2. Distribution of the inspected churches over the Marche Region and location of the epicentres of the main events.

Table 4-1. Distribution of the sample of churches with the seismic IMs (PGA and I$_{MCS}$).

PGA (g)	<0.009	0.009÷0.030	0.030÷0.090	0.090÷0.310	0.310÷1.020	> 1.020
I$_{MCS}$	<4	5	6	7	8	9
Number of Churches	0	32	334	148	27	0

Taking into account the architectural background previously discussed and the related difficulties in grouping churches of the Marche Region according to architectural styles, a typological sorting of the sample was adopted, as shown in Figure 4-3a.

Although typological groups are not necessarily representative of the expected seismic response, being difficult a direct correlation between structural performance and architectural characteristics of the church (Lagomarsino and Podestà 2004b), they provide indirect information on church importance, quality of materials, and state of preservation (having reasonably assumed that important churches were made of better materials and subjected to periodic maintenance). It is also noted that detailed structural information on the sample churches was not reported by the inspecting teams as out of their reaches. For example, masonry type could not be identified in many cases due to the presence of plaster, it was not possible to clearly assess if vaults were in structural masonry or non-structural "camorcanna" (commonly found in churches and palaces of the Marche Region) as direct inspection was impossible, construction evolutions and relevant discontinuities could not be evaluated due to the lack of time and documentation, foundations could not be accessed. Indeed, acquiring such information would have required an integrated approach involving historic investigations,

material identifications, and accurate geometric and structural survey (e.g., Chellini et al. 2014; Dall'Asta et al. 2019), largely exceeding the scope as well as time and financial resource of post earthquake reconnaissance. Hence, more detailed classifications from a structural point of view of the inspected churches were not feasible. Figure 4-3b shows the distribution of the churches of the sample over the proposed typological classes; most churches fall into categories A and B (70% of the sample), the 23% in the C-H classes, while for the remaining 7% it was not possible to identify a suitable class for the lack of data available in the A-DC survey forms. Assuming five ranges for the plan area (<100 m², 100-200 m², 200-500 m², 500-1000 m² and > 1000 m²), most churches have a surface less than 200 m² (70%), 23% of the sample has a surface ranging between 200 and 500 m² while only 7% has a surface greater than 500 m² (Figure 4-3c).

(a)

(b)

(c)
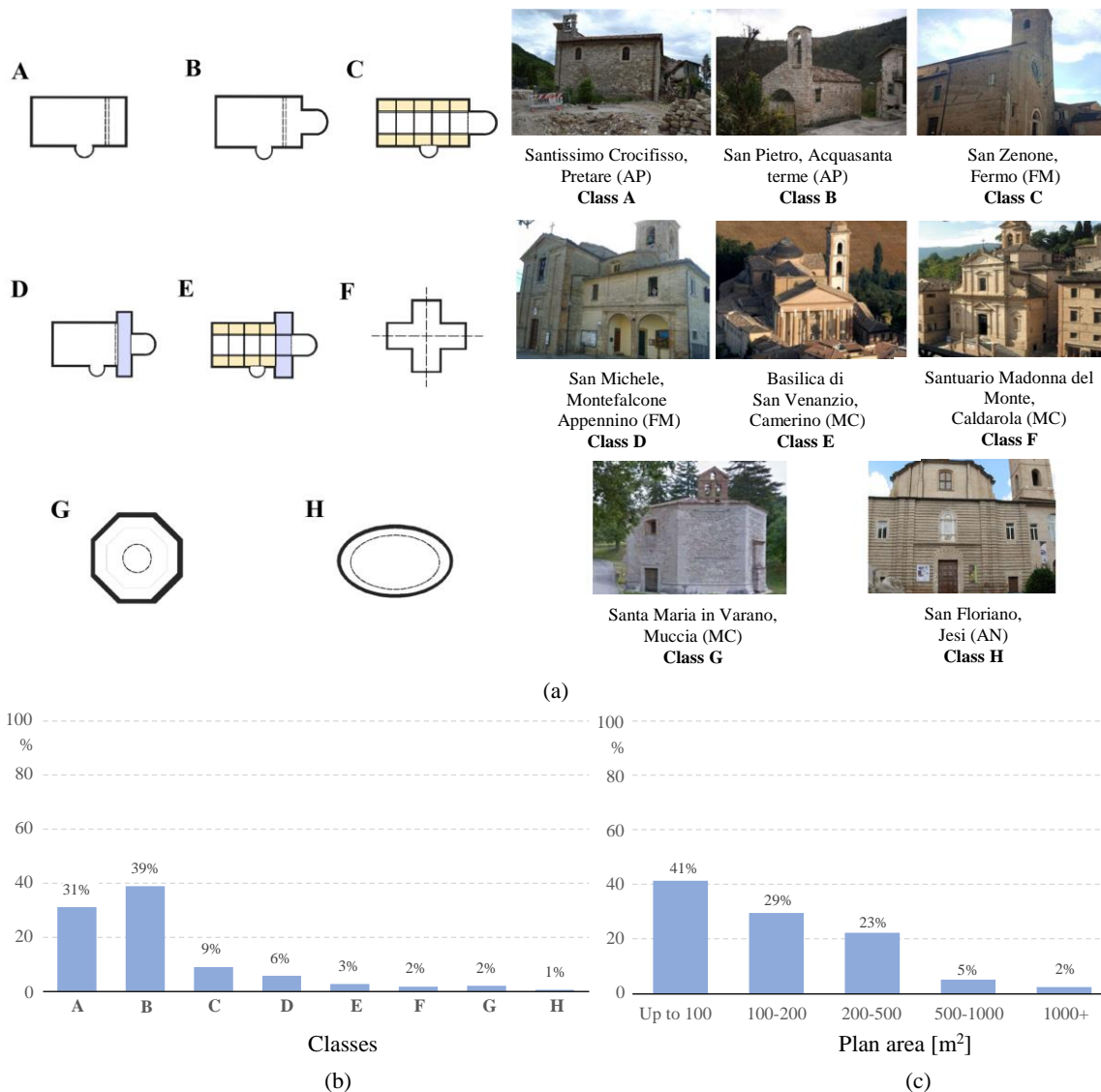
Figure 4-3. Typological classification and sample distribution: (a) schemes of churches plan with examples; (b) typological distribution of the sample; (c) distribution with the plan area.

Considering the above information, in conjunction with data relevant to the distribution of churches over the typological classes, it can be concluded that most part of the sample is constituted by medium-small size churches characterized by a simple layout.

Concerning the state of preservation of the sampled churches, the analysis of the information available in the survey forms led to the distribution reported in Figure 4-4b. A good state of maintenance was observed in almost half of the sample while poor maintenance conditions were noted in only 19.1% of the churches. Figure 4-4a superimposes the state of preservation of each church with the shake map obtained by enveloping accelerations of the mainshocks, in order to provide a big picture and ballpark figure of the unfavorable conditions experienced by some churches due to the combination of experienced PGAs and state of preservation.
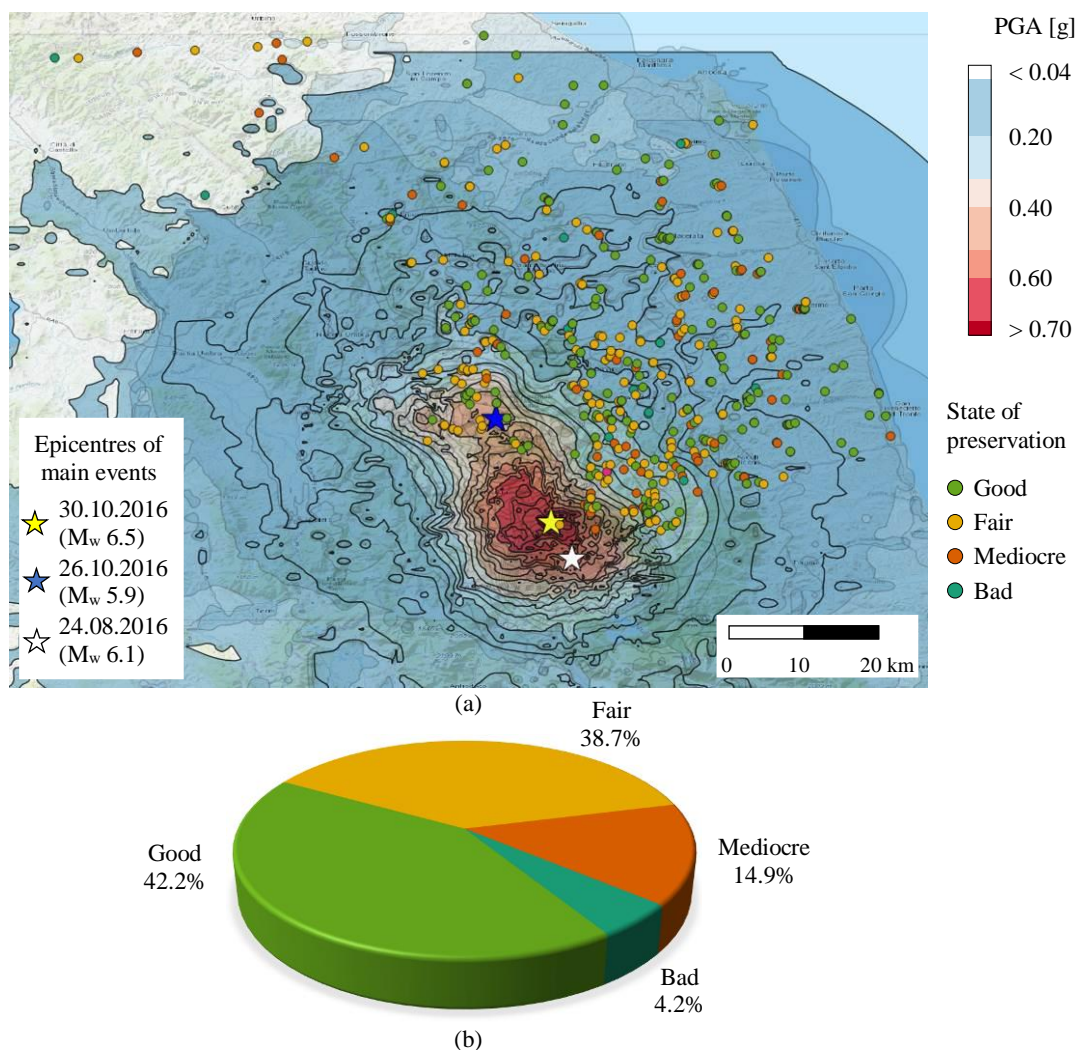
Figure 4-4. State of preservation: (a) map of the state of preservation of churches; (b) distribution of the sample.

Information about the existing structural damage in the sampled churches (i.e. the damage developed before the earthquake on August 24th, 2016) is reported in Figure 4-5b. Data reveal that almost half of the sample exibited no damage, consistently with previous considerations relevant to the state of preservation, and only

12.3% of the sample showed extensive and severe damage; 39.1% of churches were characterized by a limited existing damage. Figure 4-5a superimposes the damage state of each church before the earthquake with the shake map of all the mainshocks, providing useful information to understand the high damage indexes of some churches subjected to moderate accelerations.

(a)

(b)
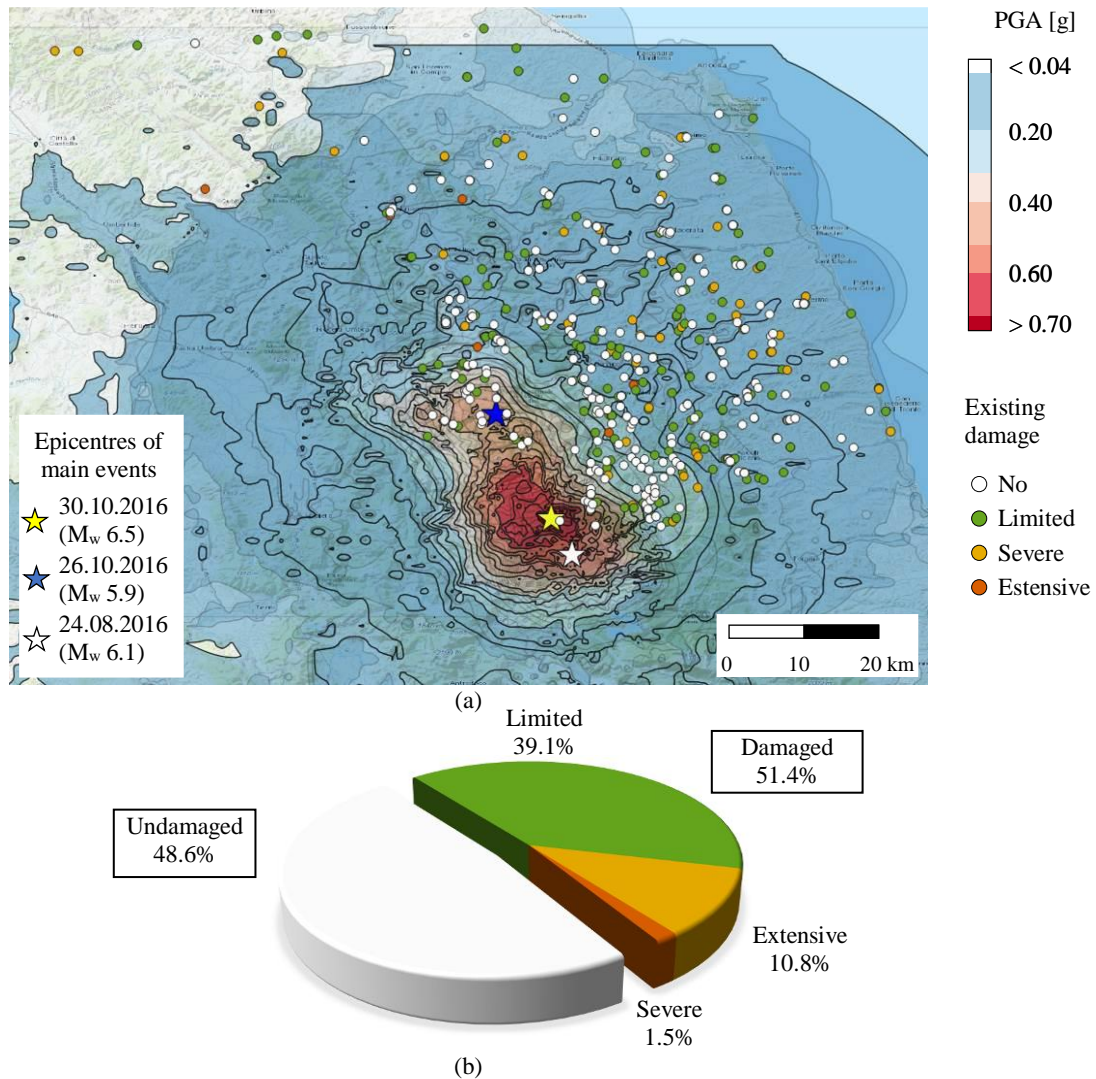
Figure 4-5. Existing damage: (a) map of the existing damage in the churches; (b) distribution of the sample.

Another important feature, useful to understand the observed seismic damage, is the topographic condition of the site where churches are located. By post-processing data from the survey forms, five site configurations (Figure 4-6) were identified. The distribution of the sample over the different topographic conditions is shown in Figure 4-6b. Figure 4-6a superimposes the topographic condition of each church with the shake map in order to highlight possible detrimental effects due to particular site response, such in the case of crest or valley configurations.

(a)

(b)
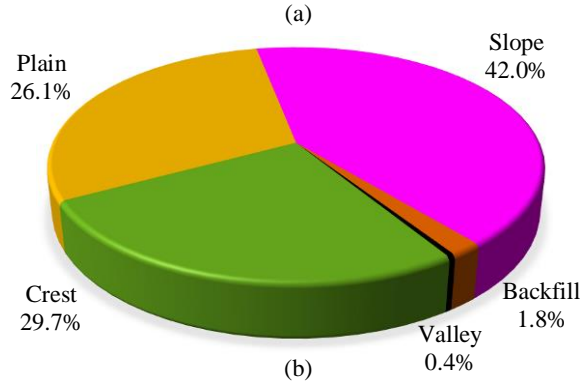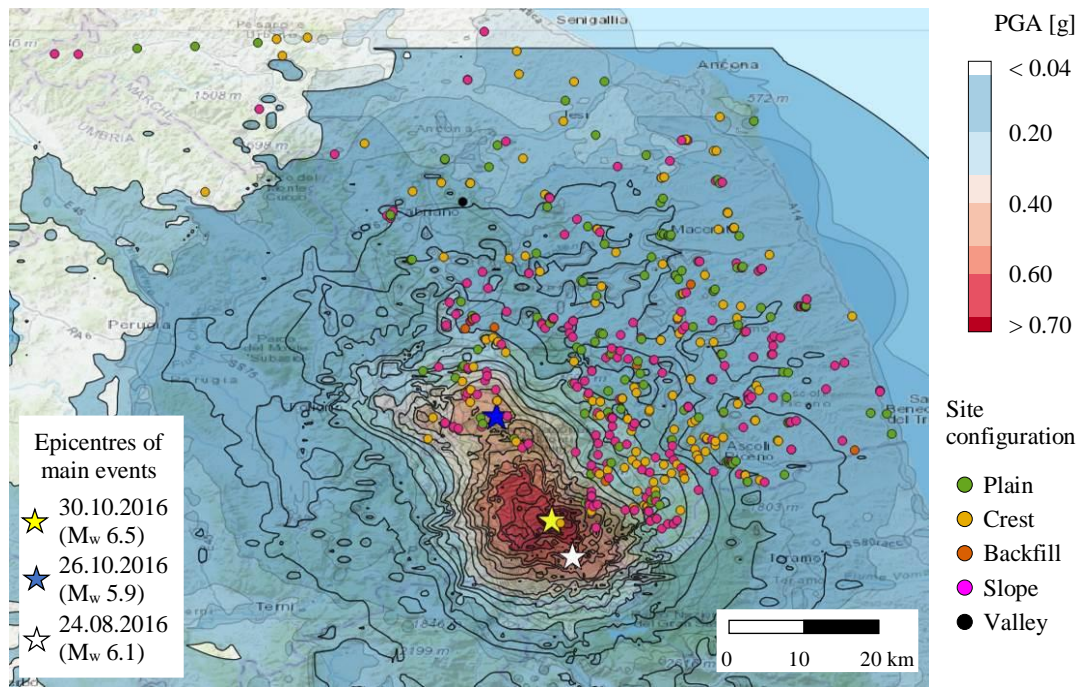
Figure 4-6. Site configuration: (a) map of the site configuration of the churches; (b) distribution of the sample.

4.2.2.3 Analysis of the damage of mechanisms and global damage index

The A-DC survey form identifies 28 damage mechanisms (Figure 4-7) with a six-level scale of damage d_k, from $k=0$ (no damage) to $k=5$ (partial or total collapse of the macro-element), according to EMS-98 equivalent criterion for gravity evaluation (Grünthal et al. 1998).
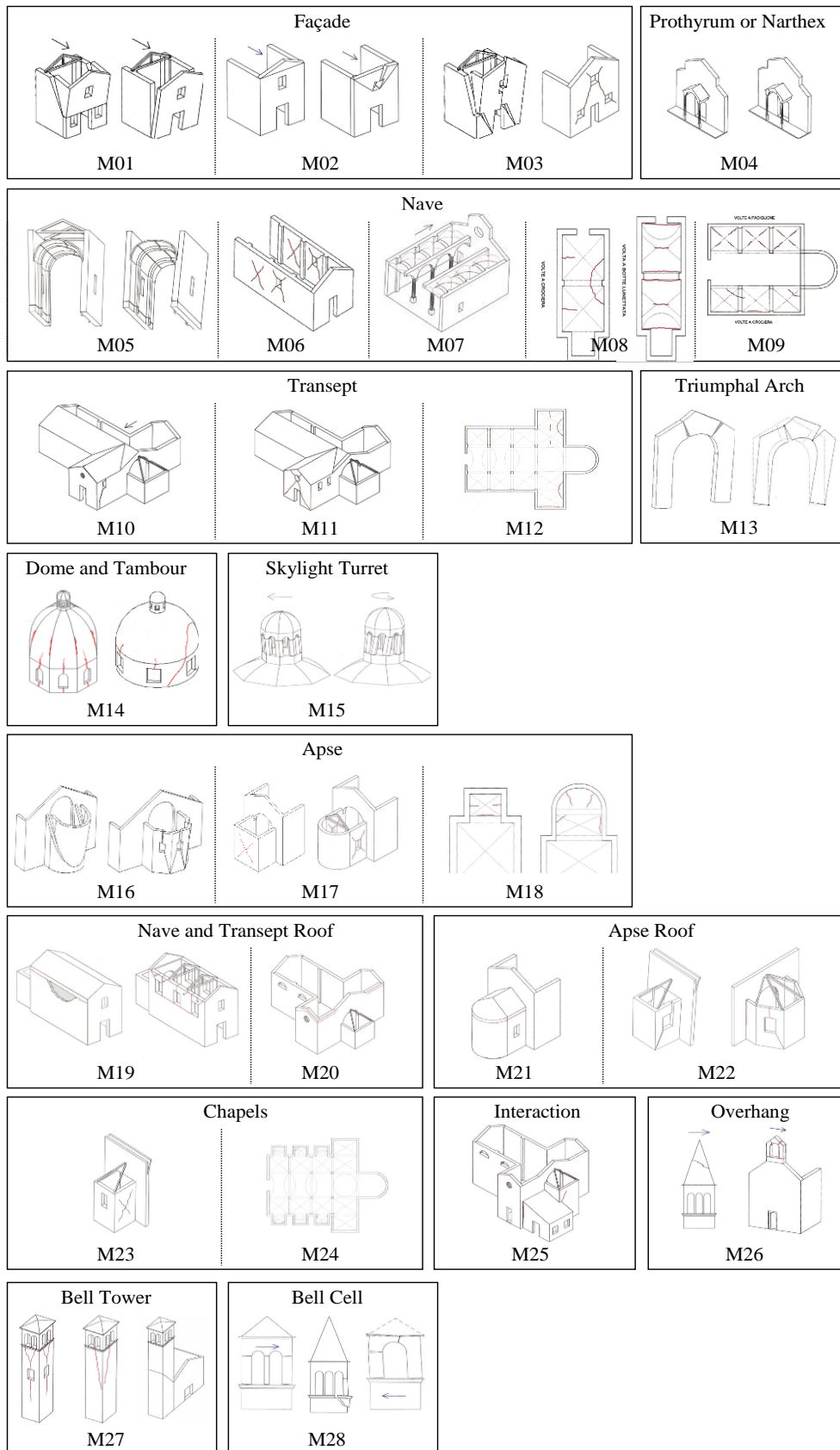
Figure 4-7. Damage mechanisms provided in the A-DC survey form.

Figure 4-8a compares the percentage of potential mechanisms that could be activated with the percentage of actually activated mechanisms, i.e. mechanisms activated with at least the d_1 damage level. It can be observed that the most common potential mechanisms refer to the façade (in-plane and out-of-plane), the lateral walls, the vaults, the apse, the triumphal arch, the roof, the bell tower, and the sailing bell. This observation is consistent with the typological distribution of the sample, characterized by churches having medium-small dimensions and simple layout. In particular, mechanisms relevant to vaults (M08 and M09) and the triumphal arch (M13) were very often activated (73% and 77% of cases, respectively), while the absolute most activated mechanism is the dome one (M14 and M15) (90% of cases). Damage observed in the churches of the Abruzzo Region after the 2009 L'Aquila earthquake (da Porto et al. 2012) presents very similar trends, as evident from Figure 4-8b, consistently with the significant similarities between the religious buildings of the two adjacent Abruzzo and Marche Regions. Figure 4-8c-d refers to damage occurred to churches of the Emilia and Veneto Regions following the Emilia 2012 Earthquake (Taffarel et al. 2016). In this case the typologies of churches present some differences compared to those in the Marche and Abruzzo Regions, as can be observed in Figure 4-8c and Figure 4-8d analysing the percentages of mechanisms that may potentially activate. Nevertheless, damage trends are almost similar referring to the most widespread macro-elements (e.g. façade, lateral walls, vaults, apse, triumphal arch, roof, bell tower and sailing bell).
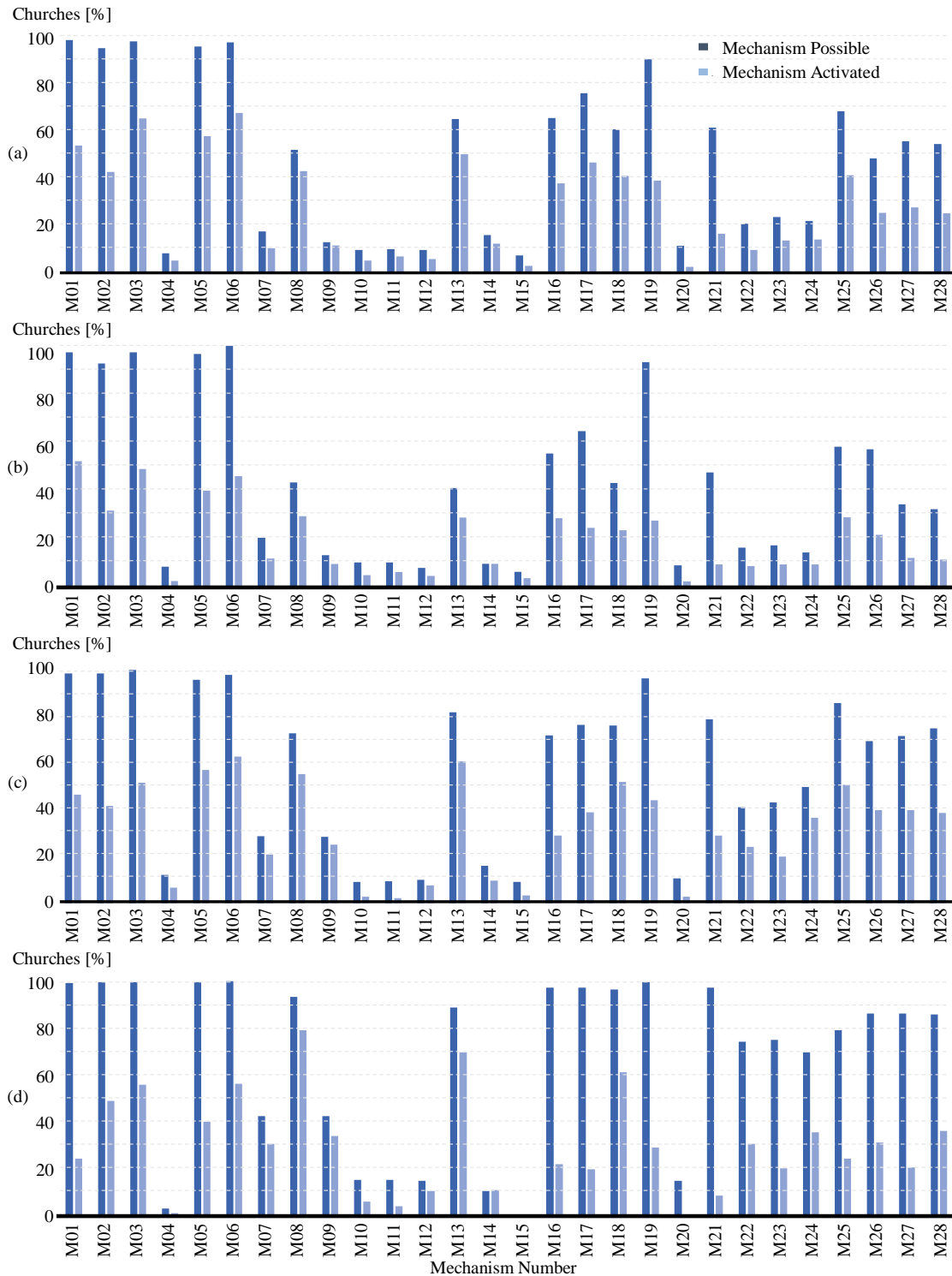
Figure 4-8. Analysis of damage of single mechanisms: (a) churches of the Marche Region following the 2016 Central Italy earthquakes; (b) churches of the Abruzzo Region following the 2009 L'Aquila earthquakes; (c) churches of the Emilia Region following the 2012 Emilia earthquakes; (d) churches of the Veneto Region following the 2012 Emilia earthquakes.

According to the A-DC survey form, the global damage index i_d is obtained by averaging the damage of all mechanisms, i.e. considering the level of damage of all the activated mechanisms over the achievable

maximum damage, corresponding to the collapse of the mechanisms that may potentially activate in the church. By associating a score k ranging from 0 to 5 to each damage level d_k, the definition of i_d translates in the following mathematical expression:

$$i_d = \frac{1}{5N} \sum_{j=1}^{N} d_{k,j} \qquad (4.2)$$

where N is the number of mechanisms that may potentially activate and $d_{k,j}$ is the level of damage k exhibited by j-th single potential mechanism.

The damage indexes are grouped into damage classes (Lagomarsino and Podestà 2004a, 2004b; De Matteis et al. 2016) to make the vulnerability analysis of churches consistent with that of buildings, expressed by six Dk damage levels (from $D0$ to $D5$) defined by the EMS-98 intensity. The correlation proposed by Lagomarsino and Podestà (2004b) between the i_d index and the overall damage levels Dk is adopted in this work and reported in Table 4-2, together with the percentages of churches presenting each damage level. 75.7% of churches developed an overall low damage ($D1$ and $D2$), 15.1% of the sample underwent a severe damage, and only 1.5% attained a near collapse condition.

Table 4-2. Distribution of the sample of churches with the global damage levels based on the damage index i_d.

Global level Dk	Damage Score	Description	Percentage of churches
0	$i_d \leq 0.05$	No damage: light damage only in one or two mechanisms	7.7
1	$0.05 < i_d \leq 0.25$	Negligible to slight damage: light damage in some mechanisms	50.7
2	$0.25 < i_d \leq 0.40$	Moderate damage: light damage in many mechanisms, with one or two mechanisms active at medium level	25.0
3	$0.40 < i_d \leq 0.60$	Substantial to heavy damage: many mechanisms have been active at medium level with severe damage in some mechanisms	12.7
4	$0.60 < i_d \leq 0.80$	Very heavy damage: severe damage in many mechanisms, with the collapse of some macroelements of the church	2.4
5	$i_d > 0.80$	Destruction: at least 2/3 of the mechanism exhibit severe damage	1.5

Figure 4-9 superimposes the damage level of each church with the shake maps of the main shocks, taking into account the maximum acceleration experienced by the church up to the inspection. As already mentioned, surveys were interrupted for safety reasons after the events at the end of October. Thus, 51.5% of churches,

inspected before October 26th, is reported in Figure 4-9a together with the shake map of the August earthquake, while the remaining 48.5% of churches, inspected starting from November, is reported in Figure 4-9b, which includes the shake map obtained by enveloping accelerations of all the mainshocks. As expected, the highest damage levels are associated to churches falling near the mainshocks epicentres; however, there are also significant cases in which a moderate damage ($D1$ and $D2$) is developed by churches far from the epicentres. These cases are probably triggered from unfavourable situations resulting from the combinations of different factors, such as the existence of previous damage, the bad state of preservation of the church, and the site condition.
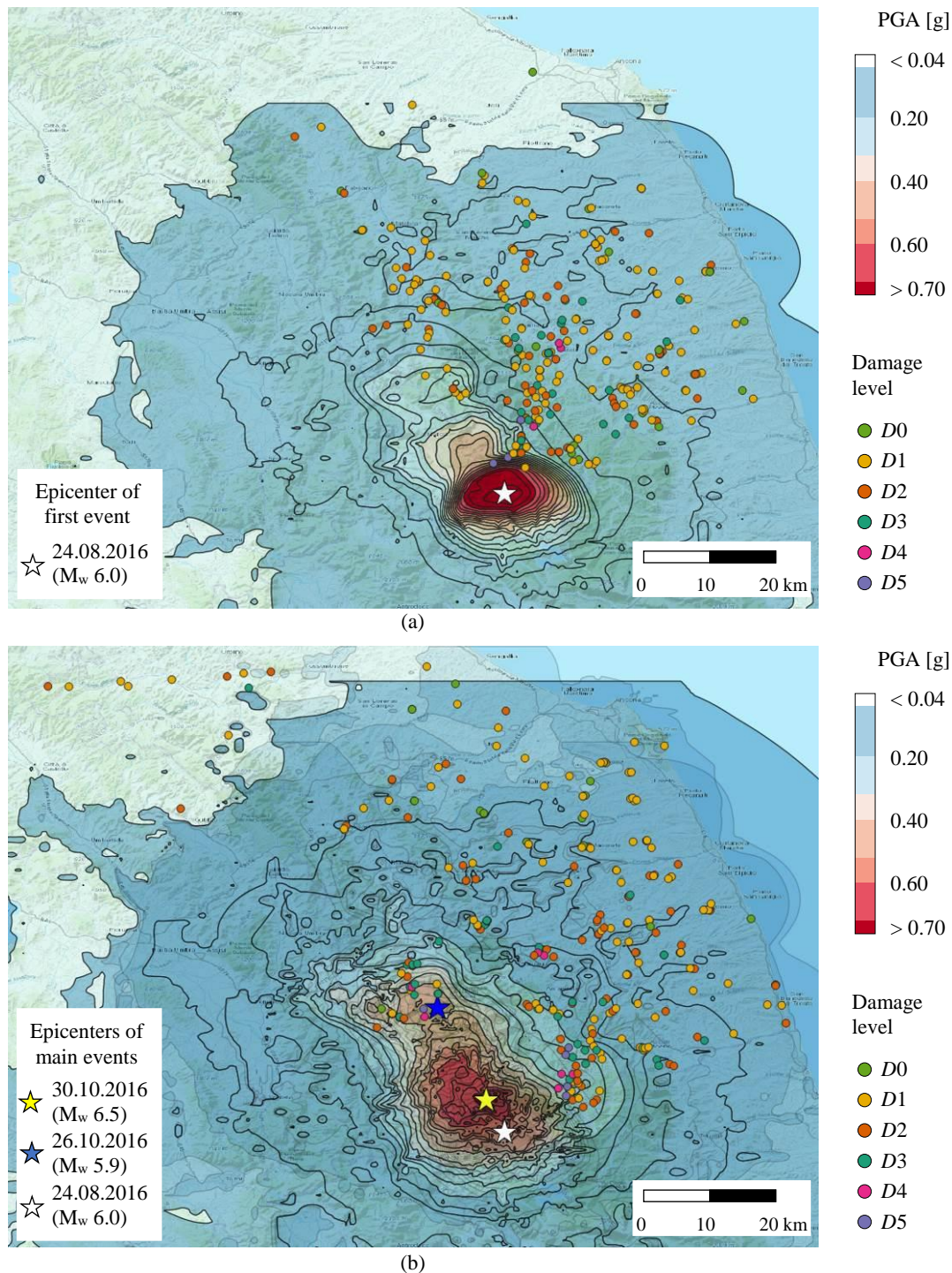
Figure 4-9. Shake maps of PGA and indications of global damage of churches inspected: (a) before October 26th, 2016; (b) after October 30th, 2016.

Similarly, damage data relevant to the most widespread mechanisms are presented in Figure 4-10 and Figure 4-11. In detail, damage relevant to mechanisms of the façade (M01 and M03) and the lateral walls (M05 and M06) are reported in Figure 4-10, while damage of the apse (M16 and M17) and the bell tower (M27 and M28) mechanisms are addressed in Figure 4-11. In this cases, the damage scale is that adopted in the A-DC survey form, ranging from d_0 (absence of damage) to d_5 (partial or total collapse). It is worth noting that selected

mechanisms are all characterized by a high damage for a significant number of churches far from the epicentres of the mainshocks, thus, in areas that experienced low values of accelerations. Despite previous considerations concerning the unfavourable combinations of factors apply, such mechanisms revealed to be highly vulnerable.

With reference to the entire set of mechanisms, Figure 4-12 shows the mean damage μ_D obtained by considering churches falling within four ranges of the macro-seismic intensity I_{MCS}, indicated with different colours. As expected, for the majority of mechanisms, the mean damage level increases with the IM even if there are also some mechanisms that deviate from the above trend (i.e. M04, M09, M10, M11, and M20). It should be noted that the latter are not fully representative, considering the low percentage of cases where they can develop (Figure 4-8a). Furthermore, mechanisms of the façade, lateral walls, apse, and bell tower, considered for plots of Figure 4-10 and Figure 4-11, are those developing the highest damage and configure as the most vulnerable ones.
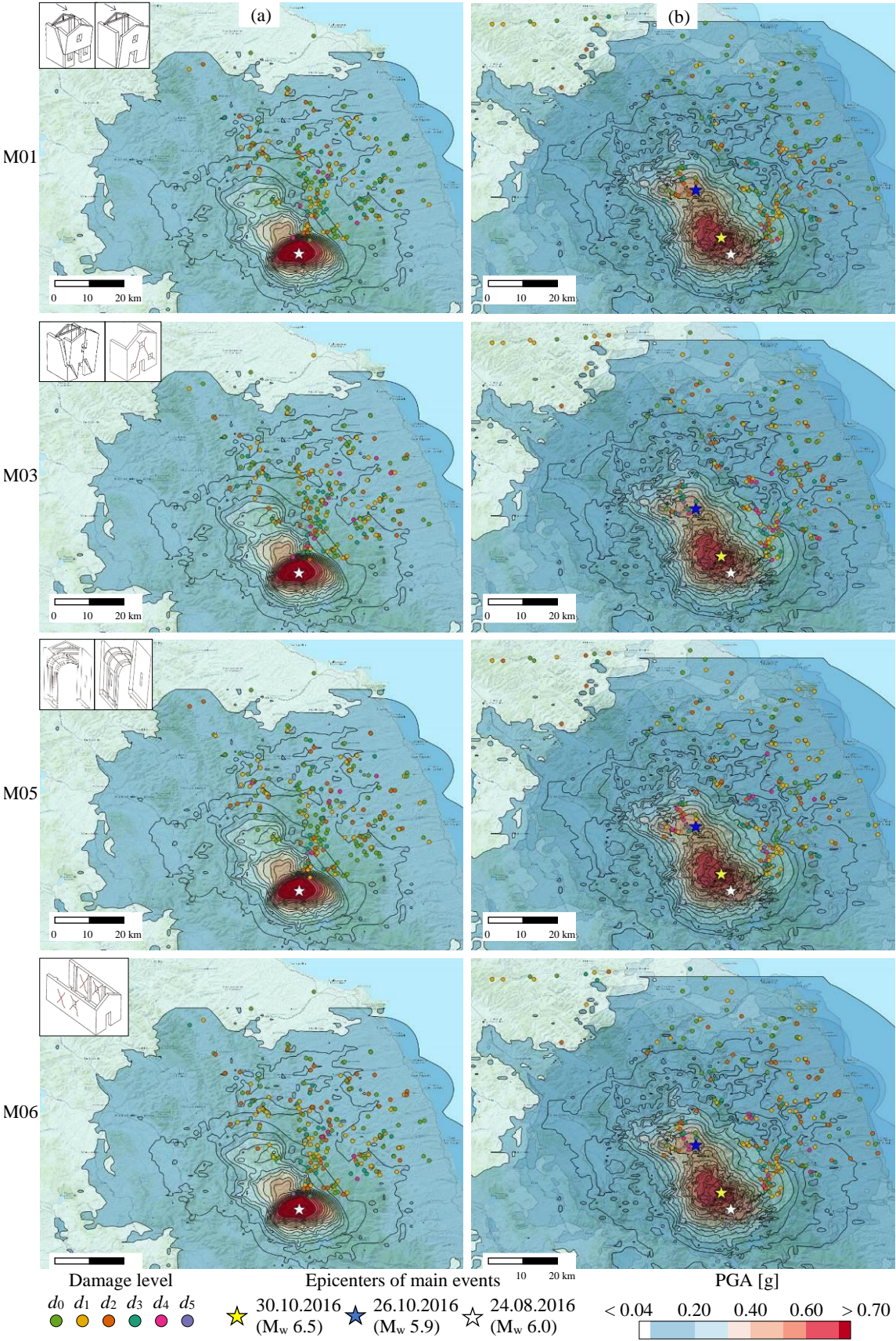
Figure 4-10. Shake maps of PGA and indications of damage of common mechanisms in churches inspected: (left-hand side column a) before October 26th, 2016; (right-hand side column b) after October 30th, 2016.
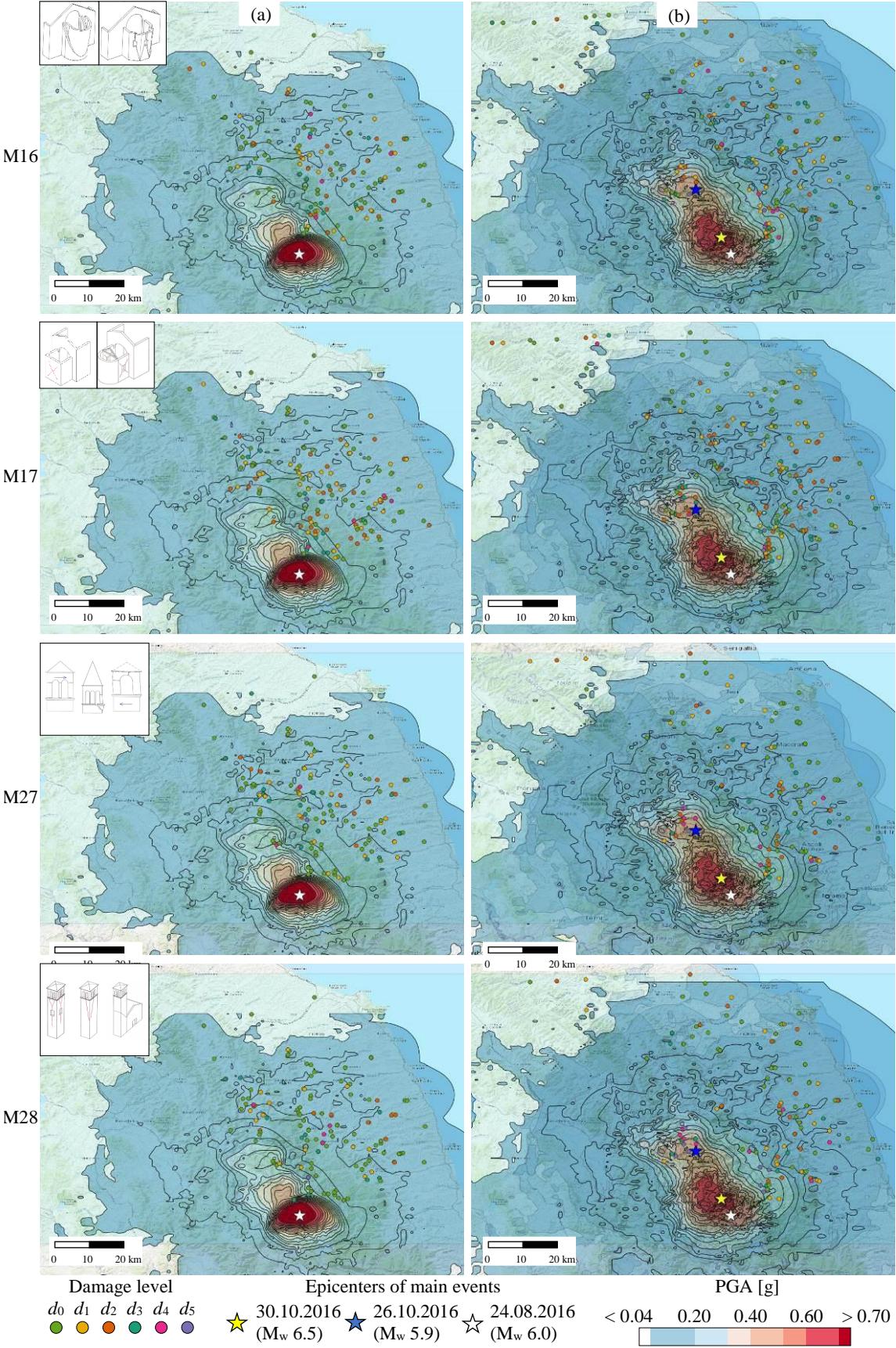
Figure 4-11. Shake maps of PGA and indications of damage of common mechanisms in churches inspected: (left-hand side column a) before October 26th, 2016; (right-hand side column b) after October 30th, 2016.
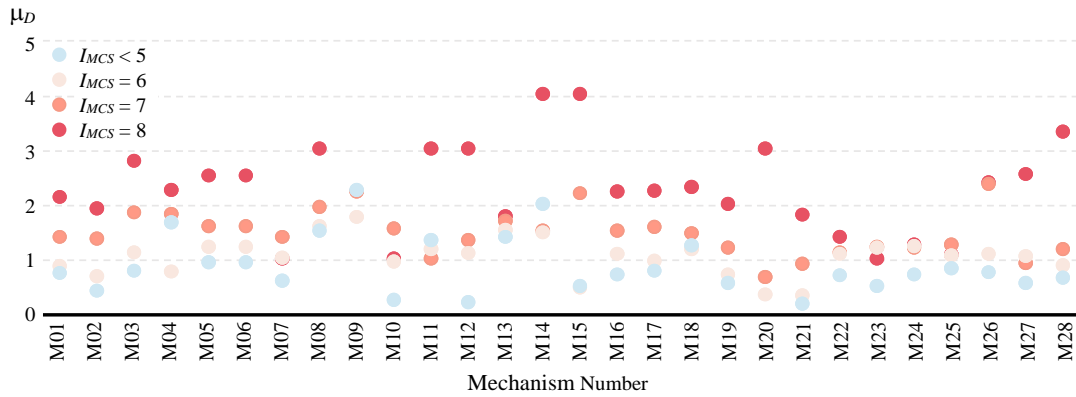
Figure 4-12. Average damage for each mechanism for different ranges of I_{MCS}.

4.2.2.4 Usability outcomes

Another important statistical aspect is the outcome relevant to the usability of churches following the first event of the seismic sequence. Usability during a seismic emergency is evaluated starting from expert judgment during surveys for the damage identification and classification. The question is whether the building, hit by the seismic event, is able to withstand a lower or equal earthquake and if its use does not endanger its occupants. For unusable outcomes, possible problems concerning public safety must also be considered. In this framework, the presence of damage, also of moderate level, should be carefully taken into account since it reveals that the building has partially spent its resistance and ductility resources.

The A-DC form foresees six different possibilities to judge the church usability and the need of provisional protections to mitigate risks for public safety. In detail, the church may be considered safe, safe with countermeasures, unsafe, partially safe and temporarily unsafe. If a church is declared safe, the structure is immediately usable; on the contrary, if an unsafe judgement is expressed, the church is not usable and possible protection measures can be indicated to protect public safety. If the usability only refers to some portions of the church, the building may be declared partially safe and the unusable parts, whose possible collapse does not compromise the stability of usable portions, must be clearly indicated. Churches defined safe with countermeasures are unusable until the indicated provisional interventions are carried out. Finally, the structure can be judged temporarily unsafe if a final decision was not possible and further investigations are needed.

Figure 4-13a plots the percentages of cases relevant to each usability outcome; about half of the inspected churches is judged unsafe (51%) while a significant number of cases (29%) is considered usable with countermeasures. Only 14% of churches, presenting limited damage, is immediately usable after the earthquake. Finally, a limited number of cases are partially safe and temporarily unsafe (5% and 1%, respectively). Figure 4-13b shows the percentage distribution of the outcomes, normalized with respect to the number of cases belonging to different IMs, namely that experienced similar seismic intensities. As expected, by increasing the IM, an increase of the unsafe churches can be observed; on the contrary, the trend of

percentages relevant to both the safe and safe with countermeasures outcomes appears to be not consistent moving from IM=5 to IM= 6. This is probably due the limited number of churches relevant to IM = 5. Finally, Figure 4-13c superimposes the shake map obtained from the envelops of accelerations of the mainshocks of the sequence with the usability outcomes of the inspected churches. It can be observed that churches with an unsafe outcome are quite distributed over the whole territory, in areas with both high and moderate accelerations. It is worth mentioning that a direct correlation between damage index and the usability outcome is quite difficult to determine, because the safe judgement may be often related to few mechanisms, which affect the overall damage index in a limited manner; this issue is confirmed by data reported in Figure 4-10 and Figure 4-11, which show that important and recurrent mechanisms with medium-high damage levels are quite widespread in the Region, also in areas characterized by moderate accelerations. However, from an overall point of view, results generally show that damage indexes greater than 0.3 are associated to the unsafe outcome.
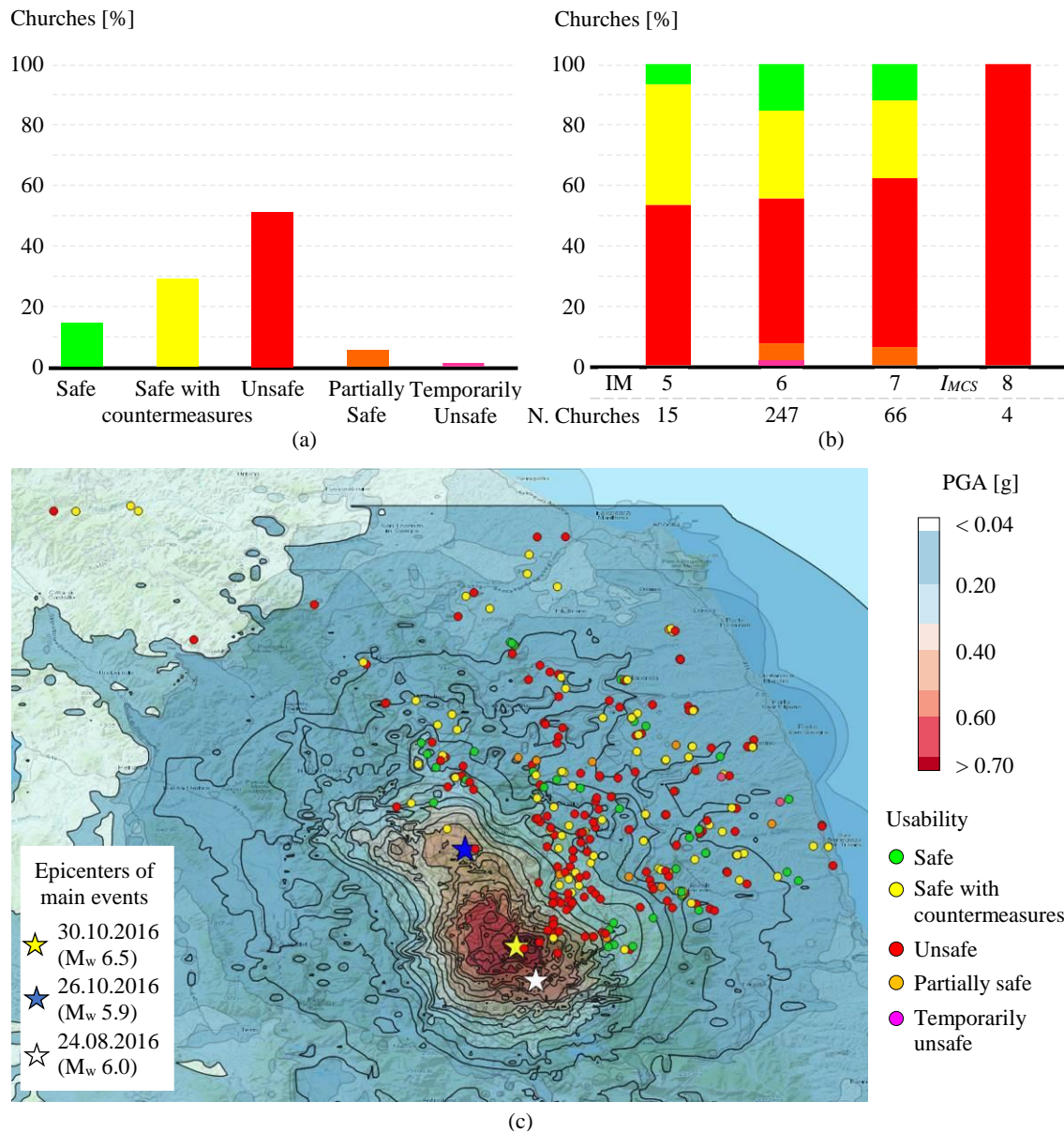
Figure 4-13. Usability outcomes: (a) distribution of the sample; (b) percentage of each usability outcome with respect to the I_{MCS}; (c) map of the usability outcomes of churches.

4.2.3 Damage and vulnerability assessments from observational data

In this chapter, the evaluation of the damage occurred to churches and the vulnerability assessment is provided. The global damage and local mechanisms of collapse were analysed in recent years by various authors with a statistical approach, applying to churches a procedure originally developed for buildings (Lagomarsino e Podestà 2004b; Lagomarsino 2006; De Matteis et al. 2014 and 2016). In such studies, the macro-seismic approach for the assessment of the seismic vulnerability was considered, generally adopting the I_{MCS} as IM, and correlating the continuous variable i_d to six discrete Dk damage levels (from $D0$ to $D5$) defined by the EMS-98 intensity (Grünthal et al., 1998). In accordance with previous definition, the correlation proposed by

Lagomarsino and Podestà (2004b) between the i_d index and the overall damage levels Dk is adopted (Table 4-2).

The statistical analysis of the global damage (expressed by the global damage index) was here performed by computing the Damage Probability Matrix (DPM) that collects for the considered IMs, the frequency of occurrence of each damage level Dk (with $k = 0\text{-}5$). The Damage Probability Histograms (DPHs) derived from the DPMs obtained for the inspected churches are shown in Figure 4-14. The DPHs were fitted with the following binomial distribution (Braga et al., 1982):

$$p_k = \frac{5!}{k!(5-k)!}\left(\frac{\mu_D}{5}\right)^k\left(1-\frac{\mu_D}{5}\right)^{1-k} \tag{4.3}$$

described by the mean damage μ_D for each IM, which is the average of the global damage indexes Dk defined by

$$\mu_D = \sum_{k=0}^{5} kP_k \tag{4.4}$$

where P_k is the probability of the k-th observed damage.

DPHs for the whole sample and the relevant binomial distributions considering four intervals of the IM ($I_{MCS} = 5 \div 8$) are compared in Figure 4-14. It can be observed that the binomial distribution fits quite well the observational data for all the considered levels of I_{MCS}; these results are in line with those obtained in previous works by Lagomarsino and Podestà (2004b, c) for churches damaged by the Molise and Marche-Umbria earthquakes. Furthermore, values of the mean damage μ_D evaluated from Equation (4) are reported in Figure 4-14. With reference to the latter, Table 4-3 compares results of this study with those of past researches, relevant to seismic events characterized by M_w greater than 6; it can be observed that for all the considered I_{MCS}, the mean damage obtained from the observational data is in line with that resulting from previous studies.
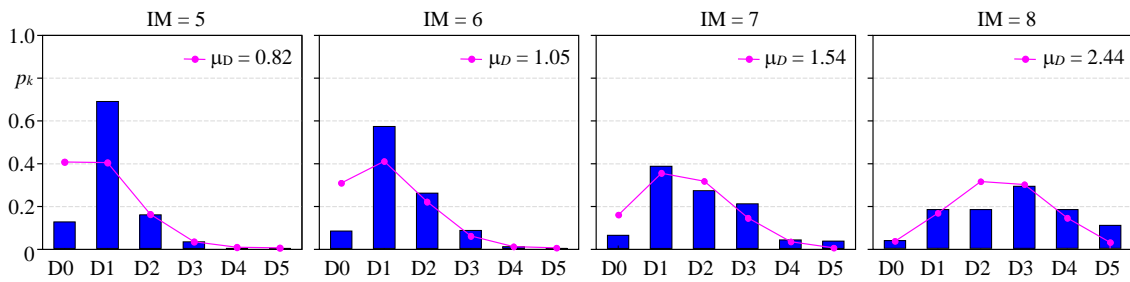
Figure 4-14. DPHs of the global damage index.

Table 4-3. Mean damage of churches following different Italian earthquakes (Lagomarsino, 2012).

Events	I_{MCS}					
	4	5	6	7	8	9
Irpinia (1980)		1.21	1.41	1.86	2.71	3.25
Marche-Umbria (1997)	-	1.05	1.38	2.02	3.00	-
Molise (2002)	0.4	0.54	1.28	2.90	-	-
Aquila (2009)	-	0.73	1.28	1.97	2.60	3.43
Mean from past studies	-	**0.88**	**1.33**	**2.19**	**2.77**	-
Central Italy (2016)	-	**0.82**	**1.05**	**1.54**	**2.44**	-

The same procedure can be developed for each single mechanism (M01-M28) addressed in the survey form; to this purpose, damage level $d_{k,Mi}$ of the i-th mechanism is considered instead of the global damage index Dk, and the mean damage is labelled with $\mu_{D,Mi}$. DPHs relevant to mechanisms of the façade (M01 and M03) and the lateral walls (M05 and M06) are reported in Figure 4-15, while DPHs of the apse (M16 and M17) and the bell tower (M27 and M28) mechanisms are addressed in Figure 4-16. Even for the single mechanisms, the binomial distribution approximates quite well the DPHs. It is worth observing that the in-plane mechanisms are slightly more vulnerable than the out-of-plane ones. This outcome, in conjunction with the observation that the mean damage of each mechanism appears slightly lower than those from the 1997 Marche-Umbria earthquake (Lagomarsino and Podestà 2004b), likely due to the fact that seismic improvements were widely made in the churches of the Region following the 1997 earthquake, often aimed to prevent out-of-plane mechanisms.
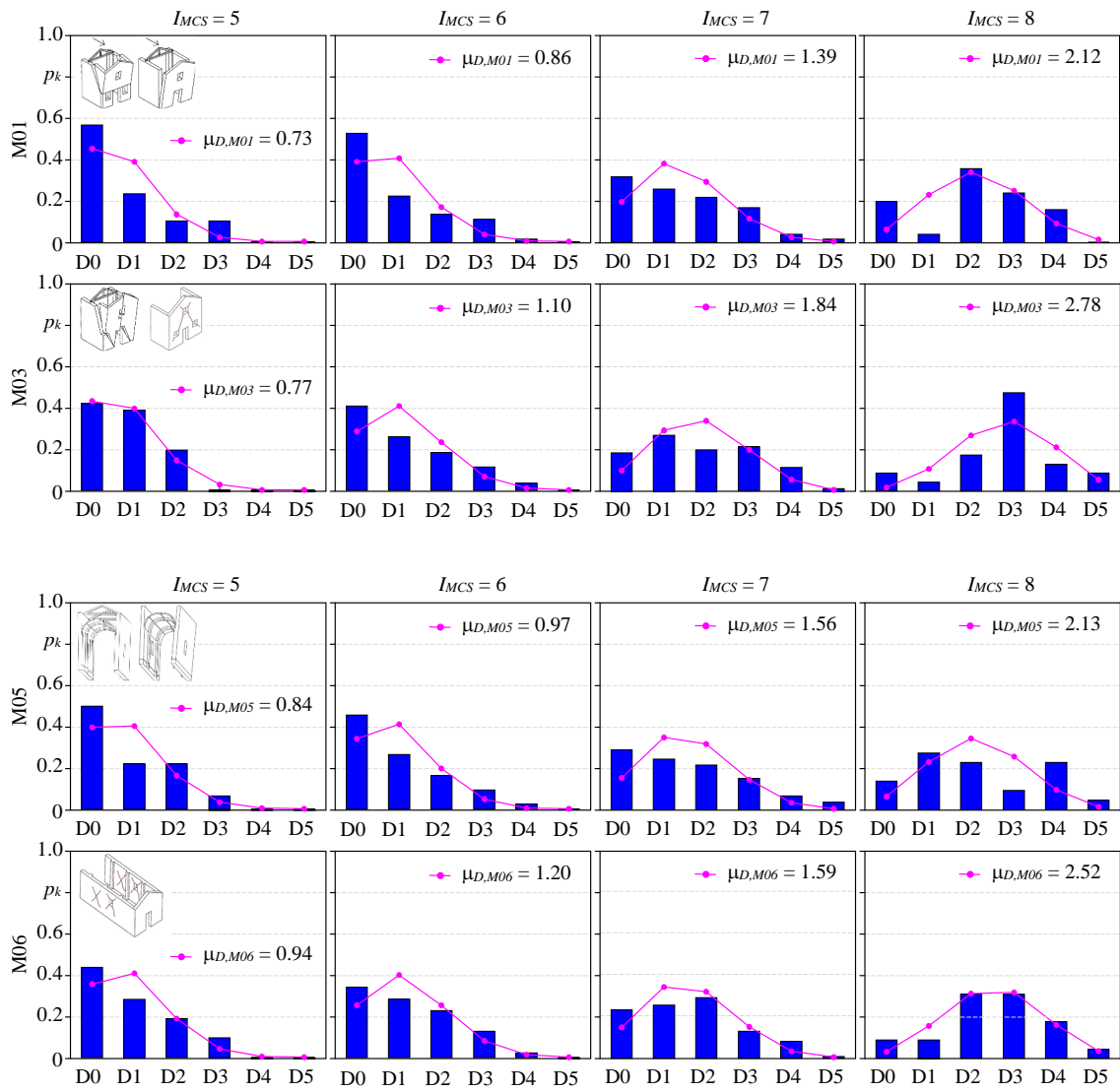
Figure 4-15. DPHs for mechanisms M01, M03, M05 and M6.
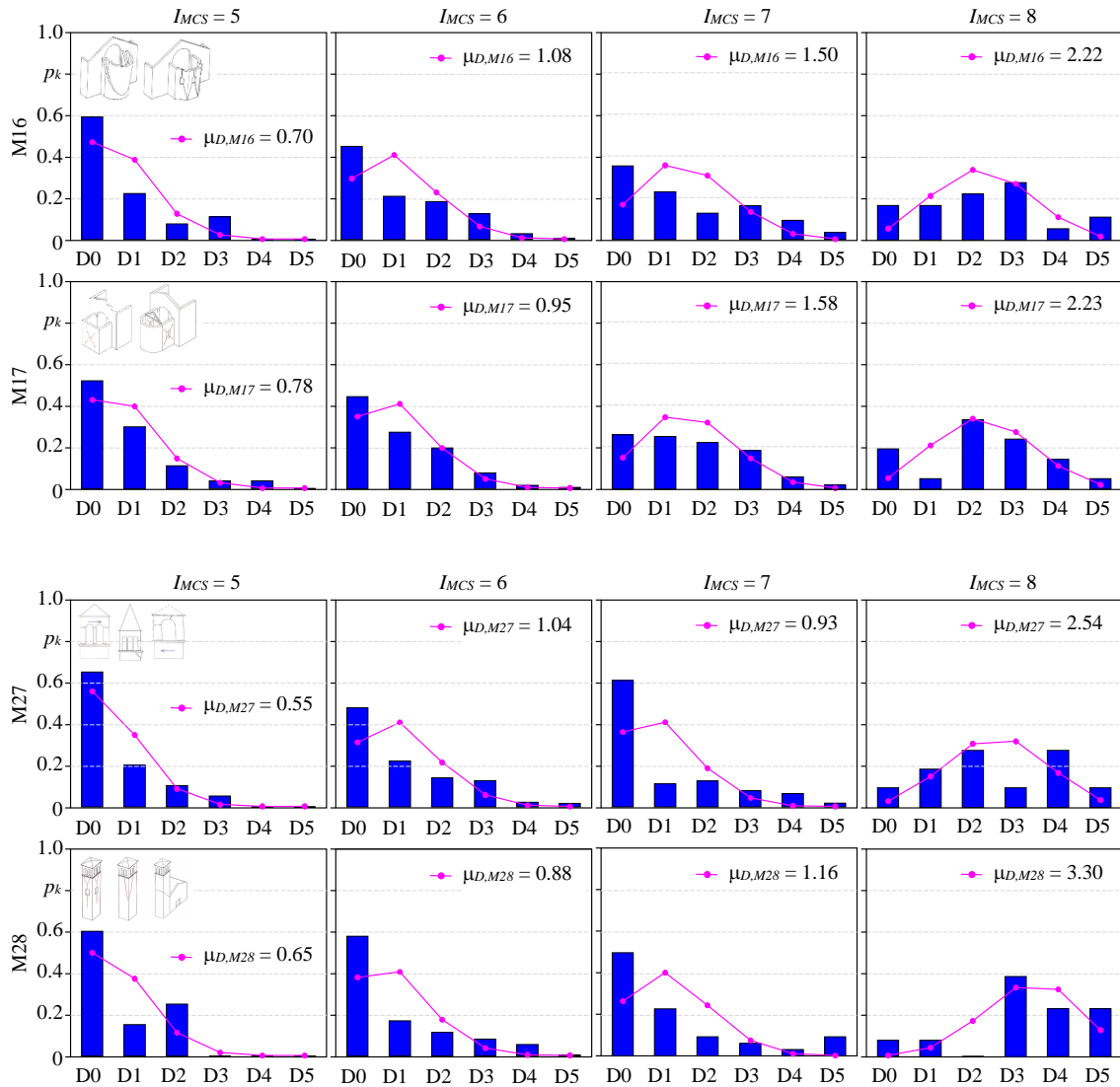
Figure 4-16. DPHs for mechanisms M16, M17, M27 and M28.

The correlation between the IM and the average damage μ_D allows defining a model of observational vulnerability. According to Lagomarsino (2006), the vulnerability curves assume the general form:

$$\mu_D = 2.5 \cdot \left[1 + \tanh \left(\frac{IM + 6.25V - 13.1}{Q} \right) \right] \qquad (4.5)$$

It is a function of two parameters, namely the vulnerability V and the ductility index Q, which represents the rate of increase in damage with intensity and controls the slope of the curve. Parameters V and Q are defined based on the typological categories of monuments (e.g. churches, towers, and palaces) and were introduced in Lagomarsino et. al. (2004b). Starting from the post-processing of data from inspections of churches damaged

by the 1997 Marche-Umbria earthquakes, Lagomarsino and Podestà (2004a, 2004b) and Lagomarsino et al. (2006), proposed the following expression for the vulnerability curve of churches

$$\mu_D = 2.5 \cdot \left[1 + \tanh\left(\frac{I_{MCS} + 3.3475 \cdot iv - 8.9125}{3} \right) \right] \tag{4.6}$$

where *iv* represents the vulnerability index; according to the same authors, vulnerable churches have *iv* > 0.4.

Figure 4-17 compares the vulnerability curves obtained from Equation (6) (continuous red lines and dotted blue line) with those resulting from processing the observational damage of this study (black line). Curves from Equation (6) are plotted considering *iv*=0.2, 0.4 and 0.6, in order to account for different vulnerabilities, assuming 0.4 as the value dividing vulnerable churches from less vulnerable ones (Lagomarsino and Podestà 2004b). In addition, curves obtained from observational data following other Italian seismic events are reported for comparison; the latter are based on data provided by Lagomarsino (2012). It can be observed that results of the current study are in line with those relevant to previous researches for macro-seismic intensities greater than 7, and have, consistently with the typological nature of the sample, a very similar trend of those obtained after the 1997 Marche-Umbria earthquake, although shifted towards a lower vulnerability. The analysed sample, which presents a vulnerability curve that fits quite well the analytical one (i.e. from Equation (6)) for *iv* = 0.2, has an overall moderate vulnerability; this is not fully conforming to previous existing studies and may be due to the fact that seismic improvements were made in most churches of the sample after the 1997 Marche-Umbria earthquake (RiMARCANDO 2007). In addition, it should be remarked that vulnerability curves obtained from observed data may be affected by a subjective parameter, which is the technician sensitivity in judging the damage level. Anyway, it can be observed that for IM lower than 7, results are in line with the analytical curve obtained for a higher vulnerability index (*iv* = 0.4).

Mechanisms relevant to the bell tower and the bell cell are worth of being also analysed independently, since they are typical of structural portions characterized by different vibration periods. Figure 4-18 compares the observational vulnerability curves for the bell tower and bell cell mechanisms with the analytical ones, resulting from the application of Equation (5) in which *V*=0.89 and *Q*=2.0 for the bell tower and *V*=0.94 and *Q*=1.49 for the bell cell, as suggested in Curti et., 2006. Even for these two mechanisms, results comply very well with data from the literature.
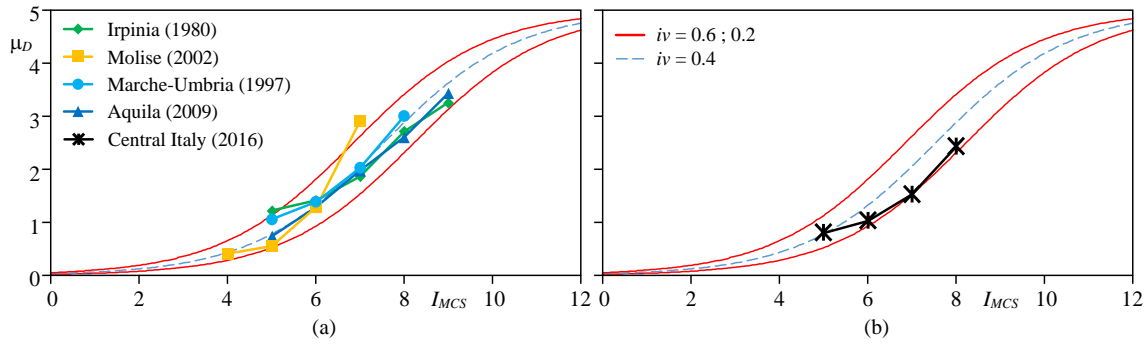
Figure 4-17. Comparison of the observational vulnerability with curves from the literature: (a) past events; (b) analysed sample.
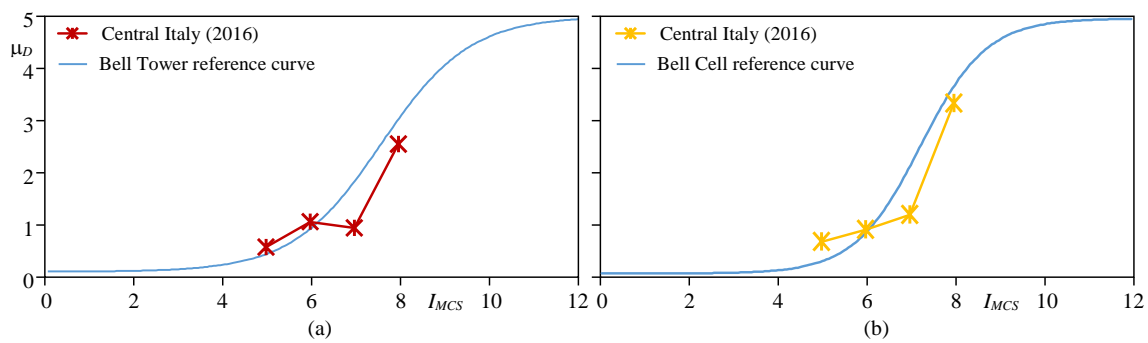
Figure 4-18. Comparison of the observational vulnerability of single mechanisms with curves from the literature: (a) bell tower; (b) bell cell.

4.2.4 Fragility Curves definition and mean damage response

According to the statistical results shown in the subchapter 4.2.2, the sample considered now on for the definition of the fragility curves and for the definition of its mean response, is the one formed by about 370 churches falling in class A or B. Indeed, Figure 4-19 and Figure 4-20 show the statistical trend of this reduced sample of churches. In particular, Figure 4-19 compares the percentage of potential mechanisms that could be activated with the percentage of actually activated mechanisms, i.e. mechanisms activated with at least the d_1 damage level. The distribution of potential mechanisms that could be activated, highlights that most of them are referred to the façade (M01-M02-M03) and to the lateral walls, both in-plane (M06) and out-of-plane mechanisms (M05-M19). Figure 4-20 superimposes the overall damage of each church with the shake maps obtained by enveloping accelerations of all the mainshocks. Figure 4-20b shows the distribution in a cake diagram. As for the whole dataset, the highest damage levels are associated to churches falling near the mainshocks epicentres; however, there are also significant cases in which a moderate damage (D1 and D2) is developed by churches far from the epicentres.
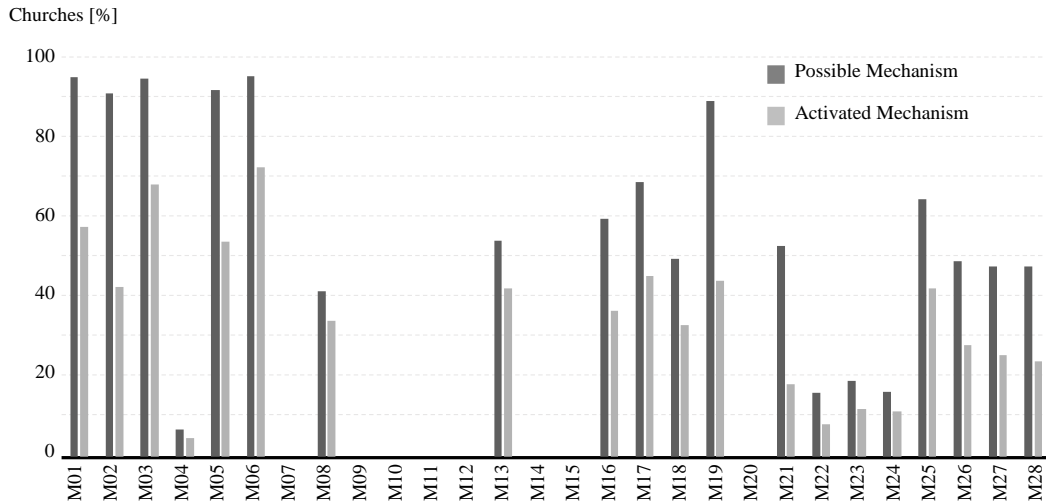
Figure 4-19. Comparison between possible/activated damage mechanisms for A and B churches typologies.
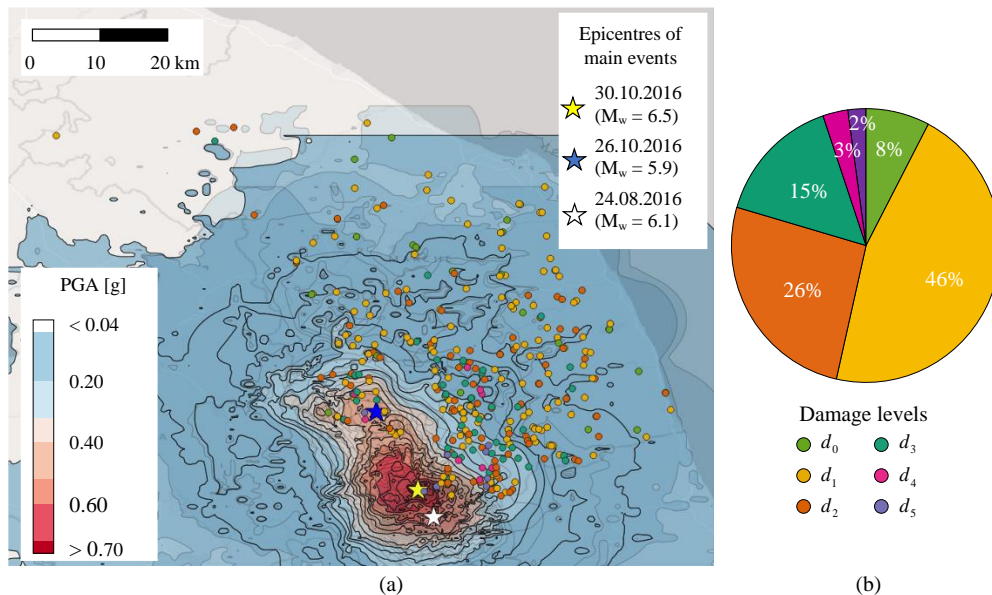
Figure 4-20. (a) Shake maps of PGA and indications of overall damage of A and B churches (b) distribution of the damage levels for A and B churches.

Fragility curves describe the probability of exceedance of a given damage level as a function of the intensity measure of the seismic ground motion. Generally, the damage state is described by a discrete variable d_k ($k = 0,1,..,N_D$) which denotes the damage within a finite number $N_D + 1$ of ordered possible damage states. By denoting by D the random variable that describes the church damage, the fragility curve $G_D(d_k|i)$ ($k = 0,1,..,N_D$) describes the probability that, for a seismic intensity, the damage state is equal or higher than d_k . Usually, the fragility curves are efficiently approximated by the two-parameter function (Singhal et al. 1996, Ibarra et al. 2005, Bradley et al. 2008):

$$G_D(d_k \mid i) \approx \Phi\left[\frac{\ln(i) - \mu_k}{\beta_k}\right] \qquad (4.7)$$

where Φ is the cumulative normal distribution function, i is the intensity measure expressed in PGA and μ_k and β_k are the two-parameters associated to the response of the structure.

Data observed from churches consist of pairs (d_m, i) where the measure of experienced damage state d_m, is derived from the damage index i_d on the basis of the equivalences reported in Table 4-4, and the intensity measure i is obtained from the shaking registered on site.

On the basis of the assumed probabilistic model, given an intensity measure i, the probability to observe a damage d_m equal or higher than d_k can be expressed as:

$$p[d_m \geq d_k \mid i] = G_D(d_k \mid i)^y \left(1 - G_D(d_k \mid i)\right)^{1-y} \qquad (4.8)$$

where y is a binary variable that is equal to 1 if $d_m \geq d_k$, 0 otherwise. Considering a number of observations $(d_{m,l}, i_l)$ with $l = 1,.., N$ where N is the total number of observed churches and assuming that data are independent and identically distributed, the associated likelihood function L_k for the general damage level d_k can be defined as follows (Dang et al. 2017, Straub et al. 2008, Lallemant et al. 2015).

$$L_k(\mu_k, \beta_k) = \prod_{l=1}^{N} p\left[d_{m,l} \geq d_k \mid i_l\right] \qquad (4.9)$$

The values of μ_k and β_k are obtained maximizing the likelihood function L_k for each damage level d_k:

$$\left(\hat{\mu}_k, \hat{\beta}_k\right) = \arg\max\left(L_k(\mu_k, \beta_k)\right) \qquad (4.10)$$

Figure 4-21 reports the fragility curves obtained considering the expression proposed in Equation (4.7) and five pairs of parameters $\left(\hat{\mu}_k, \hat{\beta}_k\right)$ estimated by Equation (4.10) are reported in Table 4-5.
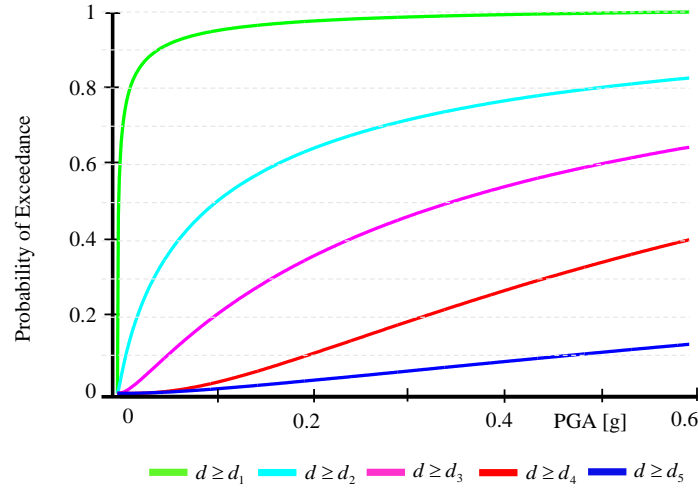
Figure 4-21. Fragility curves for damage levels from d₁ to d₅

Table 4-4. Definition of structural damage levels based on damage index id (Lagomarsino and Podestà, 2004b).

Level	Damage Score	Description
d_0	$i_d \leq 0.05$	No damage: light damage only in one or two mechanisms
d_1	$0.05 < i_d \leq 0.25$	Negligible to slight damage: light damage in some mechanisms
d_2	$0.25 < i_d \leq 0.40$	Moderate damage: light damage in many mechanisms, with one or two mechanisms active at medium level
d_3	$0.40 < i_d \leq 0.60$	Substantial to heavy damage: many mechanisms have been active at medium level with severe damage in some mechanisms
d_4	$0.60 < i_d \leq 0.80$	Very heavy damage: severe damage in many mechanisms, with the collapse of some macroelements of the church
d_5	$i_d > 0.80$	Destruction: at least 2/3 of the mechanism exhibit severe damage

Table 4-5. Parameters of the fragility curves derived by the MLE

	$d \geq d_1$	$d \geq d_2$	$d \geq d_3$	$d \geq d_4$	$d \geq d_5$
$\hat{\mu}_k$	-6.6175	-2.2346	-1.0242	-0.2291	1.2783
$\hat{\beta}_k$	2.8691	1.9379	1.4893	1.0708	1.5663

A further step is represented by the evaluation of the mean response model based on the fragility curves, then compared with the mean response preformed in a continuous way directly from the experimental data.

To do that, the relationship between the seismic intensity i and the expected overall damage index i_d is analysed. This information can be recovered by computation from the probabilistic model defined in the previous section or can be directly determined by interpolation techniques, starting from surveyed pairs $(i_{d,j}, i_j)$. The results coming from the two approaches are compared in the following. The damage functions, derived by the former and latter approach, are denoted by $I_C(i)$ and $\bar{I}_C(i)$ respectively. For what concerns the former approach, the probability $f_D(d_k | i)$ that a church is in the k-th damage state, given the intensity, can be derived from the previous fragility curves as follows:

$$f_D\left(d_k \mid i\right) = \begin{cases} 1 - G_D\left(d_1 \mid i\right) & k = 0 \\ G_D\left(d_k \mid i\right) - G_D\left(d_{k+1} \mid i\right) & k = 1, 2, .., N_D - 1 \\ G_D\left(d_{N_D} \mid i\right) & k = N_D \end{cases} \tag{4.11}$$

The model provided by the fragility curves collects, in each damage state d_k, values of the overall index i_d belonging to the intervals reported in Table 4-4 and does not provide information about the distribution of i_d values within each interval. In order to estimate the mean response for each intensity, it is assumed that the mean of the indexes belonging to each interval, coincides with the centre of the interval itself. Consequently, the mean damage indexes for the six damage states are: 0.025, 0.15, 0.325, 0.50, 0.70, and 0.90.

On the other hand, the second approach is based on the definition of a reference curve starting from the experimental data. The data were fitted considering a two-parameter function (Baker, 2015)

$$\bar{I}_C(i) = \Phi\left(\frac{\ln(i) - \bar{\mu}}{\bar{\beta}}\right) \tag{4.12}$$

and the parameters $\bar{\mu}$ and $\bar{\beta}$, evaluated through the SSE, technique assume the values -0.523 and 2.991, respectively. In this case, no statistical meaning can be associated to the curve obtained.

Figure 4-22 reports the global damage index function obtained from the fragility functions (blue curve), and the dot points represent the expected damage index derived from fragility curves for the sample of churches considered. The red curve depicts the empirical damage index fitted by the SSE technique. The global damage index evaluated starting from the fragility curves is in agreement with the one obtained from the data fitted with the SSE.
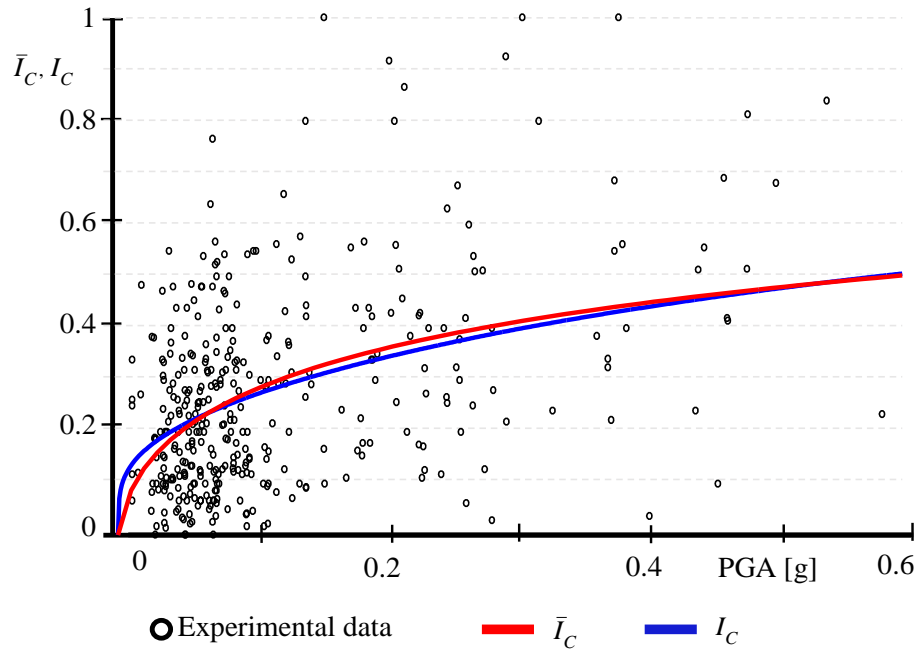
Figure 4-22. Global damage index functions obtained from the fragility functions and from the experimental data fitted by SSE

A new comparison has been made considering the mean response derived from the model proposed and the results from the past researches relevant to seismic events characterized by M_w greater than 6 after the Italian seismic events. In particular, the 1980 Irpinia earthquake, the 1997 Marche Umbria earthquake, the 2002 Molise earthquake and the 2009 L'Aquila earthquake have been considered; data used are described in Table 4-6, where the mean damage values given I_{MCS} as intensity measure have been reported for the considered seismic events.

For sake of simplicity, in order to make a comparison with the past events, only the global damage index function obtained from the fragility functions has been considered (blue curve of Figure 4-22) because there is a good agreement with the mean function obtained from the model.

Considering that the model gives the mean response using the PGA as seismic intensity, the macroseismic intensities have been converted in PGA [g] using the expression proposed by Faenza and Michelini (2010).

Figure 4-23 shows the trend of the mean curve obtained from the model proposed and the results from past seismic events. It is possible to highlight that the experimental mean curve seems to be lower than the past events. In particular, if it is considered the comparison between the model and the results derived from Umbria Marche 1997 earthquake, the churches show less vulnerability and they have been subjected to lower damaged even though the seismic events had a higher intensity.

Table 4-6. Mean damage for churches after different Italian seismic events.

Events	IMCS					
	4	**5**	**6**	**7**	**8**	**9**
Irpinia (1980)		1.21	1.41	1.86	2.71	3.25
Marche-Umbria (1997)	-	1.05	1.38	2.02	3.00	-
Molise (2002)	0.4	0.54	1.28	2.90	-	-
Aquila (2009)	-	0.73	1.28	1.97	2.60	3.43
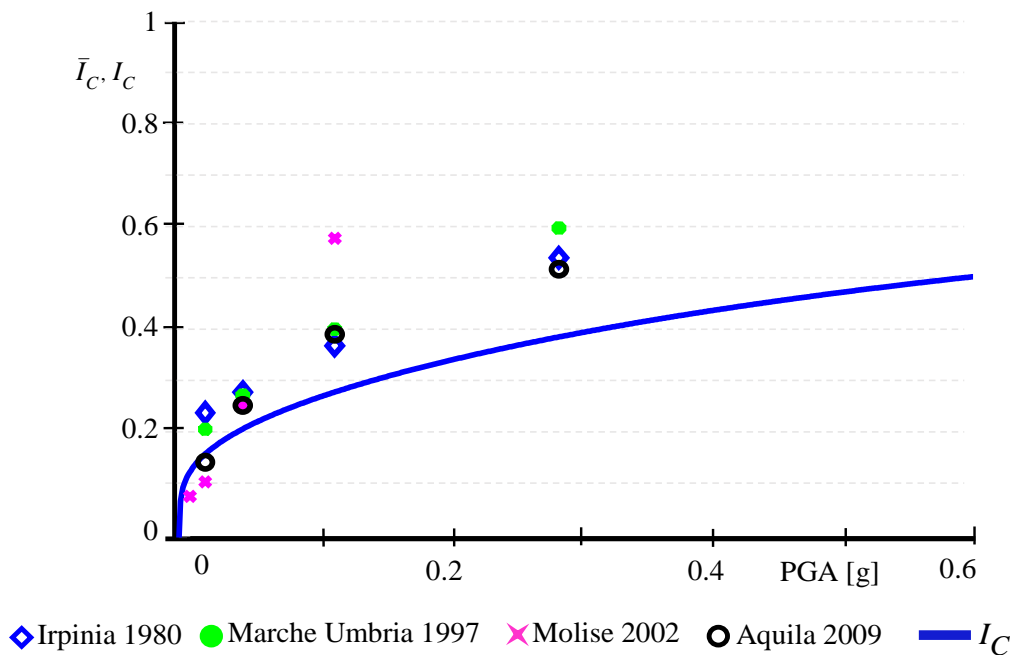
Figure 4-23. Comparison between global damage index function obtained from fragility curves and the experimental data available in literature

4.3 Empirical predictive model for seismic damage and repairing costs of historical churches

The damage observed after earthquakes is fundamental for testing existing predictive models, and for providing expected damage related to seismic intensity. The availability of new data from damage surveys allows defining more refined predictive models. Previous works on this topic generally aimed to provide statistical analyses for a set of limit states defined according to a discrete description of damage levels (Lagomarsino and Podestà 2004b; Lagomarsino 2006; Lagomarsino 2012; De Matteis et al. 2016; De Matteis et al. 2019; De Matteis and Zizi 2019; Hofer et al. 2018; Cescatti et. al. 2019). However, damage surveys often measure earthquake consequences by continuous indexes and a conventional translation from available data into a discrete number of limit states is required (Lagomarsino and Podestà 2004b).

Furthermore, seismographic networks have been significantly enhanced in recent years and more detailed information is available for what concerns seismic action intensity, therefore recorded ground motions permit to develop more precise relationships between objective measures of the ground motion intensity and observed

damage. Even if most of the existing studies are based on a macro-seismic scale, recent works are based on objective measures of the ground motion, such as the Peak Ground Acceleration (PGA) (e.g. Hofer et al. 2018; Cescatti et. al. 2019; De Matteis and Zizi 2019).

This Chapter presents a probabilistic response model relating the measure of the ground motion intensity to the overall damage index, continuous in the range [0,1]. The model is based on the analysis of data coming from post-earthquake surveys of historical churches. Different parametric models have been proposed to infer dataset from surveys, model parameters have been determined by using the maximum likelihood method and a solving strategy has been developed to handle some irregularities in the probabilistic response.

The alternative discrete description of damage, usually associated to limit state fragility curves and presented before, has been derived from the proposed model, once a relationship between the two descriptions is defined, e.g. by using proposal reported in the technical literature (Lagomarsino and Podestà, 2004b).

The model and the procedure developed to evaluate relevant parameters have been used to provide a damage predictive model by starting from a set of data surveyed after the recent Central Italy earthquake of 2016. It is worth noting that damage surveys carried out after the earthquake during the emergency generally provide partial information because they do not include the undamaged and fully collapsed churches, but only damaged ones. Therefore, a complete data set has been obtained by integrating the post-earthquake survey with in-field data collected by the authors. The dataset used for parameters evaluation concerns 514 churches located in the Archdiocese of Camerino-San Severino that have the same architectural background of the other database due to their location in the Marche Region, and includes data spanning quite a large range of PGA and damage index values. Moreover, a demonstrative application is presented in order to illustrate the potential use of the model in the prediction of post-earthquake damage scenarios and in the support of decision-making processes oriented to mitigate the seismic risk.

Prevention is clearly one of the most effective way to mitigate seismic risk, but also the post-earthquake scenarios should be considered in order to reduce direct and indirect socio-economic losses. Historically, the impact of a medium-strong earthquake on the economy of a country has been always remarkable. Many economic losses have not been reported in databases, and therefore it is important to deal with changes of economic trends due to the seismic events taking into consideration all the features of a country such as the population, insurance information exchange rate, etc. (Daniell et al, 2010). Consequently, the built environment vulnerability should be reduced but the community preparedness should be increased, minimising recovery time. Evaluations and management on architectural resources from an economic point of view should be deeply analysed and considered. In this optic, Della Spina and Calabrò (Della Spina and Calabrò, 2018) proposed a support instrument in order to find the best use of a historic buildings of Southern Italy to help the public decision in terms of conservation and reuse. The complexity of this strategy identification process in terms of financial resources is due to its interdisciplinary that involves the culture, the social and environmental aspects. Contribute at the development of sustainable strategies against the abandoned of cultural heritage

maintaining its strengths, capitalizing on opportunities and finding solutions for structure weaknesses are object of different studies. In addition, the prioritization of the protection and interventions of restoration became a necessary aspect, identifying tangible valuation criteria, sub-criteria, and ratings of historical resources (Bottero et al 2019, Bottero et al 2020, D'Alpos and Valluzzi, 2020).

At territorial level, studies on consequences evaluation from an economic point of view related to historical churches are few. The main reasons are the different architectural background of the churches related to their areas, or their complex internal architecture that do not follow a linear and simple design. This is why, many works based on consequences evaluation, are related to ordinary buildings of prone areas and they may be of interest to understand the consequences evaluation methodology. The technical principles and the procedure used to calibrate the repair costs for reinforced concrete and masonry buildings using the existing repair costs monitored in the reconstruction process after the recent Italian earthquakes, have been illustrated in the work of Cosenza et al. (Cosenza et al., 2018). It emerges that the expected losses are becoming a key parameter to evaluate and to compare the structure performances in their reference life. Other studies have been developed for reinforced concrete buildings after L'Aquila earthquake of 2009, in order to monitor and collect data related to the repairing cost for structural and non-structural components (Del Vecchio et al., 2018), or to compare predicted repair costs with actual repairing costs for different types of building stock (De Martino et al., 2017). For steel structures some studied related to cost have been proposed. A new methodology has been developed to quickly estimate the erection cost with early design information. In particular, the total installed costs have been estimated with the result of defining a cost-optimal frame early in the design process (Barg et al., 2018). In addition, for areas struck by other seismic events there have been presented studies on prediction the losses for groups of buildings hit by the 1999 Athens earthquake (Kappos et al., 2007). An analytical methodology has been used, where the statistical repair cost was estimated through data collected after in situ survey for a sample of building blocks. A comparison between predicted and statistical costs for the whole area has been performed, considering also separate classes for different geological and geophysical areas. The methodology proposed by Kappos et al., can be also adapted for other urban areas by considering a proper calibration of the damage and loss assessment models, useful in risk mitigation intervention, as well as in prior policies for seismic areas. Another study was performed for sample building types in the area of Tehran, Iran (Zolfaghari et al., 2012). In order to improve the seismic performance of a building or building groups, retrofitting is an effective approach for reducing seismic losses. The complexity for decision makers to determine the retrofitting performance level and the considerable cost of retrofitting itself, make the loss assessment a crucial phase. In that work, probabilistic economic losses were estimated for each structure before and after retrofitting process, useful to estimate the replacement cost and to assess an index for retrofitting process, which could be used in cost/benefit analyses.

Focusing on historical buildings, and in particular on historical churches, the literature does not provide many studies on consequences evaluations. Indeed, especially for these kind of assets, it is very important to have a prior estimation of the economic damage in the first phase of post emergency. The work of Lagomarsino and

Podestà (Lagomarsino and Podestà, 2004a) is one of the first study aimed at evaluating the economic loss. Different kind of damages have been considered for churches and in particular: the structural damage, the economic damage that represents the cost of repair of the structural damage due to the seismic events and the cultural damage that is the restoration cost of the artistic asset. The method is not focused on a detailed crack survey but it is based on the identification of activation of different seismic collapse mechanisms, by evaluating the assessment of the damage in terms of macroelements and not considering the restoration of artistic assets. Thanks to this approach, a preliminary design for the repair of damage for churches has been formulated, estimating also the cost of intervention (economic damage). From another point of view, the work of Curti et al. (Curti et al., 2008) focused on the importance of decisions and technical procedures for the reconstruction process. Their main objective is to prevent inadequate interventions and ensure a correct distribution of funding, and it is applied to the reconstruction of the Molise area after the 2002 earthquake. The main consideration of their work is the importance of having an effective planning tool for retrofitting design that is capable to perform reliable judgment in terms of seismic strengthening costs as primary priority especially at territorial level, where the churches are more heterogeneous.

In the final part of this Chapter, a probabilistic response consequence model that relates the repairing costs of historical churches with the seismic damage defined based on the empirical damage model previously described in the chapter, is shown. A final demonstrative application is presented in order to illustrate the potential use of the model in the prediction of repairing cost scenarios. This probabilistic response consequence model may be of interest in the development of effective strategies to mitigate and prevent the risk and can be a tool of supporting the reduction of direct economic losses.

4.3.1 Probabilistic model for damage evaluation

In this paragraph, a probabilistic damage model is presented. The damage index is a continuous random variable D, whose values d belong to the domain $[0,1]$ and the seismic intensity is described by a positive scalar random variable I, defined in the domain $i \in (0, \infty)$. In particular, the boundary value $d = 0$ represents the case of negligible damage and $d = 1$ the case of collapsed or not recoverable church.

The system response is described by the probability of observing a damage level lower than an assigned value d, given the seismic intensity i, and it is described by the following Cumulative Density Function (CDF)

$$F_{D|I}(d|i) = P[D < d|i] \quad d \in [0,1] \tag{4.13}$$

Generally, for an assigned value of the intensity i, the expected conditional Probability Density Function (PDF) can be expressed by a continuous function in the open interval $(0,1)$, while discontinuities are expected at $d = 0$ (no damage) and $d = 1$ (collapse) (Figure 4-24a). Therefore, the conditional CDF of damage, given i, can be expressed in the form:

$$F_{D|I}(d|i) = F_0(i)H(d) + (1 - F_0(i) - F_1(i))F^*_{D|I}(d|i) + F_1(i)H(d-1) \quad d \in [0,1] \tag{4.14}$$

where $F_0(i)$ provide the probability of observing $d = 0$, $F_1(i)$ the probability of observing a damage $d = 1$, while the regular function $F^*_{D|I}(d|i; \Theta_d)$ is a conditional CDF describing the distribution of damage probability within the reduced set of cases where the damage is in the range $0 < d < 1$ i.e. the damage has occurred but the structural system has not collapsed. Finally $H(x)$ is the Heaviside step function, such that $H(x) = 1$ or $x \geq 0$ and it is 0 elsewhere. The associated conditional PDF assumes the form

$$f_{D|I}(d|i) = F_0(i)\delta(d) + (1 - F_0(i) - F_1(i))f^*_{D|I}(d|i) + F_1(i)\delta(d-1) \quad d \in [0,1] \tag{4.15}$$

where δ is the delta Dirac function expressing the derivative of the Heaviside function, and $f^*_{D|I}(d|i)$ is the derivative of $F^*_{D|I}(d|i)$ with respect to d. Figure 4-24b shows the conditional PDF $f_{D|I}(d|i)$, it is not a regular function but can be obtained by combining the three regular functions $F_0(i)$, $F_1(i)$, and $f^*_{D|I}(d|i)$.

Starting from this probabilistic response model, it is possible to derive fragility curves. Introducing a set of discrete damage levels d_s $(s = 0,1,..,N_s)$, it is possible to define a finite number of $N_k = N_S - 1$ ordered damage states D_k $(k = 1,..,N_k)$, each including damage values in the interval $d_{k-1} \leq d < d_k$; the fragility curve describes the probability that, given the intensity i, the damage state is equal or higher than D_{k*}; this probability can be evaluated by using the response model, i.e. $P[D_k \geq D_{k*}] = G_{D|I}(d = d_{k*-1}|i) = 1 - F_{D|I}(d = d_{k*-1}|i)$.
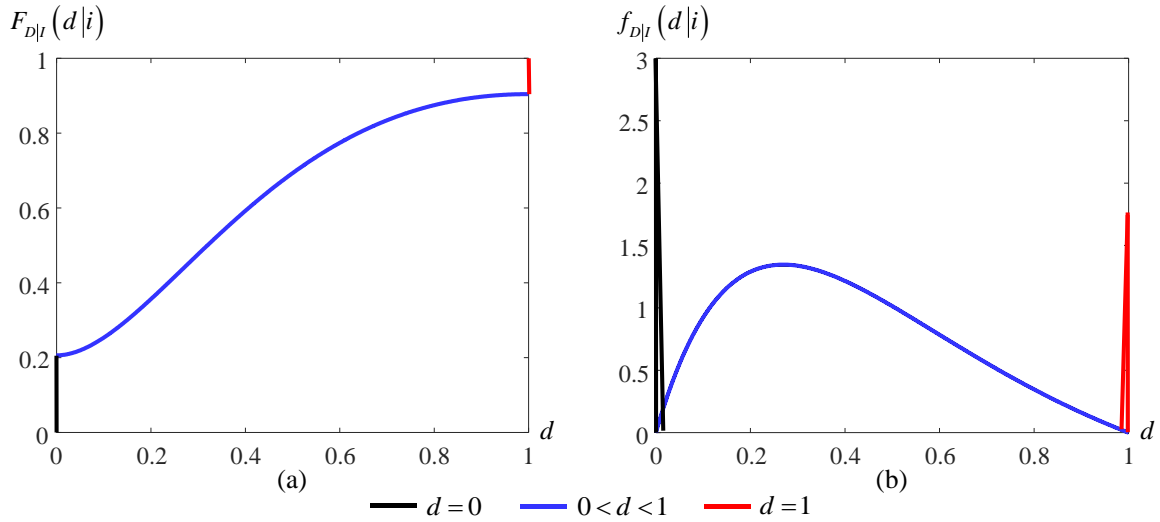
Figure 4-24. Expected conditional distribution of probability, given intensity: (a) conditional CDF and (b) conditional PDF

The assessment of an empirical numerical model is based on a set of observed pairs (d_q, i_q) $(q = 1,.., N)$, usually relied on approximate descriptions, achieved by combining a discrete number of shape functions, whose parameters are determined by inference techniques. In the following, these parameters will be collected in the vector $\Theta = [\Theta_0, \Theta_1, \Theta_d]$, where the three sub-vectors $\theta_0, \theta_1, \theta_d$ separately collect parameters regarding the three unknown functions $F_0(i; \Theta_0)$, $F_1(i; \Theta_1)$, $f_{D|I}^*(d|i; \Theta_d)$, respectively.

Some general criteria can be followed to select shape functions in a rational way. It can be assumed that the probability of damage occurrence is 0 for a seismic intensity $i = 0$ and this probability approaches to 1 when the intensity goes to infinity. Coherently, the shape functions can be chosen to reflect previous considerations, and therefore they must satisfy $F_0(0) = 1$, $F_1(0) = 0$, $F_0(\infty) = 0$, and $F_1(\infty) = 1$ for each combination of parameter values, and must be positive and not exceed 1.

Furthermore, the complementary probability $1 - F_0(i) - F_1(i)$ starts from 0 and approaches 0 when the intensity goes to infinity, it must be a positive function and this condition may imply a constraint be applied to parameters. Differently, no special constraint is required for the shape functions describing the conditional PDF $f_{D|I}^*(d|i; \Theta_d)$, beyond the conditions of positive definiteness and unitary integral along d for each value of i. However, as a desirable result for application, the set of possible solutions should be able to describe how mean value and variance vary with the intensity.

The parameters Θ will be evaluated by means of the maximum likelihood method. Some troubles arise in the application of the method, due to the lack of regularity of $f_{D|I}(d|i)$, because no value can be associated to the extreme cases $d = 0$ and $d = 1$ (Dirac function). For this reason, the problem is solved in two steps, by combining a discrete approach with a continuous approach.

In the former step the damage range is divided into 3 subsets, related to the cases $d = 0$, $0 < d < 1$, $d = 1$, respectively, and the discrete problem is solved by finding the frequency distribution of the 3 cases. Frequency distribution involves the two functions $F_0(i;\Theta_0)$ and $F_1(i;\Theta_1)$, only. More precisely, (d_q, i_q) $(q = 1,.., N)$, denotes the q-th observed pair and the model provides the corresponding probability of occurrence

$$P(d_q, i_q; \Theta_0, \Theta_1) = \begin{cases} F_0(i_q; \Theta_0) & \text{if } d_q = 0 \\ 1 - F_0(i_q; \Theta_0) - F_1(i_q; \Theta_1) & \text{if } d_q \neq 0,1 \\ F_1(i_q; \Theta_1) & \text{if } d_q = 1 \end{cases} \tag{4.16}$$

Parameters can be obtained by maximizing the likelihood function

$$L_{01}(\Theta_0, \Theta_1) = \prod_{q=1}^{N} P(d_q, i_q; \Theta_0, \Theta_1) \tag{4.17}$$

or, as usual, maximizing the log-likelihood function (Dang et al. 2017; Straub et al. 2008; Lallemant et al. 2015)

$$l_{01}(\Theta_0, \Theta_1) = \sum_{q=1}^{N} \ln P(d_q, i_q; \Theta_0, \Theta_1) \tag{4.18}$$

Once parameters Θ_0 and Θ_1 are obtained, the terms of the vector Θ_d relevant to the distribution $f_{D|I}^*(d|i; \Theta_d)$ can be evaluated by a continuous approach considering the reduced number $q_d = 1,.., N_d < N$ of cases belonging to the internal interval only ($0 < d < 1$). The expression of the log-likelihood function is

$$l_d(\Theta_d) = \sum_{q_d=1}^{N_d} \ln f_{D|I}^*(d_{q_d}, i_{q_d}; \Theta_d) \tag{4.19}$$

and the model parameters are obtained maximizing the log-likelihood function.

4.3.2 Application of the damage model to historical churches

In this paragraph, the proposed methodology is applied to establish a probabilistic response model based on damage observed after the seismic events of Central Italy 2016. For this purpose, all the churches belonging to the Archdiocese of Camerino-San Severino, for which complete information in terms of undamaged/damaged/collapsed is available, have been considered.

4.3.2.1 Database definition and damage analysis

As presented in chapter 4.2.2 the evaluation of the level of damage and state of the churches took place by compiling damage survey forms. It should be noted that the inspection was carried out only for damaged churches.

Indeed the sample considered was completed by the authors with the support of church owners with the undamaged and fully collapsed churches, combining field surveys with information derived from the BeWeb (2019) database. The complete database is constituted by 514 churches, of which 356 were inspected and the survey forms were compiled, while information about remaining 158 churches were recovered by the authors. Even if the churches present a heterogeneity relevant to different construction periods, type and complexity of the structure, the sample can be considered homogeneous in terms of construction techniques and used materials.

Figure 4-25a shows the area of the Archdiocese Camerino-San Severino and Figure 4-25b reports the location of the churches within the Archdiocese overlapping the shake maps of the envelope of the three main events of the 2016 seismic sequence. In addition, Figure 4-25b reports general information about the damage level (damaged, undamaged and collapsed churches). As already mentioned, the survey form A-DC considers a set of 28 potential mechanisms involving single sub-parts of the church (macro-elements) and for each of them a damage level is identified according to the general observational criteria introduced by EMS-1998 (Grünthal 1998) and a final overall index is obtained by combining damage levels of all the potential mechanisms. It should be emphasized that the damage index provided by the survey form is a continuous variable in the range $[0,1]$ and it will be considered in the probabilistic model presented in the following.
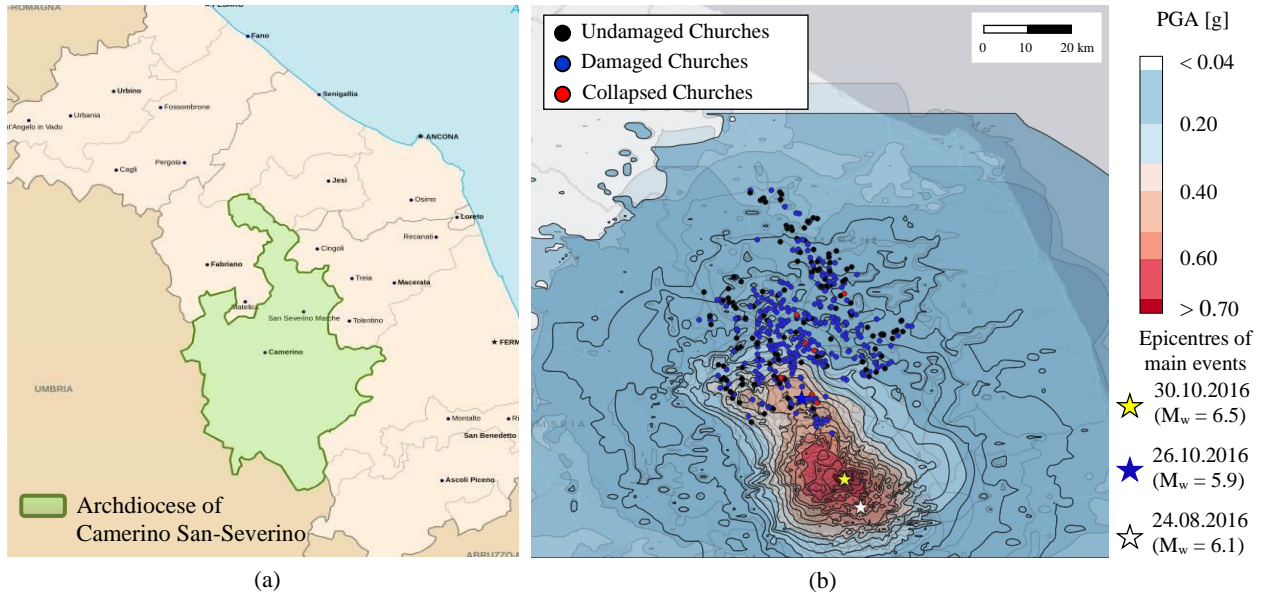
Figure 4-25. Archdiocese of Camerino-San Severino: (a) territorial extension and (b) distribution over the territory of the churches

4.3.2.2 Parametric model

In this section the parameters of the functions $F_0(i;\Theta_0)$, $F_1(i;\Theta_1)$ and $f^*_{D|i}(d|i;\Theta_d)$ are evaluated considering the database previously defined. Different sets of functions, selected according to criteria discussed in the previous section, are proposed and relevant results are compared.

Functions $F_0(i;\Theta_0)$ and $F_1(i;\Theta_1)$ are selected within the exponential family. In particular, three different options are considered and compared:

$$F_0^{LL}\left(i;\Theta_0^{LL}\right)=e^{-\Theta_{01}^{LL}\,i}\,;\qquad F_1^{LL}\left(i;\Theta_1^{LL}\right)=1-e^{-\Theta_{11}^{LL}\,i} \tag{4.20a,b}$$

$$F_0^{LG}\left(i;\Theta_0^{LG}\right)=\frac{1}{1+e^{-\left(\Theta_{00}^{LG}+\Theta_{01}^{LG}\ln(i)\right)}}\;;\quad F_1^{LG}\left(i;\Theta_1^{LG}\right)=\frac{1}{1+e^{\Theta_{10}^{LG}+\Theta_{11}^{LG}\ln(i)}} \tag{4.21a,b}$$

$$F_0^{PR}\left(i;\Theta_0^{PR}\right)=\Phi\left(\Theta_{00}^{PR}+\Theta_{01}^{PR}\ln(i)\right)\;;\qquad F_1^{PR}\left(i;\Theta_1^{PR}\right)=1-\Phi\left(\Theta_{10}^{PR}+\Theta_{11}^{PR}\ln(i)\right) \tag{4.22a,b}$$

These proposed functions are commonly adopted in the Generalized Linear Models (GLM) used for regression analysis of dichotomous data (Agresti et al. 2015, 2018). In the first case (Equation 4.20), the probability F_0 of observing $d = 0$ and the probability F_1 of observing $d = 1$ vary with the intensity i, according to a Log-Linear (LL) approximation , the second case (Equation 4.21) assumes a Log-Logit (LG) approximation, and the last case (Equation 4.22) a Log-Probit (PR) approximation (Lallemant et al. 2015; Agresti et al. 2015, 2018).

Regarding parameters, one parameter only is required in the LL function (Equation 4.20) to define the functions F_0 and F_1, i.e. $\mathbf{\Theta}_0^{\mathrm{LL}} = \left[\Theta_{01}^{\mathrm{LL}} \right]$ and $\mathbf{\Theta}_1^{\mathrm{LL}} = \left[\Theta_{11}^{\mathrm{LL}} \right]$, while in the other two cases (Equation 4.21 and 4.22) two parameters are required for each function, $\mathbf{\Theta}_0^{\mathrm{LG}} = \left[\Theta_{00}^{\mathrm{LG}}, \Theta_{01}^{\mathrm{LG}} \right]$, $\mathbf{\Theta}_1^{\mathrm{LG}} = \left[\Theta_{10}^{\mathrm{LG}}, \Theta_{11}^{\mathrm{LG}} \right]$ for LG approximation and $\mathbf{\Theta}_0^{\mathrm{PR}} = \left[\Theta_{00}^{\mathrm{PR}}, \Theta_{01}^{\mathrm{PR}} \right]$, $\mathbf{\Theta}_1^{\mathrm{PR}} = \left[\Theta_{01}^{\mathrm{PR}}, \Theta_{11}^{\mathrm{PR}} \right]$ for PR approximation, respectively.

All these parametric models satisfy conditions regarding the limit behaviours at $i = 0$ and $i = \infty$, discussed in the previous section. The constraint about the positive definiteness of the complementary probability $1 - F_0 - F_1$ is satisfied by the solution reported below.

Figure 4-26 shows the comparison among results obtained for the three proposed models, whose parameters have been obtained by the maximum likelihood method. Regarding the LL model, the function F_0^{LL} tends to zero more quickly than the LG function F_0^{LG} and PR function F_0^{PR}, while the model provided by F_1^{LL} tends to 1 more slowly than the other models. This aspect derives from the characteristic of LG and PR functions, both of them are sigmoid functions and they are smoother with respect to LL function. Minor differences can be observed between LG and PR models.

Figure 4-27 reports the trend of each type of selected function superimposed summing up the whole results between functions; it can be observed that LG and PR return quite similar response.
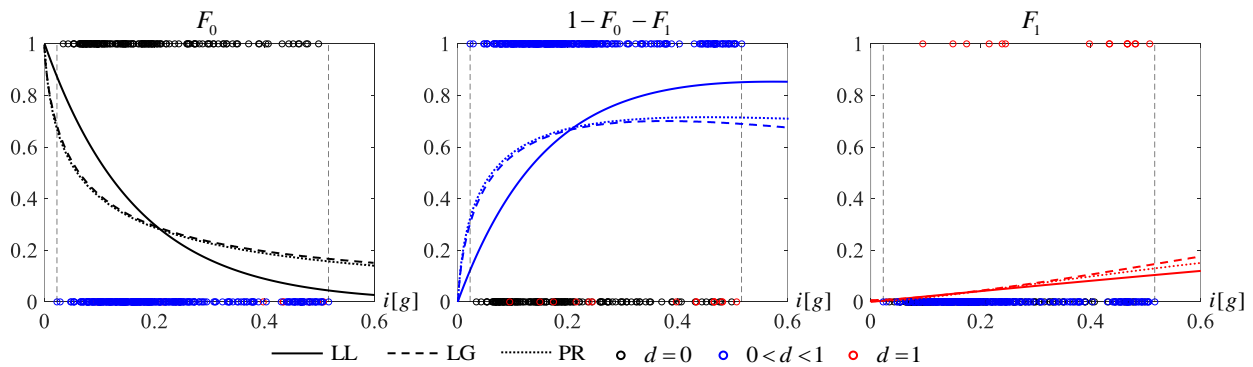
Figure 4-26. Distribution of the $F_0\left(i;\mathbf{\Theta}_0\right)$ and $F_1\left(i;\mathbf{\Theta}_1\right)$ considering the LL, LG and PR derived from the optimization procedure
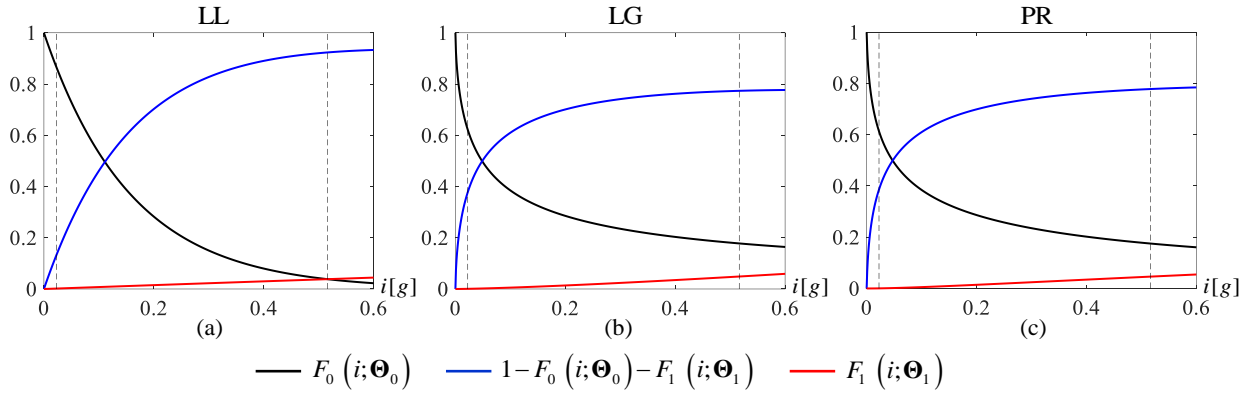
Figure 4-27. Comparisons of function F_0 and F_1 derived from the optimization procedure: (a) LL; (b) LG and (c) PR

In order to compare the performances of the different proposals, the likelihood value and the Akaike Information Criterion (AIC) are adopted. The AIC criterion is commonly used for the selection of the most effective model among a set of potential choice and it measures the goodness of fit while penalize model complexity (Akaike 1973). It is calculated as

$$AIC = -2l_{01}\left(\mathbf{\Theta}_0, \mathbf{\Theta}_1\right) + 2\xi \tag{4.23}$$

where ξ is the number of parameters adopted in the model. The model with the smallest AIC is not the model providing the best approximation, but it is the most effective under the point of view of the ratio between costs (parameters to be determined) and benefits (result accuracy).

The values of likelihood and AIC parameter are reported in Table 4-7, for the three models. It is worth noting that results concerning LG and PR are very similar, they provide lower values of likelihood and higher values of AIC index with respect to the LL approximation. Therefore, the LL approximation provides the best results considering both the absolute approximation (likelihood) and the cost-benefit ratio (AIC index), even if it requires one parameter only.

Table 4-7. Values of the parameters $\mathbf{\Theta}$ obtained from the optimization procedure for F_0 and F_1 functions and indices of goodness fit

Type	Θ_{OO}	Θ_{01}	Θ_{10}	Θ_{11}	$l_d\left(\mathbf{\Theta}_0, \mathbf{\Theta}_1\right)$	AIC value
LL	-	6.32	-	0.076	366.69	-729.38
LG	-1.96	-0.65	2.07	-1.37	346.64	-685.28
PR	-3.06	2.57	2.49	1.87	346.68	-685.36

121

Regarding the conditional PDF $f^*_{D|I}\left(d\,|i;\mathbf{\Theta}_d\right)$ two solutions have been analysed. The first proposal consists of a combination of two Exponential Distribution Functions (EDF), defined in the domain $[0,1]$:

$$f^*_{D|I}\left(d\,|i;\mathbf{\Theta}_d^{\text{EDF}}\right) = \frac{1}{A(i)}\left(e^{-a\left(i;\mathbf{\Theta}_d^{\text{EDF},a}\right)d} - e^{-a\left(i;\mathbf{\Theta}_d^{\text{EDF},a}\right)}\right)\left(e^{-b\left(i;\mathbf{\Theta}_d^{\text{EDF},b}\right)(1-d)} - e^{-b\left(i;\mathbf{\Theta}_d^{\text{EDF},b}\right)}\right) \qquad (4.24)$$

where $a\left(i;\mathbf{\Theta}_d^{\text{EDF},a}\right)$ and $b\left(i;\mathbf{\Theta}_d^{\text{EDF},b}\right)$ are two parameters varying with the seismic intensity i. The term $A(i)$ is a normalization coefficient

$$A(i) = \int_0^1\left(e^{-a\left(i;\mathbf{\Theta}_d^{\text{EDF},a}\right)d} - e^{-a\left(i;\mathbf{\Theta}_d^{\text{EDF},a}\right)}\right)\left(e^{-b\left(i;\mathbf{\Theta}_d^{\text{EDF},b}\right)(1-d)} - e^{-b\left(i;\mathbf{\Theta}_d^{\text{EDF},b}\right)}\right)dd \qquad (4.25)$$

required to have $\int_0^1 f^*_{D|I}\left(d\,|i;\mathbf{\Theta}_d\right)dd = 1$. For each value of i, Equation (4.24) provides a two-parameter distribution that permits controlling both the mean value and the dispersion of the system response. The EDF function is quite flexible and it is very effective in describing asymmetric distribution functions, as required for very high and low intensity level. A polynomial expression has been assumed to describe the variation of coefficients a and b due to variation of i. It has been assumed that the two coefficients vary independently from each other and a linear approximation has been chosen for both; this provides a satisfactory balance between computational effort required by the maximum likelihood procedure and the quality of the approximation. The polynomial expressions of coefficients a and b are

$$a\left(i;\mathbf{\Theta}_d^{\text{EDF},a}\right) = \Theta_{d0}^{\text{EDF},a} + \Theta_{d1}^{\text{EDF},a}i \qquad (4.26a)$$

$$b\left(i;\mathbf{\Theta}_d^{\text{EDF},b}\right) = \Theta_{d0}^{\text{EDF}b} + \Theta_{d1}^{\text{EDF},b}i \qquad (4.26b)$$

and the parameters are collected in the vector $\mathbf{\Theta}_d = \left[\mathbf{\Theta}_d^{\text{EDF},a}, \mathbf{\Theta}_d^{\text{EDF},b}\right]$.

A different choice can be carried out by assuming a truncated Normal Distribution Function (NDF) for $f_{D|I}^{*}\left(d\,|i;\mathbf{\Theta}_{d}\right)$, considering two parameters for each value of i, as in the previous case. The NDF function is based on the normal distribution commonly used to describe problems characterized by a large level of uncertainty (e.g. seismic attenuation laws, magnitude-frequency laws, etc.). The expression of the conditional PDF is

$$f_{D|I}^{*}\left(d\,|i;\mathbf{\Theta}_{d}^{\mathrm{NDF}}\right)=\frac{n(d;i,\mathbf{\Theta}_{d}^{\mathrm{NDF}})}{N(1;i,\mathbf{\Theta}_{d}^{\mathrm{NDF}})-N(0;i,\mathbf{\Theta}_{d}^{\mathrm{NDF}})} \tag{4.27}$$

where

$$n(d;i,\mathbf{\Theta}_{d}^{\mathrm{NDF}})=\frac{1}{\sigma\left(i;\mathbf{\Theta}_{d}^{\mathrm{NDF},\sigma}\right)\sqrt{2\pi}}e^{-\frac{d-\mu\left(i;\mathbf{\Theta}_{d}^{\mathrm{NDF},\mu}\right)}{2\left[\sigma\left(i;\mathbf{\Theta}_{d}^{\mathrm{NDF},\sigma}\right)\right]^{2}}} \tag{4.28}$$

is the normal distribution, and $N\left(d;i,\mathbf{\Theta}_{d}^{\mathrm{NDF}}\right)$ is the cumulative density function of the normal distribution. As above, it is assumed that the two coefficients μ and σ, expressing mean and variance of the distribution, vary linearly with the intensity. The expression of two coefficients μ and σ assumes the form

$$\mu\left(i;\mathbf{\Theta}_{d}^{\mathrm{NDF},\mu}\right)=\Theta_{d0}^{\mathrm{NDF},\mu}+\Theta_{d1}^{\mathrm{NDF},\mu}i \tag{4.29a}$$

$$\sigma\left(i;\mathbf{\Theta}_{d}^{\mathrm{NDF},\sigma}\right)=\Theta_{d0}^{\mathrm{NDF},\sigma}+\Theta_{d1}^{\mathrm{NDF},\sigma}i \tag{4.29b}$$

and the parameters are collected in the vector $\mathbf{\Theta}_{d}^{\mathrm{NFD}}=\left[\mathbf{\Theta}_{d}^{\mathrm{NDF},\mu},\mathbf{\Theta}_{d}^{\mathrm{NDF},\sigma}\right]$.

Figure 4-28 reports the trends of the polynomial expressions describing the conditional PDF obtained from the optimization procedure, highlighting the intensity ranges in which the parameters were assessed (out of range in grey).

In particular, Figure 4-28a shows the trends of linear functions $a\left(i;\mathbf{\Theta}_{d}^{\mathrm{EDF},a}\right)$ and $b\left(i;\mathbf{\Theta}_{d}^{\mathrm{EDF},b}\right)$. They are characterized by opposite trends, positive values of $a\left(i;\mathbf{\Theta}_{d}^{\mathrm{EDF},a}\right)$ together with negative values of $b\left(i;\mathbf{\Theta}_{d}^{\mathrm{EDF},b}\right)$

moves the peak of $f_{D|I}^*\left(d\,|\,i;\mathbf{\Theta}_d\right)$ toward $d=0$; while negative values of $a\left(i;\mathbf{\Theta}_d^{\mathrm{EDF},a}\right)$ and positive values of $b\left(i;\mathbf{\Theta}_d^{\mathrm{EDF},b}\right)$ move the peak of the distribution toward $d=1$.

Figure 4-28b shows trends of linear functions $\mu\left(i;\mathbf{\Theta}_d^{\mathrm{NDF},\mu}\right)$ and $\sigma\left(i;\mathbf{\Theta}_d^{\mathrm{NDF},\sigma}\right)$. In detail, the mean parameter $\mu\left(i;\mathbf{\Theta}_d^{\mathrm{NDF},\mu}\right)$ increases by increasing the intensity measure, moving the peak of the conditional PDF toward $d=1$, while the standard deviation $\sigma\left(i;\mathbf{\Theta}_d^{\mathrm{NDF},\sigma}\right)$ decreases in the interval of interest, causing a reduction of the bell curve opening.

Extrapolation of results out from the range of data is generally not admitted, however it could be necessary in the evaluation of risk assessment. It is suggested to assume constant values equal to the ones obtained at range boundary, in order to avoid inconsistencies (e.g. $\sigma<0$).

Table 4-8 collects the numerical values of parameters obtained from optimization procedure, the maximum likelihood and the AIC values evaluated by means Equations (4.23) considering $l_d\left(\mathbf{\Theta}_d\right)$ instead of $l_{01}\left(\mathbf{\Theta}_0,\mathbf{\Theta}_1\right)$. It should be pointed out that results of the exponential combination provide an upper value of likelihood and a lower value of AIC index, with respect to the normal distribution approximation. Therefore, the exponential approximation seems to be more efficient in the considered case.

Figure 4-29 on the left side, shows the median, 1st and 3rd quartile trends of the distributions $f_{D|I}^*\left(d\,|\,i;\mathbf{\Theta}_d\right)$ of damage in the subset $d\in(0,1)$, i.e. , $d\neq0$ and $d\neq1$. The right side of Figure 4-29 reports the conditional PDF $f_{D|I}^*\left(d\,|\,i;\mathbf{\Theta}_d\right)$ of the damage for five intensities i ($i=0.1$g, 0.2g, 0.3g, 0.4g, 0.5g). It should be underlined that in the case of exponential distribution (Figure 4-29a), the maximum value of the distribution moves from $d=0$ to $d=1$ passing from low to high intensities and the shape of the function notably varies. In the case of the normal distribution (Figure 4-29b), the amplitude of the bell is similar at all the intensity levels while the function translates from low to high damage by increasing the seismic intensity.
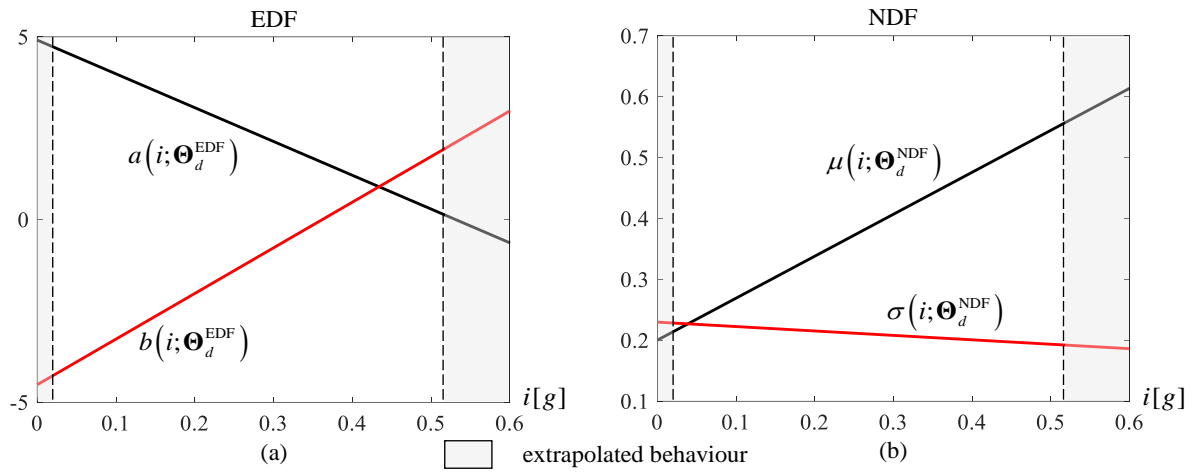
Figure 4-28. Trend of linear combinations of parameters derived from the optimization procedure: (a) EDF, and (b) NDF

Table 4-8. Values of the parameters $\mathbf{\Theta}_d$, $l_d\left(\mathbf{\Theta}_d\right)$ and AIC value obtained from the optimization procedure for EDF and NDF distribution

Type of Function	Parameters	Θ_{d0}	Θ_{d1}	$l_d\left(\mathbf{\Theta}_d\right)$	AIC value
EDF	$a\left(i;\mathbf{\Theta}_d^{\text{EDF},a}\right)$	4.9111	-9.2474	-96.59	201.19
	$b\left(i;\mathbf{\Theta}_d^{\text{EDF},b}\right)$	-4.5176	12.4867		
NDF	$\mu\left(i;\mathbf{\Theta}_d^{\text{NDF},\mu}\right)$	0.2000	0.6890	-102.42	212.84
	$\sigma\left(i;\mathbf{\Theta}_d^{\text{NDF},\sigma}\right)$	0.2299	-0.0726		
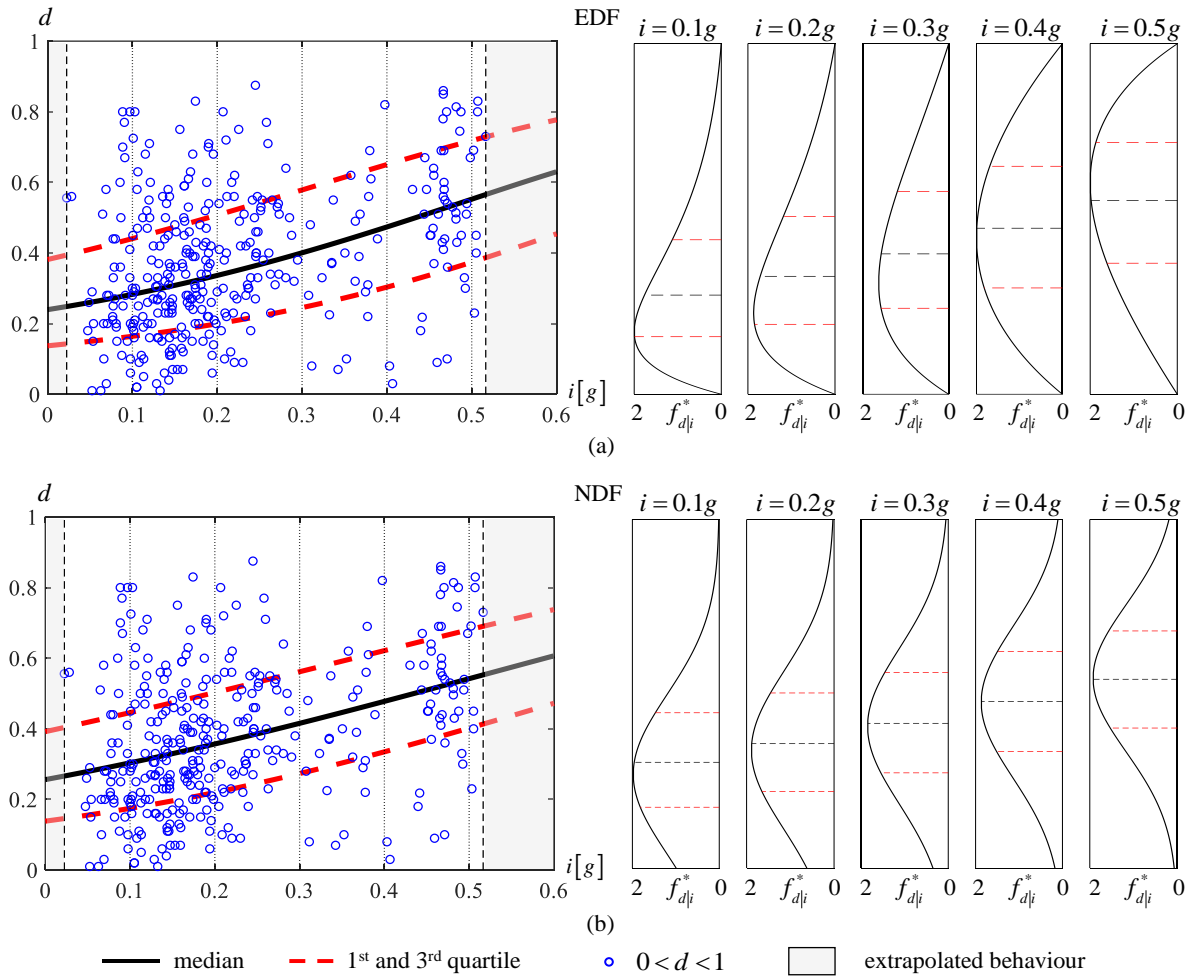
Figure 4-29. Median, 1st and 3rd quartile of distributions $f_{D|I}^{*}\left(d\,|i;\Theta_{d}\right)$ depending of intensity (left) and distribution of

$f_{D|I}^{*}\left(d\,|i;\Theta_{d}\right)$ *given a discrete intensity (right): (a) EDF and (b) NDF*

Starting from results of $F_{0}\left(i;\Theta_{0}\right)$, $F_{1}\left(i;\Theta_{1}\right)$, and distribution $f_{D|I}^{*}\left(d\,|i;\Theta\right)$ previously obtained, the LL functions and the EDF combination are the best selections to describe the model response. Figure 4-30 shows the global probabilistic model obtained by combining previous results regarding approximating functions. The conditional CDF $F_{D|I}\left(d\,|i;\Theta\right)$ and conditional PDF $f_{D|I}\left(d\,|i;\Theta\right)$ of the proposed model have been reported for a set $i_{z}=i_{1}<...<i_{N_{z}}$ of seismic intensity levels. It should be noted the percentage of undamaged churches notably varies by increasing the seismic intensity, while the percentage of collapsed or not recoverable churches is quite small also for high intensities. Furthermore, the shapes of conditional PDF of damage distribution vary significantly with the seismic intensity.
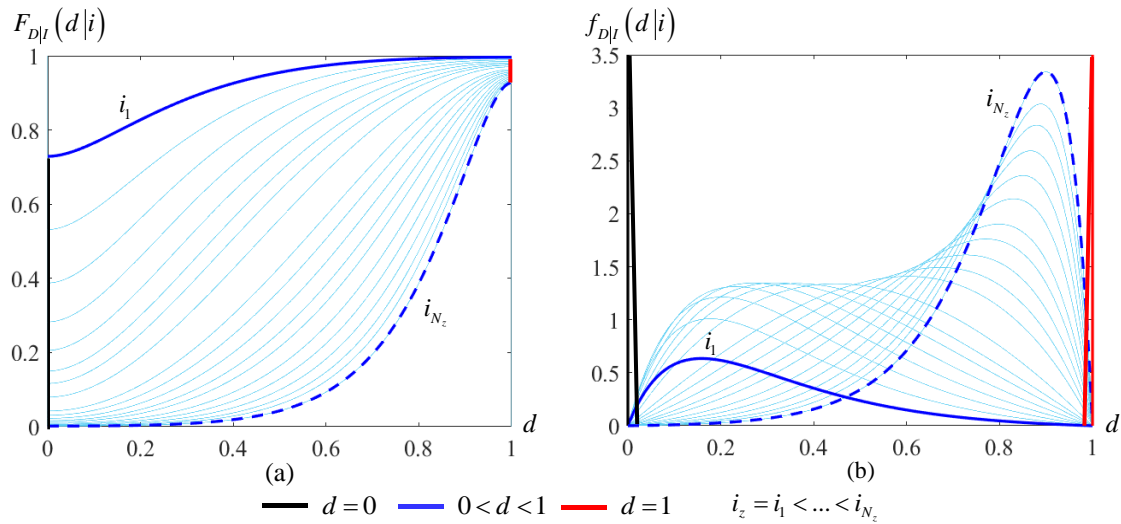
Figure 4-30. Expected conditional distribution of probability given intensity: (a) conditional CDF $F_{D|I}(d|i;\Theta)$ and (b) conditional PDF $f_{D|I}(d|i;\Theta)$

4.3.2.3 Fragility curves derived from the empirical probabilistic model

In this section, fragility curves, introduced in the probabilistic model paragraph, are evaluated. In particular, the discrete levels of damage have been selected according to Grünthal (1998), considering five ordered levels of damage, denoted as D_k $(k=1,..,5)$, defined on the basis of five disjoint and complementary damage intervals (Lagomarsino and Podestà 2004b).

Figure 4-31 shows the fragility curves for these levels of damage, derived from previous models combining different functions for $f_{D|I}^*$, F_0 and F_1. More precisely, the rows of Figure 4-31 represent the different functions considered in which the first shows the exponential distribution, while the second the normal one. Furthermore, the columns of Figure 4-31 specify the LL function, LG function and PR function respectively in the first, second and third column. In addition, the grey windows report the extrapolated curves evaluated out of the range of intensity where the curves have been approximated. It can be observed that the fragility curves for LG and PR functions show a similar behaviour due to the smoothness of their sigmoid function for both EDF and NDF distributions. Moreover, the fragility curves of the LL function move to 1 faster than the curves of the other two functions.
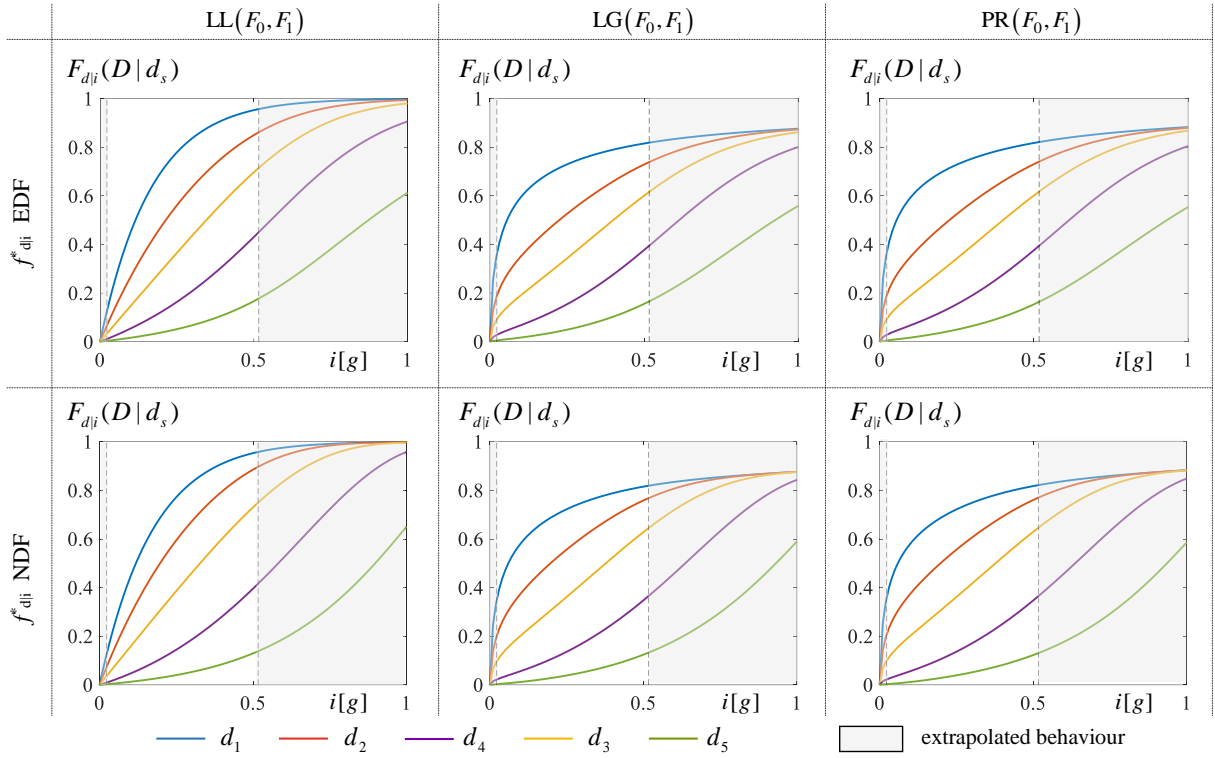
Figure 4-31. Fragility curves derived combining different proposed functions for F_0, F_1 and $f_{D|I}^*$

4.3.3 Illustrative example of the damage model

In this section, the proposed damage model is applied to evaluate the potential damage scenario following a single seismic event. The considered region is near the Archdiocese of Camerino-San Severino Diocese, and it is assumed that seismic response of churches is similar to the response observed in the post-event survey used for parameter calibration. For this purpose, the seismogenetic fault of Senigallia, located in the coast of Marche Region, is considered. This fault originated a seismic event of magnitude $M_w = 5.8$ in 1930, causing significant damage to cultural heritage.

It is a blind thrust fault and it is characterized by a potential magnitude $M_w = 5.9$ with a mean depth of 7 km (Vannoli et al. 2015; Laurenzano et al. 2008). Figure 4-32a reports the location of seismogenetic source and the parameters of the 1930 event (Vannoli et al. 2015), while Figure 4-32b shows the area interested by the single event.

The distribution of intensity measure $f_I(i|M,r)$ in terms of PGA, given an epicentral distance r, and magnitude M of a single event, is evaluated by the same GMPE adopted for shake maps used in model calibration. The expression of the attenuation law is (Ambraseys et al. 1996)

$$\log_{10} I = C_1 + C_2 M_S + C_4 \log_{10} \rho + C_A S_A + C_S S_S + \varepsilon \tag{4.30}$$

where I is a random variable describing the expected intensity measure, that is the PGA (g) in the considered case, M_S is the surface-wave magnitude, $\rho = \sqrt{r^2 + h_0^2}$ contains the epicentral distance r, C_1=-1.48, C_2=0.266, C_4=-0.922, C_A=0.117, C_S=0.124, and h_0=3.5 are coefficients and S_A, S_S assume value [0,1] depending on the superficial soil category (rock, stiff, soft and very soft soil). The term ε is a normally distributed random variable with 0-mean and constant standard deviation σ =0.25, that describes uncertainties on the prediction of intensity measure.
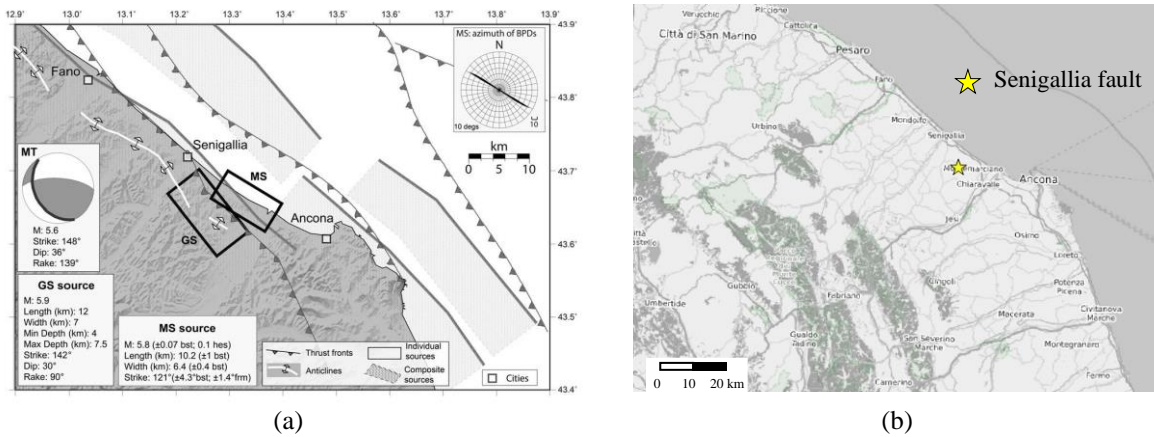
Figure 4-32. Senigallia fault: (a) Macroseismic Source (MS) and Geological Source (GS) parameters for the 1930 earthquake and (b) area considered in the application

The shear-wave magnitude M_S is calculated from the M_W = 5.9 adopting the relation proposed by Scordilis (2006) and assumes a value of M_S = 5.72. For what concern the soil category, stiff soil is assumed as average behaviour and coefficients S_A and S_S get values of 0 and 1 respectively.

Figure 4-33a shows the trend of the median value of intensity measure I with respect to the epicentral distance, while Figure 4-33b reports the PDF $f_I(i|M,r)$ of the intensity expected at different epicentral distances r_k from r_1 = 5 km to r_{max} = 150 km spacing 5 km (grey lines), and the highlighted curves correspond to distance values equal to 5 km, 20 km, 50 km, 100 km. It is worth to note that both the mean value and the standard deviation of the expected intensity increase as the epicentral distance decreases. In the sequel, the maximum considered epicentral distance is r_{max} = 150 km, since the average PGA is less than 0.029 g, and therefore negligible with respect to a possible damage of churches.
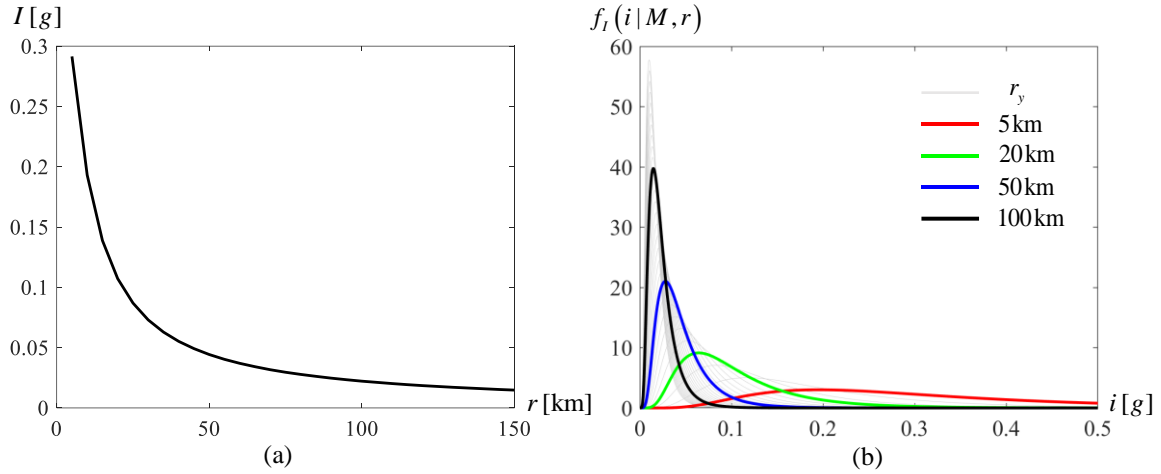
Figure 4-33. Seismic hazard: (a) mean expected intensity measure (PGA) and (b) distribution of intensity $f_I(i|M,r)$ given epicentral distance

The distribution of damage at a distance r can be evaluated by combining the proposed model with the distribution of seismic intensity, as follow

$$F_{D|R}(d|r) = \int_{\Re^+} F_{D|I}(d|i) f_I(i|r) di \tag{4.31}$$

where $F_{D|I}(d|i)$ is the CDF of the damage. In this application a LL function is adopted to describe the F_0 and F_1, and the EDF combination is adopted to describe $f_{D|I}^*$ as the best solutions, according to previous section outcomes.

Figure 4-34 reports the CDF $F_{D|R}(d|r_y)$ and the related PDF $f_{D|R}(d|r_y)$ of damage for different values of the distance r_y from $r_1 = 5$ km to $r_{max} = 150$ km spacing 5 km (grey lines), and the highlighted curves correspond to distance values equal to 5 km, 20 km, 50 km, 100 km.

It can be argued that the probability to have undamaged churches (d=0) increases with the increase of r while the probability to have churches with damage between (0-1) and its standard deviation decreases by increasing r. Finally, the probability to have a damage $d = 1$ (collapsed churches) is less than 3% for $r = 5$ km and almost null for $r = 150$ km.
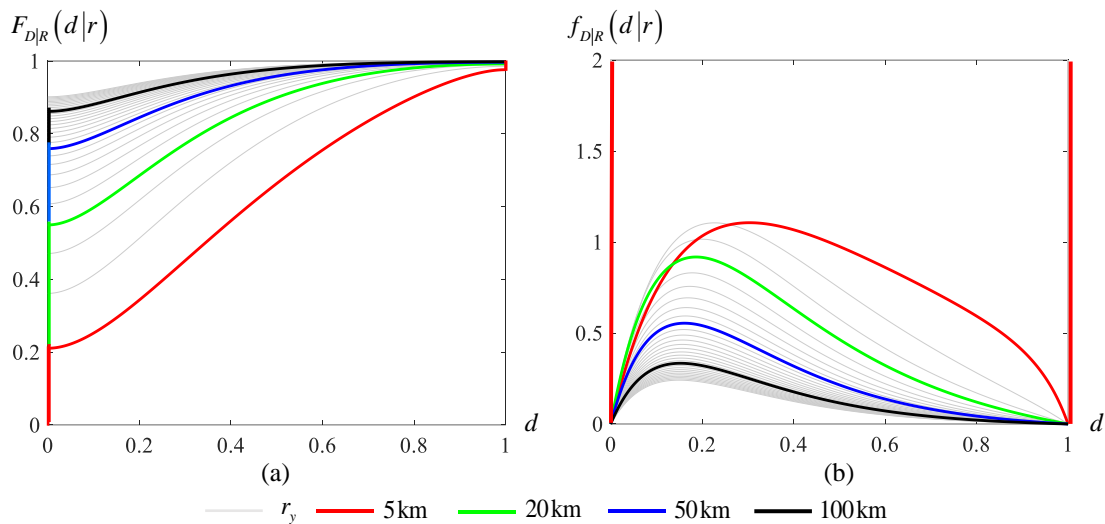
Figure 4-34. Damage distribution given epicentral distance: (a) CDF $F_{D|R}(d|r)$ and (b) PDF $f_{D|R}(d|r)$

Figure 4-35a shows the trend of mean damage $\mu_D(r)$ and standard deviations $\sigma_D(r)$ depending on the epicentral distance, while Figure 4-35b reports the box plot of median $Q_2(r)$, 25nd percentile $Q_1(r)$ and 75nd percentile $Q_3(r)$ of the damage depending on the epicentral distance; in additions dashed lines represent the extreme values corresponding 5 and 95 percentiles respectively. The percentage of damaged churches is lower that 50% for churches located at a distance larger than 25 km, while the percentages are lower than 25% for distances larger than 50 km.
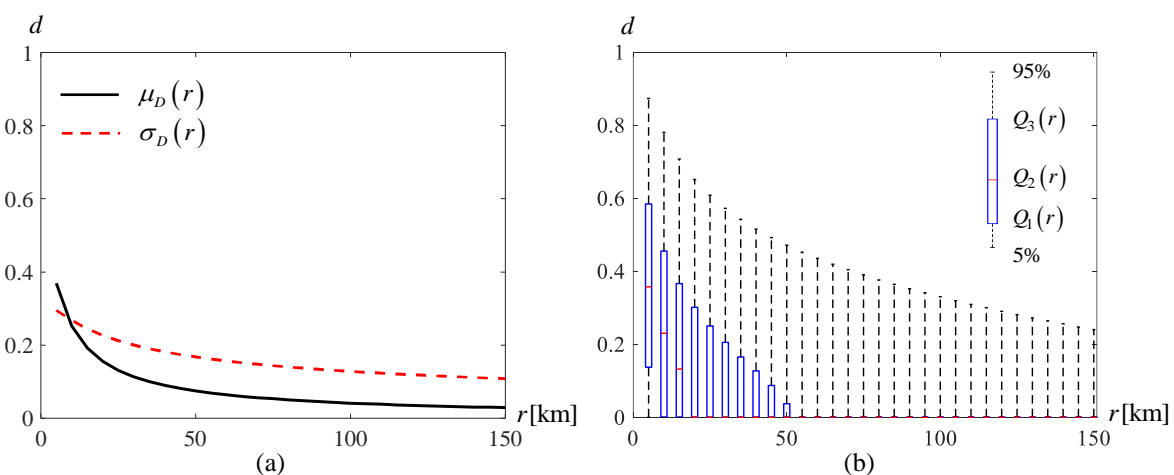
Figure 4-35. Damage distribution given epicentral distance: (a) mean damage and (b) median, 1st quartile, and 3rd quartile of damage

Finally, Figure 4-36 describes the overall damage scenario expected in the region, by combining results obtained from the proposed predictive models with the real location of the historical churches provided by the national catalogue (GeoNue 2019). More precisely, the expected value of d (mean value) of each church is reported by a color scale and the table reports the number of churches suffering different levels of damage.
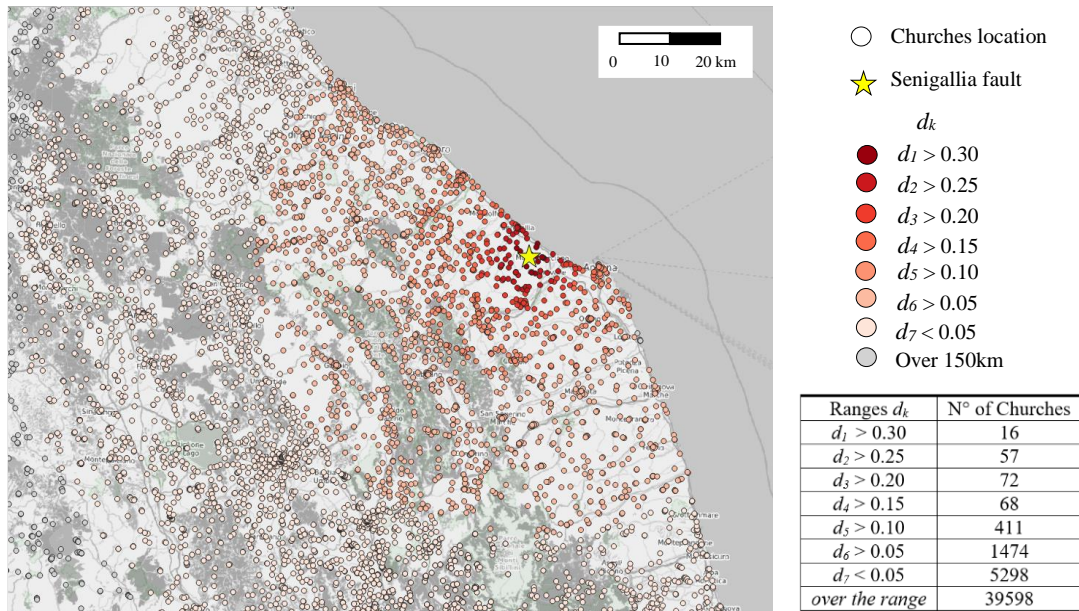
Figure 4-36. Damage distribution over the territory considering a maximum radius of 150 km

4.3.4 Decision making

In this paragraph, the damage scenario, obtained combining response model and seismic hazard, is used to take decisions about specific actions oriented to mitigate the seismic risk. The following problem is considered as an example: fixed a damage threshold, the region must be divided into two sub-regions: in the former, a damage larger than the threshold is expected; in the latter, it is expected a damage lower than the threshold. Given the response variability, a percentage of misclassification is expected in both the regions, and the study aims to divide the total region in such a way that the misclassification is minimized. The analysis outcome can be of interest to plan risk reduction measures or retrofit actions on churches more prone to damage.

The damage threshold is denoted by $\bar{d}$ and the domain of the expected damage is divided in two subsets, related to the occurrence of two different events: E_0, denoting the occurrence of a damage lower to the threshold ($d < \bar{d}$), and E_1 corresponding to the occurrence of a damage greater or equal to the threshold ($d \geq \bar{d}$). The conditional probability of the two events E_0 or E_1 at the distance r can be derived from the risk analysis

$$P\left[E_0|r\right] = \int_0^{\bar{d}} f_{D|X}\left(d|r\right)dd \qquad P\left[E_1|r\right] = 1 - P\left[E_0|r\right] \tag{4.32a,b}$$

It is assumed that the churches are homogeneously smeared over the region. This is a simplifying assumption introduced to derive a closed form solution in this example with illustrative purpose. The joint probability to observe a church with a damage higher/lower than the threshold $\bar{d}$ (event E_0 or E_1) at a distance r is distributed as follow

$$f_{E_0}\left(E_0,r\right) = P\left[E_0|r\right]f_R\left(r\right) \qquad f_{E_1}\left(E_1,r\right) = \left(1 - P\left[E_0|r\right]\right)f_R\left(r\right) \tag{4.33a,b}$$

where $f_R\left(r\right)$ is the density of the probability to find a church at the distance r, its expression is $f_R\left(r\right) = 2r/r_{\max}^2$ where $r_{\max} = 150$ km is the maximum distance considered, according to homogeneous distribution, and increases with the distance.

The separation of the total region into two sub-regions is controlled by the distance r_0, splitting the total surface into an inner region ($r < r_0$) and an outer region ($r > r_0$). The marginal probability to observe event E_0, or event E_1, in the inner region bounded by r_0 can be evaluated by

$$P_{E_0}\left(r_0\right) = \int_0^{r_0} P\left[E_0|r\right]f_R\left(r\right)dr \qquad P_{E_1}\left(r_0\right) = \int_0^{r_0}\left(1 - P\left[E_0|r\right]\right)f_R\left(r\right)dr \tag{4.34a,b}$$

In order to take a decision based on the probability of occurrence of one of the two events, the extension r_0 of region should minimize the probability of mispredictions. In this case, the optimal value of r_0 is located at the intersection between the two functions $f_{E_0}\left(E_0,r\right)$ and $f_{E_1}\left(E_1,r\right)$ (Bishop 2006), or when $P_{E_0}\left(r_0\right) = P_{E_1}\left(r_0\right)$.

Two threshold damage values have been considered $\bar{d} = 0.1$ and $\bar{d} = 0.2$, in particular Figure 4-37 shows the marginal probability and the joint probability for the two damage thresholds considered in the analysis, as well as the distance r_0 that minimize the probability of misprediction. This distance r_0 assumes the value 13.80 km for $\bar{d} = 0.1$, and 9.50 km for $\bar{d} = 0.2$.
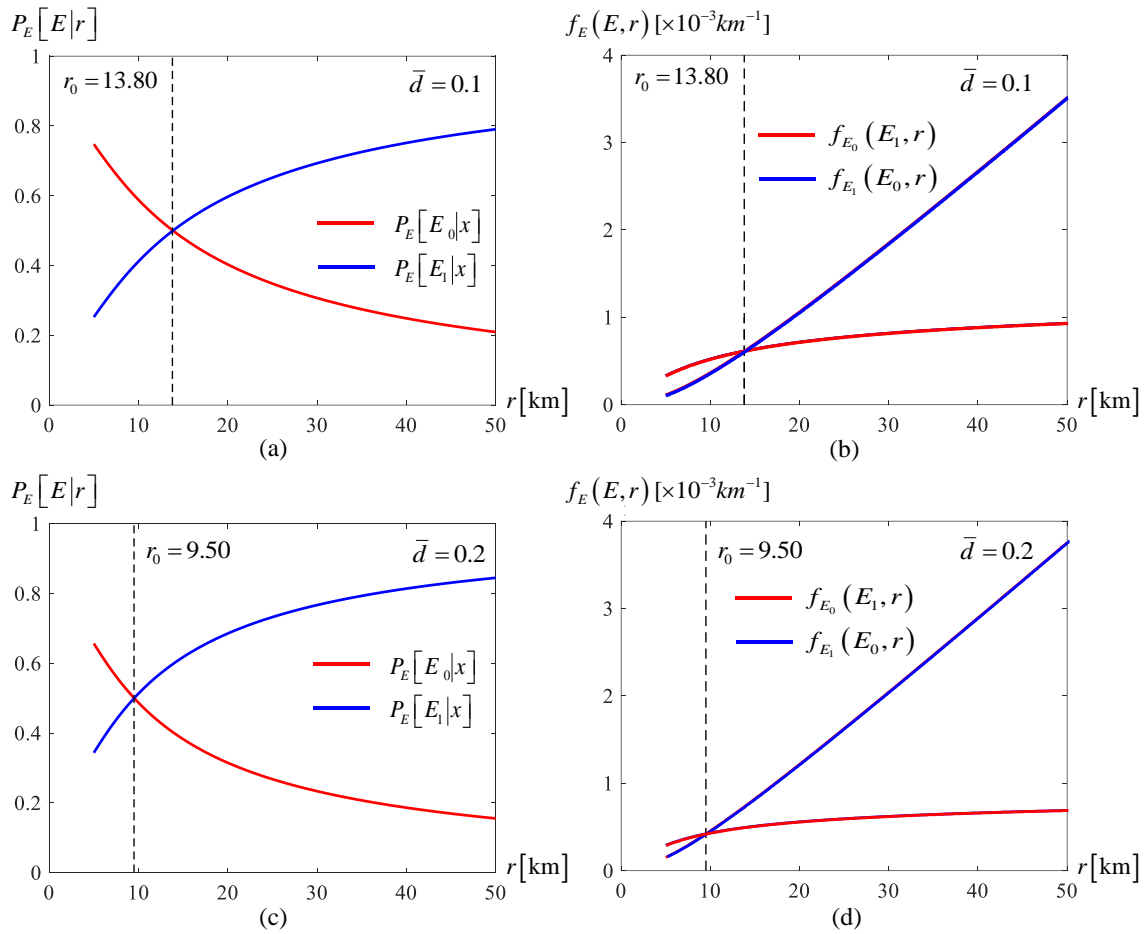
Figure 4-37. Probability of the two events E_0 and E_1 in the inner region, for $\bar{d}$ =0.1 (first row) and $\bar{d}$ =0.2 (second row): (a),(c) marginal probability, and (b),(d) joint probability distribution

4.3.5 Probabilistic model for evaluating the consequences

In this paragraph, the probabilistic response consequences model is presented. The consequences evaluation is a key point of the risk analysis. The quantities that describe the consequences of the response, may be substantially different each other but connected on the same seismic scenario. In this paragraph, the Repair Cost (RC) is assumed as quantity that describes the consequence considered and it is represented by the cost in euros for unit of the church surface (€/mq).

In the proposed RC model, the repair cost is a continuous random variable C, whose values c belong to the domain $[0,\infty)$, and that are related to a damage index described by a scalar random variable D defined in the domain $[0,1]$. The probability of observing a cost level lower than an assigned value c, given the damage level d, is described by the following CDF

$$F_{C|D}\left(c|d\right) = P\left[C < c|d\right] \qquad\qquad c \in \left[0,\infty\right) \qquad\qquad (4.35)$$

Generally, for an assigned value of the damage d, the expected conditional PDF $f_{C|D}\left(c|d\right)$, can be expressed by a continuous function in the interval $[0,\infty)$. The assessment of PDF $f_{C|D}\left(c|d;\Theta_c\right)$ is based on a set of observed pairs $\left(c_q,d_q\right)$ $\left(q = 1,..,N\right)$, achieved fixing the shaped function, whose parameters Θ_c are determined by inference techniques.

To evaluate the parameters of these functions, the maximum likelihood estimation has been employed according with the following expression:

$$L\left(\Theta_c\right) = \prod_{q=1}^{N} P\left(c_q,d_q;\Theta_c\right) \qquad\qquad (4.36)$$

or, as usual, the parameters are obtained by maximizing the log-likelihood function (Dang et al. 2017; Straub et al. 2008; Lallemant et al. 2015)

$$l\left(\Theta_c\right) = \sum_{q=1}^{N} \ln P\left(c_q,d_q;\Theta_c\right) \qquad\qquad (4.37)$$

where $\left(c_q,d_q\right)$ $\left(q = 1,..,N\right)$ denotes the *q-th* observed pair of damage and repairing cost and the model provides the corresponding probability of occurrence. N represents the number of churches that present a repairing cost value. The vector Θ_c collects the parameters regarding the options functions for describing the model.

4.3.6 Application of the RC model to historical churches

In this paragraph, the proposed RC model is applied to historical churches struck by the 2016 Central Italy seismic sequence.

4.3.6.1 Database definition

The dataset is built considering the historical churches of the Archdiocese of Camerino-San Severino that have received a repairing cost value or an economic contribution furnished by the Italian Government (Ordinanza n. 105) after the 2016 Central Italy seismic sequence. Indeed, the Italian Government provided an estimated cost suitable for the reconstruction of the church or intervention costs on it. There are calculated costs per area for each church, by considering the surface of the church as the maximum dimensional surface between the area of the ground floor and the area of the covering.

Figure 4-38a shows the location of the churches and their relative value of reconstruction cost per meter square within the Archdiocese, superimposed the envelope of shake maps relevant to the three main events of the 2016 seismic sequence. In addition, Figure 4-38b reports the distribution sample referred to the cost per area, and Table 4-9 shows the number of churches in each reconstruction cost values range.

(a)   (b)
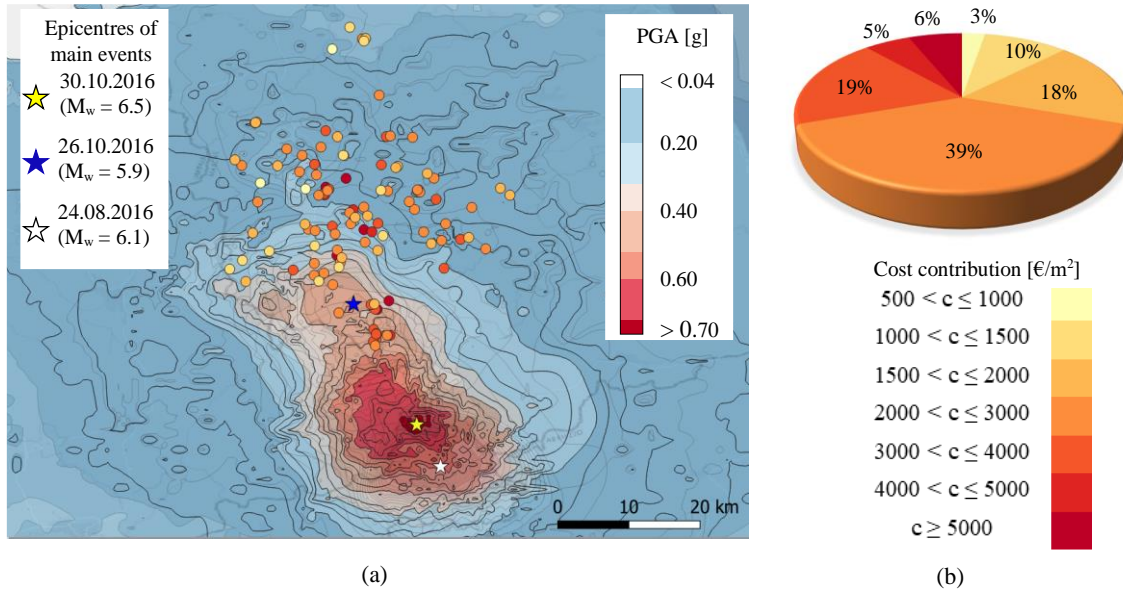
Figure 4-38. Distribution of the churches with a cost contribution: (a) distribution over the territory of the churches considering their cost contribution and (b) distribution of the cost contribution of the churches

Table 4-9. Ranges of cost levels and number of churches in each interval for both GMPEs and distribution functions.

Ranges of cost [€/m2]	Number of churches
$550 < c \leq 1000$	3
$1000 < c \leq 1500$	11
$1500 < c \leq 2000$	20
$2000 < c \leq 3000$	44
$3000 < c \leq 4000$	21
$4000 < c \leq 5000$	6
$c \geq 5000$	7

4.3.6.2 Parametric model

In this section, two distributions proposal have been selected. The first proposal consists in using a Lognormal Distribution Function (LDF) for $f_{C|D}\left(c|d\right)$:

$$f_{C|D}\left(c|d\right) = \frac{1}{c \cdot \sigma(d;\Theta_c^{LDF})\sqrt{2\pi}} \exp(-\frac{(\ln c - \mu(d;\Theta_c^{LDF}))^2}{2\sigma \cdot (d;\Theta_c^{LDF})^2}$$ (4.38)

where $\mu(d;\Theta_c^{LDF})$ and $\sigma(d;\Theta_c^{LDF})$ are the parameters varying with the damage index d.

The second proposal for the distribution function is the Gamma Distribution Function (GDF), defined by:

$$f_{C|D}\left(c|d\right) = \frac{1}{b(d;\Theta_c^{GDF,b})^{a(d;\Theta_c^{GDF,a})} \cdot \Gamma(a(d;\Theta_c^{GDF,a}))} c^{a(d;\Theta_c^{GDF,a})-1} \exp(\frac{-c}{b(d;\Theta_c^{GDF,b})}) \tag{4.39}$$

where $\Gamma(\cdot)$ is the gamma function, $a(d;\Theta_c^{GDF})$ and $b(d;\Theta_c^{GDF})$ are the parameters of GDF depending on the damage index d.

For both couple of parameters μ,σ and a,b, polynomial expressions have been assumed to describe the variation of parameters given d. Three choices have been considered to describe these polynomial expressions.

The first choice is a linear approximation for both expressions μ,σ and a,b:

$$\mu(d;\Theta_c^{LDF_1}) = \Theta_{c1}^{LDF_1} + d \cdot \Theta_{c2}^{LDF_1} ; \qquad \sigma(d;\Theta_c^{LDF_1}) = \Theta_{c3}^{LDF_1} + d \cdot \Theta_{c4}^{LDF_1} \tag{4.40a,b}$$

$$a(d;\Theta_c^{GDF_1}) = \Theta_{c1}^{GDF_1} + d \cdot \Theta_{c2}^{GDF_1} ; \qquad b(d;\Theta_c^{LDF_1}) = \Theta_{c3}^{GDF_1} + d \cdot \Theta_{c4}^{GDF_1} \tag{4.41a,b}$$

where the parameters are collected in the vectors $\Theta_c^{LDF_1} = \left[\Theta_{c1}^{LDF_1}, \Theta_{c2}^{LDF_1}, \Theta_{c3}^{LDF_1}, \Theta_{c4}^{LDF_1}\right]$ and $\Theta_c^{GDF_1} = \left[\Theta_{c1}^{GDF_1}, \Theta_{c2}^{GDF_1}, \Theta_{c3}^{GDF_1}, \Theta_{c4}^{GDF_1}\right]$

The second choice assumes an exponential expression for μ and a defined by two parameters, while for σ and b a linear approximation described by two parameters has been considered:

$$\mu(d;\Theta_c^{LDF_2}) = \Theta_{c1}^{LDF_2} \cdot d^{\Theta_{c2}^{LDF_2}} ; \qquad \sigma(d;\Theta_c^{LDF_2}) = \Theta_{c3}^{LDF_2} + d \cdot \Theta_{c4}^{LDF_2} \tag{4.42a,b}$$

$$a(d;\Theta_c^{GDF_2}) = \Theta_{c1}^{GDF_2} \cdot d^{\Theta_{c2}^{GDF_2}} ; \qquad b(d;\Theta_c^{LDF_2}) = \Theta_{c3}^{GDF_2} + d \cdot \Theta_{c4}^{GDF_2} \tag{4.43a,b}$$

The parameters are collected in the vectors $\Theta_c^{LDF_2} = \left[\Theta_{c1}^{LDF_2}, \Theta_{c2}^{LDF_2}, \Theta_{c3}^{LDF_2}, \Theta_{c4}^{LDF_2}\right]$ and $\Theta_c^{GDF_2} = \left[\Theta_{c1}^{GDF_2}, \Theta_{c2}^{GDF_2}, \Theta_{c3}^{GDF_2}, \Theta_{c4}^{GDF_2}\right]$.

Finally, the third choice assumes the same exponential expression adopted in the second case for μ and a, while for σ and b a constant expression has been chosen:

$$\mu(d;\Theta_c^{LDF_3}) = \Theta_{c1}^{LDF_3} \cdot d^{\Theta_{c2}^{LDF_3}} \; ; \qquad\qquad \sigma(\Theta_c^{LDF_3}) = \Theta_{c3}^{LDF_3} \qquad\qquad (4.44a,b)$$

$$a(d;\Theta_c^{GDF_3}) = \Theta_{c1}^{GDF_3} \cdot d^{\Theta_{c2}^{GDF_3}} \; ; \qquad\qquad b(\Theta_c^{GDF_3}) = \Theta_{c3}^{GDF_3} \qquad\qquad (4.45a,b)$$

and the parameters are collected in the vectors $\Theta_c^{LDF_3} = \left[\Theta_{c1}^{LDF_3}, \Theta_{c2}^{LDF_3}, \Theta_{c3}^{LDF_3}\right]$ and $\Theta_c^{LDF_3} = \left[\Theta_{c1}^{GDF_3}, \Theta_{c2}^{GDF_3}, \Theta_{c3}^{GDF_3}\right]$ respectively.

Regarding the GDF, a constraint is imposed for the polynomial function $a(d;\Theta_c^{GDF,a})$ that it must be lower than 2.

In Figure 4-39 - Figure 4-44 (a) the trend of the polynomial expressions options for the two distribution functions is shown, respectively for LDF from Figure 4-39 to Figure 4-41 and for GDF from Figure 4-42 to Figure 4-44, considering three type of functions. In Figure 4-39 - Figure 4-44 (b) the probability density function of the cost given a damage $f_{C|D}(c|d)$ is reported. Finally, Figure 4-39 - Figure 4-44 (c) display the 50th percentile in black, the 25th and 75th percentiles with dashed blue lines, and the mean function with red curve.
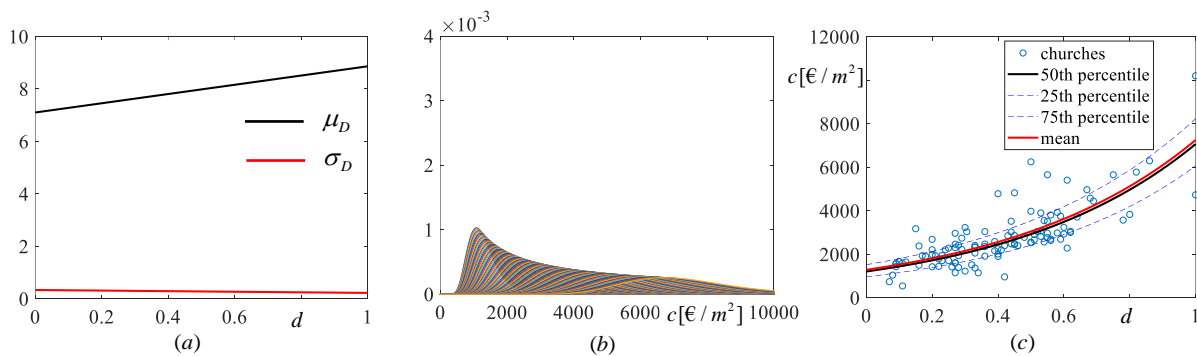
Figure 4-39. LDF considering the first choice of polynomial expression

138
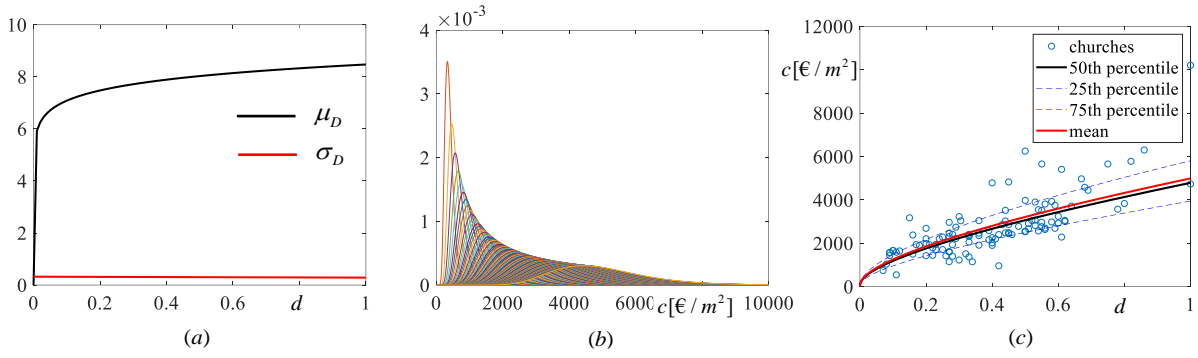
Figure 4-40. LDF considering the second choice of polynomial expression
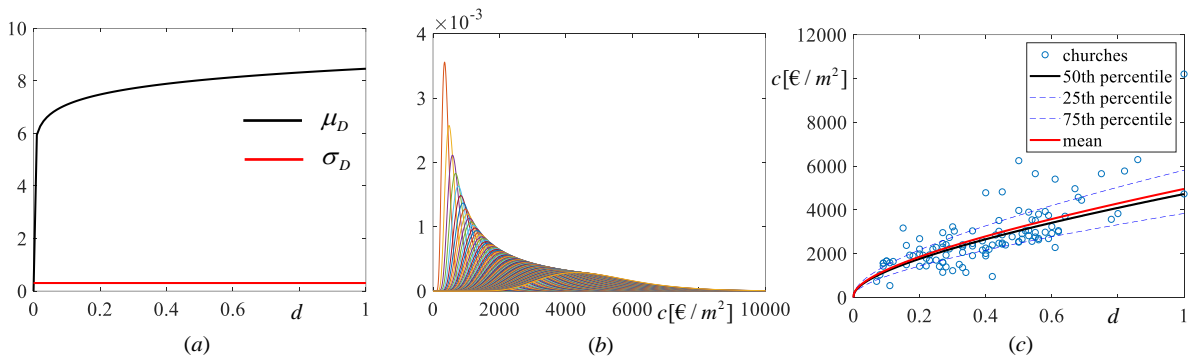
Figure 4-41. LDF considering the third choice of polynomial expression
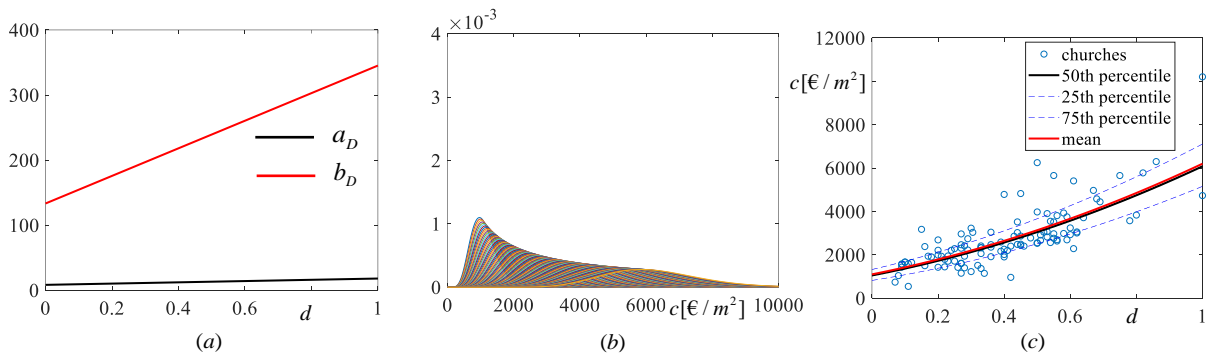
Figure 4-42. GDF considering the first choice of polynomial expression
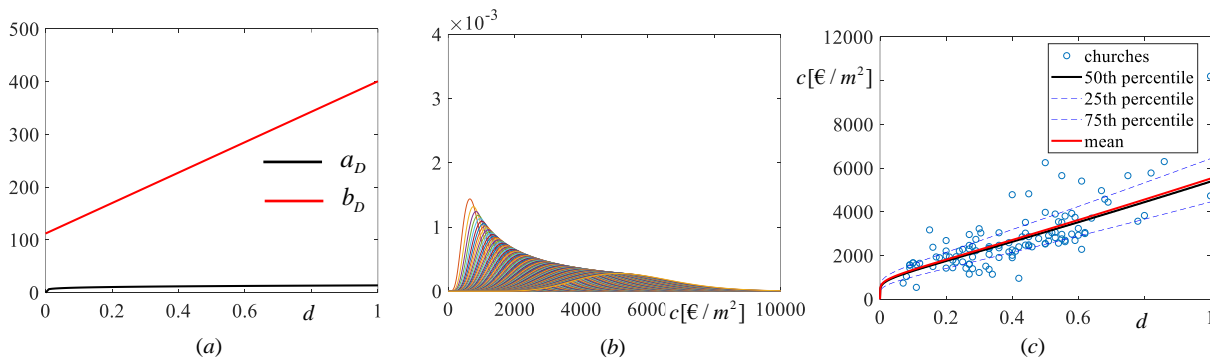
Figure 4-43. GDF considering the second choice of polynomial expression
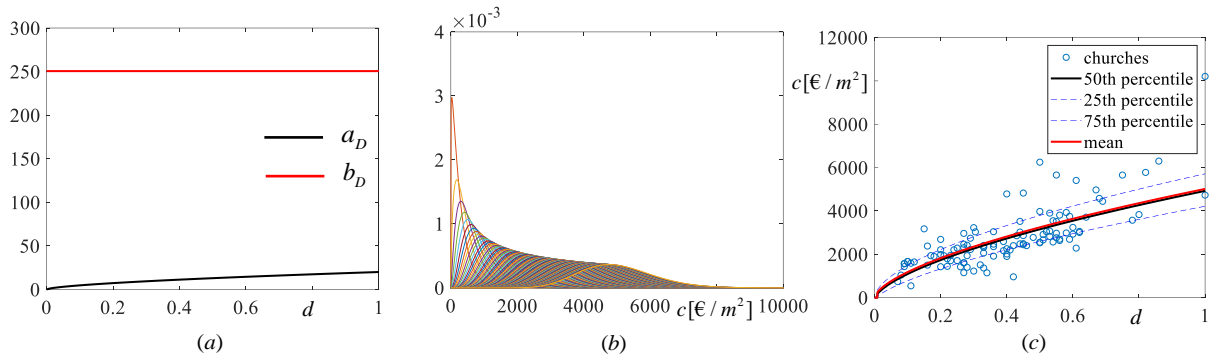
Figure 4-44. GDF considering the third choice of polynomial expression

In order to compare the performances of the different proposals, the likelihood value and the AIC are adopted. The values of likelihood and AIC parameter are reported in Table 4-10 and Table 4-11, for the three options of each distribution function.

Focusing on LDF, it is worth noting that the results concerning LDF_2 and LDF_3 are very similar: they provide higher values of likelihood and lower values of AIC index with respect to the LDF_1 approximation. Therefore, the LDF_3 approximation provides the best results considering both the absolute approximation (likelihood) and the cost-benefit ratio (AIC index), even if it requires three parameters only.

Considering now the GDF, it is shown the same general trend as the LDF. The best absolute approximation is furnished by the GDF_3 in terms of likelihood and AIC value.

Finally, comparing the two distribution functions LDF and GDF over all, the model that provides the best results is the GDF_3 in terms of maximum likelihood and AIC value.

Table 4-10. Values of the parameters Θ obtained from the optimization procedure for $f_{C|D}(c|d)$ functions considering LDF and indices of goodness fit.

Type	Θ_{c1}	Θ_{c2}	Θ_{c3}	Θ_{c4}	$l_c(\Theta_{c1},\Theta_{c2},\Theta_{c3},\Theta_{c4})$	AIC value
LDF[1]	7.103	1.761	0.337	-0.111	896.146	-1784.292
LDF[2]	8.474	0.078	0.321	-0.036	901.847	-1795.693
LDF[3]	8.462	0.077	0.307	-	901.922	-1797.843

Table 4-11. Values of the parameters Θ obtained from the optimization procedure for $f_{C|D}(c|d)$ functions considering GDF and indices of goodness fit.

Type	Θ_{c1}	Θ_{c2}	Θ_{c3}	Θ_{c4}	$l_c(\Theta_{c1},\Theta_{c2},\Theta_{c3},\Theta_{c4})$	AIC value
GDF[1]	8.247	9.713	133.312	211.959	896.520	-1785.039
GDF[2]	13.778	0.158	112.129	288.701	898.239	-1788.479
GDF[3]	20.019	0.629	250.558	-	905.359	-1804.718

4.3.7 Illustrative Example of the RC model

In this section, a demonstrative application of the RC consequence model is proposed. Starting from the model previously illustrated, the RC response consequence model described above is applied to evaluate the potential damage and cost scenario following a single seismic event. The Camerino fault has been considered as the seismic source and the damage expected in the set of historical churches belonging to Archdiocese of Camerino-San Severino, has been evaluated. The Fault is located to a depth of 9-15 km (Figure 4-45b) and it is characterized by a potential magnitude Mw=5.8, testified by the seismic event of 1799 that had a complex, and probably multiple, source that produced two separate areas of maximum damage (Monachesi et al., 2016). The fault belongs to the Central Apennines fault system, where the active faults consist of arrays of distinct overlapping segments which may be unconnected or linked into a single continuous fault surface (Tondi and Cello, 2003) as illustrated in Figure 4-45c. In addition, unconnected adjacent faults may interact each other through their stress fields, activating different earthquake sequences (Tondi and Cello, 2003). However, according with (Tondi, 2000), it is possible to assume that the surface faults, belonging to each seismogenic zone responsible for generating single seismic events with multiple ruptures, are the surface manifestations of earthquake-related deformation. Figure 4-45a reports the geographic location of Camerino fault, and Figure 4-45b shows the distribution of the historical and recent seismic activity of the region and the areas mainly damaged after the event of 1799, identified with light blue rectangles (Monachesi et al., 2016). Finally, Figure 4-45c displays the Central Apennines Fault System where measured active surface faults and related deep seismogenic structures are also shown (Tondi and Cello, 2003).
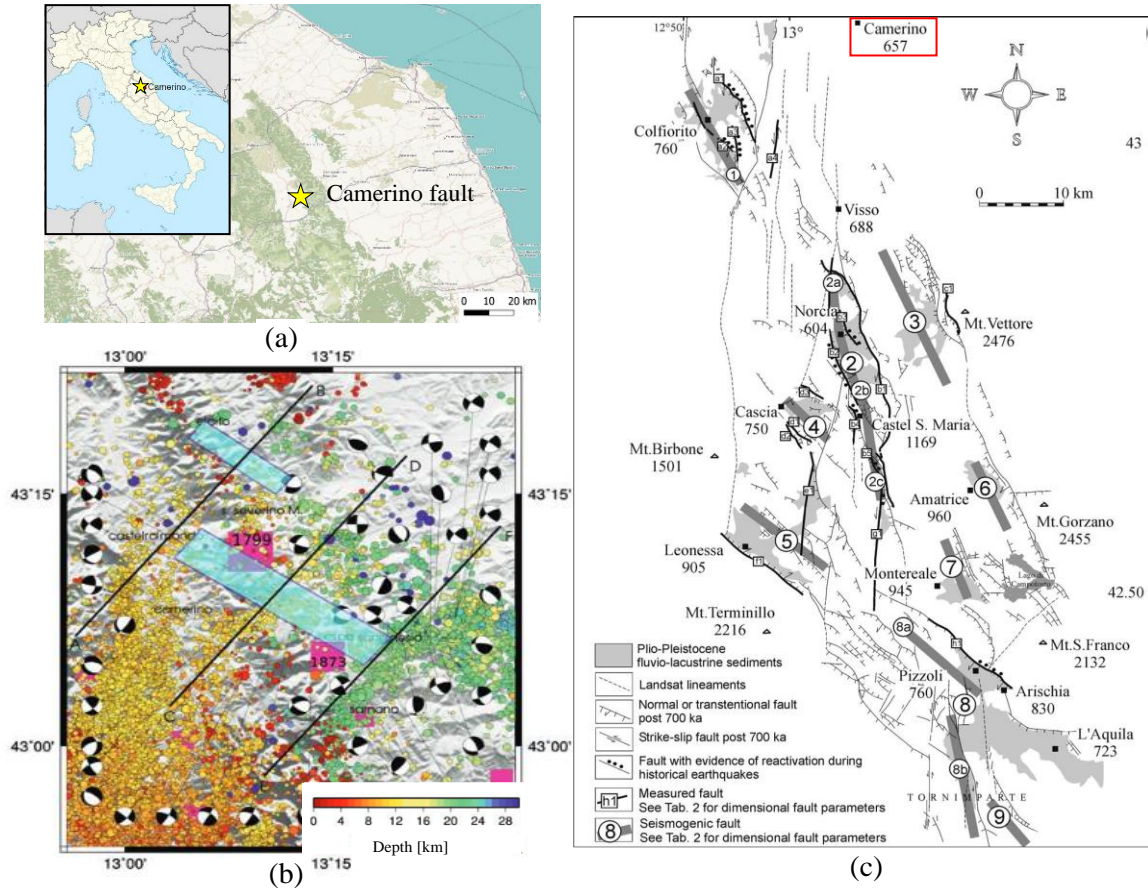
Figure 4-45. (a) Geographic location of Camerino fault; (b) Distribution of the historical and recent seismicity of the area with the areas mainly damaged after the 1799 earthquake (Monachesi et al., 2016); (c) the Central Apennines Fault System (Tondi and Cello, 2003).

The distribution of intensity measure $f_I(i|M,r)$ in terms of PGA, given an epicentral distance r, and magnitude M of a single event, is evaluated by the same GMPE adopted in Morici et al. In particular, the expression of the attenuation law is (Ambraseys et al. 1996)

$$\log_{10} I = C_1 + C_2 M_S + C_4 \log_{10} \rho + C_A S_A + C_S S_S + \varepsilon \tag{4.46}$$

where I is a random variable describing the expected intensity measure, that is the PGA (g) in the considered case, M_S is the surface-wave magnitude, $\rho = \sqrt{r^2 + h_0^2}$ contains the epicentral distance r that in this case is the specific distance church-seismogenetic fault, C_1 =-1.48, C_2 =0.266, C_4 =-0.922, C_A =0.117, C_S =0.124, and h_0 =3.5 are coefficients and S_A, S_S assume value [0,1] depending on the superficial soil category (rock, stiff, soft and very soft soil). The term ε is a normally distributed random variable with 0-mean and constant standard deviation σ =0.25, that describes uncertainties on the prediction of intensity measure. The shear-wave

magnitude M_S is calculated from the chosen $M_W = 5.8$ adopting the relation proposed by Scordilis (2006) and assumes a value of $M_S = 5.57$.

To make a comparison, the expression of the attenuation law of Lanzano et al. (Lanzano et al., 2019) has been used. It takes into account a dataset of Italian waveforms, adding 12 worldwide events with magnitude range 6.1 - 8.0. Its functional form is the following:

$$\log_{10} I = a + F_M(M_w, SOF) + F_D(M_w, R) + F_S(V_{S,30}) + \sigma \tag{4.47}$$

where

$$F_M(M_W, SOF) = f_i SOF_j + b_1(M_W - M_h) \, where \, M_W \leq M_h$$
$$F_M(M_W, SOF) = f_i SOF_j + b_2(M_W - M_h) \, where \, M_w > M_h \tag{4.48}$$

$$F_D(M_w, R) = \left[c_1(M_w - M_{ref}) + c_2 \right] \log_{10} \sqrt{R^2 + h^2} + c_3 \sqrt{R^2 + h^2} \tag{4.49}$$

$$F_S(V_{S,30}) = k \log_{10}(\frac{V_0}{800})$$
$$with \, V_0 = V_{S,30} \, for \, V_{S,30} \leq 1500 m/s$$
$$with \, V_0 = 1500 m/s \, for \, V_{S,30} > 1500 m/s \tag{4.50}$$

$$\sigma = \sqrt{\tau^2 + \varphi_{S2S}^2 + \varphi_0^2} \tag{4.51}$$

where I is a random variable describing the expected intensity measure, that is the PGA (g) in the considered case, M_W is the moment magnitude, R is the source site distance, V_{S30} is the shear wave velocity and the SOFj are the styles of faulting such as strike-slip (j=1), reverse (j=2), and normal (j=3) fault types. The hinge magnitude is represented by M_h, the reference magnitude by M_{ref} and the pseudo-depth by h. The coefficients a, b1, b2, c1, c2, c3, k and f_j (f_1 for strike-slip, f_2 for thrust fault, and f_3 for normal fault) are derived by a second step mixed-effect linear regression; τ and φ_{S2S} represent between-event and site-to-site variability, respectively, and φ_0 is the standard deviation of the event- and site- corrected residuals.

The main difference between the two GMPEs is the IM used (Boore and Kishida, 2017). In particular, Ambraseys et al. GMPE uses the Larger IM intended as the larger intensity of the two as recorded horizontal components, while Lanzano et al. expression uses the RotD50 that represents the 50th percentile values of response spectra of the two horizontal components projected onto all non-redundant azimuths (Boore, 2010).

Therefore, in order to be coherent with the two expressions, a conversion from RotD50 IM to Larger IM has been applied to the IM obtained from Lanzano et al. GMPE, even though it is an approximation (Beyer and

Bommer, 2006). The amplification factor that should be applied to the PGAs obtained from Lanzano et al. GMPE is equal to 1.1156 and it is obtained from the regression analysis proposed by Beyer and Bommer.

The reason that brings the authors to choose these two GMPEs is their consistency with the analysis under different points of view. The Ambraseys et al. GMPE has been used in the work of Morici et al. (2020) because consistent with the Shake maps proposed by INGV. However, it is not a contemporary expression and it provides relationships related to the Europe and Middle East areas. On the other hand, the Lanzano GMPE is more recent and it is based on a collection of recent year's data after the major seismic sequences in Italy (Emilia 2012; Central Italy 2016-2017). From this point of view, this expression could be more suitable with the response consequence model, but on the other side, it uses a median IM that should be convert in larger IM to ensure higher safety standards and to make then a comparison with the IM obtained from Ambraseys et al. GMPE.

For what concern the soil category, a specific $V_{S,30}$, the time-averaged shear-wave velocity to 30 m depth, has been selected for each church. The possible effects of local amplification caused by the local geology of the site and identified by the category of soil, are evaluated by means of the $V_{S,30}$ parameter. The $V_{S,30}$ value represents the time-averaged shear-wave velocity to 30 m depth, and it is representative of the soil deformability. The specific $V_{S,30}$ of each church site has been selected on the basis of the studies of USGS (Vs30 Map Viewer website; Heath et al., 2020). In particular, for the Italian map, data are derived from the Shake Map provided by the work of Michelini et al. (Michelini et al., 2008).

This is an improvement of the study that, in this way, gives completeness and extensiveness to better develop effective strategies for supporting seismic risk reduction and of the economic losses from a holistic perspective. In literature, many studies have been highlighted the importance of $V_{S,30}$ in the GMPEs, showing that the advantage of the use of $V_{S,30}$ measurements is the ability to apply the very limited existing data to important regional hazard mapping applications (Wald et al., 2011). Generally, this parameter is used in the classification of the soil response. Indeed, the building code Eurocode8 (EN 1998-1, 2005) classifies sites by considering five major categories of soil types, and two specific categories that correspond to very loose or liquefiable material (Table 4-12). Therefore, a suitable characterization of the local site effects, main task of the seismic microzonation, can be performed by determining the resonance frequency of soft sedimentary layers or by estimating the local shear-wave velocity profiles.

Table 4-12. Soil Classification according to Eurocode 8

Ground Type	Description of the stratigraphic profile	Vs,30 (m/s)
A	Rock or other rock-like geological formation, including at most 5 m of weaker material at the surface	> 800

B	Deposit of very dense sand, gravel or very stiff clay, at least several tens of meters in thickness, characterized by gradual increase of mechanical properties with depth	360-800
C	Deep deposit of dense or medium-dense sand, gravel or stiff clay with thickness from several tens to many hundreds of meters	180-360
D	Deposits of loose-to-medium cohesionless soil (with or without some soft cohesive layers), or of predominantly soft-to-firm cohesive soil.	< 180
E	A soil profile consisting of a surface alluvium layer with Vs values of type C or D and thickness varying between about 5 m and 20 m, underlain by stiffer material with Vs> 800 m/s	
S1	Deposits consisting of, or containing, a layer at least 10m thick, of soft clays/silts with a high plasticity index (PI> 40) and high water content.	< 100 (Indicative)
S2	Deposits of liquefiable soils, of sensitive clays, or any other soil profile not included in types A-E or S1.	

Figure 4-46 shows the distribution of the $V_{S,30}$ of the churches according with the data of USGS Map over the contour map of Marche Region (Regione Marche, Paesaggio Territorio Urbanistica Genio Civile, website). The table reports the number of historical churches placed in sites with different range of $V_{S,30}$. The distribution shows an expected trend: the majority of the churches located on the Appennini mountain chain, exhibit higher values of $V_{S,30}$ around 700 m/s^2 while the more eastern located churches or the ones not placed on the chain, show lower values of $V_{S,30}$ between 600m/s^2 and 200m/s^2.

Ranges of $V_{s,30}$	N° of churches
$0 < V_{s,30} \leq 240$	1
$240 < V_{s,30} \leq 300$	3
$300 < V_{s,30} \leq 360$	13
$360 < V_{s,30} \leq 490$	114
$490 < V_{s,30} \leq 600$	142
$600 < V_{s,30} \leq 760$	241
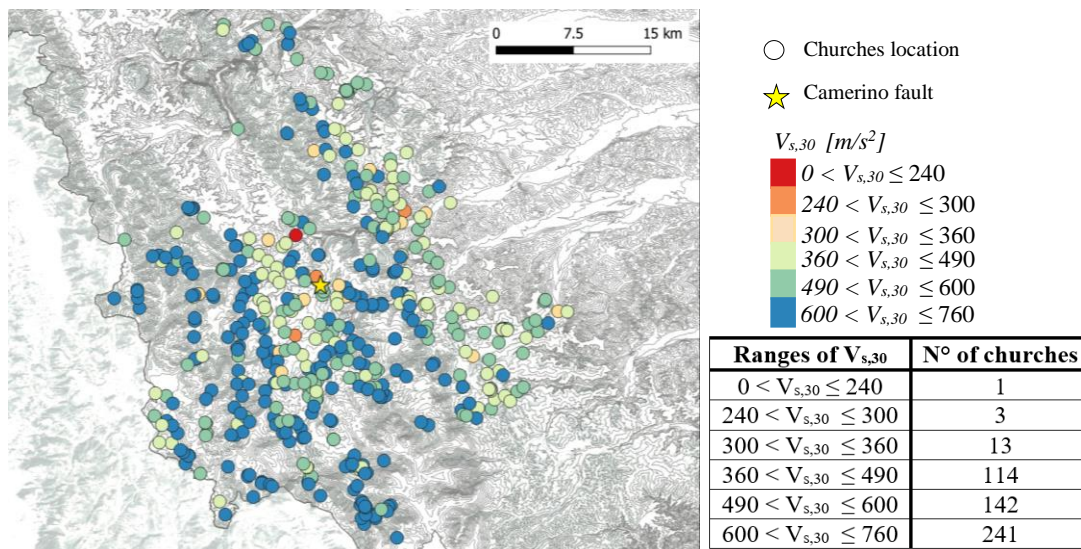
Figure 4-46. Distribution of the $V_{S,30}$ of each church derived from the value of USGS map over the contour map.

The two GMPEs used in this illustrative example, consider the soil amplification and so the influence of $V_{S,30}$ in different ways.

Ambraseys et al. GMPE considers the classes of site geology defined by ranges of average $V_{S,30}$: rock >750 m/s; stiff soil between 360-750 m/s; soft soil between 180-360 m/s, and very soft soil <180 m/s. Therefore the coefficients S_A, S_S that appear in the equation, assume value 0,1 depending on the superficial soil category, and in particular: for $V_{S,30} < 180\,\mathrm{m/s}$, $S_A = 0$ and $S_S = 1$ (very soft soil), for $180\,\mathrm{m/s} \le V_{S,30} < 360\,\mathrm{m/s}$, $S_A = 0$ and $S_S = 1$ (soft soil), for $360\,\mathrm{m/s} \le V_{S,30} < 750\,\mathrm{m/s}$, $S_A = 1$ and $S_S = 0$ (stiff soil), and for $V_{S,30} > 750\,\mathrm{m/s}$, $S_A = 0$ and $S_S = 0$ (rock).

Lanzano et al. GMPE assumes that the site term varies linearly with $V_{S,30}$ in respect to a velocity of 800 m/s up to 1500 m/s and this because 800 m/s is representative for rock sites in Italy (Norme Tecniche per le Costruzioni [NTC], 2018). Due to a lack of record sampling data of very hard-rock sites, in this GMPE, an upper bound on the $V_{S,30}$ has been fixed 1500 m/s, above which the amplification is not anymore dependent on $V_{S,30}$. Applying the chosen GMPEs to the area of interest and using the value of $V_{S,30}$ for each point of the selected area, the result is the distribution of the PGA (Figure 4-47). It is possible to observe that the $V_{S,30}$ values are not influencing the distribution of the PGA when the GMPE of Ambraseys et al. is used. In fact, Figure 4-47a shows a circular distribution for all the PGA levels. This behaviour demonstrates that the decisive importance in the distribution of the acceleration is attributable to the distance from the considered sismogenetic source. On the other hand, for the case of the amplified Lanzano et al. GMPE, the PGA distribution shows a higher importance of the $V_{S,30}$ values, and a nonlinear distribution of the PGA levels. Moreover, in this last case lesser points of the grid reach higher values of PGAs, differently from the Ambraseys et al. case where more grid points are in the last PGA range (0.35-0.45g).

PGA [g]
< 0.05
0.10
0.20
0.30
> 0.35

(a)   ⭐ Camerino fault   (b)
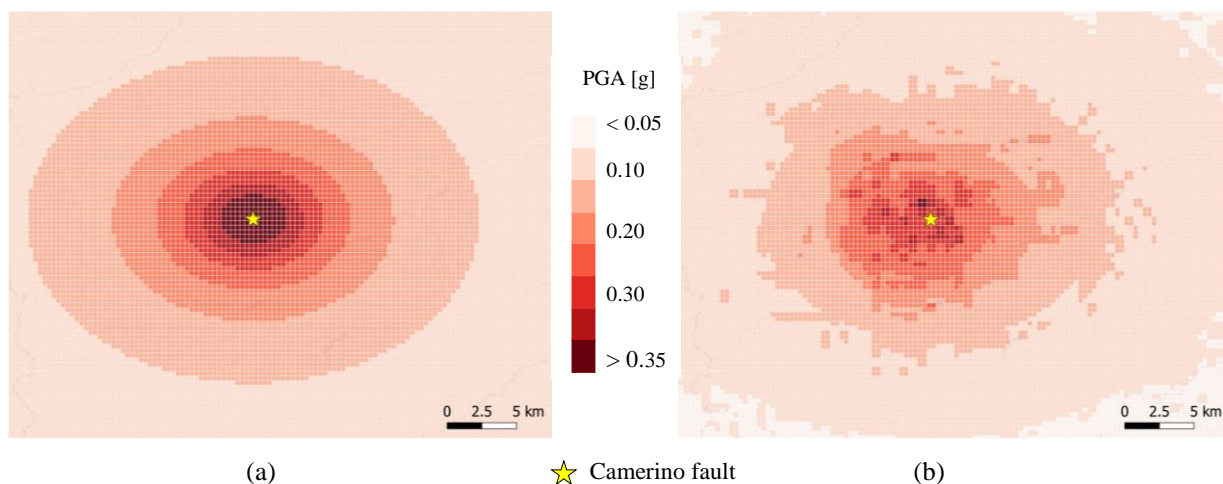
Figure 4-47. Distribution of the PGA considering the specific value of $V_{S,30}$ *for a delimited area using two different GMPE: (a) Ambraseys et al. 1996 and (b) amplified Lanzano et al. 2019.*

Figure 4-48 reports the PDF $f_I^k(i)$ of the intensity expected at each kth church ($k=1,..,514$), considering their epicentral distance and the relevant $V_{S,30}$.

Finally, Figure 4-49 shows the distribution of the PGA of each church by applying the Ambraseys et al. and the amplified Lanzano et al. GMPEs, considering for each of them their specific value of $V_{S,30}$. It is possible to highlight that the results obtained from Ambraseys et al. GMPE leads to more churches with higher PGA distribution in respect to the amplified Lanzano et al. GMPE. Indeed, it is clear that from Figure 4-48 by increasing the source-church distance the probability of exceedance given a seismic intensity, is higher with Ambraseys et al. GMPE respect to the results obtained by using amplified Lanzano et al. This feature clarifies and confirms the behaviour in the maps of Figure 4-49.
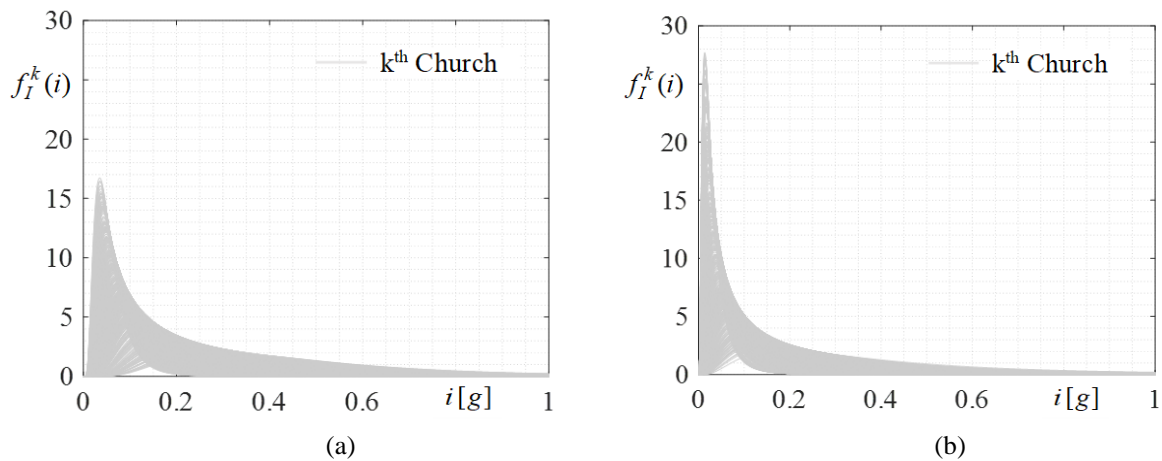
Figure 4-48. Seismic hazard: distribution of intensity $f_I^k(i)$ given epicentral distance for (a) Ambraseys et al. 1996 (b) and for Lanzano et al. 2019 GMPEs
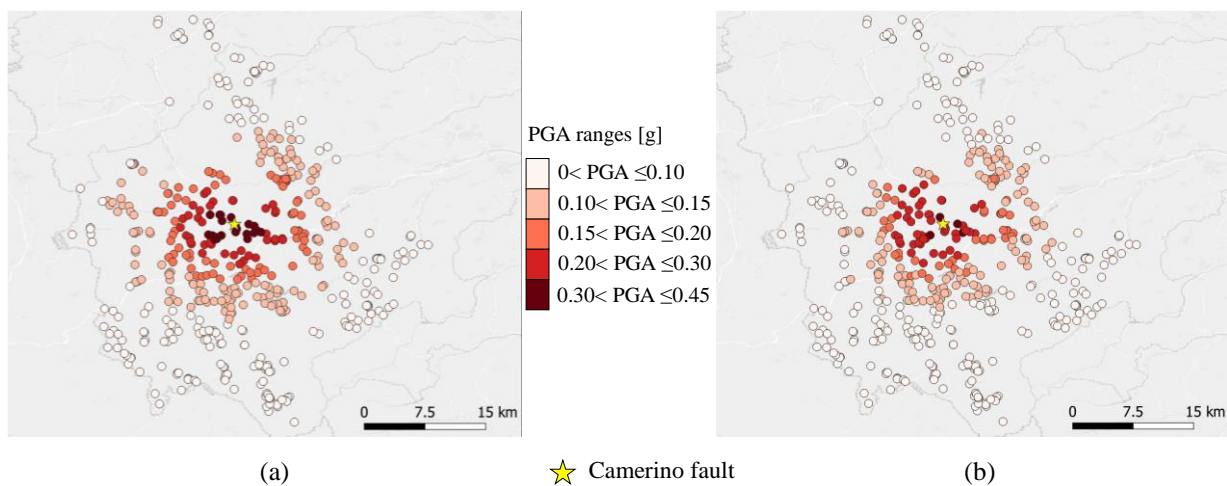
Figure 4-49. Distribution of the PGA considering the specific value of $V_{S,30}$ for each church of the dataset by using (a) Ambraseys et al. 1996 and (b) amplified Lanzano et al. 2019 GMPEs.

Moreover, the distribution of damage d for each church has been evaluated by combining the model proposed by Morici et al., with the distribution of seismic intensity, as follow

$$F_D^k(d) = \int_{\Re^+} F_{D|I}(d|i) f_I^k(i) di \tag{4.52}$$

where $F_D^k(d)$ is the CDF of the damage relative to the kth church and $F_{D|I}(d|i)$ is the conditional CDF of damage, given i as previously presented (Figure 4-24).

Regarding the functions $F_0(i;\Theta_0)$ and $F_1(i;\Theta_1)$, according to Morici et al. they are selected from the exponential family, and they assume the form $F_0(i) = e^{-6.32i}$ and $F_1(i) = 1 - e^{-0.076i}$. The conditional PDF $f_{D|I}^*(d|i;\Theta_d)$ consists of a combination of two Exponential Distribution Functions (EDF),

$$f_{D|I}^*(d|i) = \frac{1}{A(i)} \left(e^{-(4.9111-9.2474i)d} - e^{-(4.9111-9.2474i)} \right) \left(e^{-(-4.5176+12.4867i)(1-d)} - e^{-(-4.5176+12.4867i)} \right)$$ where the term $A(i)$ is a

normalization coefficient $A(i) = \int_0^1 f_{D|I}^*(d|i) dd$.

The final step of this example is the use of the empirical RC model. The distribution of repairing cost at damage d is evaluated by combining the cost consequences model with the distribution of seismic damage, as follow:

$$F_C^k(c) = \int_{\Re^+} F_{C|D}(c|d) \cdot f_D^k(d) dd \tag{4.53}$$

where $F_{C|D}(c|d)$ is the CDF of the repairing cost given the damage.

Figure 4-50 reports the CDF $F_C^k(c)$ for all distances churches to seismic source for both GMPEs. The first row represents the results from Ambraseys et al. GMPE (Figure 4-50a, b) while the second row represents the results by using the amplified Lanzano et al. GMPE (Figure 4-50c, d). In addition, also both the distribution functions LDF$_3$ and GDF$_3$ have been considered: Figure 4-50a, c report the LDF$_3$ and Figure 4-50b, d report the GDF$_3$. It can be noted that not important differences are visible from the two distribution functions. Only a slight change is noted between the two GMPEs: Ambraseys et al. GMPE presents curves with a little lower exceeding probability considering the same repairing cost in respect to amplified Lanzano et al. GMPE. Moreover, if the two distributions are compared, the first stroke of the *LDF₃* curve shows a small slope respect to the *GDF₃*.
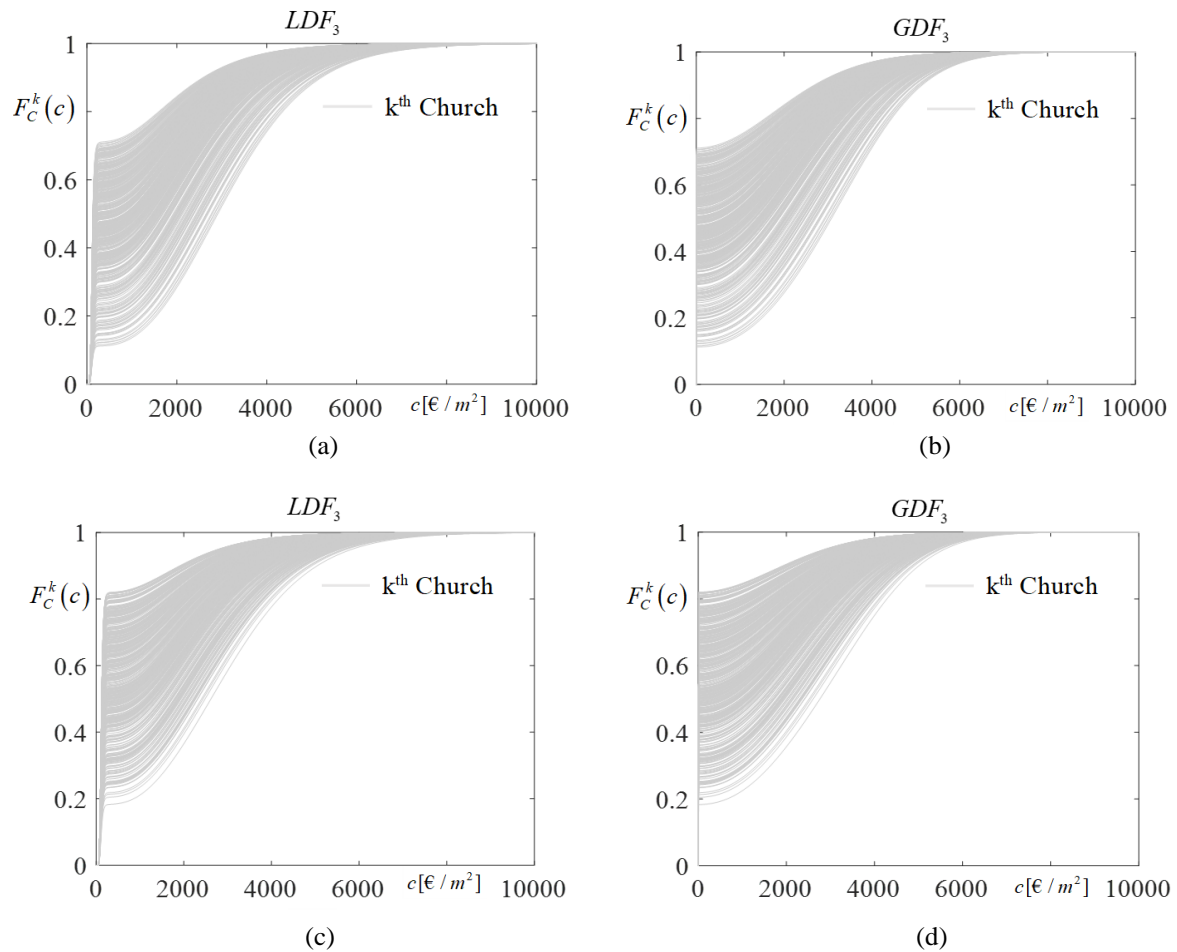
Figure 4-50. CDF $F_C^k(c)$ of the cost distribution given epicentral distance for Ambraseys et al. 1996 (a, b) and for amplified Lanzano et al. 2019 (c, d) GMPEs and for different distribution functions: (a), (c) CDF for LDF₃ and (b), (d) CDF for GDF₃

Figure 4-51 describes the overall damage scenario expected for the churches for both GMPEs, by combining results obtained from the damage predictive model of Morici et al. with the real location of the historical churches. More precisely, the expected value of d (mean value) of each church is reported by a colour scale and Table 4-13 reports the number of churches suffering different levels of damage. Figure 4-51 and Table 4-13 confirm the results obtained from Figure 4-49 showing a higher number of churches classified in the maximum level of damage for Ambraseys et al. GMPE respect to amplified Lanzano et al. GMPE.
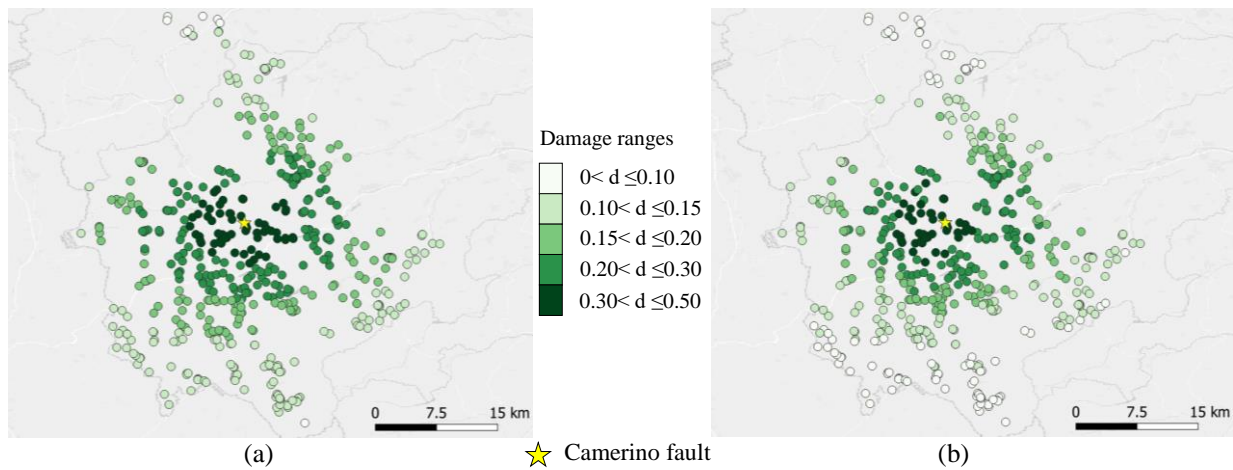
Figure 4-51. Distribution of the damage *d* for the churches of the dataset by using (a) Ambraseys et al. 1996 and (b) amplified Lanzano et al. 2019 GMPEs.

Table 4-13. Ranges of damage levels and number of churches in each interval for both GMPS

Ranges of d	Number of churches (Ambraseys et al. 1996 GMPE)	Number of churches (Lanzano 2019 GMPE)
0 < d ≤ 0.10	12	113
0.10 < d ≤ 0.15	154	137
0.15 < d ≤ 0.20	135	105
0.20 < d ≤ 0.3	149	112
0.3 < d ≤ 0.50	64	47

Consequently, Figure 4-52 describes the overall cost scenario expected for the churches, by combining results obtained from the proposed predictive RC model with the real location of the historical churches. More precisely, the expected mean value of c of each church is reported by a colour scale. In particular, Figure 4-52a, b report the results of Ambraseys et al. GMPE respectively for LDF_3 and GDF_3 distributions, while Figure 4-52c, d report the same results for amplified Lanzano et al. GMPE. In Table 4-14 the number of churches with their different value of costs are written down. Table 4-14 does not shows important differences from LDF_3 and GDF_3 for both GMPEs. Only the GDF_3 derived from the amplified Lanzano et al. GMPE displays a distribution of churches in each range of costs.
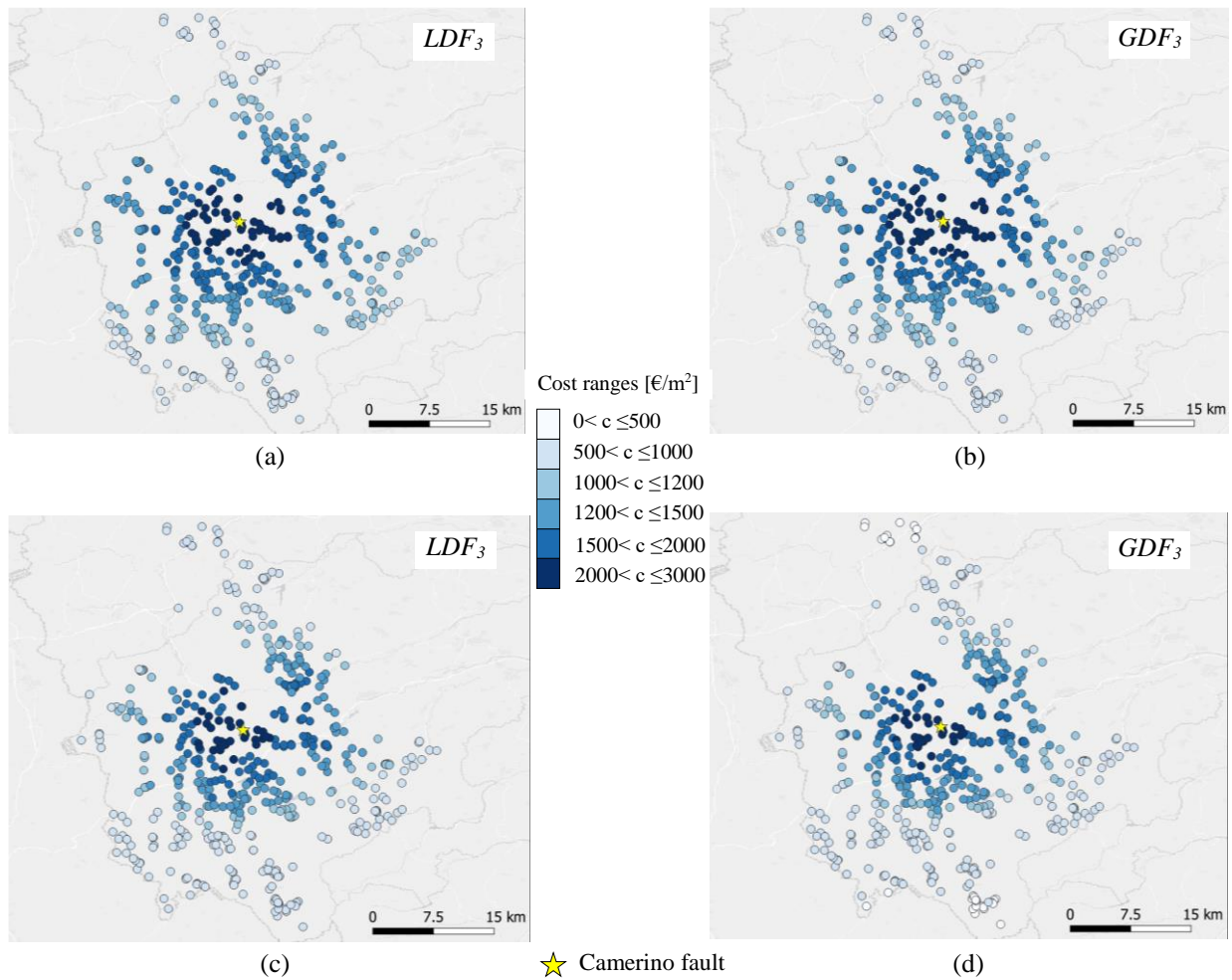
Figure 4-52. Distribution of the repairing costs c for the churches of the dataset for the two distributions (a,c) LDF$_3$ and (b,d) GDF$_3$ by using (a,b) Ambraseys et al. 1996 and (c,d) amplified Lanzano et al. 2019 GMPEs.

Table 4-14. Ranges of cost levels and number of churches in each interval for both GMPEs and distribution functions.

Ranges of c	Number of churches (Ambraseys et al.)		Number of churches (amplified Lanzano et al.)	
	LDF$_3$	GDF$_3$	LDF$_3$	GDF$_3$
$0 < c \leq 500$	0	0	0	35
$500 < c \leq 1000$	104	140	204	201
$1000 < c \leq 1200$	100	83	72	55
$1200 < c \leq 1500$	118	113	102	102
$1500 < c \leq 2000$	128	115	95	86
$2000 < c \leq 3000$	64	63	41	35

In addition to the mean response, also the percentiles have been reported for the damage and costs, by using for sake of simplicity only the amplified Lanzano et al. GMPE a *LDF$_3$* distribution.

In particular, Figure 4-53 shows the 25th percentile, the median and 75th percentile of the damage, while Figure4-54 displays the respectively results for the repairing costs, where a gradual increase of the damage and costs is noticeable from the 25th to the 75th percentile.
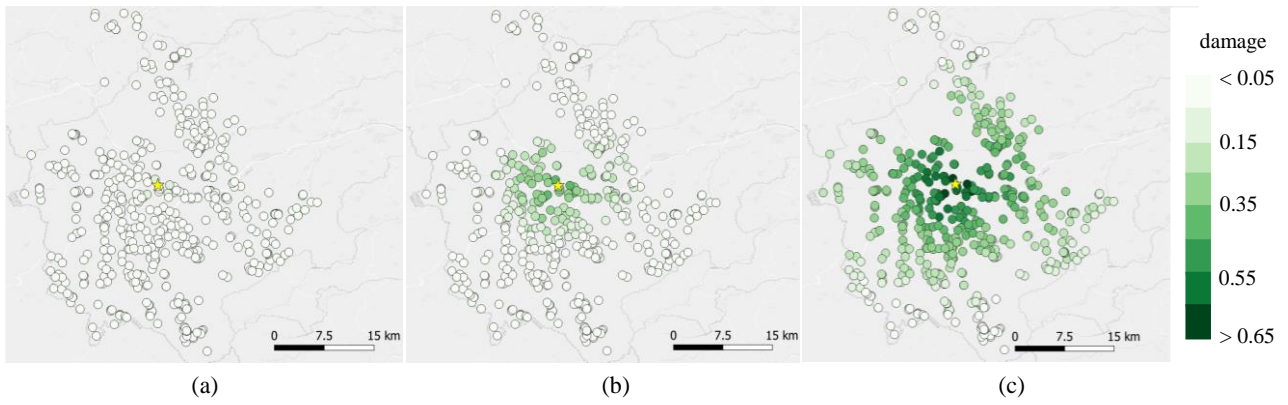
Figure 4-53. Damage distribution of churches: (a) 1st quartile, (b) median and (c) 3rd quartile of damage
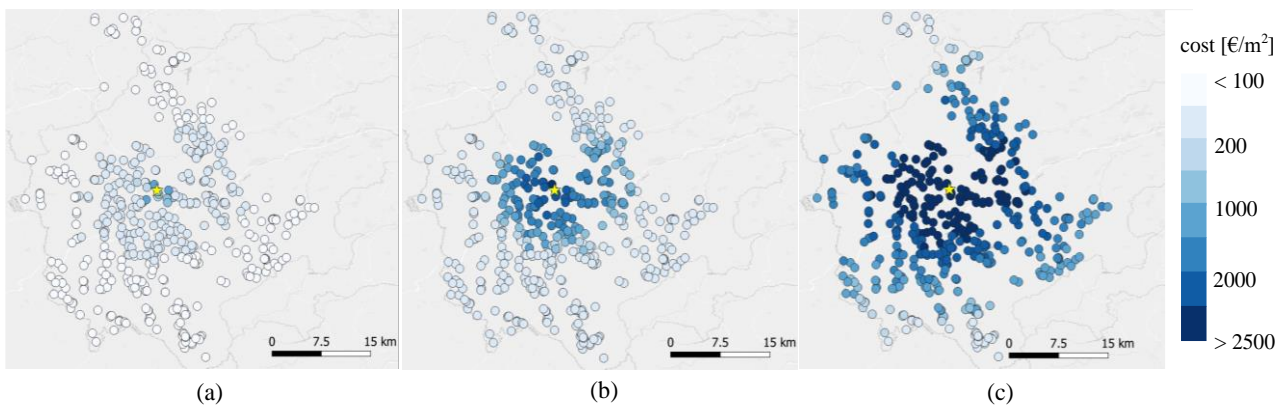
Figure 4-54. Cost distribution of churches: (a) 1st quartile, (b) median and (c) 3rd quartile of cost.

Chapter's References

Agresti, A., 2018. An Introduction to Categorical Data Analysis., 3rd Edition. ed. Wiley.

Agresti, A., 2015. Foundations of Linear and Generalized Linear Models., Hoboken, NJ. ed.

Akaike, H., 1974. Information Theory and an Extension of the Maximum Likelihood Principle, in: Parzen, E., Tanabe, K., Kitagawa, G. (Eds.), Petrovand BN, Caski F (Eds) Proceeding of the Second International Symposium on Information Theory. Akademiai Kiado, Budapest., pp. 267–281. https://doi.org/10.1007/978-1-4612-1694-0_15

Ambraseys, N.N., Simpson, K.A., Bommer, J.J., 1996. Prediction of Horizontal Response Spectra in Europe. Earthquake Engineering & Structural Dynamics 25, 371–400. https://doi.org/10.1002/(SICI)1096-9845(199604)25:4<371::AID-EQE550>3.0.CO;2-A

Baker, J.W., 2015. Efficient Analytical Fragility Function Fitting Using Dynamic Structural Analysis. Earthquake Spectra 31, 579–599. https://doi.org/10.1193/021113EQS025M

Baraccani, S., Silvestri, S., Gasparini, G., Palermo, M., Trombetti, T., Silvestri, E., Lancellotta, R., Capra, A., 2015. A Structural Analysis of the Modena Cathedral. International Journal of Architectural Heritage 15583058.2015.1113344. https://doi.org/10.1080/15583058.2015.1113344

Barg, S., Flager, F., Fischer, M., 2017. An Analytical Method to Estimate the Total Installed Cost of Structural Steel Building Frames during Early Design. Journal of Building Engineering 15. https://doi.org/10.1016/j.jobe.2017.10.010

Bellaveglia, S., Bistocchi, R.M., Gattoni, M., 2018. Microzonazione sismica di III livello. Relazione illustrativa.

Berto, L., Doria, A., Faccio, P., Saetta, A., Talledo, D., 2017. Vulnerability Analysis of Built Cultural Heritage: A Multidisciplinary Approach for Studying the Palladio's Tempietto Barbaro. International Journal of Architectural Heritage 11, 773–790. https://doi.org/10.1080/15583058.2017.1290853

Betti, M., Vignoli, A., 2011. Numerical assessment of the static and seismic behaviour of the basilica of Santa Maria all'Impruneta (Italy). Construction and Building Materials 25, 4308–4324. https://doi.org/10.1016/j.conbuildmat.2010.12.028

Betti, M., Vignoli, A., 2008. Modelling and analysis of a Romanesque church under earthquake loading: Assessment of seismic resistance. Engineering Structures 30, 352–367. https://doi.org/10.1016/j.engstruct.2007.03.027

BeWeB | Portale dei beni culturali ecclesiastici. beweb.chiesacattolica.it. URL https://beweb.chiesacattolica.it/ (accessed 5.11.21).

Beyer, K., 2006. Relationships between Median Values and between Aleatory Variabilities for Different Definitions of the Horizontal Component of Motion. Bulletin of the Seismological Society of America 96, 1512–1522. https://doi.org/10.1785/0120050210

Binda, L., 2004. The importance of the investigation for the diagnosis of historic building: application at different scale (centres and single buildings). Presented at the 4th International Seminar on Structural Analysis of Historical Constructions, Padova, Italy, pp. 29–42.

Bishop, C., 2006. Pattern Recognition and Machine Learning, Information Science and Statistics. Springer-Verlag, New York.

Boore, D.M., 2010. Orientation-Independent, Nongeometric-Mean Measures of Seismic Intensity from Two Horizontal Components of Motion. Bulletin of the Seismological Society of America 100, 1830–1835. https://doi.org/10.1785/0120090400

Boore, D.M., Kishida, T., 2017. Relations between Some Horizontal-Component Ground-Motion Intensity Measures Used in Practice. Bulletin of the Seismological Society of America 107, 334–343. https://doi.org/10.1785/0120160250

Bottero, M., D'Alpaos, C., Marello, A., 2020. An Application of the A'WOT Analysis for the Management of Cultural Heritage Assets: The Case of the Historical Farmhouses in the Aglié Castle (Turin). Sustainability 12, 1071. https://doi.org/10.3390/su12031071

Bottero, M., D'Alpaos, C., Oppio, A., 2019. Ranking of Adaptive Reuse Strategies for Abandoned Industrial Heritage in Vulnerable Contexts: A Multiple Criteria Decision Aiding Approach. Sustainability 11, 785. https://doi.org/10.3390/su11030785

Bradley, B.A., Dhakal, R.P., 2008. Error estimation of closed-form solution for annual rate of structural collapse. Earthquake Engng Struct. Dyn. 37, 1721–1737. https://doi.org/10.1002/eqe.833

Braga, F., Dolce, M., Liberatore, D., 1982. A statistical study on damaged buildings and an ensuing review of the MSK-76 scale - CORE. Presented at the Proc. of the 7th European Conference on Earthquake Engineering, Athens, pp. 431-450.

Capera, A., Albarello, D., Gasperini, P., 2007. Aggiornamento relazioni fra l'intensità macrosismica e PGA. Progetto INGV-DPC S1, Deliverable D11.

Carbonari, S., Dall'Asta, A., Dezi, L., Gara, F., Leoni, G., Morici, M., Prota, A., Zona, A., 2019. First analysis of data concerning damage occurred to churches of the Marche region following the 2016 central Italy earthquakes. BGTA. https://doi.org/10.4430/bgta0271

Casarin, F., Modena, C., 2008. Seismic Assessment of Complex Historical Buildings: Application to Reggio Emilia Cathedral, Italy. International Journal of Architectural Heritage 2, 304–327. https://doi.org/10.1080/15583050802063659

Cescatti, E., Salzano, P., Casapulla, C., Ceroni, F., da Porto, F., Prota, A., 2019. Damages to masonry churches after 2016–2017 Central Italy seismic sequence and definition of fragility curves. Bull Earthquake Eng 18, 297–329. https://doi.org/10.1007/s10518-019-00729-7

Chellini, G., Nardini, L., Pucci, B., Salvatore, W., Tognaccini, R., 2014. Evaluation of Seismic Vulnerability of Santa Maria del Mar in Barcelona by an Integrated Approach Based on Terrestrial Laser Scanner and Finite Element Modeling. International Journal of Architectural Heritage 8, 795–819. https://doi.org/10.1080/15583058.2012.747115

Cherubini, A., 2000. Presenza monastica nelle Marche dopo il Mille. Presented at the Atti del convegno di studi, Jesi.

Cosenza, E., Del Vecchio, C., Di Ludovico, M., Dolce, M., Moroni, C., Prota, A., Renzi, E., 2018. The Italian guidelines for seismic risk classification of constructions: technical principles and validation. Bull Earthquake Eng 16, 5905–5935. https://doi.org/10.1007/s10518-018-0431-8

Curti, E., Lagomarsino, S., Podestà, S., 2006. Dynamic Models for the Seismic Analysis of Ancient Bell Towers, in: Structural Analysis of Historical Constructions. New Delhi, p. 8.

Curti, E., Podestà, S., Resemini, S., 2008. The Post-Earthquake Reconstruction Process of Monumental Masonry Buildings: Suggestions from the Molise Event (Italy). International Journal of Architectural Heritage 2, 120–154. https://doi.org/10.1080/15583050701646703

D. Min. Infrastrutture e Trasporti, 2018. NORME TECNICHE PER LE COSTRUZIONI (NTC 2018).

da Porto, F., Silva, B., Costa, C., Modena, C., 2012. Macro-Scale Analysis of Damage to Churches after Earthquake in Abruzzo (Italy) on April 6, 2009. Journal of Earthquake Engineering 16, 739–758. https://doi.org/10.1080/13632469.2012.685207

Dall'Asta, A., Leoni, G., Meschini, A., Petrucci, E., Zona, A., 2019. Integrated approach for seismic vulnerability analysis of historic massive defensive structures. Journal of Cultural Heritage 35, 86–98. https://doi.org/10.1016/j.culher.2018.07.004

D'Alpaos, C., Valluzzi, M.R., 2020. Protection of Cultural Heritage Buildings and Artistic Assets from Seismic Hazard: A Hierarchical Approach. Sustainability 12, 1–14.

D'Amato, M., Laterza, M., Diaz Fuentes, D., 2018. Simplified Seismic Analyses of Ancient Churches in Matera's Landscape. International Journal of Architectural Heritage 14, 119–138. https://doi.org/10.1080/15583058.2018.1511000

Dang, C.-T., Le, T.-P., Ray, P., 2017. A novel method based on maximum likelihood estimation for the construction of seismic fragility curves using numerical simulations. Comptes Rendus Mécanique 345, 678–689. https://doi.org/10.1016/j.crme.2017.06.011

Daniell, J., Wenzel, F., Khazai, B., 2010. The Cost of Historic Earthquakes Today – EconomicAnalysis since 1900 through the use of CATDAT.

De Martino, G., Di Ludovico, M., Prota, A., Moroni, C., Manfredi, G., Dolce, M., 2017. Estimation of repair costs for RC and masonry residential buildings based on damage data collected by post-earthquake visual inspection. Bull Earthquake Eng 15, 1681–1706. https://doi.org/10.1007/s10518-016-0039-9

De Matteis, G., Brando, G., Corlito, V., 2019. Predictive model for seismic vulnerability assessment of churches based on the 2009 L'Aquila earthquake. Bull Earthquake Eng 17, 4909–4936. https://doi.org/10.1007/s10518-019-00656-7

De Matteis, G., Criber, E., Brando, G., 2016. Damage Probability Matrices for Three-Nave Masonry Churches in Abruzzi After the 2009 L'Aquila Earthquake. International Journal of Architectural Heritage 27.

De Matteis, G., Criber, E., Brando, G., 2014. Damage evaluation on churches belonging to the sulmona-valva diocese after the 2009 L'Aquila earthquake. Presented at the Proc. of the 2nd International Conference on Protection of Historical Constructions (PROHITECH 2014), Antalya, Turkey.

De Matteis, G., Mazzolani, F.M., 2010. The Fossanova Church: Seismic Vulnerability Assessment by Numeric and Physical Testing. International Journal of Architectural Heritage 4, 222–245. https://doi.org/10.1080/15583050903078903

De Matteis, G., Zizi, M., 2019. Seismic Damage Prediction of Masonry Churches by a PGA-based Approach. International Journal of Architectural Heritage 13, 1165–1179. https://doi.org/10.1080/15583058.2019.1597215

Del Vecchio, C., Di Ludovico, M., Pampanin, S., Prota, A., 2018. Repair Costs of Existing RC Buildings Damaged by the L'Aquila Earthquake and Comparison with FEMA P-58 Predictions. Earthquake Spectra 34, 237–263. https://doi.org/10.1193/122916EQS257M

Della Spina, L., Calabrò, F., 2018. Decision Support Model for Conservation, Reuse and Valorization of the Historic Cultural Heritage, in: Gervasi, O., Murgante, B., Misra, S., Stankova, E., Torre, C.M., Rocha, A.M.A.C., Taniar, D., Apduhan, B.O., Tarantino, E., Ryu, Y. (Eds.), Computational Science and Its Applications – ICCSA 2018, Lecture Notes in Computer Science. Springer International Publishing, Cham, pp. 3–17. https://doi.org/10.1007/978-3-319-95168-3_1

Despotaki, V., Silva, V., Lagomarsino, S., Pavlova, I., Torres, J., 2018. Evaluation of Seismic Risk on UNESCO Cultural Heritage sites in Europe. International Journal of Architectural Heritage 12, 1231–1244. https://doi.org/10.1080/15583058.2018.1503374

Di Ludovico, M., DE Martino, G., Santoro, A., Prota, A., Manfredi, G., Calderini, C., Carocci, C., da porto, F., Dall'Asta, A., De Santis, S., Fiorentino, G., Digrisolo, A., Dolce, M., Moroni, C., Ferracuti, B., Ferretti, D., Graziotti, F., Penna, A., Mannella, A., Sorrentino, L., 2019. Usability and damage assessment of public buildings and churches after the 2016 Central Italy earthquake: The ReLUIS experience F. da Porto A. Mannella.

Doglioni, F., Moretti, A., Petrini, V., Angeletti, P., 1994. Le Chiese e il Terremoti: Dalla Vulnerabilità Constatata nel Terremoto del Friuli al Miglioramento Antisismico nel Restauro, Verso una Politica di Prevenzione., Edizioni Lint. ed. Trieste, Italy.

DPCM 23-02-2006 - Normativa Nazionale, URL http://www.normativaitaliana.it/nazionale/DPCM%2023-02-2006.asp (accessed 5.7.21).

EN 1998-1, 2005, Eurocodice 8 – Progettazione delle strutture per la resistenza sismica, 2005.

Fabbrocino, F., Vaiano, G., Formisano, A., 2019. Parametric analysis on local collapse mechanisms of masonry churches. Presented at the CENTRAL EUROPEAN SYMPOSIUM ON THERMOPHYSICS 2019 (CEST), Banska Bystrica, Slovakia, p. 4. https://doi.org/10.1063/1.5114430

Fabbrocino, G., Marra, A., Savorra, M., Fabbrocino, S., Santucci de Magistris, F., Rainieri, C., Brigante, D., Celiento, A., 2016. Increasing the resilience of cultural heritage to earthquakes by knowledge enhancement: the lesson of the Carthusian monastery in Trisulti. in: Atti Dei Convegni Lincei "Resilienza Delle Città d'arte Ai Terremoti – XXXIII Giornata Dell'Ambiente. BARDI EDIZIONI, Roma, pp. 553–556.

Faccioli, E., Cauzzi, C., 2006. Macroseismic intensities for seismic scenarios estimated from instrumentally based correlations. https://doi.org/10.13140/RG.2.1.3984.2641

Faenza, L., Michelini, A., 2010. Regression analysis of MCS intensity and ground motion parameters in Italy and its application in ShakeMap. Geophysical Journal International 180, 1138–1152. https://doi.org/10.1111/j.1365-246X.2009.04467.x

Formisano, A., Landolfo, R., Mazzolani, F., Florio, G., 2010. A quick methodology for seismic vulnerability assessment of historical masonry aggregates. https://doi.org/10.13140/2.1.1706.3686

Fortunato, G., Funari, M.F., Lonetti, P., 2017. Survey and seismic vulnerability assessment of the Baptistery of San Giovanni in Tumba (Italy). Journal of Cultural Heritage 26, 64–78. https://doi.org/10.1016/j.culher.2017.01.010

Fuentes, D.D., Laterza, M., D'Amato, M., 2019. Seismic Vulnerability and Risk Assessment of Historic Constructions: The Case of Masonry and Adobe Churches in Italy and Chile, in: Aguilar, R., Torrealva, D., Moreira, S., Pando, M.A., Ramos, L.F. (Eds.), Structural Analysis of Historical Constructions, RILEM Bookseries. Springer International Publishing, Cham, pp. 1127–1137. https://doi.org/10.1007/978-3-319-99441-3_122

GeoNue | Le chiese in Italia, geonue.com/le-chiese-in-italia. URL https://geonue.com/le-chiese-in-italia/ (accessed 5.11.21).

Giovinazzi, S., Lagomarsino, S., 2004. A Macroseismic Method for the Vulnerability Assessment of Buildings, in: 13th World Conference on Earthquake Engineering. Vancouver, B.C., Canada, p. 16.

Gizzi, S., 2017. Paesaggio architettonico, paesaggio dipinto e paesaggio archeologico nella regione italiana delle marche: relazioni reciproche e aspetti materiali e immateriali. Tavares Dias L., Alarcão P.(eds.), Paisagem antiga, sua construção e (re)uso, reptos e perspetivas, CITCEM – Centro de Investigação Transdisciplinar «Cultura, Espaço e Memória», 24.

Goded, T., Ingham, J.M., Giovinazzi, S., Lagomarsino, S., Clark, W., Cattari, S., Ottonelli, D., Marotta, A., Lourenço, P.B., McClean, R., 2014. Results on most probable MMI values for Christchurch URM churches, Report part of the EQC Project 14/660 Vulnerability analysis of unreinforced masonry churches. GNS Science, Lower Hutt, New Zealand.

Grünthal, G., 1998. European Macroseismic Scale 1998 (EMS-98).

Guerreiro, L., Azevedo, J., Proença, J., Bento, R., Lopes, M., 2000. Damage in ancient churches during the 9th of July 1998 Azores earthquake.

Heath, D.C., Wald, D.J., Worden, C.B., Thompson, E.M., Smoczyk, G.M., 2020. A global hybrid VS30 map with a topographic slope–based default and regional map insets. Earthquake Spectra 36, 1570–1584. https://doi.org/10.1177/8755293020911137

Hofer, L., Zampieri, P., Zanini, M.A., Faleschini, F., Pellegrino, C., 2018. Seismic damage survey and empirical fragility curves for churches after the August 24, 2016 Central Italy earthquake. Soil Dynamics and Earthquake Engineering 111, 98–109. https://doi.org/10.1016/j.soildyn.2018.02.013

I A E G Commision No 16- Engineering Geology and Protection of Ancient Monuments and Archaeological Sites, 2003. users.auth.gr. URL http://users.auth.gr/users/2/4/004042/public_html/assets/iaeg16/index.htm (accessed 5.7.21).

Ibarra, L.F., Krawinkler, H., 2005. Global collapse of frame structures under seismic excitations, Blume Center Technical Report.

ICOMOS-International Charter for the Conservation and Restoration of Monuments and Sites, Decision and Resolutions, 1964.

Indirli, M., Marghella, G., Marzo, A., 2012. Damage and collapse mechanisms in churches during the Pianura Padana Emiliana earthquake Energia Ambiente Innovaz, 69–94.

INGV - Italy ShakeMaps. shakemap.rm.ingv.it. URL http://shakemap.rm.ingv.it/shake/index.html (accessed 5.7.21).

Kappos, A., Lekidis, V., Panagopoulos, G., Sous, I., Theodulidis, N., Karakostas, C., Anastasiadis, T., Salonikios, T., Margaris, B., 2007. Analytical Estimation of Economic Loss for Buildings in the Area Struck by the 1999 Athens Earthquake and Comparison with Statistical Repair Costs. Earthquake Spectra 23, 333–355. https://doi.org/10.1193/1.2720366

Lagomarsino, S., 2012. Damage assessment of churches after L'Aquila earthquake (2009). Bull Earthquake Eng 10, 73–92. https://doi.org/10.1007/s10518-011-9307-x

Lagomarsino, S., 2006. On the vulnerability assessment of monumental buildings. Bull Earthquake Eng 4, 445–463. https://doi.org/10.1007/s10518-006-9025-y

Lagomarsino, S., 1998. A new methodology for the post-earthquake investigation of ancient churches.

Lagomarsino, S., Podestà, S., 2004c. Damage and Vulnerability Assessment of Churches after the 2002 Molise, Italy, Earthquake. Earthquake Spectra 20, 271–283. https://doi.org/10.1193/1.1767161

Lagomarsino, S., Podestà, S., 2004a. Seismic Vulnerability of Ancient Churches: I. Damage Assessment and Emergency Planning. Earthquake Spectra 20, 377–394. https://doi.org/10.1193/1.1737735

Lagomarsino, S., Podestà, S., 2004b. Seismic Vulnerability of Ancient Churches: II. Statistical Analysis of Surveyed Data and Methods for Risk Analysis. Earthquake Spectra 20, 395–412. https://doi.org/10.1193/1.1737736

Lallemant, D., Kiremidjian, A., Burton, H., 2015. Statistical procedures for developing earthquake damage fragility curves. Earthquake Engineering & Structural Dynamics 44. https://doi.org/10.1002/eqe.2522

Lanzano, G., Luzi, L., Pacor, F., Felicetta, C., Puglia, R., Sgobba, S., D'Amico, M., 2019. A Revised Ground-Motion Prediction Model for Shallow Crustal Earthquakes in Italy. Bulletin of the Seismological Society of America 109, 525–540. https://doi.org/10.1785/0120180210

Laurenzano, G., Barnaba, C., Romano, M.A., Priolo, E., Bertoni, M., Bragato, P.L., Comelli, P., Dreossi, I., Garbin, M., 2018. The Central Italy 2016–2017 seismic sequence: site response analysis based on seismological data in the Arquata del Tronto–Montegallo municipalities. Bull Earthquake Eng 17, 5449–5469. https://doi.org/10.1007/s10518-018-0355-3

Laurenzano, G., Priolo, E., Tondi, E., 2008. 2D numerical simulations of earthquake ground motion: examples from the Marche Region, Italy. J Seismol 12, 395–412. https://doi.org/10.1007/s10950-008-9095-1

Leite, J., Lourenco, P.B., Ingham, J.M., 2013. Statistical Assessment of Damage to Churches Affected by the 2010–2011 Canterbury (New Zealand) Earthquake Sequence. Journal of Earthquake Engineering 17, 73–97. https://doi.org/10.1080/13632469.2012.713562

Marotta, A., Sorrentino, L., Liberatore, D., Ingham, J.M., 2017. Vulnerability Assessment of Unreinforced Masonry Churches Following the 2010–2011 Canterbury Earthquake Sequence. Journal of Earthquake Engineering 21, 912–934. https://doi.org/10.1080/13632469.2016.1206761

Masi, A., Santarsiero, G., Chiauzzi, L., Gallipoli, M.R., Piscitelli, S., Vignola, L., Bellanova, J., Calamita, G., Perrone, A., Lizza, C., Grimaz, S., 2016. Different damage observed in the villages of Pescara del Tronto and Vezzano after the M6.0 August 24, 2016 Central Italy earthquake and site effects analysis 1–12.

Mele, E., De Luca, A., Giordano, A., 2003. Modelling and analysis of a basilica under earthquake loading. Journal of Cultural Heritage 4, 355–367. https://doi.org/10.1016/j.culher.2003.03.002

Michelini, A., Faenza, L., Lauciani, V., Malagnini, L., 2008. Shakemap Implementation in Italy. Seismological Research Letters 79, 688–697. https://doi.org/10.1785/gssrl.79.5.688

Mochi, G., Predari, G., 2016. La vulnerabilità sismica degli aggregati edilizi. Una proposta per il costruito storico, Edicom Edizioni. ed. Gorizia.

Modello A-DC PCM-DPC MiBAC. Scheda per il rilievo del danno ai beni culturali – Chiese (in Italian), 2006.

Monachesi, G., Castelli, V., Camassi, R., 2016. Quaderni di Geofisica, Aggiornamento delle conoscenze sul terremoto del 28 luglio 1799 nel sub-Appennino maceratese.

Morici, M., Canuti, C., Dall'Asta, A., Leoni, G., 2020. Empirical predictive model for seismic damage of historical churches. Bull Earthquake Eng 18, 6015–6037. https://doi.org/10.1007/s10518-020-00903-2

Ordinanza n. 105, Semplificazione della ricostruzione degli edifici di culto. 2020.

Pavlova, I., Makarigakis, A., Depret, T., Jomelli, V., 2017. Global overview of the geological hazard exposure and disaster risk awareness at world heritage sites. Journal of Cultural Heritage 28, 151–157. https://doi.org/10.1016/j.culher.2015.11.001

Peña, F., Chávez, M.M., 2015. Seismic Behavior of Mexican Colonial Churches. International Journal of Architectural Heritage 15583058.2015.1113341. https://doi.org/10.1080/15583058.2015.1113341

Penna, A., Calderini, C., Sorrentino, L., Carocci, C.F., Cescatti, E., Sisti, R., Borri, A., Modena, C., Prota, A., 2019. Damage to churches in the 2016 central Italy earthquakes. Bull Earthquake Eng 17, 5763–5790. https://doi.org/10.1007/s10518-019-00594-4

QGIS Development Team, QGIS geographical information system. Open Source Geospatial Foundation Project, 2015. www.qgis.org/en/site/. URL https://www.qgis.org/en/site/ (accessed 5.7.21).

Regione Marche, Paesaggio Territorio Urbanistica Genio Civile. URL https://www.regione.marche.it/Regione-Utile/Paesaggio-Territorio-Urbanistica-Genio-Civile/Cartografia-e-informazioni-territoriali/Repertorio#DTM (accessed 5.12.21).

RiMARCANDO 1997 - 2007: a 10 anni dal sisma, 2007, Bollettino Direzione Regionale per i Beni Culturali e Paesaggistici delle Marche, 2.

Rossi, A., Tertulliani, A., Azzaro, R., Graziani, L., Rovida, A., Maramai, A., Pessina, V., Hailemikael, S., Buffarini, G., Bernardini, F., Camassi, R., Del Mese, S., Ercolani, E., Fodarella, A., Locati, M., Martini, G., Paciello, A., Paolini, S., Arcoraci, L., Castellano, C., Verrubbi, V., Stucchi, M., 2019. The 2016–2017

earthquake sequence in Central Italy: macroseismic survey and damage scenario through the EMS-98 intensity assessment. Bull Earthquake Eng 17, 2407–2431. https://doi.org/10.1007/s10518-019-00556-w

Salzano, P., Cescatti, E., Casapulla, C., Ceroni, F., Prota, A., 2019. 2016-17 Central Italy: macroscale assessment of masonry churches vulnerabilit. https://doi.org/10.7712/120119.6974.19936

Scordilis, E.M., 2006. Empirical Global Relations Converting M S and m b to Moment Magnitude. J Seismol 10, 225–236. https://doi.org/10.1007/s10950-006-9012-4

Sextos, A., De Risi, R., Pagliaroli, A., Foti, S., Passeri, F., Ausilio, E., Cairo, R., Capatti, M.C., Chiabrando, F., Chiaradonna, A., Dashti, S., De Silva, F., Dezi, F., Durante, M.G., Giallini, S., Lanzo, G., Sica, S., Simonelli, A.L., Zimmaro, P., 2018. Local Site Effects and Incremental Damage of Buildings during the 2016 Central Italy Earthquake Sequence. Earthquake Spectra 34, 1639–1669. https://doi.org/10.1193/100317EQS194M

Singhal, A., Kiremidjian, A.S., 1996. Method for Probabilistic Evaluation of Seismic Structural Damage. Journal of Structural Engineering 122, 1459–1467. https://doi.org/10.1061/(ASCE)0733-9445(1996)122:12(1459)

Sorrentino, L., Cattari, S., da Porto, F., Magenes, G., Penna, A., 2019. Seismic behaviour of ordinary masonry buildings during the 2016 central Italy earthquakes. Bull Earthquake Eng 17, 5583–5607. https://doi.org/10.1007/s10518-018-0370-4

Sorrentino, L., Liberatore, L., Decanini, L.D., Liberatore, D., 2014. The performance of churches in the 2012 Emilia earthquakes. Bull Earthquake Eng 12, 2299–2331. https://doi.org/10.1007/s10518-013-9519-3

Stewart, J.P., Zimmaro, P., Lanzo, G., Mazzoni, S., Ausilio, E., Aversa, S., Bozzoni, F., Cairo, R., Capatti, M.C., Castiglia, M., Chiabrando, F., Chiaradonna, A., d'Onofrio, A., Dashti, S., De Risi, R., de Silva, F., della Pasqua, F., Dezi, F., Di Domenica, A., Di Sarno, L., Durante, M.G., Falcucci, E., Foti, S., Franke, K.W., Galadini, F., Giallini, S., Gori, S., Kayen, R.E., Kishida, T., Lingua, A., Lingwall, B., Mucciacciaro, M., Pagliaroli, A., Passeri, F., Pelekis, P., Pizzi, A., Reimschiissel, B., Santo, A., de Magistris, F.S., Scasserra, G.,

Sextos, A., Sica, S., Silvestri, F., Simonelli, A.L., Spanò, A., Tommasi, P., Tropeano, G., 2018. Reconnaissance of 2016 Central Italy Earthquake Sequence. Earthquake Spectra 34, 1547–1555. https://doi.org/10.1193/080317EQS151M

Straub, D., Der Kiureghian, A., 2008. Improved seismic fragility modeling from empirical data. Structural Safety 30, 320–336. https://doi.org/10.1016/j.strusafe.2007.05.004

Taffarel, S., Giaretton, M., da porto, F., Modena, C., 2016. Damage and vulnerability assessment of URM buildings after the 2012 Northern Italy earthquakes. pp. 2455–2462. https://doi.org/10.1201/b21889-321

Tondi, E., 2000. Geological analysis and seismic hazard in the Central Apennines (Italy). Journal of Geodynamics - J GEODYNAMICS 29, 517–533. https://doi.org/10.1016/S0264-3707(99)00048-4

Tondi, E., Cello, G., 2003. Spatiotemporal evolution of the Central Apennines fault system (Italy). Journal of Geodynamics 36, 113–128. https://doi.org/10.1016/S0264-3707(03)00043-7

Vannoli, P., Vannucci, G., Bernardi, F., Palombo, B., Ferrari, G., 2015. The Source of the 30 October 1930 Mw 5.8 Senigallia (Central Italy) Earthquake: A Convergent Solution from Instrumental, Macroseismic, and Geological Data. Bulletin of the Seismological Society of America 105. https://doi.org/10.1785/0120140263

Vicente, R., Lagomarsino, S., Ferreira, T.M., Cattari, S., Mendes da Silva, J.A.R., 2018. Cultural Heritage Monuments and Historical Buildings: Conservation Works and Structural Retrofitting, in: Costa, A., Arêde, A., Varum, H. (Eds.), Strengthening and Retrofitting of Existing Structures, Building Pathology and Rehabilitation. Springer Singapore, Singapore, pp. 25–57. https://doi.org/10.1007/978-981-10-5858-5_2

Vs30 Map Viewer: Topographic Slope as a Proxy for Seismic Site-Conditions (VS30) and Amplification around the Globe. Allen, T.I., Wald. D.J., URL https://usgs.maps.arcgis.com/apps/webappviewer/index.html?id=d3c32c758316402dbd8292b7ffea720e (accessed 5.12.21).

Wagner-Rieger, R., 1957. Die italienische Baukunst zu Beginn der Gotik. I Teil : Oberitalien. Bulletin Monumental 115, 161–162.

Wald, D.J., McWhirter, L., Thompson, E., Hering, A.S., 2011. A new strategy for developing Vs30 maps. Presented at the 4th IASPEI/IAEE International Symposium: Effects of Surface Geology on Seismic Motion.

Zolfaghari, M.R., Mahboubi, S., Peyghaleh, E., n.d. Estimation of Financial Added Value for Retrofitted Buildings 8.

Chapter 5.

Application of the analytical method

Claudia Canuti, Andrea Dall'Asta, Graziano Leoni, Michele Morici, (2019), Risk assessment of Camerino municipality: a case study of Vallicelle district, COMPDYN 2019, 7th ECCOMAS Thematic Conference on Computational Methods in Structural Dynamics and Earthquake Engineering, Crete, Greece, 24–26 June 2019

Claudia Canuti, Lucia Barchetta Michele Morici, Enrica Petrucci, Alessandro Zona, (2019), Analisi dei parametri locali per la riduzione delle incertezze nelle valutazioni di vulnerabilità dei centri storici: il caso di Vezzano (Arquata del Tronto, Marche), XIX Convegno Nazionale, L'ingegneria sismica in Italia–ANIDIS 2019, Ascoli Piceno15-19 settembre 2019.

5.1 Introduction

A proper quantification of the losses plays an important role to develop resilient and sustainable communities especially in areas hit by frequent seismic sequences. Prediction of potential economic losses and, more generally, consequences due to hazardous events, is a key point for prevention planning and emergency organization. To this aim, it is necessary to define reliable models for event predictions, building response and consequences evaluation. The Performance Based Earthquake Engineering framework (PBEE) presented by the Pacific Earthquake Engineering Research Center (PEER) is a robust methodology to evaluate the structural performance in a rigorous probabilistic manner without relying on expert opinion, considering the uncertainty in the seismic hazard, structural response, potential damage and economic losses.

The PBEE involves four different stages, namely: hazard analysis, structural analysis, damage analysis and loss analysis (Cornell and Krawinkler, 2000; Deierlein et al., 2003). The latter culminates with the calculation of one or more Decision Variables, which depending on the specific interests of the involved stakeholders may be expressed in terms of fatalities, economic losses and/or downtimes (Porter, 2003). A complete methodology of loss estimation is presented in Hazus (HAZUS, 2001) and Risk-UE (Milutinovic and Trendafi, 2003), where all the aspects of the PBEE framework are investigated (Whitman et al., 1997; Kircher et al., 1997a; Kircher et al., 1997b).

In this chapter an analysis of the capacity of the PBEE framework to estimate the expected losses at level of urban district is performed, taking into account the propagation of the uncertainties as well.

For this purpose, the Reinforced Concrete (RC) buildings of the Vallicelle district of Camerino in Marche Region are considered. These type of structures may be included in the cultural heritage because their historical value is not represented only by the long history but mainly by a construction technique that it is now obsolete and abandoned (Morabito and Podestà, 2015).

The district is composed by different typologies of RC structure (Low, Middle and High-rise) built at different times and designed considering the seismic actions provided by early versions of seismic Italian code. Furthermore, the area of Vallicelle district experienced the seismic sequence of Central Italy 2016, which included many events with similar magnitude. The sequence started from August 24th with an event of magnitude Mw= 6.1 followed by other two events characterized by Mw= 5.9 and Mw= 6.5 in October 26th and 30th (Sextos et al, 2018), respectively. After these seismic events, most of structures of the district exhibited different level of damage.

The seismic response of the structures, necessary to perform the PBEE framework, is defined starting from the fragility curves available in literature. In particular the Syner-G document (Pitilakis, et al., 2014a; Pitilakis, et al., 2014b) provides groups of fragility curves for different building typologies classified on the type of structure (masonry and reinforced concrete), the height of buildings (three classes depending on the number of floors), the design level of seismic load (High-Code, Moderate-Code, Low-Code, Pre-Code) and the use of the constructions (residential, commercial etc.). The seismic hazard of the area is evaluated based on the Italian standard definition, providing the values of Peak Ground Acceleration (PGA) expected for different levels of mean annual rate of exceedance. In addition, specific studies on the seismic wave amplification phenomena due to the geological and geotechnical local site condition have been recently developed and they are considered in the analysis. Finally, the losses are evaluated in terms of Expected Annual Loss (EAL) considering the replacement costs available in the Hazus documents (HAZUS, 2003). Furthermore, the registered damage after seismic sequence of Central Italy 2016 is compared with the EAL furnished by the PBEE framework, in order to validate the result of the numerical analysis.

A further step has been done by considering the propagation of the uncertainties in the framework of the risk. In particular, the approach proposed by Cosenza et al (2018) has been chosen for evaluating the variability in the fragility curves parameters. The sensitivity analysis has been conducted for two limit states evaluating the First-Order sensitivity index and the Total sensitivity index (Saltelli et al. 2004, Saltelli et al. 2008), considering also different hazard references curves.

5.2 Risk assessment of Camerino municipality

5.2.1 Definition of the sample

Camerino is a Municipality of the Marche Region (Central Italy) and Vallicelle is one of the most populated district of the small town of Camerino. It is located on the southern area near the historical centre (Figure 5-1).

The area was built mainly after the 1980, and the most recent buildings were risen few years ago. This area experienced a higher levels of damage after the seismic sequence of 2016, due to the proximity of the second and third mainshock epicentres (October 26th and 30th) and due to the geology of the area.
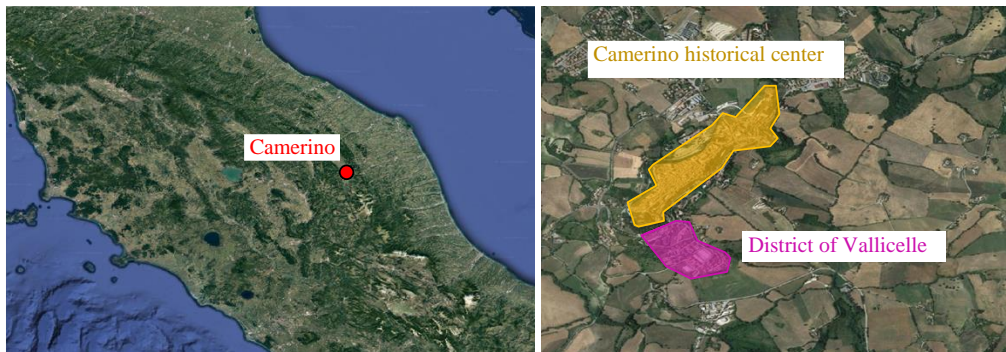

Figure 5-1. Location of Camerino city and Vallicelle district.

Most of the buildings of Vallicelle district are made by RC structures designed according to early versions of the seismic Italian design code. Therefore, these type of structures, even though they are formed by concrete, may be considered part of the Italian cultural heritage, due to a construction technique that it is now obsolete and abandoned (Morabito and Podestà, 2015). This version of the code defines the seismic structural response by linear static analysis, without considering the damage control at low intensities and without specific checks in terms of ductile and fragile mechanisms. In addition, the possible amplification of the seismic input due to the local site effect was considered in a simplified manner.

In order to evaluate the seismic response of buildings in the context of a district-oriented risk assessment, it is necessary to classify the structures into building typologies (classes) characterised by similar structural behaviours. Consistently with the level of the building knowledge, the subdivision in typologies based on the number of floors represents a satisfactory approach. Based on this strategy, it is possible to group the RC buildings in three classes: Low Rise (LR) characterized by 1-3 floors, Middle Rise (MR) by 4-7 floors and High Rise (HR) constituted by 8-19 floors. Moreover, it is possible to associate the range of possible first elastic periods of vibration T_1 to each typology of buildings. In particular, the range [0.1s, 0.5s] is associated to LR structures, the range [0.4s, 0.8s] to MR structures and the range [0.7s, 1.1s] to HR structures. Figure 5-2 shows the distribution over the Vallicelle district of the building typologies; in particular 27 buildings fall in the LR typology, 21 buildings in MR typology and only one building falls in HR typology.

Figure 5-2. Building typologies distribution of Vallicelle district.

The RC building sample considered has been hit by the Central Italy seismic sequence that occurred on August 24th of 2016 and that generated about 300 causalities and important damages to buildings with great economic losses. As described in Chapter 4, the mainshock was characterized by a magnitude Mw=6.1 with epicentre at 1 km W of Accumoli, and the PGAs recorded nearby the epicentre was about 0.45g. After this mainshock other two events characterized by Mw=5.9 and Mw=6.5 in October 26th and 30th were occurred in the Region; these last events were characterized by a location of the epicentre 3 km S away from Visso and 4 km NE from Norcia respectively. During the last mainshock, the maximum PGA recorded nearby the epicentre was nearly 0.48g. The area was interested by about 6500 aftershocks with magnitude Mw ranging from 2.3 to 5.5, occurred between August 2016 and January 2017. It should be emphasized that the PGAs estimated by INGV (ShakeMap – Home, website) do not consider the possibility of the local shaking amplification due to the geological condition. Table 5-1 reports the values of the PGA estimated in the Vallicelle district by means the INGV data processing after the mainshocks, and it is visible that the event of 30th October produced a maximum value of PGA in the area.

Table 5-1: Estimated PGA in Vallicelle district after the mainshocks

Event	Estimated PGA
August 24th, 2016	0.055g
October 26th, 2016	0.126g
October 30th, 2016	0.168g

5.2.2 Seismic risk assessment

Analytical loss estimation can be determined by following a direct method, where the annual rate of exceedance of a loss value is determined by considering all the uncertainties in a unitary way and by assuming probabilistic models for all of them (Scozzese et al., 2019; Bradley et al., 2009). As an alternative approach, the problem can be separated in blocks, as proposed in the PEER frameworks (Porter, 2003; Günay and Mosalam, 2013), by exploiting some advantages coming from the conditional evaluation of rare events (Scozzese et al., 2019). In the following, the latter approach has been considered, by determining the annual rate of exceedance of costs by the equation:

$$\lambda_C(c) = \iint G_C(c \mid d) f_D(d \mid i) dd \left| \lambda_I^{'}(i) \right| di \tag{5.1}$$

In this study, "loss" is referring to the random variable C providing the cost required to repair/replace the facilities after an earthquake, the random variable D describes the building damage and I is a random variable measuring the ground motion intensity. Notation $G_X(x)$ indicates the complementary distribution function of the argument x, and $f_X(x) = -G_X^{'}(x)$ denotes the related probability density function and apex denotes derivative. In the following, the results are presented and discussed with reference to the EAL per year, provided by the integral:

$$EAL = \int c \left| \lambda_C^{'}(c) \right| dc \tag{5.2}$$

Seismic hazard assessment

Taking into account the potential seismogenic sources, Italian standard (Opcm n. 3519, 2006) defines the seismic hazard over the territory, providing the expected PGA for a discrete number of mean annual frequency of exceedance rate λ in the interval between 0.004 - 0.033.

Generally, the relationship between annual rate of exceedance and ground-motion intensity is well fitted by a power law expression (Cornell et al., 2002; Kennedy 1999)

$$\lambda_I(i) = k_0(i)^{-k} \tag{5.3}$$

where k_0 and k are empirical constants. In this study, the seismic intensity i is measured by PGA and the parameters of the power law expression are estimated considering two earthquake intensity levels corresponding to 63% and 5% probabilities of exceedance in 50 years. The former is associated to $\lambda = 0.02$ and it is suggested for checks related to the Damage Limit State (DLS) and the latter is associated to $\lambda = 0.001$ and it is suggested for checks related to Collapse Limit State (CLS). Adopting this strategy, k and k_0 assume the values -2.726 and 2.257E^{-5} respectively. Figure 5-3 shows the hazard curve adopted in the analysis.
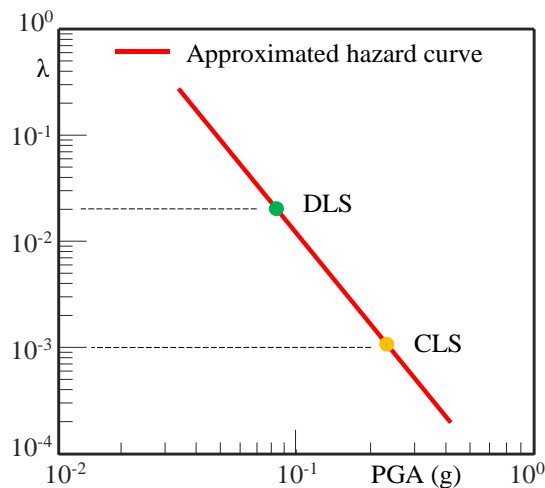
Figure 5-3. Exceedance rates for seismic hazard intensity parameter at bedrock site.

In addition, in the evaluation of the seismic hazard, the local amplification phenomena due to the geological and geotechnical local site condition are considered. The Vallicelle area is characterized by a large wave amplification caused by local site effects. Studies of Seismic Microzonation (SM), performed by the Italian Center of Microzonation (Maccari, 2017), provide a general overview of the spatial distribution of

amplification factors (Figure 5-4a). These effects were evaluated considering three ranges of periods for the superstructure, [0.1s, 0.5s], [0.4s, 0.8s], [0.7s, 1.1s], providing for each range the corresponding Amplification Factor (FA). These ranges of period are coherent with the building typologies mentioned above (LR, MR and HR). The SM of Vallicelle district identifies two sub areas characterized by high (Area 1) and low (Area 2 and Area 3) amplification effects. Figure 5-4b reports for each range of period the relevant FA. In particular, Area 1 is characterized by FA between 1.5 (LR buildings) and 2.8 (for MR buildings), while for the Area 2 and Area 3 the maximum value of FA is 1.4 (LR buildings).

Figure 5-4. Vallicelle geology: (a) soil stratigraphy and (b) FA for each homogeneous sub-area.

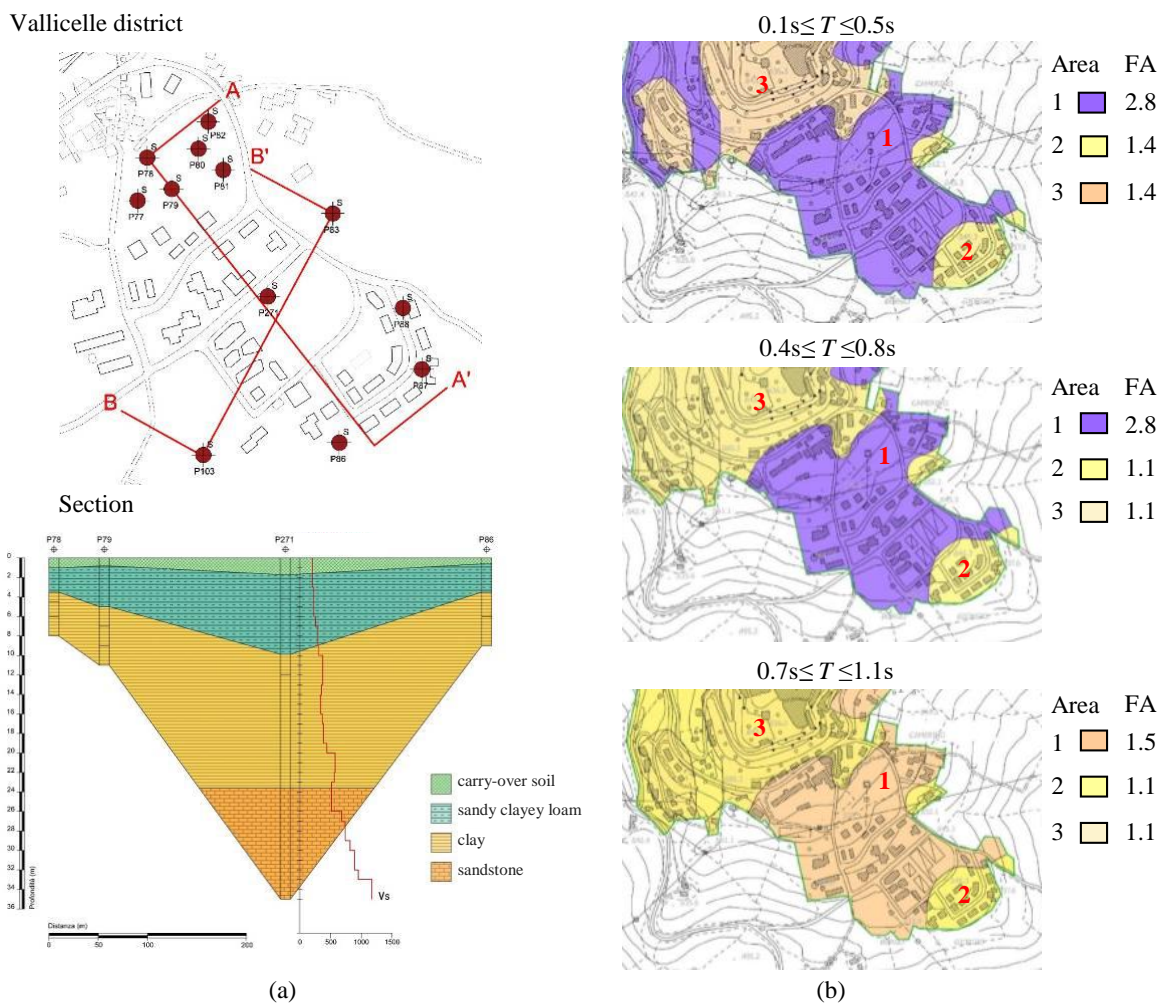Figure 5-5 illustrates the extrapolated seismic hazard of Camerino according to the Equation (5.3) (red line) with respect to the hazard evaluation of the site amplification effects (blue line).

Finally, Table 5-2 reports for each building the relative area of amplification considered in the following analyses.
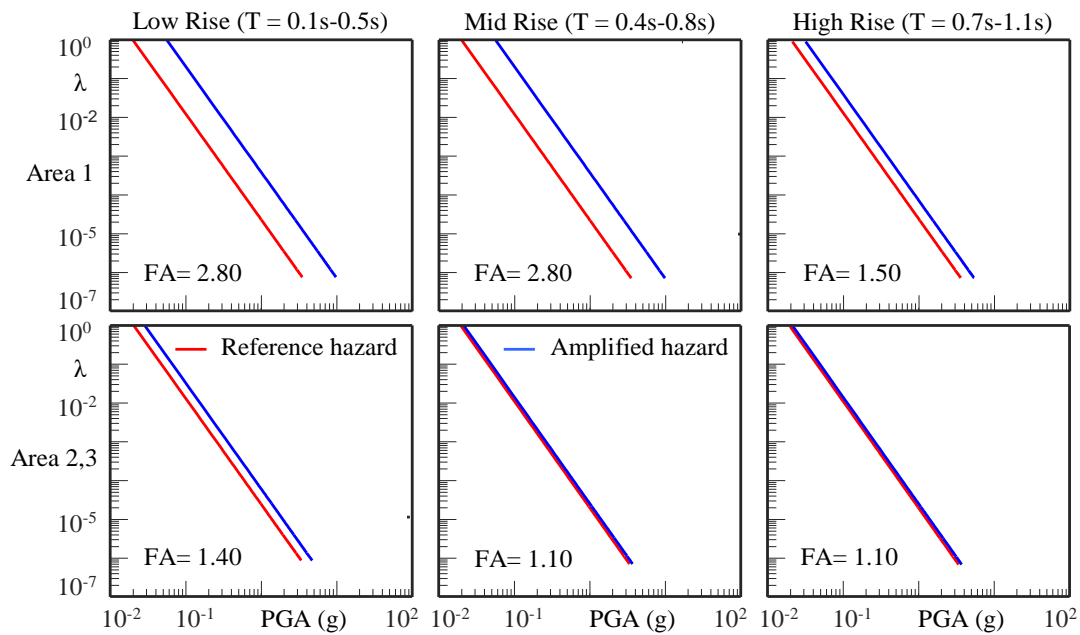
Figure 5-5: Seismic hazard considering the site effect amplification.

Table 5-2: Buildings grouped by amplification area.

Buildings	Amplification Area
A, B, C, D, E, F, G, H, I, L, M and O	Area 1
N	Area 2
K, and J	Area 3

Loss estimation

The loss estimation can be evaluated by damage functions $G_c(c|d)$, which describe the probability of exceedance of the loss value c, given the damage level d. Generally, the damage level is described by a discrete variable; in this case d_k ($k = 0,1,..,N_D$) denotes the damage level within a finite number $N_D + 1$ of ordered possible damage states and the functions $G_c(d_k|i)$ ($k = 0,1,..,N_D - 1$) describe the probability that the damage state is larger than d_k, given the seismic intensity i. The most common way to define earthquake consequences is a classification based on qualitative approach (0 = no damage; 1 = slight/negligible; 2 = moderate; 3 = heavy; 4 = very heavy, 5 = destruction) (Grünthal 1998), which requires a description of each damage state.

The fragility curves are often efficiently approximated by a closed form expression based on a lognormal probability distribution function:

$$G_c(d_k \mid i) = \Phi\left[\frac{\ln(i) - \mu_k}{\beta_k}\right] \tag{5.4}$$

where i is the intensity measure expressed in PGA and μ_k and β_k are the parameters associated with the response of the structure.

The probability $f_D(d_k \mid i)$ of structure being in the k-th damage state given intensity i, derives from previous Equation (5.4) and can be evaluated by:

$$f_D(d_k \mid i) = \begin{cases} 1 - G_D(d_0 \mid i) & k = 0 \\ G_D(d_k \mid i) - G_D(d_{k-1} \mid i) & k = 1, 2, .., N_D - 1 \\ G_D(d_{N_D-1} \mid i) & k = N_D \end{cases} \tag{5.5}$$

The Syner-G documents (Pitilakis et al., 2014a; Pitilakis et al., 2014b) collected an inventory of fragility functions grouping the structures in classes, characterized by a similar response to earthquake (with respect to material, geometry, design code level). In particular, the classification of the buildings is made considering the type of structure (masonry and reinforced concrete), the height of buildings (three classes depending on the number of floors), the design level of seismic load (High-Code, Moderate-Code, Low-Code, Pre-Code) and the use of the constructions (residential, commercial etc.).

In this work, three classes of RC buildings have been considered, LR, MR and HR respectively, designed for a moderate intensity earthquake (PGA=0.1-0.3g). Furthermore, three levels of damage state d_k (with $k = 0, 1, 2$) have been considered and connected with a particular Limit State of the structure provided by the Italian standard code, which provides the boundary between two different damage conditions defining a damage threshold. In particular, the structure is considered damaged with level d_0 (undamaged) if the LS of DLS has not been reached, and damaged with level d_2 if the LS of CLS is exceeded. Finally, the structure is damaged with level d_1 if only the DLS is exceeded. Figure 5-6 reports the fragility curves adopted for each class of structure assuming the parameters μ_k and β_k collected in Table 5-3 (Pitilakis et al., 2014a) and describing the mean values of parameters relevant to fragility curves observed within each class.
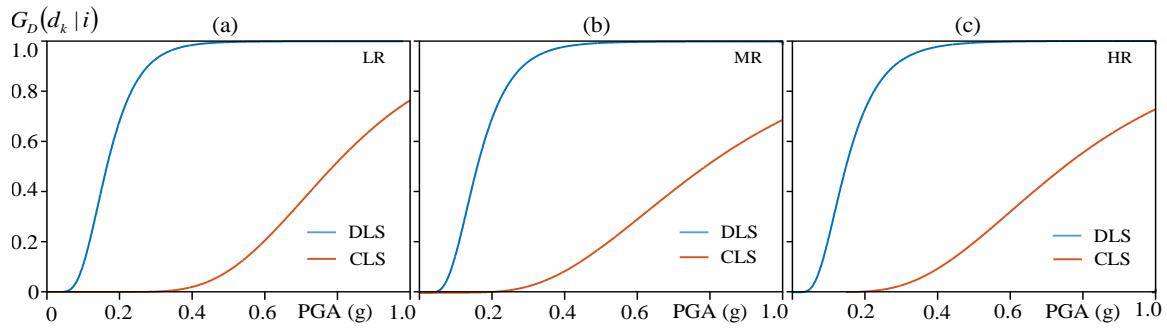
Figure 5-6: Fragility curves adopted in the analyses: (a) LR buildings; (b) MR buildings and (c) HR buildings.

Table 5-3: Parameters adopted in the analyses

LR				MR				HR			
DLS		CLS		DLS		CLS		DLS		CLS	
μ_k(g)	β_k	μ_k(g)	β_k	μ_k(g)	β_k	μ_k(g)	β_k	μ_k(g)	β_k	μ_k(g)	β_k
0.16	0.43	0.84	0.26	0.16	0.43	0.77	0.46	0.16	0.43	0.78	0.46

With respect to the set of damage states previously discussed and referred to European Macroseismic Scale EMS of 1998 (Grünthal, 1998), in the reduced set used here the damage state d_0 includes both the case of no damage and slight/minor damage, the damage state d_1 includes both moderate and heavy damage and the damage state d_2 concerns heavy damage and collapse.

The economic implication of damage state is specified in terms of loss ratio c defined as ratio between repair costs and the total replacement cost rc (value of the facility), and $G_c(c|d_k)$ represents the probability of exceedance of the cost connected to the level of damage d_k. Based on the Hazus study (HAZUS, 2003), a deterministic relation is assumed between damage level and costs. The values $c_0 = 1\%$, $c_1 = 26\%$, and $c_2 = 100\%$ have been associated to the damage states d_0, d_1, and d_2 respectively, and $G_c(c|d_k)$ can be reduced to the Heaviside function $H(c - c_k | d_k)$. Thus, the Equation (5.1) assumes the simplified form:

$$\lambda_C(c) = \sum_k \int H(c - c_k | d_k) f_D(d_k | i) |\lambda_I'(i)| di \tag{5.6}$$

where f_D varies class by class of structures and λ_I varies according to the shake local amplification phenomena of the site.

Results

In this part of the chapter, results of the seismic risk assessment of Vallicelle district, reported in Figure 5-7, are presented and commented.

Figure 5-7a reports the distribution of the EAL over Vallicelle district, measured by the ratio between the repair costs and the replacement costs. The values of EAL observed in buildings located in Area 1 are generally larger than EAL of buildings in Area 3 and 2, despite different typologies are present in both the areas. Therefore, in this case study, the FA is the main parameter influencing EAL.

In Area 1 the EAL values vary from 2.50% to 3.24% and the highest values regard the MR typology. In Area 2 the EAL value is 0.38% due to the presence of only one class of buildings. Finally, Area 3 shows the lowest values of EAL, varying from 0.25% to 0.36%.

Figure 5-7b reports the distribution of the EAL over Vallicelle district in terms of total repair cost per year. The total replacement cost rc is evaluated considering a unitary cost 1500 €/m² (Asprone et al., 2013) multiplied by the area and the number of floors of each facility. The maximum value of EAL (212k €/year) is obtained for the building group *L*, while the value of 4.7k €/year is related to the building group *N* and *K* due to their low risk area.

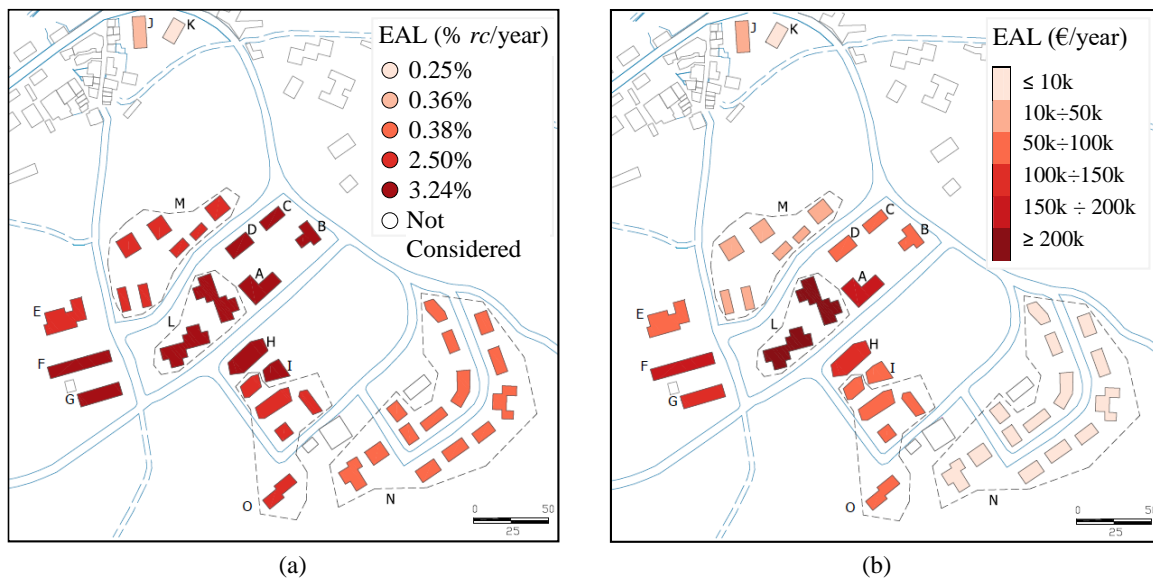(a)   (b)

Figure 5-7. Estimated EAL expressed as: (a) percentage of replacement costs; (b) total replacement costs.

5.2.3 Observed damage after the seismic sequence of 2016

This section reports the damage suffered by the buildings after the Central Italy seismic sequence of 2016 and compares this with the expected damage evaluated starting from the fragility curves adopted in the analysis. The damage assessment is based on visual inspections (Di Ludovico et al., 2017), and it is classified following the EMS98 scale (Grünthal, 1998), considering six levels of damage (D0-D5). In details, Table 5-4 reports for each damage level the classification of the RC buildings damage according with the observational approach adopted as follow.

Table 5-4: Classification of damage to buildings of reinforced concrete.

Damage Level	Description
D0	No damage
D1	Negligible damage (no structural damage, slight non-structural damage)
D2	Moderate damage (slight structural damage, moderate non-structural damage)
D3	Substantial to heavy damage (moderate structural damage, heavy non-structural damage)
D4	Very heavy damage (heavy structural damage, very heavy non-structural damage)
D5	Destruction (very heavy structural damage)

Figure 5-8 shows the damage distribution recorded in the Vallicelle district; it can be observed that the main damages were registered in the buildings A-F falling in the Area 2 characterized by a higher values of FA according to the MS study. In particular the building B suffered a serious structural damage (D4) probably due to the irregularity in the structural and non-structural systems (pilotis floor, ribbon window at the ground floor, eccentric staircase). However, the building groups L, and M are fully operative, while a level damage D1 was registered in the buildings E and G. Finally, the buildings J and K falling in the Area 3 experienced a level of damage D2 and D1 respectively, while all the buildings in the Area 2 are fully operative.
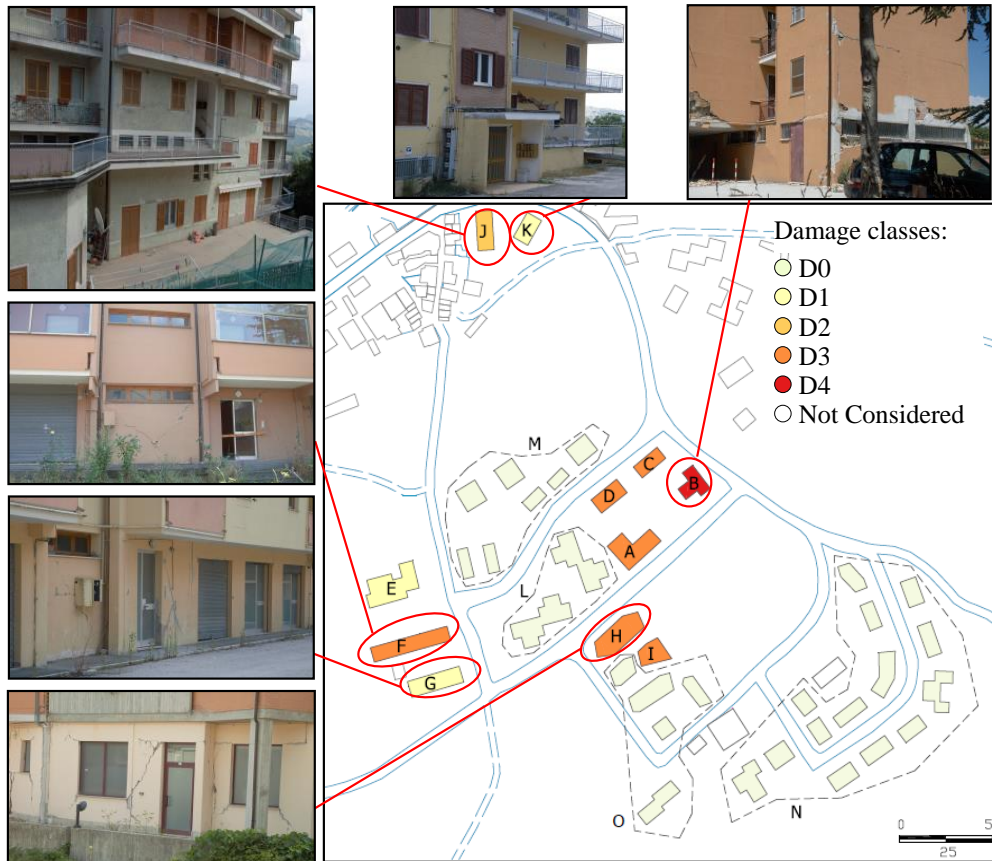
Figure 5-8. Observed damage after the Central Italy 2016 seismic sequence

The expected damage scenario is evaluated with reference to the October 30th event characterized by a magnitude M_w of 6.5 and epicentral distance relevant to Vallicelle district of about 30 km. The estimated PGA for the considered event, over the rigid soil (soil type A) in the area is i_{max} = 0.168g. The frequency distributions of expected damage state, conditioned by the event with intensity i_{max}, is described by the discrete function $f_D(d_k | i_{max})$ introduced in Equation (5.5). According to the reduced set of damage state previously introduced and discussed, the damage d_0 is related to damages D0-D1, the damage state d_1 is related to damages D2-D3, and d_2 is related to damages D4-D5 expected by the EMS98 scale.

Table 5-5 and Table 5-6 report the frequency distributions of the expected damage after the event of October 30th for the building falling in the Area 1, Area 2 and 3. Figure 5-9 reports the distribution of probability of damage over the Vallicelle district. The damage level d_1 (equivalent to D2-D3 in EMS98 scale) results to be the most probable, with a probability greater than 67 % in all cases. The major probability of having a damage level d_2 (D4-D5 in EMS98) is expected for the MR building falling in the Area 1 and it is in agreement with the registered damage. Indeed the greatest damage is registered in the Area 1 for the buildings A, D, C, F, H, and I. Moreover, it can be observed that the distribution of relative frequency is quite dispersed in many cases and this justifies the deviation from predicted damage mode and observed damage.

Table 5-5: Frequency distribution of damage for the buildings fallen in Area 1 after the event of October 30th.

	$f_D(d_0\,|\,i_{max})$	$f_D(d_1\,|\,i_{max})$	$f_D(d_2\,|\,i_{max})$	Building groups
LR	0.49%	93.44%	6.08%	M, E, O
MR	0.81%	84.14%	15.05%	A,B,C,D,F,G,H,I
HR	14.03%	84.85%	1.12%	-

Table 5-6: Frequency distribution of damage for the buildings fallen in Area 2 and 3 after the event of October 30th.

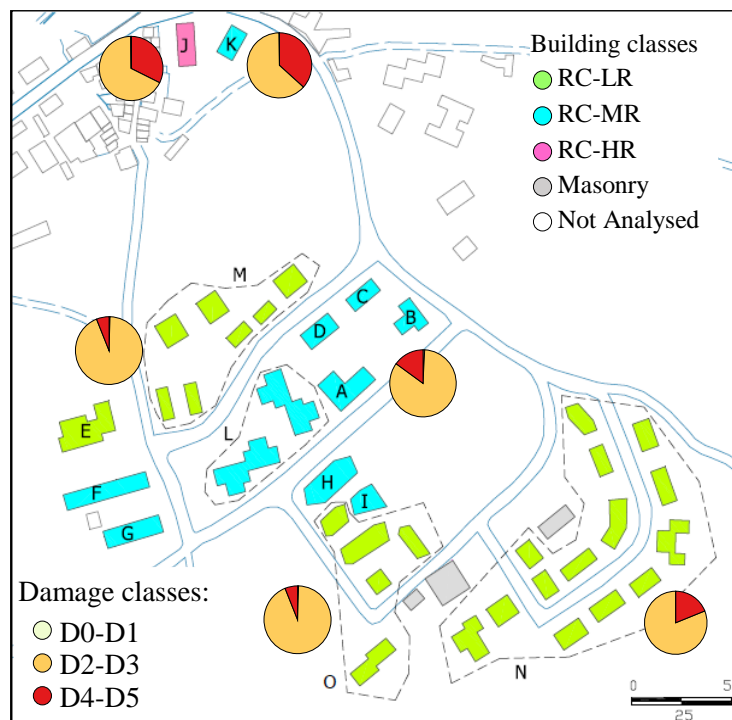|	$f_D(d_0\,|\,i_{max})$	$f_D(d_1\,|\,i_{max})$	$f_D(d_2\,|\,i_{max})$	Building groups
LR	18.89%	81.10%	0.01%	N
MR	36.65%	63.18%	0.17%	K
HR	32.32%	67.52%	0.17%	J

Figure 5-9. Distribution of damage probability of given by the October 30th event.

181

5.3 Uncertainties propagation in the risk framework

In this section, the effects on the uncertainties propagation for one of the structural classes presented above have been evaluated.

5.3.1 Loss evaluation framework

The evaluation of the effects of the parameters uncertainties, which affect the fragility curves and consequently the final result in terms of expected losses, can be issued by using the sensitivity analysis (Saltelli et al. 2004, Saltelli et al. 2008). Indeed, Saltelli et al. gave a possible definition of the sensitivity analysis affirming that is the study of how uncertainty in the output of a model (numerical or otherwise) can be apportioned to different sources of uncertainty in the inputs.

Saying that, in the sensitivity analysis there have been evaluated the effects of the input parameters variability of the model over the variability response of the model itself. For this aim, the model response should be described by means of a scalar function, evaluated from the following expression:

$$\lambda_C(c) \quad = \lambda_0 \sum_k \int G_C(c|ls_k) f_{LS}(ls_k|i) |G_I'(i)| di \tag{5.7}$$

where $\lambda_0 G_I(i) = MAF[I > i|year]$ means the hazard of the site, $f_{LS}(ls_k|i) = P[ls = ls_k|i]$ represents the fragility curve of the structure referred to the *k*-th Limit State ls_k and $G_C(c|ls_k) = P[C > c|ls_k]$ represents the exceedance probability of the costs (or expected consequences) conditional to the ls_k limit state occurrence.

Starting from the value of λ_c, it is possible to define a new scalar parameter named EAL useful for the sensitivity analysis.

In Equation (5.7), the fragility curves $f_{LS}(ls_k|i; \vartheta_k)$ for each building class and for each limit state are useful to describe the structural response given the seismic intensity. The uncertain system parameters of the fragility curves are described by means of random variables ϑ_k that belong to the domain Θ_k. These parameters are defined for each limit state, they are correlated each other, and their variability will affect the reliability of the EAL evaluation.

5.3.2 Hazard step evaluation

Starting from the sites analysed in the RINTC project (RINTC, 2018), there have been evaluated different hazard sites considering in particular the locations of Milan, Rome, Caltanissetta, Naples and L'Aquila. In addition, there have been considered two soil categories A and C (NTC, 2018, EN 1998-1) in the analysis.

As mentioned in subchapter related to "Seismic hazard assessment", the law used to describe the hazard is the Cornell's exponential law (Cornell et al. 2002, Kennedy 1999) that links the mean annual frequency of exceedance with the seismic intensity. As previously mentioned in this chapter, the seismic intensity is represented by the PGA and the parameters of the exponential law are evaluated to interpolate the damage and collapse limit states provided by the code. Therefore, the parameters assume the same values cited before, that are $k_0 = -2.726$ and $k = 2.257E^{-5}$.

5.3.3 Structural step evaluation

The parameters that are defining the fragility curves, derive from the SYNER-G document (Pitilakis et al. 2014a, 2014b) that provides for each building class the parameters ϑ_k and their variability. In particular, for the sensitivity analysis the mid-rise RC building (number of floors between 3 and 9) class is chosen. As mentioned before, the fragility curves follow the normal distribution with two parameters $\vartheta_k = [\mu_k, \beta_k]$.

Table 5-7 shows the parameters used to define the fragility curves for RC buildings of different typological classes and for damage and collapse limit states. In particular, in Table 5-7, highlighted in red, the typological class "mid-rise building with moment resisting frame" has been used to generate the sample useful for the sensitivity analysis.

Figure 5-10 displays the sample generated by using Monte Carlo analysis (Hasting, 1970), in particular Figure 5-10a reports all the fragility curves of the sample for the two limit states considered, while Figure 5-10b shows the probability distribution function of the two parameters useful to define the fragility curve for damage and collapse limit state.

Table 5-7 Parameters $\vartheta_k = \left[\mu_k, \beta_k \right]$ *for different typological building class (Pitilakis et al. 2014a, 2014b)*

RC buildings		Yielding		Collapse	
		Logarithmic Mean	Logarithmic Standard Deviation	Logarithmic Mean	Logarithmic Standard Deviation
mid-rise building with moment resisting frame	Mean	-1.853	0.481	-0.879	0.452
	c_v (%)	26	19	48	23
mid-rise building with moment resisting frame with lateral load design	Mean	-1.876	0.476	-0.738	0.430
	c_v (%)	28	21	67	28
mid-rise building with bare moment resisting frame with lateral load design	Mean	-1.939	0.458	-0.821	0.452
	c_v (%)	28	23	64	25
mid-rise building with bare non-ductile moment resisting frame with lateral load design	Mean	-1.832	0.474	-1.091	0.485
	c_v (%)	33	21	48	24
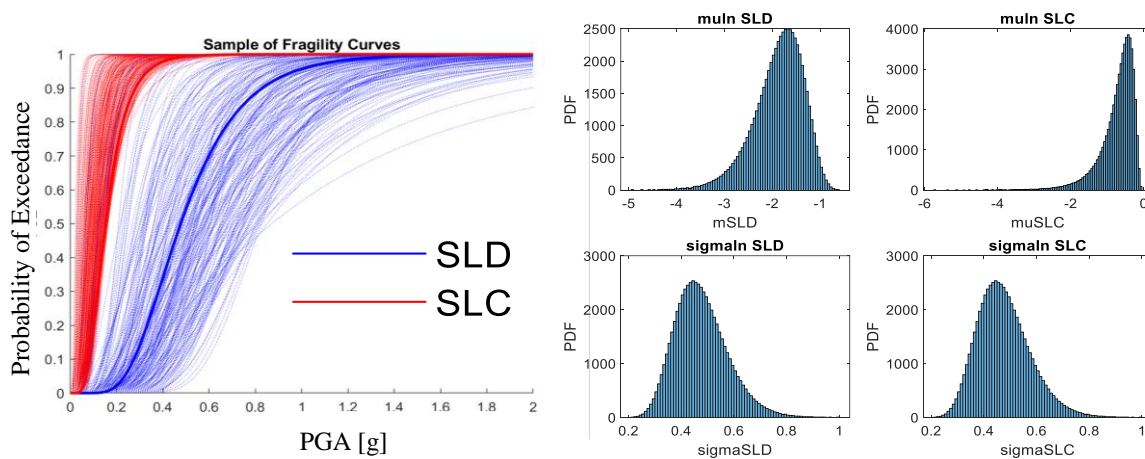
Figure 5-10. Sample of the parameters for the "mid-rise building with moment resisting frame" class: (a) fragility curves sample; (b) PDF for each parameter and for each limit state.

5.3.4 Results

To evaluate the EAL considering the definition of λ_{sl} it has been used the approach defined by Cosenza et al. 2018. This simplified approach allows to define all the limit states starting from the damage and collapse limit states (Figure 5-11).
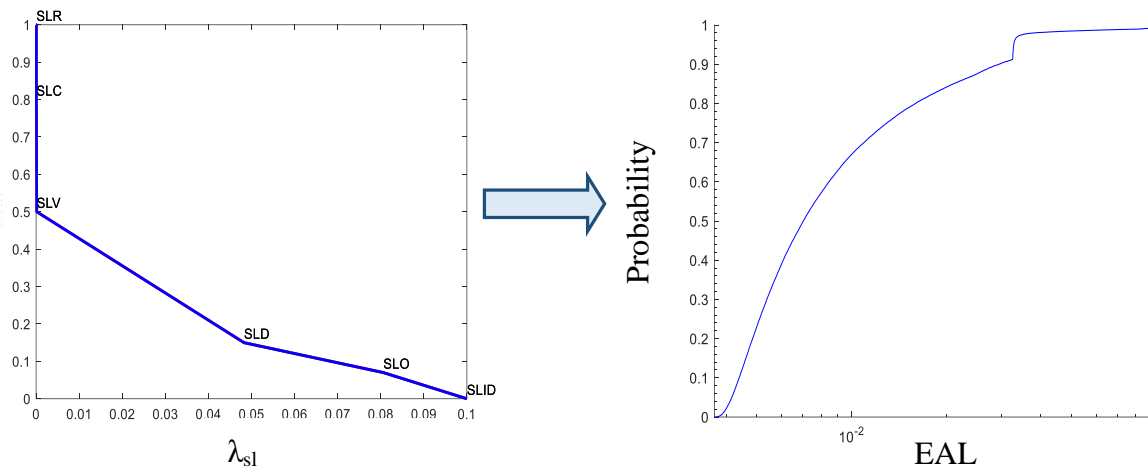
Figure 5-11: EAL definition starting from λ_{sl}.

The influence of the variability of the damage limit state and collapse limit state curves over the output value of the EAL, has been evaluated by sensitivity analysis and in particular by the definition of the First-Order sensitivity index and of the Total sensitivity index (Saltelli et al. 2004, Saltelli et al. 2008).

This approach has been applied for all the sites considered and for the two soil types A and C. Figure 5-12 to Figure 5-16 show the results for all these locations and type of soil. It is possible to highlight that by increasing the seismicity of the area such as going from Milan to L'Aquila, the EAL curves tend to move away from the y axis and tent to became flatter.

Table 5-8 shows the sensitivity analysis results for the different hazard locations and soil types, considering the mid-rise building with moment resisting frame class. Each of that sensitivity indexes states the amount of parameter variability of each fragility curve that affect the final variability of the EAL.

The total sensitivity indexes confirm the evidences seen in the EAL curves: by increasing the seismicity of the area, the parameter that represents the mean value of the fragility curve for the collapse limit state is the most important and influences the most the EAL curve. Instead, for the lower seismic areas such as the location of Milan, the parameter that represents the mean value of the fragility curve for the damage limit state, becomes the most important.
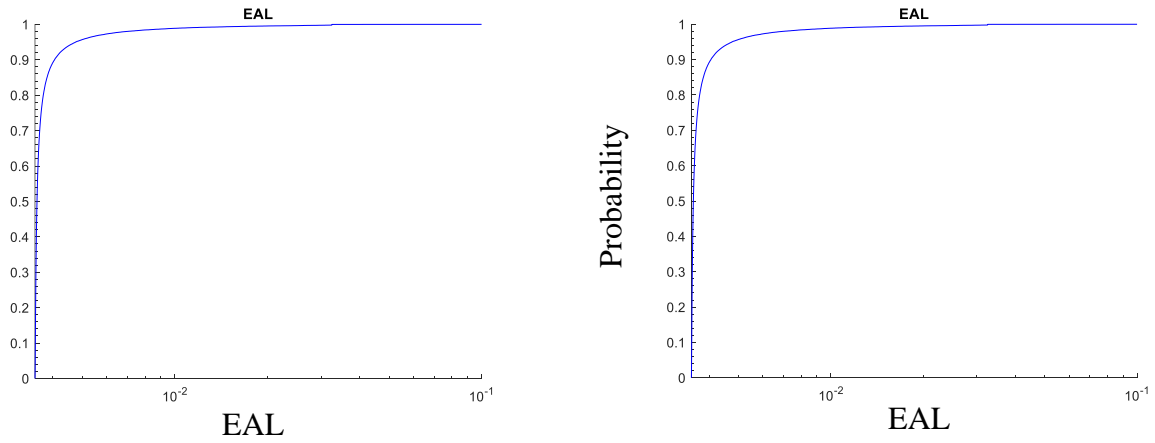
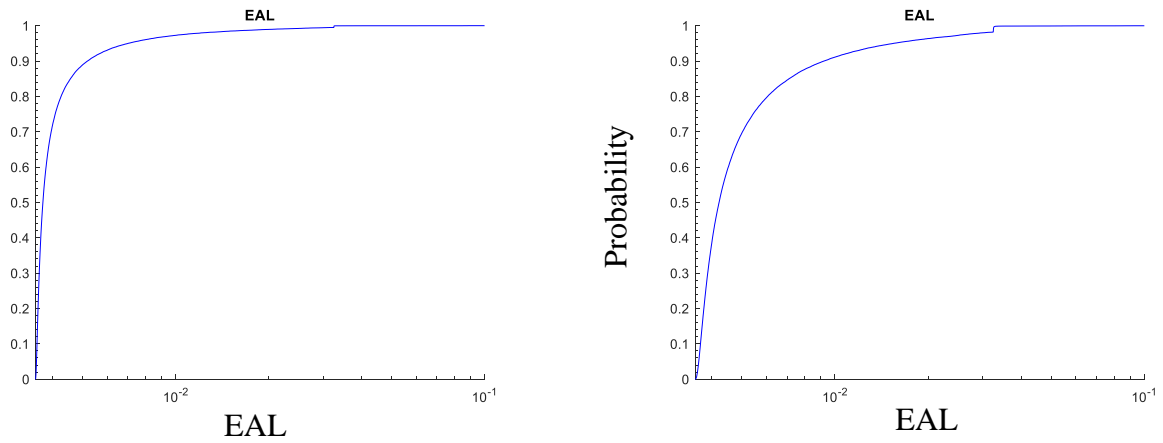*Figure 5-12. EAL curves related to the site of Milano: (a) Soil Type A, (b) Soil Type C*

Figure 5-13. EAL curves related to the site of Caltanissetta: (a) Soil Type A, (b) Soil Type C
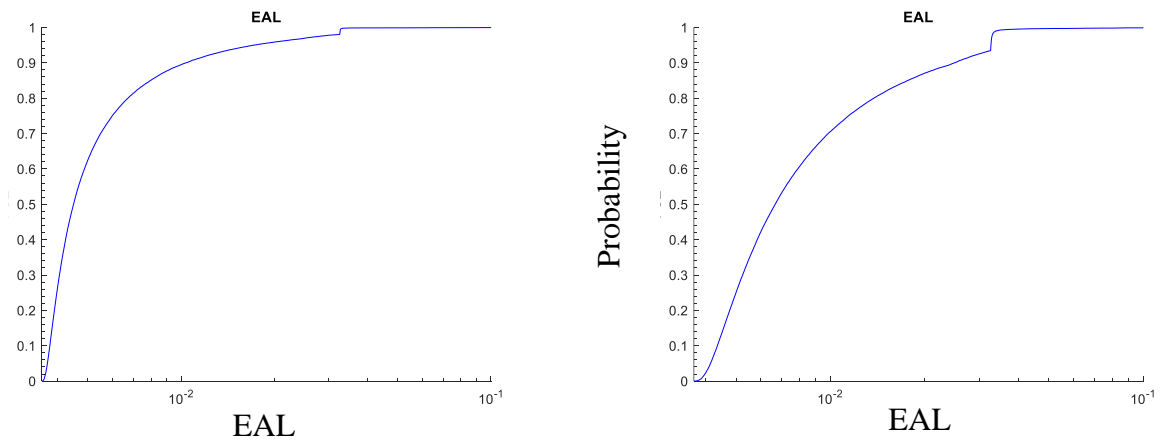
Figure 5-14. EAL curves related to the site of Rome: (a) Soil Type A, (b) Soil Type C
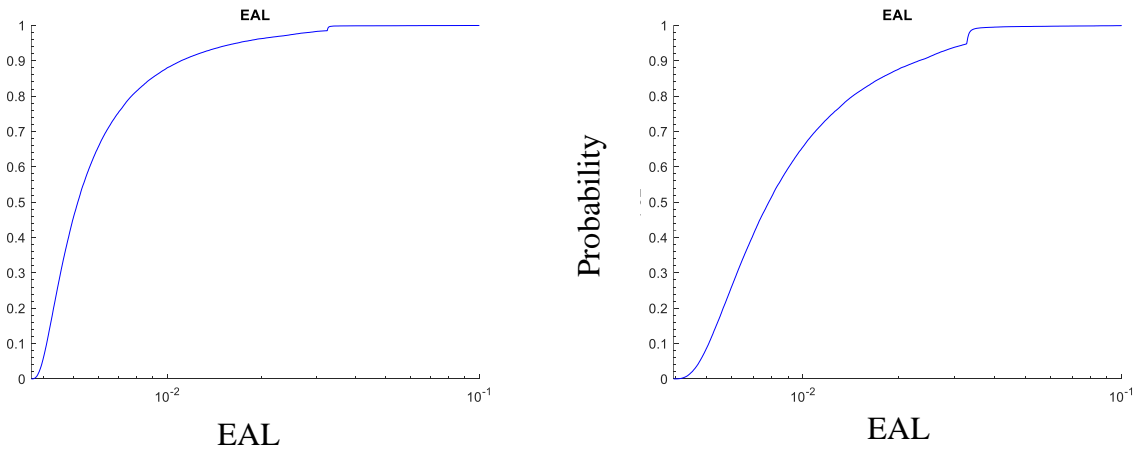
Figure 5-15. EAL curves related to the site of Naples: (a) Soil Type A, (b) Soil Type C
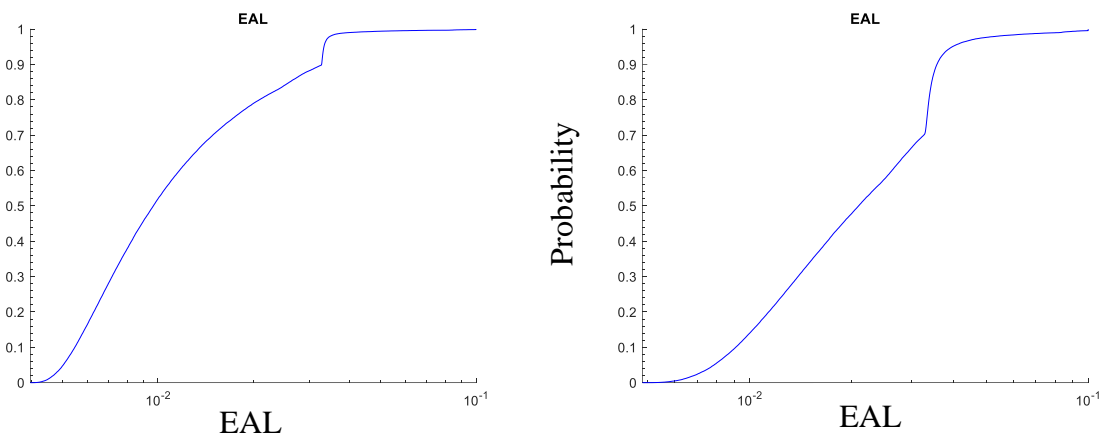
Figure 5-16. EAL curves related to the site of L'Aquila: (a) Soil Type A, (b) Soil Type C

Table 5-8. Total sensitivity indexes for each site, soil category and limit state.

	Yielding		Collapse	
Sites	Logarithmic Mean	Logarithmic Standard Deviation	Logarithmic Mean	Logarithmic Standard Deviation
Milan - A	83%	11%	21%	3%
Milan - C	83%	11%	21%	3%
Caltanissetta - A	79%	7%	23%	3%
Caltanissetta - C	77%	8%	21%	2%
Rome - A	76%	7%	22%	1%
Rome - C	72%	7%	23%	2%

Naples - A	74%	4%	25%	1%
Naples - C	70%	4%	27%	1%
Aquila - A	68%	5%	29%	2%
Aquila - C	51%	4%	46%	4%

Chapter's References

Asprone, D., Jalayer, F., Simonelli, S., Acconcia, A., Prota, A., Manfredi, G., 2013. Seismic insurance model for the Italian residential building stock. Structural Safety 44, 70–79. https://doi.org/10.1016/j.strusafe.2013.06.001

Bradley, B.A., Dhakal, R.P., Cubrinovski, M., MacRae, G.A., Lee, D.S., 2009. Seismic loss estimation for efficient decision making. BNZSEE 42, 96–110. https://doi.org/10.5459/bnzsee.42.2.96-110

Cornell, C.A., Jalayer, F., Hamburger, R.O., Foutch, D.A., 2002. Probabilistic Basis for 2000 SAC Federal Emergency Management Agency Steel Moment Frame Guidelines. Journal of Structural Engineering 128, 526–533. https://doi.org/10.1061/(ASCE)0733-9445(2002)128:4(526)

Cornell, C.A., Krawinkler, H., 2000. Progress and Challenges in Seismic Performance Assessment.

Cosenza, E., Del Vecchio, C., Di Ludovico, M., Dolce, M., Moroni, C., Prota, A., Renzi, E., 2018. The Italian guidelines for seismic risk classification of constructions technical principles and validation. Bulletin of Earthquake Engineering 16, 5905–5935.

D. Min. Infrastrutture e Trasporti, 2018. NORME TECNICHE PER LE COSTRUZIONI (NTC 2018).

Deierlein, G., Krawinkler, H., Cornell, C., 2003. A framework for performance-based earthquake engineering.

Di Ludovico, M., Digrisolo, A., Graziotti, F., Moroni, C., Belleri, A., Caprili, S., Carocci, C., Dall'Asta, A., Martino, G.D., Santis, S.D., Ferracuti, B., Ferretti, D., Fiorentino, G., Mannella, A., Marini, A., Mazzotti, C., Sandoli, A., Santoro, A., Silvestri, S., Sorrentino, L., Magenes, G., Masi, A., Prota, A., Dolce, M., Manfredi, G., 2017. The contribution of ReLUIS to the usability assessment of school buildings following the 2016 central Italy earthquake. Bollettino di geofisica teorica ed applicata 58, 353–376. https://doi.org/10.4430/bgta0192

EN 1998-1, 2005, Eurocodice 8 – Progettazione delle strutture per la resistenza sismica, 2005.

Grünthal, G., 1998. European macroseismic scale 1998 (EMS-98). Cahiers du Centre Européen de Géodynamique et de Séismologie.

Günay, S., Mosalam, K.M., 2013. PEER Performance-Based Earthquake Engineering Methodology, Revisited. Journal of Earthquake Engineering 17, 829–858. https://doi.org/10.1080/13632469.2013.787377

Hastings, W.K., 1970. Monte Carlo Sampling Methods Using Markov Chains and Their Applications. Biometrika 57, 97–109. https://doi.org/10.2307/2334940

Hazus®–MH 2.1, Technical Manual, 2001. . Department of Homeland Security Federal Emergency Management Agency Mitigation Division, Washington, D.C.

Hazus®–MH, MR4 Technical Manual, Multi-hazard Loss Estimation Methodology Earthquake Model, 2003. . Department of Homeland Security Emergency Preparedness and Response Directorate FEMA Mitigation Division, Washington, D.C.

Kennedy, R.P., 1999. Risk based seismic design criteria. Nuclear Engineering and Design 192, 117–135.

Kircher, C., Nassar, A., Kustu, O., Holmes, W., 1997a. Development of Building Damage Functions for Earthquake Loss Estimation. https://doi.org/10.1193/1.1585974

Kircher, C., Reitherman, R., Whitman, R., Arnold, C., 1997b. Estimation of Earthquake Losses to Buildings. Earthquake Spectra 13, 703–720. https://doi.org/10.1193/1.1585976

Maccari, M., 2017. Relazione illustrativa per la microzonazione di terzo livello (Comune di Camerino), in Italian.

Milutinovic, Z.V., Trendafiloski, G.S., 2003. RISK-UE, An advanced approach to earthquake risk scenarios with applications to different European towns, WP4: Vulnerability of current buildings.

Morabito, G., Podestà S., 2015, Edifici storici in conglomerato cementizio armato, D. Flaccovio, Palermo, ISBN 9788857904306©

Opcm n. 3519 del 28 aprile 2006: criteri generali per l'individuazione delle zone sismiche e per la formazione e l'aggiornamento degli elenchi delle stesse zone - Normativa, 2006.

Pitilakis, K., Crowley, H., Kaynia, A. (Eds.), 2014a. SYNER-G: Typology Definition and Fragility Functions for Physical Elements at Seismic Risk: Buildings, Lifelines, Transportation Networks and Critical Facilities, Geotechnical, Geological and Earthquake Engineering. Springer Netherlands. https://doi.org/10.1007/978-94-007-7872-6

Pitilakis, K., Franchin, P., Khazai, B., Wenzel, H. (Eds.), 2014b. SYNER-G: Systemic Seismic Vulnerability and Risk Assessment of Complex Urban, Utility, Lifeline Systems and Critical Facilities: Methodology and Applications, Geotechnical, Geological and Earthquake Engineering. Springer Netherlands. https://doi.org/10.1007/978-94-017-8835-9

Porter, K.A., 2003. An Overview of PEER's Performance-Based Earthquake Engineering Methodology. Presented at the Ninth International Conference on Applications of Statistics and Probability in Civil Engineering (ICASP9), San Francisco.

RINTC Workgroup (2018). Results of the 2015-2017 Implicit seismic risk of codeconforming structures in Italy (RINTC) project. ReLUIS report, 2018, Rete dei Laboratori Universitari di Ingegneria Sismica (ReLUIS), Naples, Italy.

Saltelli, A. (Ed.), 2008. Global sensitivity analysis: the primer. John Wiley, Chichester, England ; Hoboken, NJ.

Saltelli, A. (Ed.), 2004. Sensitivity analysis in practice: a guide to assessing scientific models. Wiley, Hoboken, NJ.

Scozzese, F., Dall'Asta, A., Tubaldi, E., 2019. Seismic risk sensitivity of structures equipped with anti-seismic devices with uncertain properties. Structural Safety 77, 30–47. https://doi.org/10.1016/j.strusafe.2018.10.003

Sextos, A., De Risi, R., Pagliaroli, A., Foti, S., Passeri, F., Ausilio, E., Cairo, R., Capatti, M.C., Chiabrando, F., Chiaradonna, A., Dashti, S., De Silva, F., Dezi, F., Durante, M.G., Giallini, S., Lanzo, G., Sica, S., Simonelli, A.L., Zimmaro, P., 2018. Local Site Effects and Incremental Damage of Buildings during the 2016 Central Italy Earthquake Sequence. Earthquake Spectra 34, 1639–1669. https://doi.org/10.1193/100317EQS194M

ShakeMap - Home , INGV. URL http://shakemap.rm.ingv.it/shake4/ (accessed 4.15.21).

Whitman, R.V., Anagnos, T., Kircher, C.A., Lagorio, H.J., Lawson, R., Schneider, P., 1997. Development of a National Earthquake Loss Estimation Methodology. Earthquake Spectra 13, 643–661. https://doi.org/10.1193/1.1585973

Chapter 6.

Final remarks and future developments

This Thesis analyses the uncertainties propagation in the seismic risk evaluation at territorial level of urban centres, estimated in the interclass variability of the response. In the risk assessment process, the prediction of potential economic losses and, more generally, consequences due to hazardous events, are a key point for prevention planning and emergency organization. To this aim, it is necessary to define reliable models for event predictions, both empirical or analytical, building response and consequences evaluation.

Two different methods have been used to evaluate the vulnerability: the empirical method, based on observational data of historical churches and the analytical one based on the sample analysis using the Monte Carlo method. This latter is applied to a sample of reinforced concrete structures, classified on the basis of the height of the buildings. The reasons that bring this study to use the two methods are different. The main advantage of the empirical approach is the credibility of the data: they represent a realistic picture of the location analysed, that can be useful to analyse the risk at territorial level, grouping the structures into classes' vulnerability. On the other hand, the main drawbacks of the empirical method are the incompleteness of the observational data for some case studies and the fact that many buildings types have not yet experienced strong motion. Therefore, the analytical vulnerability method is used as well. It considers stochastic or numerical simulations of the seismic response of any type of structure and it is very useful when observed data or expert judgments are not fully available or when there are buildings that not have experienced strong motion. However, it is a time consuming method when the building or class of buildings behaviour are estimated and it is an approach that induces a significant variability.

The level of accuracy of the evaluation of the seismic vulnerability depends on the size of the study performed. For structural risk assessment, the uncertainties analysis is part of the evaluation. The uncertainties have a crucial role in the analysis and modelling of disasters in general, both natural and human, having a meaningful impact on the risk based decisions and to develop a reliable probabilistic model for structural seismic risk assessment. In order to rigorously assess the seismic risk of a structure, all the uncertainties related to the ground motions affecting a given site, the structural response, the associated damage and the cost to repair a damaged structure should be accounted for. A number of uncertainties are present in the earthquake action, in the choice of the materials and geometrical structural properties, in the modelling and analysis of the structure and in the numerical prediction of structural seismic performance. In particular, in this Thesis the uncertainties analysis is focalized on the vulnerability assessment, where the response variability of classes' vulnerability depends on the size of the class itself.

Therefore, in analysing the seismic risk at territorial level for a delimited centre, a methodology must be developed which is capable of simulating the response for increasing level of the seismic intensity considering in particular the damage and the direct consequences. At the same time, this methodology should be able to propagate the uncertainty affecting the model parameters, which define the systems through the whole process of response and vulnerability assessment.

The first part of the Thesis is focused on reviewing the issue of seismic vulnerability assessment and methods to evaluate it, and the sources of uncertainty that may affect the earthquake input, the model parameters and the final step of the risk evaluation related to the loss estimation. The most relevant methodologies proposed by the literature, which have already been defined and applied to account for these uncertainties in the seismic structural response and vulnerability assessment, are also presented and investigated.

In the second part of the Thesis, a deep evaluation of the empirical method has been done, applying it at the case study of historical churches. Firstly, an evaluation of the post-earthquake damage and vulnerability assessment of historical churches using a discrete and continuous approach are investigated. This first investigation shows that the damage distribution over the Marche Region might be due to possible effects induced by factors such as local site condition, state of maintenance, and damage already present in the construction. The results, both in terms of local (i.e., single mechanisms) and global damage, exhibit similarities with those available in literature relevant to investigations carried out after some major Italian earthquakes. This behaviour supports the conclusion that damage mechanisms of churches are characterized by recurrent characteristics, despite the peculiarities of each building. The vulnerability curves obtained from the observational data fit are not fully conforming to previous existing studies that demonstrated a higher vulnerability for existing churches. This is probably due to the contribution of seismic improvements made after the 1997 Marche-Umbria earthquake. Even if it is well known that interventions might not always lead to a clear improvement of the seismic behaviour of churches (especially when based on the use of reinforced concrete), they probably revealed effective in reducing the vulnerability of Marche churches after the 1997 Marche-Umbria earthquake. Anyway, for low seismic intensities, the observed vulnerability is in line with the previous studies. Finally, concerning the judgment on church usability, the analysis of data clarified that a direct correlation between the damage index and the usability outcome is quite difficult to establish, given that building safety might be compromised by only few activated mechanisms.

Moreover, also a continuous approach of the damage has been considered and empirical fragility curves have been proposed. They are derived from groups of churches refereed to homogeneous typologies characterized by similar structural response of the same sample. The fragility model is defined by evaluating relevant parameters using the Maximum Likelihood Estimation. In addition, from the defined fragility curves the global damage index function is derived and then compared with the curve obtained by fitting data registered on field with a Sum Square Estimation technique, as well as with the results from past researches related to previous

seismic events. This comparison shows a good agreement between the two approaches (the discrete and the continuous ones).

Moving on the empirical predictive model for seismic damage, it provides a probabilistic description of the relationship between the damage, expressed by a continuous random variable, and the ground motion intensity, by considering a complete database of historical churches that represents a news in the literature for the cultural heritage. Finally, an illustrative example has been carried out in order to depict the potentialities of the model in the prediction of damage scenarios and in supporting decision making processes for risk reduction. Some concepts about the response model are quite general and can be of interest in the development of empirical predictive models of other types of constructions.

To complete the process of the seismic risk evaluation, also the repairing cost model for churches has been developed. It is a probabilistic consequence model based on the damage model previously defined, with the peculiarities of analysing the soil type that represents an important advancement in the seismic risk analysis because it is one of the main reason of local amplification effects.

In the last part of the Thesis, the analytical method has been investigated by considering a delimited urban district formed by Reinforced Concrete buildings classified in three vulnerability groups according with their height. The main objective is evaluating the capacity of probabilistic based procedure framework to assess the expected annual losses at territorial scale. This probabilistic procedure uses Monte Carlo simulation in order to propagate the uncertainties affecting the model parameters through the response and vulnerability assessment. The seismic hazard is assessed considering the geological and geotechnical condition of the soil, useful for the evaluation of the shake amplification. The most representative fragility curves for specific limit state are selected from the state of the art and then they are applied to the three specific classes of building: high, medium and low height.

The loss analysis is expressed in terms of expected annual losses considering the replacement costs available in literature. Finally, a comparison with the observed damage is provided. The outcomes of the study are particularly relevant and highlight that the differences between the results of the analytical analysis and the reality are due to the large variability presents in the classes of fragility curves valid for groups of buildings with similar structural response. Therefore, it is important to point up the needs of uncertainty analysis due to the influence of model parameters uncertainty on the seismic response and fragility of the investigated systems. Considering that, the sensitivity analysis have been conducted for two limit states evaluating the First-Order sensitivity index and the Total sensitivity index, considering as well different hazard references curves.

The work in the present study should be extended through additional research in the following areas:
- considering the empirical approach: a comparison of the output of the empirical model with the data of past earthquakes can be of interest. In addition, the application of the empirical model to the churches that have been invested by the Umbria Marche 1997 earthquake could also be proposed and a comparison with the churches stuck by Central Italy 2016 could be considered,

- considering the analytical approach: different considerations and developments can be make. The first aspect is a deep investigation on the final result of the expected annual losses, considering a standard deviation or its variability. Then, in the uncertainties analysis step, other types of buildings could be considered (different height, different construction type or construction period) and then it could be evaluated the output with its variability and the importance of the structural analysis step input parameters in terms of output influence. In addition, also other fragility curves references can be selected even if the state of the art does not propose fragility curves fitted for groups of buildings and covariance matrix at the same time.

The variability of the input and so a record-to record variability could be included to provide a proper seismic risk assessment. Finally, also the consequences analysis can be considered on the analytical approach, focusing on the direct and indirect losses and providing an estimation of the risk assessment in a holistic way.